2018

Liner characterisation and leak detection using electrical resistivity techniques

Lopa M S Pandey
Edith Cowan University

Edith Cowan University

Copyright Warning

Liner Characterisation and Leak Detection Using Electrical Resistivity Techniques

By

Lopa Mudra S. Pandey

MScEng Civil and Environmental Engineering (Edith Cowan University, Australia)

BTech Environmental Engineering (Indian Instituite of Technology, ISM, India)

Associate Professor Sanjay Kumar Shukla, Principal Supervisor

Professor Daryoush Habibi, Associate Supervisor

This thesis is presented in fulfillment of the requirements for the

Degree of Doctor of Philosophy

2018

School of Engineering

Edith Cowan University

USE OF THESIS

The Use of Thesis statement is not included in this version of the thesis.

ABSTRACT

Engineered lining systems are often designed for waste containment facilities, such as landfills, leachate ponds, tailing dams, red mud ponds, sump wells, etc. to prevent soil and groundwater contamination. Although the integrity of liners during their intended lifespan is critical, harsh physico-chemical operating conditions and poor installation practices generally cause defects in the liners. These defects result in the leakage of leachates which contaminate the underlying liner base soil. The use of a suitable leak detection system for the prevention and mitigation of pollution due to the lining system failures is integral to the proper management of waste containment facilities. A detailed review of the literature shows that in the current practice, there are several conventional methods for leak detection; however, these methods are limited in their usefulness as they are generally time-consuming and expensive. Therefore, there is a huge scope for an innovative method of leak detection which can detect leakages at the onset.

In the present research, an attempt has been first made to assess the current state of landfilling in Australia with a focus on the lining practices and leak detection methods. Based on the survey and the information available on the public domain, it has been observed that different landfill sites practice non-uniform set of directives for waste classification, siting, design, operation and rehabilitation. Majority of the facilities have been found to be publicly owned. Further, various leak detection methods to detect liner defects have been scrutinised. The need for the online monitoring of lining systems for the proper management of waste containment facilities has been discussed. The use of groundwater monitoring wells for leakage detection is more prevalent, while the use of sensor-beds for real-time monitoring of liners is found to be very limited.

In this thesis, an effort has been made to characterise the lining materials using the electrical resistivity method, so that later this property can be utilised to detect liner leakages in leak detection systems. The results of an investigation into the effect of the state of compaction on the electrical resistivity of sand-bentonite mixtures, with the bentonite content varying from 0 to 100%, have been presented. The resistivity values of mixtures at their different states of compaction have been investigated. The resistivity of the lining mixture decreases as the water content increases, but the rate of decrease is reduced significantly above specific water content for each mixture. Furthermore, this specific water content is noted to be on the wet-side of the optimum for sand-bentonite mixtures and on the dry-side of the optimum for pure sand and pure bentonite. Increasing the bentonite content over 20% demonstrates an insignificant impact

on resistivity. It is observed that at higher water contents, the bentonite addition has negligible effect on resistivity. Correlations applicable to the sand, bentonite and pore fluid used in this study have also been presented.

In addition, this thesis also presents a new technique based on the electrical resistivity method to detect the leakage of leachates through defects in liners by the simulation of lining system as used in actual practice. The design of this innovative system as developed for the detection and localization of leaks in geomembrane liner placed over soil has been detailed. A new leak detection system is developed by pairing a resistivity sensing technique with a four-probe ground resistance testing equipment to measure the resistivity profile. The guidelines given by the Australian Standard AS 1289.4.4.1-1997 are used for the design of the soil box, which was used as the resistivity sensing system. The box was designed to represent an actual waste containment site with a geomembrane (GMB) liner placed on top of a soil layer. The box with an internal dimensions of 500 mm length, 200 mm width and 400 mm height, was fabricated using 12-mm thick non-conducting perspex sheet. It was installed with two brass current plate electrodes of dimensions 200 mm by 200 mm, and 16 brass potential measuring pins of 4 mm diameter. On one side of the box, sixteen holes were made, through which the potential pin electrodes could be inserted into the box after filling it with the soil specimen. Soil was filled into the box, overlain with the GMB and covered with a standing head of leachate. Leak was introduced intentionally in the GMB liner. Controlled leakage through the liner was then established to study the resistivity profile of the soil layer, in order to detect the liner leak.

Furthermore, to show the efficacy of the innovative leak detection system, the results from the experimental demonstration using water, have been presented. The leak was introduced intentionally in the geomembrane and the resulting changes in the electrical resistivity of the underlying soil were observed. The resulting resistivity profiles for Perth soil in Australia were obtained at an interval of 10 min. The resistivity of soil was found to be in the range of 90-100 Ωm. The electrical resistivity decreases with an increase in the leakage duration. The resistivity was found to increase with an increase in the distance/depth from the leak point. The electrode sensing system that is the closest to the liner was found to have better ability to detect leakage. The resistivity values recorded using the sensors at a depth of 120 mm and above, showed insignificant variation with distance and leakage duration. This method is found to be effective in detecting and locating liner leakage issues within 30 min from the instant when the defect develops.

Additional tests were conducted using municipal solid waste (MSW) landfill leachates to evaluate the performance of the new technique by use of controlled leakage. Leachates for the test were procured from actual landfill sites in Perth metropolitan region. A sharp decrease of resistivity of soil is noticed with an increase in the leakage duration, irrespective of the leachate composition. However, the effect of distance/depth on the soil resistivity is negligible at leakage duration greater than 60 min for Leachate #1 and 160 min for Leachate #2. The resistivity of soil ranges from 7-15 Ωm for Leachate #1 to 20-50 Ωm for Leachate #2. The resistivity decreases with an increase in the proximity to the leak point. Furthermore, the resistivity values obtained with water were nearly 10 times the values observed with landfill leachate as the leaching liquid. Based on the resistivity profiles of soil as observed at different time intervals, the method is found to be effective in determining leakages in the liner.

The test results have also been presented for the leakage of Bayer liquor obtained from aluminium manufacturing company in Western Australia. The resistivity values were found to range from 1 to 3 Ωm. A similar trend in the resistivity values was found with distance/depth for Bayer liquor contamination as observed with other leachates. Therefore, the installation of this innovative detection system below the liners in the aluminium industry can enable the effective monitoring of the lining systems and in case of failures, to take timely action for hazard mitigation.

Finally, based on the leak detection test results, empirical correlations and analytical modelling have been developed and presented for the relationship between resistivity, leakage duration and distance/depth. These can be used to predict the velocity of flow of leachate at any point within a liner base soil specimen. A numerical model for the seepage analysis of the leak detection test has been developed using the SEEP/W software. The flow velocity obtained from this model has then been used in conjunction with the new correlations to generate resistivity profiles for any specific soil type and leachate, in the leak detection test. Any other suitable seepage analysis software (e.g. GGU-SEEP, GGU-SS-FLOW2D, GGU-SS-FLOW3D, etc.) can be used by practicing engineers to predict resistivity, and therefore, to design a suitable lining system for waste containment facilities.

This research work is particularly useful in generating awareness about the state of landfilling and will help various environmental protection agencies in making informed decisions for the development of rules and regulations to govern landfills. It is demonstrated that this system can be used to effectively detect and locate the liner leaks by simulating the field condition. The newly developed innovative diagnostic technique can be useful in designing the monitoring systems for waste storage and handling facilities, subbase

contamination detection, liner leak detection, development and placement of sensors, soil and corrosion studies and so on, in Australia as well as worldwide.

DEDICATION

This thesis is dedicated to my parents, Mr Lalit K. Pathak and Mrs Poonam Pathak, for their endless love, support and encouragement. Thank you both for giving me the strength to chase my dreams.

ACKNOWLEDGEMENTS

First and foremost, I would like to express heartfelt appreciation and gratitude to my supervisor, Associate Professor Sanjay Kumar Shukla, who is a constant source of support and guidance. Without his help and encouragement, this dissertation could not have been completed so timely. He is professionally and personally inspirational and I have learnt a lot from him. His dedication and perseverence throughout this research journey have been outstanding and immeasurable.

I would like to acknowledge my co-supervisor, Professor Daryoush Habibi, for his insightful suggestions and kind help. A special word of appreciation goes to the technical staff, Mr. Mohamed Ismail, Mr. Adrian Styles, Mr. Xiaoli Zhao, Mr. Kourosh Sheikhzadeh and Mr. Greg Yu for their unrelenting support at all stages in the development of my thesis.

A special thanks to Mr Sreten Askraba for his unwaivering help and encouragement at every stage of the research. Furthermore, I would like to include a special note of thanks to Mr. Tim Morris and Mr Andrew Murphy (City of Joondalup) for their invaluable assistance through various aspects of the research. Their guidance, kindness and willingness to support academic research are highly appreciated.

Many people contributed in different but meaningful ways to my thesis. In particular, Mike Haynes (Henderson Waste Recovery Park, WA), John Jones (SUEZ Recycling and Recovery, NSW), Glen Maslen (Red Hill Landfill Facility, WA), Shane Middleton (City of Greater Geelong, Victoria), Eugene Olman (North Bannister Resource Recovery Park, WA), Alicia Sheen (Newcastle City Council, WA), Sarah Wallrodt (Armadale Landfill and Recycling Facility, WA), Elonn Tyl (Water Corporation, WA), Elise Matthews (Water Corporation, WA), Tom Widenbar (North Bannister Resource Recovery Facility, SUEZ, WA), Kerryn Suthern (EPA, SA), Michael Leahy (Alcoa, WA), Peter DiDonna (Worsley Alumina, WA), and so on. Without the help and the friendship of these people, this thesis would not have been possible. I, as well as, anyone who gains from reading the words herein owe them a debt of gratitude.

In addition, I also wish to acknowledge the dedication of the administrative staff, especially Ms. Muriel Vaughan, Mrs. Audrey Gan and Mrs. Olga Samul. All these people have tremendous impact on my work. Indeed, they understood the needs of a research student and were always available to meet them. The library and the computer facilities of the university

have been indispensable. Finally, I wish to thank all the kind people that I had the pleasure of interacting with during my work, to only some of whom it is possible to give mention here.

Last but not the least; I would like to thank my husband, Shashwat S. Pandey, for his steady faith and understanding during this journey. His support and encouragement have been crucial for this success. He has been a pillar of strength and it would not have been possible to successfully complete this PhD without him.

Lopa Mudra S. Pandey

COPYRIGHT AND ACCESS DECLARATION

I certify that this thesis does not, to the best my knowledge and belief:

I. incorporate without acknowledgement any material previously submitted for a degree or diploma in any institution of higher education;

II. contain any material previously published or written by another person except where due reference is made in the text; or

III. contain any defamatory material

I also grant permission to the Library at the Edith Cowan University to make duplicate copies of my thesis as required.

Signature: [redacted]..

Date: 18th Dec 2018.....

TABLE OF CONTENTS

LIST OF FIGURES

LIST OF TABLES

LIST OF SYMBOLS

Basic SI units are given in parentheses.

a	constant (Ωm)
a_o	geomembrane hole area (m^2)
α	ratio of bentonite addition (dimensionless)
A	cross-sectional area of specimen (m^2)
A_l	area through which the leachate flows (m^2)
a_1 and a_2	positive constants (dimensionless)
b	constant corresponding to a soil type and pore fluid (dimensionless)
b_1 and b_2	positive constants (dimensionless)
c , m	fitting parameters (dimensionless)
c_1	constant (Ωm)
c_2 and c_3	specific constants corresponding to a particular soil type and pore fluid (dimensionless)
C_0	variable dependent on the composition of the pore fluid (dimensionless)
C_c	coefficient of curvature (dimensionless)
C_u	coefficient of uniformity (dimensionless)
d	soil parameter (dimensionless)
d^*	critical pore diameter for porous systems (m)
D	diffusion coefficient for same ionic species in clay (m^2/s)
D_{10}	effective size of the soil particles (mm)
D_{60}	diameter of the soil particles for which 60% of the particles are finer (mm)
D_r	relative density (dimensionless)
e	void ratio of soil (dimensionless)
$e_{\min}$	minimum void ratio (dimensionless)
$e_{\max}$	maximum void ratio (dimensionless)
EC_0	bulk soil electrical conductivity (S/m)

EC_w	pore water electrical conductivity (S/m)
EC_s	apparent soil-particle-surface electrical conductivity (S/m)
FF	formation factor (dimensionless)
F_{sat}	structural coefficient at saturated condition (dimensionless)
G_s	specific gravity of soil solids (dimensionless)
h	head of leachate on top of the liner (m)
h_w	depth of water on top of the geomembrane (m)
i	input current (A)
I	induced electric current in the medium between outer electrodes (A)
k	coefficient of permeability of soil (m/s)
k_1	coefficient of permeability of soil using Leachate #1 (m/s)
k_2	coefficient of permeability of soil using Leachate #2 (m/s)
K	absolute permeability of soil (m^2)
k^*	permeability (m^2)
k_s	soil hydraulic conductivity (m/s)
k_{sat}	saturated hydraulic conductivity (m/s)
$K4P$	four probe conductivity (S/m)
$K(SE)$	electrical conductivity of saturation (S/m)
$K(1:5)$	electrical conductivity for 1:5 extracts (S/m)
Kx	$K(SE)$ or $K(1:5)$ (S/m)
L	length of specimen (m)
m_b	mass of dry bentonite (kg)
m_s	mass of dry sand (kg)
η	viscosity of leachate (Pas or Ns/m^2)
η_1	viscosity of Leachate #1 (Pas or Ns/m^2)
η_2	viscosity of Leachate #2 (Pas or Ns/m^2)
n^*	efficient porosity (dimensionless)
p	percentage of clay fraction in soil (dimensionless)

p_b	bentonite content (dimensionless)
p_l	leachate content (dimensionless)
Q	rate of leachate migration through the geomembrane defect (m^3/s)
r	radial distance between an electrode pair (mm)
R	electrical resistance (ohm, Ω)
R'	radius of geomembrane defect (m)
S	degree of saturation (dimensionless)
S_r	degree of saturation (dimensionless)
t	duration for which the leakage through liner was allowed/leakage duration (min)
V	velocity of flow of leachate (m/s)
v_1	velocity of flow of Leachate #1 (m/s)
v_2	velocity of flow of Leachate #2 (m/s)
ΔV	electrical potential difference between the two inner electrodes (V)
V	potential difference across the outer conductors/ input voltage (V)
w	gravimetric water/fluid content (dimensionless)
w_k	water content at minimum hydraulic conductivity (dimensionless)
w_l	liquid limit (dimensionless)
w_p	plastic limit (dimensionless)
w_{opt}	optimum water content (dimensionless)
w_T	specific value of water content at which the trend of the resistivity curve changes (dimensionless)
x	distance of the mid-point of a pair of electrodes (mm)
x_l	distance of the liner leak (mm)
γ	total unit weight (kN/m^3)
$\gamma_{d\max}$	maximum dry unit weight (kN/m^3)
$\gamma_{d\min}$	minimum dry unit weight (kN/m^3)
γ_{dry}	dry unit weight (kN/m^3)

γ_l	unit weight of leachate (kN/m^3)
γ_{l1}	unit weight of Leachate #1 (kN/m^3)
γ_{l2}	unit weight of Leachate #2 (kN/m^3)
γ_{wet}	wet unit weight (kN/m^3)
z	depth of the mid-point of a pair of electrodes (mm)
z_l	depth of the liner leak (mm)
θ	volumetric water content (dimensionless)
θ_w	volumetric water content (dimensionless)
ρ	electrical resistivity of the soil specimen (Ωm)
ρ'	electrical resistivity of unsaturated soil (Ωm)
ρ_0	soil resistivity (Ωm)
ρ_w	resistivity of free water (Ωm)
σ	bulk conductivity of soil (S/m)
σ_w	pore water conductivity (S/m)
λ	resistivity correction factor (dimensionless)
β, e, f	various constants (dimensionless)

CHAPTER 1

INTRODUCTION

This chapter explains the problem being considered in this thesis and the importance of finding sustainable solution to address it. It includes the aim and the specific objectives of the thesis. This is followed by the scope and an explanation of how this thesis has been structured for easy understanding and convenience of the reader.

1.1 General

Lining systems are installed in waste storage and disposal facilities, such as landfills, sump wells, red mud ponds, tailing dams, leachate ponds and fly-ash collection pits for the control of soil and groundwater contamination. Figure 1.1 shows the use of a geosynthetic clay liner (GCL) at a landfilling facility. Figure 1.2 shows a typical geomembrane liner used at a landfilling facility.

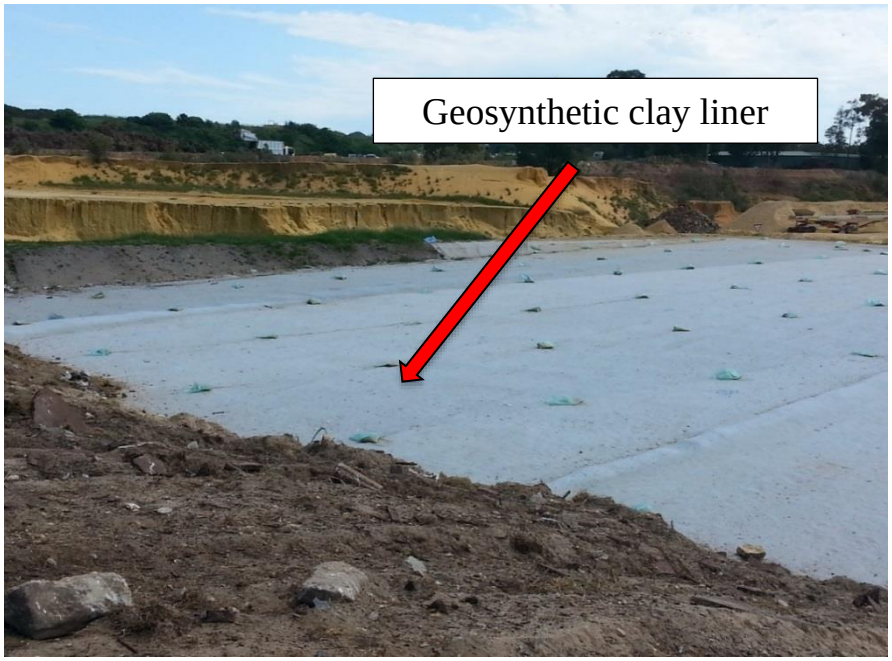

Figure 1.1: Geosynthetic liner (Courtesy: Millar road landfill and recycling facility, City of Rockingham, Perth, WA).

Engineered containment systems are essential to minimise the impact of effluents on the environment and human health. Hence, the integrity of these liners materials is critical (Daniel, 1984). However, the performance of these liners over intended design life cannot be established due to their harsh operating conditions and inadequate installation techniques (Rowe *et al.*, 2004; Oh *et al.*, 2008). Defects and subsequent contaminant leakage issues often ensue resulting in the contamination of the subbase soil layer (Nosko and Touze-Foltz, 2000).

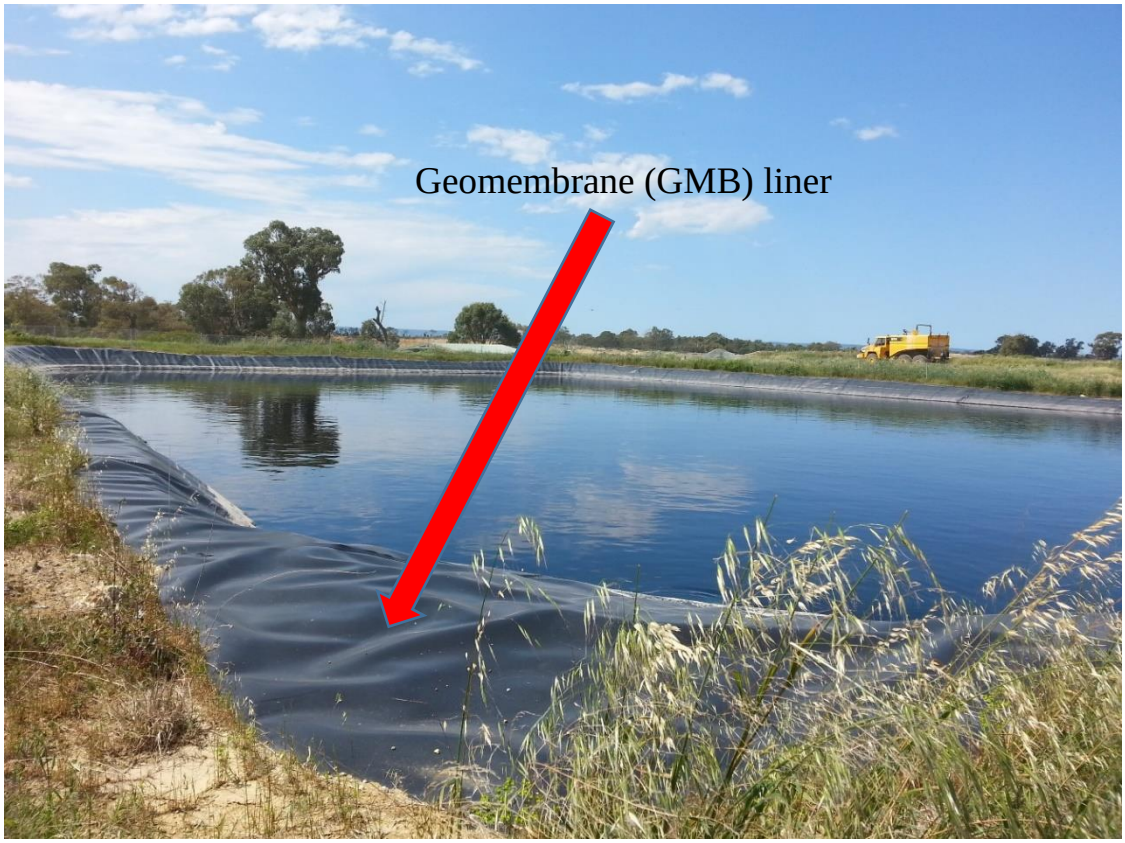

Figure 1.2: Leachate collection pond at Millar road landfill and recycling facility, Perth, WA, Australia.

Subsurface contamination detection methods such as resistivity cone penetration test (RCPT), ground penetrating radar (GPR) and time domain reflectometry (TDR) are used at sites suspected to contamination. However, for such cases the sites might have been extensively contaminated already and the cost of remediation would be very high (Oh *et al.*, 2008). Hence, an early detection and monitoring system should be designed and put in place to ensure timely leakage detection (Oh *et al.*, 2008; Ben Othmen and Bouassida, 2013). The

early detection of leaks can ensure that timely control is taken, and proper mitigation measures are implemented (Harrop-Williams, 1985).

Several technologies such as electrical methods, tracer methods, diffusion hoses, intrinsic fiber optic sensor, electro-chemical sensing cables, cable network sensors and geosynthetic membrane monitoring systems have been used for contamination detection in sublayers (Hix, 1998). Of these methods, the electrical resistivity method is more prevalent because of its ease of operation and cost-effectiveness (Oh *et al.*, 2008).

1.2 Basic Concept of Electrical Resistivity Method

The electrical resistivity method is based on the well-established fact that the electrical resistivity of any subbase/sublayer/subgrade/foundation geomaterial is much higher than the electrical resistivity of water, leachates, or any liquid effluents which may permeate the foundation material (McCarter, 1984; Yoon and Park, 2001; Munoz-Castelblanco *et al.*, 2012; Yan *et al.*, 2012; Kuranchie *et al.*, 2014; Pandey *et al.*, 2015; Pandey and Shukla, 2017). The presence of even traces of contaminants leads to a significant change in the resistivity of soils. This change can be easily detected to locate subbase contamination (Fukue *et al.*, 1999; Yoon and Park, 2001; Munoz-Castelblanco *et al.*, 2012).

The electrical resistivity (R in ohm (Ω)) of a soil is determined by providing a known current (i in ampere (A)) across a pair of electrodes and recording the subsequent voltage drop (V in volt (V)). The soil electrical resistivity is then measured using the Ohm's law as:

$$V = iR \tag{1.1}$$

However, the resistance is not a true material property as it also depends on the dimensions of the sample being tested. Hence, it is used to calculate electrical resistivity (ρ in Ohm-m (Ωm)), which is an intrinsic property of the material, using the following equation:

$$R = \frac{\rho L}{A} \tag{1.2}$$

where A is the cross-sectional area (m^2) and L is the length (m). The variations in estimated soil resistivity can then be used to effectively determine the leachate contamination of subbase

material (AS 1289.4.4.1, 1997; ASTM D6431-99, 2010). Hence, many leakage detection techniques such as, water puddle method (ASTM D7002 - 16), conductive geomembrane spark test (ASTM D7240 - 06(2011)), water lance method (ASTM D7703 - 16), arc testing method (ASTM D7953 - 14) and electrode grid method (ASTM D6747 − 15), are based on the concept of the electrical resistivity method.

1.3 Waste Management Practices in Australia

Australia is an island continent with a population of nearly 25 million people and a land mass of 7.692 million km². Waste production in Australia was 2.2 tonnes per capita in 2010–11 alone. As per DEWHA (2010), the waste production increased by 170% in the period of 1996-2015, at a compound growth rate of 7.8% per annum. 60% of this generated waste was either recovered or recycled, with the rest 40% sent for disposal to landfills (DEE, 2013). These solid wastes consisted of commercial and industrial wastes (C&I), construction and demolition wastes (C&D) and municipal solid wastes (MSW). In Australia, MSW has the lowest recovery rate out of the three main waste streams. From the 14 million tonnes of MSW generated in 2010-11, 49% could not be recovered and was sent for disposal. Most of the waste production is focused in the major urban areas (DEE, 2010).

The dumping of wastes to landfilling facilities is the major waste disposal method practiced in Australia. Figure 1.3 shows the location of various waste management facilities in Australia as per Geoscience Australia (2017).

Large amounts of wastes are also handled and stored by various waste containment facilities in industries such as red mud ponds, tailing dams, Bayer liquor storage facilities, sump wells, etc. Different combinations of natural clay liners, compacted clay liners (CCL), HDPE geomembranes, geosynthetic clay liners (GCL), geotextiles and geonets are being used in the landfills (Dixon, 2013). However, there is a lack of uniform code of practice for ground preparation and lining methods. The most popular method of leak detection in practice is the use of groundwater monitoring wells to monitor the groundwater quality upstream and downstream of landfills. Hence, the issue of proper handling and management of wastes in landfilling facilities is extremely relevant for Australia, as well as globally.

Landfills are often developed in old quarries as it is a cost-effective method of rehabilitating used quarries. However, due to geographical and geological constraints, difficulty in obtaining approval for a new site, etc., there is a scarcity of available space. Furthermore, if the landfills are situated far off from the metropolitan areas, the cost of transportation and disposal of wastes

is very high. Therefore, although Australia has a huge land mass, the siting, design, operation, and proper maintenance of landfilling facilities is a major concern (WMAA, 2013).

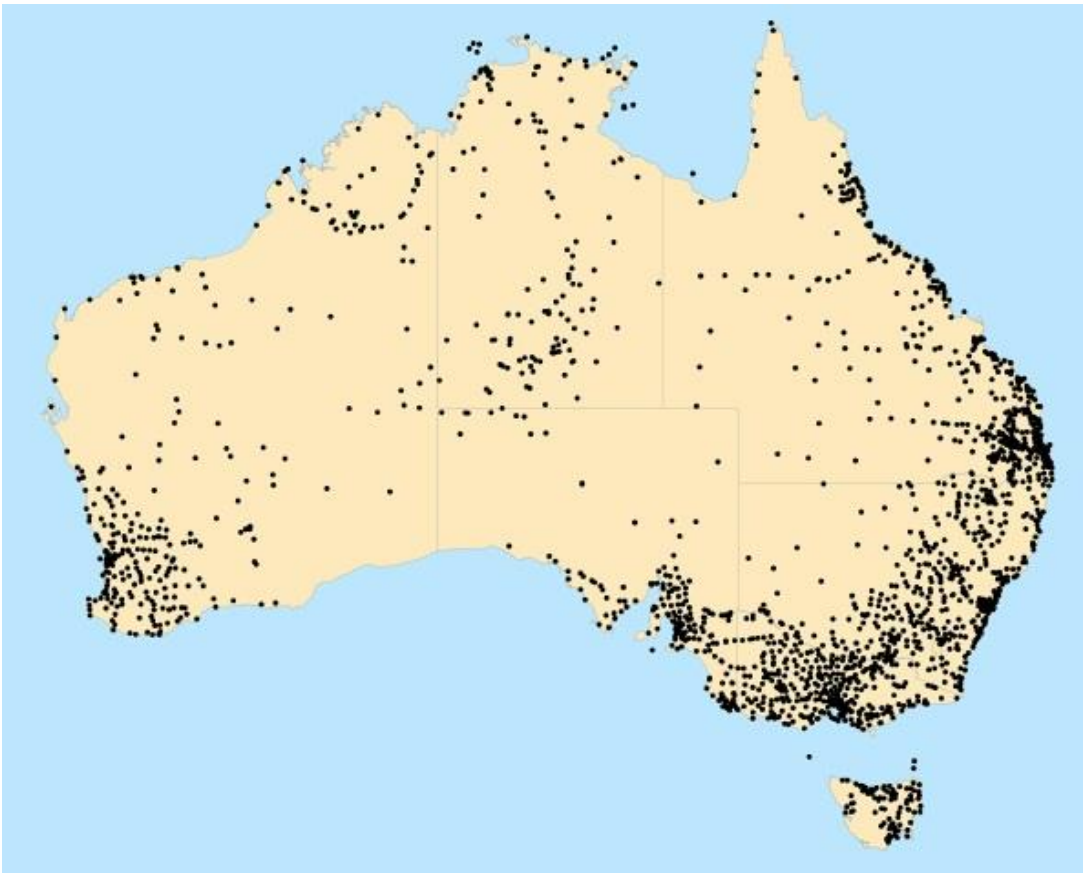

Figure 1.3: Waste management facilities in Australia (Geoscience Australia, 2017).

1.4 Significance of the Current Research

Lining systems are an essential component for contamination control in waste storage and disposal facilities (Nosko and Touze-Foltz, 2000). Ascertaining the integrity of the liners over their designed life is critical for the prevention of soil and groundwater pollution (Daniel, 1984). However, due to the intense physicochemical environment in which they operate, defects often arise in liners ((Rowe *et al.*, 2004; Oh *et al.*, 2008).

Contamination is found to increase with the passage of time, subsequently resulting in intensified adverse impact on the environment and higher mitigation costs (Oh *et al.*, 2008; Ben Othmen and Bouassida, 2013). Hence, early detection of leakage is imperative for contamination control (Harrop-Williams, 1985).

Although many methods are used for contamination detection such as electrical methods, tracer methods, diffusion hoses, intrinsic fiber optic sensor, electro-chemical sensing cables,

cable network sensors and geosynthetic membrane monitoring systems (Hix, 1998); the electrical resistivity method is the most researched. The electrical resistivity method is used more because of its low input cost and ease of operation (Oh *et al.*, 2008).

This method makes use of the well-established fact that the resistivity of the dry subbase geomaterials which are placed below liners, is very high compared to the resistivity of contaminants and even water (Rhodes *et al.*, 1976; McCarter, 1984; Yoon and Park, 2001; ANZS, 2007; Munoz-Castelblanco *et al.*, 2012; Yan *et al.*, 2012; Kuranchie *et al.*, 2014; Pandey *et al.*, 2015). Therefore, the addition of even small amounts of fluids results in changes in the electrical resistivity of the geomaterials (Yoon and Park, 2001; Pandey *et al.*, 2015). These changes can be detected easily to determine liner defects (Fukue *et al.*, 1999; Yoon and Park, 2001; Munoz-Castelblanco *et al.*, 2012).

Hence, there is a huge scope for the laboratory-based study of the electrical resistivity changes produced in subbase/sublayer/subgrade geomaterials due liner defects. This entails the characterisation studies for clay and sand-clay subbase materials, investigation of the effects of properties of leachate, the effect of leakage duration, as well as the impact of changes in the leak type, size, area, number, shape, etc.

This study aims to characterize the subbase/subgrade/sublayer liner material using the electrical resistivity method. During the course of the research work, an innovative system was developed for the detection and location of leakages by simulating actual liners. The research presents database, correlations, empirical equations, design charts and numerical models for use by practicing design engineers for anomaly detection, contamination and leakage detection, preliminary liner material selection, corrosion and salinity studies, etc. The research outcome can be useful for further research work into leak location systems and sensor development.

Based on the discussions in the previous sections, the specific topics and the objectives of this research are listed under Section 1.5.

1.5 Scope and Objectives of the Research

As defined by the problem statement above, contamination detection and leakage location are pressing issues that require in-depth research. The following specific objectives have been chosen for further investigation:

- Characterisation of bentonite and sand-bentonite liner subbase/sublayer/subgrade material using electrical resistivity method.
- Study of the effect of varying sand-bentonite ratios on the resistivity of sublayer material.

- Development of a new experimental setup for the study of leakage detection by simulating an actual liner.
- Investigation of the effect of changing leachate composition and type on the resistivity of subgrade material using the newly developed leak detection test.
- Scrutiny of the effect of time on the electrical resistivity of the subbase component.
- Analytical and numerical modeling for the prediction of the electrical resistivity profiles of liner base materials.

1.6 Publications Based on the Present Work

Attempts were made during the progress of the research to prepare the thesis as research papers for submission to peer-reviewed international journals and conference proceedings to be considered for publication. The details of the published/accepted or submitted papers are as follows:

International Journals

1. **Pandey, L.M.S**. and Shukla, S.K. (2019). Development of an innovative liner leak detection technique. *Geotechnical Testing Journal*, ASTM, USA, Vol. 42, No. 5, pp. 1-14, DOI: 10.1520/GTJ20170292.
2. **Pandey, L.M.S**. and Shukla, S.K. (2018). Effect of state of compaction on the electrical resistivity of sand-bentonite materials. *Journal of Applied Geophysics*, Netherlands, Vol. 155, No.1, pp. 208-216, DOI: 10.1016/j.jappgeo.2018.06.016.
3. **Pandey, L.M.S.,** Shukla, S.K. and Habibi, D. (2017). Resistivity profiles of Perth soil in leak detection test. *Geotechnical Research*, UK, Vol. 4, No. 4, pp. 214-221, DOI:10.1680/jgere.17.00014.
4. **Pandey, L.M.S**. and Shukla, S.K. (2018). An insight into waste management in Australia with a focus on detecting landfill liner leaks. *Journal of Cleaner Production*. (under review).
5. **Pandey, L.M.S**. and Shukla, S.K. Detection of leakage of MSW landfill leachates through a liner defect. Surveys in Geophysics. (under review).

Conference Proceedings

6. **Pandey, L.M.S** and Shukla, S.K. (2019). Use of an innovative technique to detect the leakage of Bayer liquor through a liner defect. *Proceedings of the Sustainable Waste Management through Design*, Editors: H. Singh, P. Garg and I. Kaur, 2-3 November 2018, Ludhiana, Punjab, India, pp. 1-7, DOI: 10.1007/978-3-030-02707-0_1.

7. **Pandey, L.M.S.,** Shukla, S.K. and Habibi, D. (2018). Leak detection through geomembrane liner using electrical resistivity method. *Proceedings of the 11th International Conference on Geosynthetics*, Seoul, South Korea, 16-21 September 2018, Paper No.: PP-K-02, pp. 1-6.
8. **Pandey, L.M.S**. and Shukla, S.K. (2018). Leak detection practices in Australia for sustainable landfill management. *Proceedings of the International Conference on Environmental Geotechnology, Recycled Waste Materials and Sustainable Engineering* (EGRWSE), 29-31 March 2018, Jalandhar, India, Paper No.: 105.

1.7 Structure and Organisation of the Thesis

This introduction chapter is followed by the rest of the chapters in the thesis with each chapter aiming to achieve a specific objective as stated previously. Chapter 2 is the general overview of significant, current and selected literature which is relevant to this study. This helped to identify the limitations in literature and what needs to be done in order to bridge the knowledge gaps. Parts of this chapter are based on two papers accepted for presentation and publication in the following conference proceedings: 11th International Conference on Geosynthetics, 16-21 September 2018, Coex, Seoul, Korea, and International Conference, Environmental Geotechnology, Recycled Waste Materials and Sustainable Engineering, 29-31 March 2018, Jalandhar, Punjab, India.

Chapter 3 specifically analyses the literature and uses results from an extensive survey to develop an insight into the current state of waste management in Australia, with a focus on detecting landfill liner leaks. This chapter, except with limited modifications in layout for consistency in the thesis, has been submitted to the Journal of Cleaner Production, of Elsevier/ScienceDirect Publication and is currently under review.

In chapter 4, the effect of state of compaction on the electrical resistivity of sand-bentonite lining materials has been studies using experimental investigation. Except with limited modifications in layout for consistency in the thesis, this chapter has been based on the Journal of Applied Geophysics, of Elsevier/ScienceDirect Publication.

Chapter 5 presents the detailed design for the development of an innovative liner leak detection technique. This chapter has been submitted to the Geotechnical Testing Journal, of American Society of Testing Materials (ASTM) publication and has been accepted for publication. The details presented here are the same, except some changes in the layout in order to maintain a consistency in the presentation throughout the thesis.

Chapter 6 is a practical laboratory investigation to obtain the resistivity profiles of Perth

soil in leak-detection test using water as the leachate. Except with limited modifications in layout for consistency in the thesis, this chapter has been based on the paper in Geotechnical Research of ICE Publication.

Chapter 7 is the detailed investigation of the resistivity profiles obtained by the leakage of municipal solid waste landfill leachates through a liner defect. This chapter has been submitted to Surveys in Geophysics, of Springer Publication and is currently under review.

In chapter 8, experimental results of the use of the newly developed leak detection technique to detect the leakage of Bayer liquor through a liner defect, have been presented. This chapter has been based on the conference proceeding of the 8th Sustainable Waste Management Through Design, 2-3 November 2018, Ludhiana, Punjab, India.

Based on the leak detection test results, in Chapter 9 empirical correlations and analytical modelling have also been developed and presented for the relationship between resistivity, leakage duration and distance/depth. These can be used to generate a resistivity profile for any specific soil type and leachate, in the leak detection test. Further, new equations have been given to predict the velocity of flow of leachate at any point within a soil specimen, if the resistivity is measured at a given time. A numerical model has been designed using SEEP/W for the seepage analysis in leak detection test. The generated velocity data is then used to obtain reistivity profile for the liner base material, to demonstrate the application of the newly developed correlations.

Chapter 10 briefly summarises the research and outlines the general conclusions from the previous chapters. This chapter also highlightes the contributions to knowledge through this research and suggests potential future research paths.

References

ANZS 1768:2007 (2007). Lightning protection. Australia/New Zealand Standards, Sydney, NSW, Australia.

AS 1289.4.4.1 (1997). Methods of testing soils for engineering purposes soil chemical tests - determination of the electrical resistivity of a soil - method for sands and granular materials, Standards Australia, Sydney, NSW, Australia.

ASTM D6431-99 (2010). Standard guide for using the direct current resistivity method for subsurface investigation, ASTM International, West Conshohocken, PA, USA.

ASTM D6747-15 (2015). Standard guide for selection of techniques for electrical leak location of leaks in geomembranes, ASTM International, West Conshohocken, PA, USA.

ASTM D7002-16 (2016). Standard practice for electrical leak location on exposed geomembranes using the water puddle method, ASTM International, West Conshohocken, PA, USA.

ASTM D7240-06 (2011). Standard practice for leak location using geomembranes with an insulating layer in intimate contact with a conductive layer via electrical capacitance technique (conductive geomembrane spark test), ASTM International, West Conshohocken, PA, USA.

ASTM D7703-16 (2016). Standard practice for electrical leak location on exposed geomembranes using the water lance method, ASTM International, West Conshohocken, PA, USA.

ASTM D7953-14 (2014). Standard practice for electrical leak location on exposed geomembranes using the arc testing method, ASTM International, West Conshohocken, PA, USA.

Ben Othmen, A. and Bouassida, M. (2013). Detecting defects in geomembranes of landfill liner systems: durable electrical method. *International Journal of Geotechnical Engineering* 7(2), 130-135, DOI: 10.1179/1938636213Z.00000000013.

Daniel, D.E. (1984). Predicting hydraulic conductivity of clay liners. *Journal of Geotechnical Engineering* 110(2), 285-300, DOI: 10.1061/(ASCE)0733-9410(1984)110:2(285)#sthash.g48WNynP.dpuf.

DEE (Department of the Environment and Energy) (2010). Review of the application of landfill standards. DEE, ACT, Australia. http://www.environment.gov.au/protection/national-waste-policy/publications/review-application-landfill-standards. (Accessed 05 June 2018).

DEE (Department of the Environment and Energy) (2013). National Waste Report. DEE, ACT, Australia. http://www.environment.gov.au/protection/national-waste-policy/national-waste-reports/national-waste-report-2013. (Accessed 09 Nov 2017).

DEWHA (Department of the Environment, Water, Heritage and the Arts) (2010). National Waste Report. DEWHA, ACT, Australia. http://www.environment.gov.au/system/files/resources/af649966-5c11-4993-8390-ab300b081f65/files/national-waste-report-2010.pdf. (Accessed 24 May 2018).

Dixon, A. (2013). A critical review of Australian landfill guidelines. GHD, Sydney, Australia. http://www.wmaa.asn.au/event-documents/2015_cdlf/SpeakerPresentations/Session%20Three.%20Landfill%20Planning%20and%20Developments/anthony_dixon.pdf. (Accessed 10 Nov 2017).

Geoscience Australia (2017). Waste Management Facilities. Geoscience Australia, Australian Government, ACT, Australia. Available via DIALOG. https://data.gov.au/dataset/waste-management-facilities. (Accessed 10 Nov 2017).

Harrop-Williams, K. (1985). Clay liner permeabiliy: evaluation and variation. *Journal of Geotechnical Engineering* 111(10), 1211-1225, DOI:10.1061/(ASCE)0733-410(1985)111:10(1211).

Hix, K. (1998). Leak detection for landfill liners. National Network for Environmental Management Studies Report. National Service Center for Environmental Publications, USA. https://clu-in.org/download/studentpapers/leaklnfl.pdf. (Accessed 15 June 2018).

Kuranchie, F.A., Shukla, S.K., Habibi, D., Zhao, X. and Kazi, M. (2014). Studies on electrical resistivity of Perth sand. *International Journal of Geotechnical Engineering* 8(4), 449–457, DOI: 10.1179/1939787913Y.0000000033.

McCarter, W.J. (1984). The electrical resistivity characteristics of compacted clays. *Geotechnique* 34(2), 263-267, DOI: 10.1680/geot.1984.34.2.263.

Munoz-Castelblanco, J.A., Pereira, J.M., Delage, P. and Cui, Y.J. (2011). The influence of changes in water content on the electrical resistivity of a natural unsaturated loess. *Geotechnical Testing Journal* 35(1), 11-17, DOI: 10.1520/GTJ103587.

Nosko, V. and Touze-Foltz, N. (2000). Geomembrane liner failure: modeling of its influence on contaminant transfer. *Proceedings of 2nd European Geosynthetics Conference*, Bologna, pp. 557-560.

Oh, M., Seo, M. W., Lee, S. and Park, J. (2008). Applicability of grid-net detection system for landfill leachate and diesel fuel release in the subsurface. *Journal of Contaminant Hydrology* 96(1-4), 69-82, DOI: 10.1016/j.jconhyd.2007.10.002.

Pandey, L.M.S. and Shukla, S.K. (2017). Detection of leachate contamination in Perth landfill base soil using electrical resistivity technique. *International Journal of Geotechnical Engineering*, 1-12, DOI: 10.1080/19386362.2017.1339763.

Pandey, L.M.S., Shukla, S.K. and Habibi, D. (2015). Electrical resistivity of sandy soil. *Geotechnique Letters* 5(3), 178-185, DOI: 10.1680/jgele.15.00066.

Rowe, R.K., Quigley, R.M., Brachman, R.W. and Booker, J.R. (2004). Barrier systems for waste disposal facilities (No. Ed. 2), Spon Press, London, UK.

WMAA (Waste Management Association of Australia) (2013). Analysis of Landfill Survey Data, Final Report. Blue Environment Pty Ltd, VIC, Australia. http://www.environment.gov.au/system/files/resources/91763f0e-f453-48d0-b33e-22f905450c99/files/landfill-survey-data.pdf. (Accessed 04 June 2018).

Yan, M., Miao, L. and Cui, Y. (2012). Electrical resistivity features of compacted expansive soils. *Marine Georesources and Geotechnology* 30(2), 167-179, DOI: 10.1080/1064119X.2011.602384.

Yoon, G.L. and Park, J.B. (2001). Sensitivity of leachate and fine contents on electrical resistivity variations of sandy soils. *Journal of Hazardous Materials* 84(2-3), 147-161, DOI: 10.1016/S0304-3894(01)00197-2.

CHAPTER 2

LITERATURE REVIEW

This chapter details the excerpts from relevant literature. Published research works have been collated to reflect the existing and current practices in the relevant research area. Parts of this chapter are based on two papers accepted for presentation and publication in the following conference proceedings: 11th International Conference on Geosynthetics, 16-21 September 2018, Coex, Seoul, Korea, and International Conference, Environmental Geotechnology, Recycled Waste Materials and Sustainable Engineering, 29-31 March 2018, Jalandhar, Punjab, India; as listed in Section 1.6.

2.1 Introduction

Globally a huge amount of waste is generated every year and a major portion of this ends up at landfill sites (Ministry for the Environment, New Zealand, 2001; Productivity Commission, 2006; EC, 2008; Lopes *et al.*, 2012; USEPA, 2012; Department of the Environment and Energy, Australia, 2013; Esteban-Altabella *et al.*, 2017; Geoscience Australia, 2017; Jovanov *et al.*, 2017). As per Hoornweg and Bhada-Tata (2012), 1.3 billion tonnes of municipal solid waste (MSW) are generated per annum. China has the fastest rate of MSW growth, followed by other parts of East Asia, parts of Eastern Europe, and the Middle East. A similar trend for waste generation is observed in Australia, with waste production increasing by 170% in the period of 1996-2015 at a compound growth rate of 7.8% per annum. Additionally, the rate of growth of MSW is greater than the rate of growth of urbanization (DEWHA, 2010).

The major portion of wastes is produced by domestic households (55 to 65%), followed by commercial and institutional locations (35 to 45%). The contribution by industrial sector is comparatively small due to recycling, reuse, or self-disposal practiced by industrial waste landfills (USEPA, 2011).

Figure 2.1 summarises the various MSW disposal techniques practiced globally (Hoornweg and Bhada-Tata, 2012). It can be observed that landfilling is the predominant method of waste disposal.

Waste containment facilities deal with a variety of pollutants. The leachates generated by the decomposition of these wastes are hazardous for the environment (Sharma and Reddy, 2004; Daniel and Koerner, 2007; Aboyeji and Eigbokhan, 2016; Esteban-Altabella *et al.*, 2017). Therefore, the issues of appropriate handling and management of wastes in landfilling facilities become critical. Hence, the regulatory authorities around the world have recommended that the lining systems used in landfilling facilities must be engineered, constructed and frequently monitored, such that the complete isolation of all contaminants from soil and groundwater can be ascertained over their intended design life (Shukla, 2016; Jovanov *et al.*, 2017; Parastar *et al.*, 2017).

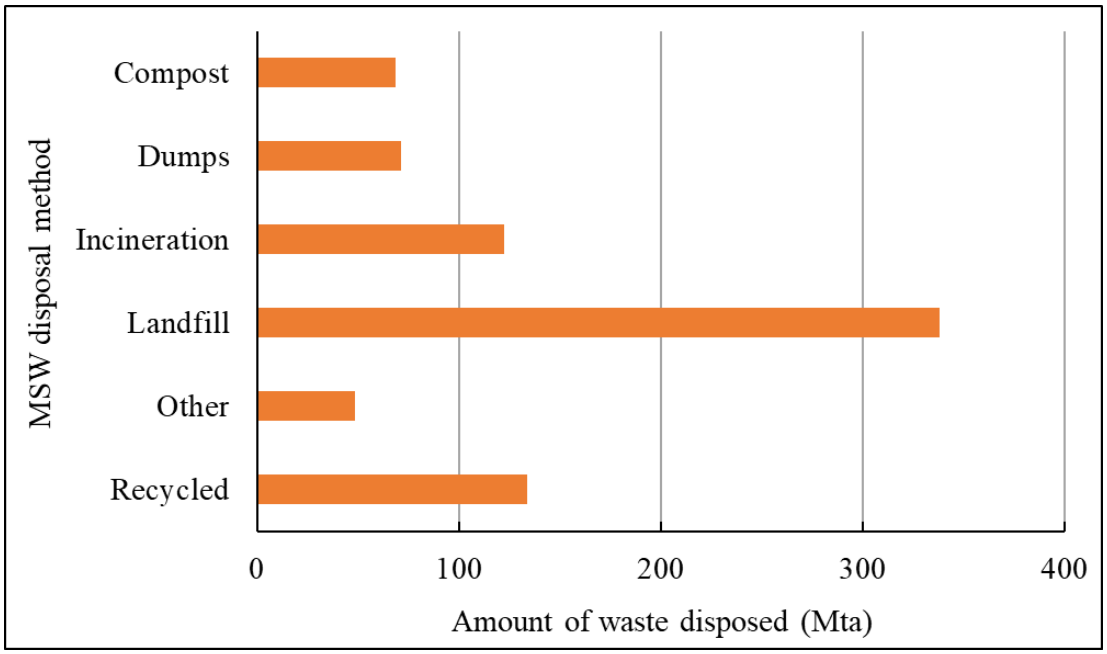

Figure 2.1: Municipal solid waste disposal methods.

Liners are engineered systems with low permeability, designed to control the movement of liquid effluents out of waste containment units. Although the liners are constructed to be intact during their design life, various factors lead to the eventual failure of the lining systems. Their integrity is frequently compromised (Giroud, 1984; Daniel and Koerner, 2007; Shukla, 2016) and the leachates tend to leak, resulting in the contamination of soil and groundwater (Oh *et al.*, 2008; Aboyeji and Eigbokhan, 2016). Subsequently, "all liners leak" (Giroud, 1984).

Figure 2.2 is a photograph of a leachate collection pond lined with geosynthetic clay liner (GCL) in Perth, Western Australia, Australia. It can be noticed that defects have developed in the liner over time. It is imperative to detect the leakage issues as early as possible, to ensure

that suitable remedial measures are taken (Lopes *et al.*, 2012). Consequently, waste impoundment facilities use different leak detection techniques for the management and control of contaminants.

It is also interesting to note that over 85% of Australians live in urban areas and nearly 70% live in the capital cities. Despite having a huge land mass, Australia's habitable land area is only about 10% of the actual land mass, with 90% being deemed uninhabitable. Majority of the population resides in the eight capital cities which have a combined population density of 378 people per km^2. Therefore, most of the waste production is focused in these major urban areas. If the landfills are situated far off from the metropolitan areas, the cost of transportation and disposal becomes extremely high. Hence, although Australia has a huge land mass, the siting, design, operation, and proper maintenance of landfilling facilities is a major concern.

Figure 2.2: Photograph of a leachate collection pond lined with geosynthetic clay liner (GCL).

Table 2.1 lists various leachate barrier systems which are currently being used in Australia (Dixon, 2013). In general, the composite liner system consisting of compacted clay and geomembrane, is used in Australian landfill facilities.

There are various leak detection methods, such as groundwater monitoring wells, lysimeters, diffusion hoses, capacitance sensors, tracers, electro-chemical sensing cables, resistivity cone penetration test (RCPT), ground penetration radar (GPR), time domain reflectometry (TDR), etc. (Oh *et al.*, 2008). Groundwater monitoring wells are the more extensively used leak

detection technique in Australia. The monitoring well system relies on detecting contamination in the groundwater. A major drawback of this method is that by the time the leakage issue is detected, a substantial amount of soil and groundwater is already contaminated (Mohamed *et al.*, 2002).

Table 2.1: The leachate barrier systems used in Australia.

State/Territory	Minimum requirements
New South Wales (NSW)	• 90 cm compacted clay with in-situ permeability less than 10^{-9} m/s • Geomembrane might be used over the compacted clay
Northern Territory (NT)	• Single clay, geomembrane (GMB) or geosynthetic clay liner (GCL) • Composite liner for MSW • Double liners with leak detection for hazardous wastes
Queensland (QLD)	• Liner chosen based on the risk assessment of the site
South Australia (SA)	• Composite liner with geomembrane
Tasmania (TAS)	• Engineered clay liner for MSW landfills • GCL for secure landfills
Victoria (VIC)	• Seepage < 10 L/ha/day for MSW landfill • Seepage < 100 L/ha/day for secure landfill

Furthermore, the field diagnostic techniques which involve on-site sampling and laboratory analysis, generally prove to be time and cost intensive. Hence, the use of the electrical leak detection methods such as water puddle method (ASTM D7002 - 16), conductive geomembrane spark test (ASTM D7240 - 06(2011)), water lance method (ASTM D7703 - 16),

arc testing method (ASTM D7953 - 14), electrode grid method (ASTM D6747 − 15), etc., has become predominant. Electrical methods are easy to install and operate, and have low costs (Oh *et al.*, 2008; Ben Othmen and Bouassida, 2013; Pandey *et al.*, 2015; Pandey and Shukla, 2017). Hence, there is a significant scope for the development of a new diagnostic technique based on the electrical resistivity method, which can investigate subsurface contamination at the onset and therefore, detect leaks across liners. However, the use of this method in field diagnostic techniques is limited by a lack of understanding of the behavior of soils under leak detection tests. Furthermore, the electrical resistivity of a soil shows a close relationship with its geotechnical parameters (Pandey *et al.*, 2015; Pandey and Shukla, 2017). Hence, a comprehensive literature survey has been conducted and presented, to reflect the existing and current practices in the relevant research area.

2.2 Electrical Resistivity for Soil Characterisation

This section summarises eminent research work involving the measurement of the electrical properties of soil and the study of its relationship with the hydraulic and geotechnical properties. Table 2.2 lists the typical resistivity values for sand and sand-clay mixtures, obtained at different water contents (AS/NZS 1768-2007).

Table 2.2: Variations in soil resistivity with water content (AS/NZS 1768-2007 Lightning protection standards)

Gravimetric water content (%)	Typical Resistivity (Ohm-m)	
	Clay mixed with sand	Silica based sand
0	10,000,000	-
2.5	1,500	3,000,000
5	430	50,000
10	185	2,100
15	105	630
20	63	290
30	42	-

2.2.1 Sands

Archie (1942) evaluated the electrical resistivity of multiple soil specimens obtained from various sand formations. The porosity of these specimens was found to range from 10 to 40%. The samples were prepared by mixing soil specimens with a brine solution of salinity 20,000 to 100,000 mg/l. Resistivity values of the specimens were determined at different degree of saturation (S_r). Based on the obtained results the following empirical equations were suggested:

$$\frac{\rho_0}{\rho_w} = (n)^{-c} \tag{2.1}$$

for saturated soils and

$$\frac{\rho'}{\rho_0} = (S_r)^{-d} \tag{2.2}$$

for unsaturated soils, where,

S_r = degree of saturation

ρ' = electrical resistivity of unsaturated soil

ρ_0 = soil resistivity

ρ_w = resistivity of free water

n = soil porosity

c and d = soil parameters.

Gupta and Hanks (1972) proposed a method for rapid soil salinity determination. The changes in the electrical conductivity of soil produced by varying its water content were scrutinised. Two soil samples were used for the study. Soil samples were prepared with different water and salt (potassium chloride, KCl) content and their bulk densities were measured. The relationship between the conductivity and salinity of these soil specimens was investigated. Eight replicate readings were taken for each sample. The cell constant K_c was determined using a solution of known electrical conductivity. Four probe conductivity ($K4P$),

electrical conductivity of saturation ($K(SE)$) and electrical conductivity for 1:5 ($K(1:5)$) extracts was noted. Based on the results, the following relation was proposed:

$$\frac{K4P}{Kx} = eW + f \tag{2.3}$$

Here Kx is $K(SE)$ or $K(1:5)$ and e, f are constants from regression analysis. A limitation of this method is that the water content must be established independently.

Kalinski and Kelly (1993) assessed the relationship between soil electrical resistivity and its hydraulic parameters. Circular four probe resistivity cells were used to measure the resistivity of soil specimen. Specimens were prepared by soaking the fine-grained soil in water and adjusting with sodium chloride (NaCl) or potassium chloride (KCl). Pressure membrane apparatus was used to adjust the volumetric water content (θ). θ was varied and specimen resistance and weight were noted. Gravimetric water content (W) and dry density was calculated. Based on the obtained results, the following equation for the bulk soil electrical conductivity EC_o was proposed:

$$EC_o = EC_s + EC_w\theta(1.04\theta - 0.09) \tag{2.4}$$

where, EC_w is the pore water electrical conductivity and EC_s is the apparent soil-particle-surface electrical conductivity. This research work concludes that provided the pore-water conductivity of a soil is known, its in-situ volumetric water content can be estimated using the relationship between the electrical resistivity and θ.

Kuranchie *et al.* (2014) studied the electrical resistivity (ρ) changes of dry Perth sand by varying its relative density. The effect of the electrode depth and the electrode spacing was also examined. The Wenner array experimental set up was used to measure the resistivity. Relative density was varied from 0 to 100%. The electrode depth was varied from 100 to 300 mm and the electrode spacing was varied from 100 to 180 mm. The simulation software COMSOL was used. The resistivity values were found to range from 60,606 for very dense condition to 142,857 Ωm for very loose condition. The resistivity was found to be inversely proportionalto electrode depth and relative density. However, electrode spacing was found to be directly proportional to resistivity. The following equation was developed for resistivity ρ:

$$\rho = 2\pi z\lambda(\frac{\Delta V}{I}) \tag{2.5}$$

where, ΔV = electrical potential difference in volts (V) between the two inner electrodes, $_I$ = induced electric current in amperes (A) in the medium between outer electrodes, and λ = resistivity correction factor.

For this particular set up, λ of 0.46 was obtained. This study concluded that the resistivity correction factor is independent of soil type.

Pandey *et al.* (2015) evaluated the effect of various geotechnical parameters (water content and relative density of the soil, and the type of water used in the experimentation) and electrical factors (AC input voltage and frequency) on the electrical resistivity of Perth sandy soil. Specimens were prepared by mixing the sand sample with various amounts of the two types of water as permeating fluids (namely distilled water and tap water). Electrical resistivity tests were conducted using resistivity boxes (fabricated as per AS 1289.4.4.1-1997) and an AEMC 6471 ground resistance tester). Two types of boxes were used for the tests. One was fitted with brass electrodes and the other with stainless steel electrodes to determine the effect of electrode material. The water content ($_w$) was varied from 4 to 20% (at an increment of 4%). Relative density (D_r) of soil specimen was varied from 0 to 100% (at an increment of 25%). Resistivity readings were taken at different AC input voltages (16 and 32 V) and AC input frequencies (55, 92, 110, 119, 128 and 513 Hz) for representative combinations of $_w$ and D_r pertaining to both types of water. Based on these results, an AC input of 16 V and 128 Hz was selected for further experimentation. Keeping $_w$ constant and varying D_r, readings were obtained for resistivity. The same tests were conducted for distilled water and tap water. Similar tests were done for both resistivity boxes. The study found that Perth sandy soil was independent of the AC input voltage and frequency for the tested range. Resistivity was observed to be inversely proportional to relative density and water content. However, the effect of water content was more significant. The effect of electrode was insignificant while the permeating fluid had a considerable effect. The study also proposed correlations for the electrical resistivity (ρ) of Perth sandy soil based on obtained results as given below:

$$\rho = 527\left(4.9 - \frac{D_r}{100}\right)(w)^{-0.832} \tag{2.6}$$

for the distilled water, and

$$\rho = 732\left(4.6 - \frac{D_r}{100}\right)(w)^{-1.258} \tag{2.7}$$

for the tap water, where,

ρ = resistivity of the sandy soil (Ωm)

D_r = relative density (%)

w = water content (%)

Pandey and Shukla (2017) investigated the effects of water and/or leachate content of soil, and composition of leachate on the electrical resistivity of Perth landfill base soil. The experimental setup given by Pandey *et al.* (2015) was used for resistivity measurements. Three leachates were used for the test. A mixture of water and leachates in varying concentration was used as the contaminating fluid. The changes to the resistivity arising from changes to the fluid content were observed to be more significant than the effect of varying the leachate content or type within any specific mixture of water and leachate. Newly developed correlations between the resistivity and the geotechnical properties of the soil infiltrated with leachates, have also been proposed. The correlation is as follows:

$$\rho = c_1 C_o\left(c_2 - \frac{D_r}{100}\right)\left[(w)^{-\left(\frac{100c_3C_o}{p_l}\right)}\right] \tag{2.8}$$

where, ρ = resistivity (Ωm), D_r = relative density (%), p_l = leachate content (%), and w = fluid content (%) for the sandy soil. Here c_1 (Ωm), c_2 (dimensionless), and c_3 (dimensionless) are specific constants corresponding to a particular soil type and pore fluid, and C_0 (dimensionless) is a variable dependent on the composition of the pore fluid.

2.2.2 Clays

McCarter (1984) investigated the relationship of electrical resistivity of two types of clay with degree of saturation using two-electrode method, keeping their water content constant. It was noted that decreasing the degree of saturation resulted in an increase in electrical resistivity of the clay samples. The gradient of resistivity versus degree of saturation curve reduces with a rise in the water content. Change in resistivity with increase in the degree of saturation becomes negligible at water content around plastic limit.

McCarter and Desmazes (1997) used soil electrical properties for the demarcation of soils. A modified consolidation cell of 66 mm internal diameter and 65 mm height was fitted with top and bottom plates along with six circumferential electrodes. Conductivity measurements were taken for diagonally opposite pairs as well as for vertical plate electrodes. The sample with 71% initial water content was subjected to standard incremental load odometer testing with 48 hours for each load increment. The void ratio and the conductivity were found to decrease with increase in effective stress. The sample was found to be of anisotropic nature. The study proposed the following relationship for porous systems:

$$k^* = \frac{\beta d^{*2}}{FF} \tag{2.9}$$

Here, k^* = permeability, FF = formation factor, d^* = critical pore diameter, and β = constant for a particular type of clay.

Fukue *et al.* (1999) studied the electrical resistivity of three clay specimens (two commercial and one natural). A model was developed to understand the soil structure, taking to account the solid, liquid and gaseous phase. The device to measure the resistivity was developed from a conventional consolidation apparatus. Based on the electrical resistivity test results, the following equations were proposed to calculate the electrical resistivity of a cylindrical sample of soil with electrical resistivity (ρ_0) and radius (r'):

$$\rho\left(\frac{\rho_0}{\rho_w}\right) = \frac{\pi r'}{n(1-F_{sat})} \tag{2.10}$$

where F_{sat} is the structural coefficient at saturated condition.

Giao *et al.* (2003) compared the electrical resistivity measured in field and obtained in the

laboratory. Four sited were chosen for the study. 2D electric imaging was carried out to map the clay deposits. RES2DINV software was used for data analysis. 50 cylindrical shaped samples (75 mm diameter and 110 mm length) were prepared. Resistivity was recorded using the four-electrode method. Additionally, the resistivity values for 20 other natural clay samples collected worldwide were obtained and compared. The layers below the depth of 27 m could not be mapped by the electrical imaging. The study found that the resistivity values of the clay specimen measured in field and in laboratory are comparable. The resistivities were found to vary from 1 to 12 Ωm. It was concluded that if the maximum dipole spacing is kept three times the depth of the clay bed, the electrical resistivity parameter could be effective for mapping clay deposits. It was also deduced that improved ground strength would lead to higher electrical resistivity. One limitation of the study is that it does not establish a correlation between electrical resistivity and geotechnical parameters. For the laboratory tests, the depth of electrode penetration and the specimen geometry had insignificant effect on the resistivity.

Sreedeep *et al.* (2004) measured the resistivity (ρ) of clayey soil using a resistivity probe and a resistivity box. Specimens for the box were prepared by mixing oven-dried soil with KCl and NaCl solutions to make different water contents. Samples were kept in airtight containers for 24hrs and compacted to achieve different dry density values. After each resistivity test with box, the probe was inserted to take another reading. Based on the results the following correlation was proposed.

$$\rho = 150 \times e^{\left(\frac{-(S_r - 20)}{25}\right)} \tag{2.11}$$

where S_r is the degree of saturation of the soil specimen.

Kibria and Hossain (2012) assessed the relationship of soil electrical resistivity with its water content, unit weight, degree of saturation, specific surface area (SSA), pore space and ion composition. Six highly plastic clay (CH) specimens were used in the study. The structure, pore distribution and composition of clay samples were determined using high energy X-ray fluorescence tests and scanning electron microscopy (SEM). Electrical resistivity measurements were made using Super Sting IP resistivity equipment. Resistivity was found to be inversely proportional to water content. However, its effect was found to decrease at water contents above 40%. Unit weight and resistivity were found to be inversely proportional for water content less than 30%. Electrical resistivity of soil was observed to be less sensitive to

unit weight compared to the water content. Increase in degree of saturation resulted in decreased resistivity. Increase in resistivity was observed with increase in SSA and percentage of Calcium at water contents below 30%. At low water contents the electrical resistivity of soil showed an increase and then a decrease with increase in pore space.

Gingine *et al.* (2016) investigated the changes in electrical resistivity of a clay sample compacted with different void ratios and molding water content. Wenner four-pin method was used on Kaolin clay specimen. The effect of the structural changes in the clay, produced due to compaction, on its electrical resistivity have been discussed.

Naghibi *et al.* (2016) measured the electrical resistivity of clays undergoing consolidation. A modified odometer cell was used to measure the resistivity of the test specimen. The results were used to develop general calibration equations.

2.2.3 Sand-clay mixtures

Kibria and Hossain (2014) investigated the changes in the electrical resistivity of sand-bentonite mixes produced by varying the bentonite content. Ten soil samples were prepared by mixing different amounts of sodium and calcium bentonite with sand. Dry unit weight and water content were varied from 11.8 to 14.9 kN/m^3 and 10 to 40%, respectively. Corresponding resistivity was recorded. Tests were done for particle-size distribution, Atterberg limits, specific gravity and cation exchange capacity (CEC) along with scanning electron microscopy (SEM) and energy dispersive spectroscopy (EDS). Decrease in bentonite content resulted in a linear increase in index properties. Considerable decrease in resistivity was observed at high mineral contents. The results indicated that bentonite type and content have significant impact on the soil resistivity. The effect of mineral content, CEC and plasticity indices on resistivity is not very significant at higher degree of saturation.

2.2.4 Compacted clay liners (CCL) and geosynthetic clay liners (GCL)

Abu-Hassanein *et al.* (1996) investigated the relationship of resistivity with compaction conditions, index properties and hydraulic conductivity. It was found that the resistivity decreased with increase in compactive effort. The resistivity was found to decrease rapidly with increase in molding water content, dry of optimum water content. Wet of optimum, the molding-water content had insignificant effect. At optimum water content, resistivity is inversely proportional to temperature, index properties, percentage fines and clay content. However, the study failed to develop correlation between hydraulic conductivity and electrical resistance. There is a scope for further research of the effect of anisotropy, electrical anomalies,

composition and liner boundaries.

2.3 Hydraulic Conductivity Studies for Soil

The presence of interstitial fluids is a major contributing factor for the flow of electricity in geomaterials. Hence, the hydraulic conductivity studies for soils have been reviewed which are relevant to the soil parameters being investigated in this research.

Chapuis (1990) investigated the permeability of 45 sand-bentonite mixtures used as landfill lining material. The hydraulic conductivity (k) did not exhibit a correlation to porosity, bentonite content or total fines content individually. However, k was found to possess a correlation to the efficient porosity (n^*).

Kenney *et al.* (1992) scrutinized the hydraulic conductivity changes of bentonite-sand mixtures due to content, compaction water content and system chemistry. The hydraulic conductivity was found to be inversely proportional to bentonite-sand ratio (B/S).

Van Ree *et al.* (1992) calculated the permeability values for natural clay and sand-bentonite liners. The study identifies the optimum for sand-bentonite liners as 10% bentonite. Original water content and cell type had insignificant effect while the degree of saturation had significant effect on permeability. The study suggested that permeability tests be carried out at complete saturation and without disturbing the sample for optimum results.

Mollins *et al.* (1996) developed a design model based on the clay void ratio, the sand porosity and tortuosity to estimate the hydraulic conductivity of a sand-bentonite mixture. For a uniform mixture, low bentonite content resulted in higher hydraulic conductivity than estimated. The study deduces that for a bentonite with known properties, the hydraulic conductivity of a sand-bentonite mixture can be predicted from the bentonite content, sand porosity and tortuosity and the vertical effect stress.

Alston *et al.* (1997) assessed various sand-bentonite mixtures to test their suitability as lining material. Based on results the 75:25 (sand to silt aggregate ratio) with 5.5% bentonite was chosen for liner construction.

Stewart *et al.* (1999) gave a model to predict the swelling and hydraulic conductivity (k) of bentonite-sand mixtures using water and salt solutions. The k exhibited a direct relationship with bentonite content and bentonite void ratio. Initial water content affected the volumetric shrinkage significantly while the bentonite content had a less significant effect.

Kodikara and Rahman (2001) scrutinized the use of optimum water content (OMC) to specify the field water content for compacted clay liner (CCL) systems. Dry unit weight was

calculated using the equation;

$$\gamma_{wet} = (1+w)\gamma_{dry} \tag{2.12}$$

Curves were plotted for wet unit weight (γ_{wet}), dry unit weight (γ_{dry}) and saturated hydraulic conductivity (k_{sat}) against water content (W). Additionally, water content at minimum hydraulic conductivity (w_k) was plotted against optimum water content (w_{opt}) and water content at maximum wet unit weight, to obtain the linear regression for each. The study puts forth that the minimum hydraulic conductivity shows a better correlation than OMC.

Frempong and Yanful (2005) evaluated the suitability of two soils for their use as landfill liner materials. Two soil samples from Ghana were used for the study while leachate was obtained from a landfill site in Ontario. Fixed- wall permeameter method was used. The acidity of both soils was found to decrease after permeation with alkaline leachate. The organic content and CEC increased while the glycol retention values decreased. Both soil samples proved to be suitable for use as lining material.

2.4 Studies to Determine Optimum Sand-Clay Ratios

The following Table 2.3 depicts the different bentonite-sand ratios used by various researchers in their published work. It has been developed from the literature discussed in the previous sections 2.2.3 and 2.3. The studies pertaining to sodium bentonite have been listed.

Table 2.3: Various bentonite-sand ratios.

Journal article	Bentonite-sand ratios used for experimentation (%)
Alston *et al.* (1997)	0, 5, 5.5, 6
Chapuis (1990)	0, 2, 2.5, 3, 4, 4.7, 5, 5.8, 6, 6.4, 7, 7.5, 8, 10, 20, 25, 33.3
Iizuka *et al.* (2003)	0, 1, 3.1, 5.3, 11.1, 17.7
Kenney *et al.* (1992)	0, 4, 8, 12, 16, 20, 24, 28, 32
Kibria and Hossain (2014)	20, 40, 60, 80, 100
Mollins *et al.* (1996)	5, 10, 20
Stewart *et al.* (1999)	10, 20
Van Ree *et al.* (1992)	5, 6, 8

The ratio of bentonite addition (α) is given as:

$$\alpha = \frac{m_b}{m_s} \times 100 \tag{2.13}$$

where m_b is the mass of dry bentonite and m_s is the mass of dry sand.

2.5 Detection of Leakage

In this section, the literature pertaining to leakage detection in lining systems has been reviewed.

2.5.1 Conventional methods of leak detection

Table 2.4 gives the various conventional methods used for leak detection. These methods are mostly redundant due to their low accuracy, limited applicability, post-contamination detection and high remediation costs.

Giroud *et al.* (1989) evaluated the rate of leakage through a composite liner constituted of a geomembrane and a layer of low-permeability soil. They proposed the following equations based on their study:

$$Q = 0.21 h_w^{0.9} a_o^{0.1} k_s^{0.74} \tag{2.14}$$

for the case of good contact, and,

$$Q = 1.15 h_w^{0.9} a_o^{0.1} k_s^{0.74} \tag{2.15}$$

for the case of poor contact, where Q is the rate of leakage, h_w is the depth of water on top of the geomembrane, a_o is the geomembrane hole area and k_s is the soil hydraulic conductivity.

2.5.2 Electrical resistivity methods for leak detection

Oh *et al.* (2008) evaluated the applicability of grid-net system for contamination detection in landfill subbase layer. The schematic diagram of the experimental setup used in laboratory

testing is as shown by Figure 2.1. The detection is based upon the variation of electrical conductivity of soil due to leachate contamination.

Table 2.4: Conventional leak detection methods (National Network for Environmental Management Studies (NNEMS) Report, 1998).

Leak detection method	Advantage	Disadvantage
Groundwater monitoring wells	detects contaminant plumes	doesn't prevent groundwater contamination, expensive, can only detect plumes that pass by the line of wells
Lysimeter	detects contamination	requires laboratory testing, high operating cost, cannot pinpoint the location of the leak
Diffusion hoses	widely available components, automatic, low operational cost	ineffective if leachate does not produce vapor
Capacitance sensors	readily available, automatic	measures all moisture, not specifically leachates
Tracers	can be used at any stage of landfilling, leachate composition not required	operational cost high due to manual collection and testing, does not locate exact leak point
Electro-chemical sensing cables	widely available	detects very narrow range of contaminants, site specific, must be installed during construction phase

Laboratory measurements indicated that the grid-net system could identify the release of landfill leachates with accuracy. One limitation of the method is that it cannot be used for existing landfills. Also, the species and quantity of the contaminant cannot be identified by this method.

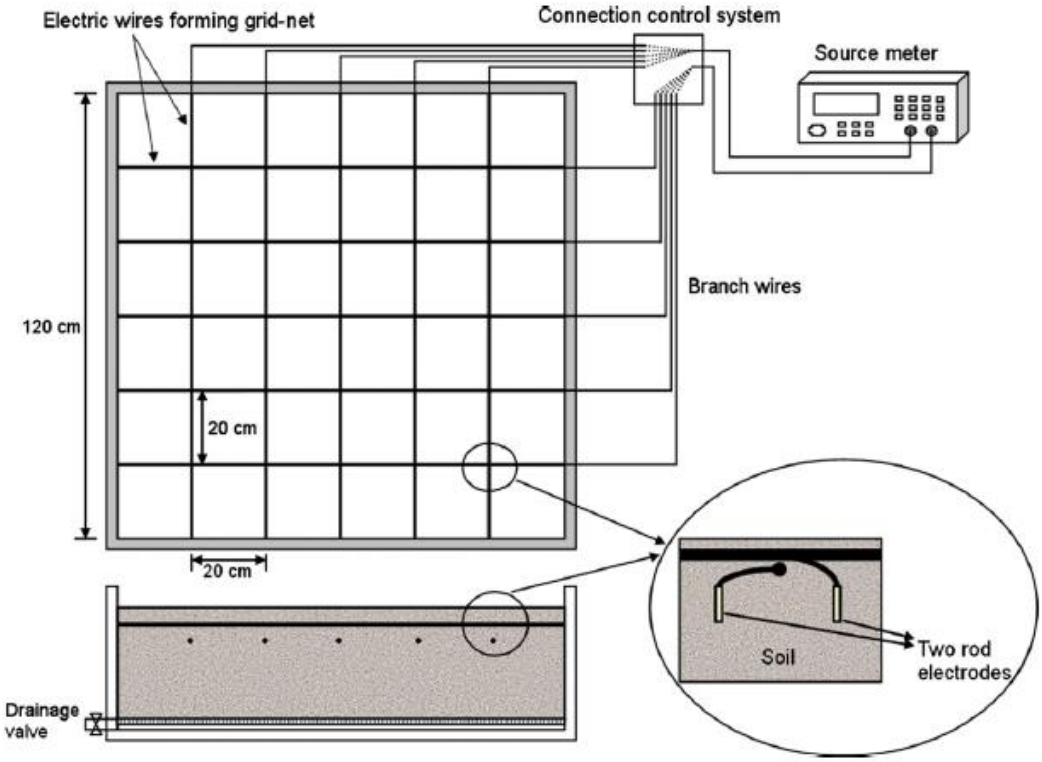

Figure 2.3: Schematic diagram of grid-net electrical conductivity measurement system (Oh *et al.*, 2008).

Ben Othmen and Bouassida (2013) developed a new electrical method for defect detection in landfill liners. This study proposed the electrical circuits method (ECM) to detect leakages in geomembranes (GMB). This method involved the placement of large parallel electrical circuits below the geomembrane at landfill facilities. This method was found to be very cost effective for GMB liner defect location. However, the system fails to predict the number and size of defects.

Panthulu *et al.* (2001) delineated potential seepage paths in earth dams using electrical resistivity and self-potential (SP) methods. Boreholes were made on predetermined profile lines along two saddle-dams and filled with water 5-6 hours before measuring SP data. Reading were taken 2-3 times for SP of each profile using two non-polarizing electrodes. Electrical profiling (EP) was done for multi electrode spacing using Schlumberger array method. It was found that weathering occurred for upto 6-m depth, while the deeper strata showed less weathering.

Sirieix *et al.* (2013) detected defects in geosynthetic clay liner (GCL) by using DC electrical methods. An experimental site of 1.5-m depth and 12×11 m^2 surface area was prepared. The lining system was constructed using 1-m thick clay layer, 6-mm thick GCL, 300-mm thick

artificial gravel layer and 150-mm thick top soil layer, from bottom to top. Defects were engineered in the GCL. Humidity and temperature were monitored at the depth of 0.7 m below the GCL. Weather was also monitored near the test site. Electrical resistivity tomography (ERT) surveys was conducted using two arrays (dipole-dipole and Wenner - Schlumberger). Compared to Wenner – Schlumberger array, dipole-dipole array was more effective. The GCL resistivity was found to drop ten times after 21 months due to chemical damage and ageing of liner.

2.6 Conclusions

Based on the literature review, the following research gaps have been identified, which require further investigation:

- Characterisation of liner subbase soil using electrical resistivity method.
- Absence of specific correlations for different geotechnical parameters of soil with electrical resistivity of clay and sand-clay mixtures.
- Study of variation of soil resistivity with changing sand-clay ratios.
- Effect of type and quantity of leachate on the electrical resistivity of liner subbase material.
- Determination of effective methods of contamination detection and leakage location for pre-existing landfill sites and other contaminant containment systems.
- Scope of innovative methods for the early detection of contaminant release in liner subbase.
- Development of new leakage detection systems for liners installed at pollutant containment facilities.
- Effect of liner leak size, number and type on the electrical resistivity of liner subbase material.
- Changes in the electrical resistivity of subbase material with time.
- Method to predict the number and size of leaks in liners.

References

Aboyeji, O.S. and Eigbokhan, S.F. (2016). Evaluations of groundwater contamination by leachates around Olusosun open dumpsite in Lagos metropolis, southwest Nigeria. *Journal of Environmental Management* 183(1), 333-341, DOI: 10.1016/j.jenvman.2016.09.002.

Abu-Hassanein, Z.S., Benson, C.H. and Blotz, L.R. (1996). Electrical resistivity of compacted clays. *Journal of Geotechnical Engineering* 122(5), 397-406, DOI: 10.1061/(ASCE)0733-9410(1996)122:5(397).

Alston, C., Daniel, D.E. and Devroy, D.J. (1997). Design and construction of sand-bentonite liner for effluent treatment lagoon, Marathon, Ontario. *Canadian Geotechnical Journal* 34(6), 841-852.

Archie, G.E. (1942). The electrical resistivity log as an aid in determining some reservoir characteristics. *Society of Petroleum Engineers* 146(1), 54–61, DOI: 10.2118/942054-G.

ASTM D6747-15 (2015). Standard guide for selection of techniques for electrical leak location of leaks in geomembranes. ASTM International, West Conshohocken, PA, USA.

ASTM D7002-16 (2016). Standard practice for electrical leak location on exposed geomembranes using the water puddle method. ASTM International, West Conshohocken, PA, USA.

ASTM D7240-06 (2011). Standard practice for leak location using geomembranes with an insulating layer in intimate contact with a conductive layer via electrical capacitance technique (conductive geomembrane spark test), ASTM International, West Conshohocken, PA, USA.

ASTM D7703-16 (2016). Standard practice for electrical leak location on exposed geomembranes using the water lance method, ASTM International, West Conshohocken, PA, USA.

ASTM D7953-14 (2014). Standard practice for electrical leak location on exposed geomembranes using the arc testing method, ASTM International, West Conshohocken, PA, USA.

Australia/New Zealand Standards (2007). AS/NZS 1768:2007: Lightning protection. Sydney, NSW: AS/NZS.

Ben Othmen, A. and Bouassida, M. (2013). Detecting defects in geomembranes of landfill liner systems: durable electrical method. *International Journal of Geotechnical Engineering* 7(2), 130-135, DOI: 10.1179/1938636213Z.00000000013.

Chapuis, R. P. (1990). Sand-bentonite liners: predicting permeability from laboratory tests. *Canadian Geotechnical Journal* 27(1), 47-57.

Daniel, D. and Koerner, R. (2007). Waste containment facilities: Guidance for construction quality assurance and construction quality control of liner and cover systems. American Society of Civil Engineers, USA.

DEE (Department of the Environment and Energy) (2013). National Waste Report. DEE, ACT, Australia. http://www.environment.gov.au/protection/national-waste-policy/national-waste-reports/national-waste-report-2013. (Accessed 09 Nov 2017).

DEWHA (Department of the Environment, Water, Heritage and the Arts) (2010). National Waste Report. DEWHA, ACT, Australia. http://www.environment.gov.au/system/files/resources/af649966-5c11-4993-8390-ab300b081f65/files/national-waste-report-2010.pdf. (Accessed 24 May 2018).

Dixon, A. (2013). A critical review of Australian landfill guidelines. GHD, Sydney, Australia. Available via DIALOG. http://www.wmaa.asn.au/event-documents/2015_cdlf/SpeakerPresentations/Session%20Three.%20Landfill%20Planning%20and%20Developments/anthony_dixon.pdf. (Accessed 10 Nov 2017).

EC (European Commission) (2008). Official Journal of the European Union. Waste Framework Directive. http://ec.europa.eu/environment/waste/framework/. (Accessed 22 April 2018).

Esteban-Altabella, J., Colomer-Mendoza, F.J. and Gallardo-Izquierdo, A. (2017). Simulation of the behavior of a refuse landfill on a laboratory scale. *Journal of Environmental Management* 204(1), 144-151, DOI: 10.1016/j.jenvman.2017.08.045.

Esteban-Altabella, J., Colomer-Mendoza, F.J. and Gallardo-Izquierdo, A. (2017). Simulation of the behavior of a refuse landfill on a laboratory scale. *Journal of Environmental Management* 204(1), 144-151, DOI: 10.1016/j.jenvman.2017.08.045.

Frempong, E.M. and Yanful, E.K. (2005). Geoenvironmental assessment of two tropical clayey soils for use as engineered liner materials. *Proceedings of the Geo-Frontiers Congress 2005*, GSP 142, ASCE, 1-10.

Fukue, M., Minato, T., Horibe, H. and Taya, N. (1999). The micro-structures of clay given by resistivity measurements. *Engineering Geology* 54(1-2), 43-53, DOI: 10.1016/S0013-7952(99)00060-5.

Geoscience Australia (2017). Waste Management Facilities. Geoscience Australia, Australian Government, ACT, Australia. Available via DIALOG. https://data.gov.au/dataset/waste-management-facilities. (Accessed 10 Nov 2017).

Giao, P.H., Chung, S.G., Kim, D.Y. and Tanaka, H. (2003). Electric imaging and laboratory resistivity testing for geotechnical investigation of Pusan clay deposits. *Journal of Applied Geophysics* 52(4), 157-175, DOI: 10.1016/S0926-9851(03)00002-8.

Gingine, V., Dias, A.S. and Cardoso, R. (2016). Compaction control of clayey soils using electrical resistivity charts. *Procedia Engineering* 143(2016), 803-810, DOI: 10.1016/j.proeng.2016.06.130.

Giroud, J.P. (1984). Impermeability: The myth and a rational approach. *Proceedings of the International Conference on Geomembranes*, Vol. 1, p. 157-162.

Giroud, J.P., Khatami, A. and Badu-Tweneboah, K. (1989). Evaluation of the rate of leakage through composite liners. *Geotextiles and Geomembranes* 8(4), 337-340, DOI: https://doi.org/10.1016/0266-1144(89)90016-2.

Gupta, S.C. and Hanks, R.J. (1972). Influence of water content on electrical conductivity of the soil. *Soil Science Society of America* 36(6), 855–857, DOI: 10.2136/sssaj1972.03615995003600060011x.

Hix, K. (1998). Leak detection for landfill liners. National Network for Environmental Management Studies Report. National Service Center for Environmental Publications, USA. https://clu-in.org/download/studentpapers/leaklnfl.pdf. (Accessed 15 June 2018).

Hoornweg, D. and Bhada-Tata, P. (2012). What a Waste (1st Ed.). World Bank. Washington D.C., USA.

Iizuka, M., Imaizumi, S., Toryuu, A. and Doi, Y. (2003). Critical ratio of bentonite addition into sandy soil to make a impermeable compacted soil liner. *Proceedings of Sardinia*.

Jovanov, D., Vujić, B. and Vujić, G. (2017). Optimization of the monitoring of landfill gas and leachate in closed methanogenic landfills. *Journal of Environmental Management* 216(0), 32-40, DOI: 10.1016/j.jenvman.2017.08.039.

Jovanov, D., Vujić, B. and Vujić, G. (2017). Optimization of the monitoring of landfill gas and leachate in closed methanogenic landfills. *Journal of Environmental Management* 216(0), 32-40, DOI: 10.1016/j.jenvman.2017.08.039.

Kalinski, R. and Kelly, W. (1993). Estimating water content of soils from electrical resistivity. *Geotechnical Testing Journal* 16(3), 323-32, DOI: 10.1520/GTJ10053J.

Kenney, T.C., Van Veen, W.A., Swallow, M.A. and Sungaila, M.A. (1992). Hydraulic conductivity of compacted bentonite-sand mixtures. *Canadian Geotechnical Journal* 29(3), 364-374, DOI: 10.1139/t92-042.

Kibria, G. and Hossain, M.S. (2012). Investigation of geotechnical parameters affecting electrical resistivity of compacted clays. *Journal of Geotechnical and Geoenvironmental Engineering* 138(12), 1520-1529, DOI: 10.1061/(ASCE)GT.1943-5606.0000722.

Kibria, G. and Hossain, M.S. (2014). Effects of bentonite content on electrical resistivity of soils. *Proceedings of the Geo-Congress 2014: Geo-characterization and Modeling for Sustainability*, p. 2404-2413, DOI: 10.1061/9780784413272.233.

Kodikara, J.K. and Rahman, F. (2001). Moisture content and hydraulic conductivity relations for compacted clay liners. *Australian Journal of Civil Engineering* 43(2001), 13-18.

Kuranchie, F.A., Shukla, S.K., Habibi, D., Zhao, X. and Kazi, M. (2014). Studies on electrical resistivity of Perth sand. *International Journal of Geotechnical Engineering* 8(4), 449–457, DOI: 10.1179/1939787913Y.0000000033.

Lopes, D.D., Silva, S.M., Fernandes, F., Teixeira, R.S., Celligoi, A. and Dall'Antônia, L.H. (2012). Geophysical technique and groundwater monitoring to detect leachate contamination in the surrounding area of a landfill–Londrina (PR–Brazil). *Journal of Environmental Management* 113(0), 481-487, DOI: 10.1016/j.jenvman.2012.05.028.

McCarter, W.J. and Desmazes, P. (1997). Soil characterization using electrical measurements. *Géotechnique* 47(1), 179–183.

Ministry of Environment (2001). A guide for the management of closing and closed landfills in New Zealand, ISBN 0-478-24021-X.

Mohamed, A.M.O., Said, R.A., and Al-Shawawreh, N.K. (2002). Development of a methodology for evaluating subsurface concentrations of pollutants using electrical polarization technique. *Geotechnical Testing Journal* 25(2), 157–167, DOI: 10.1520/GTJ11359J.

Mollins, L.H., Stewart, D. I. and Cousens, T.W. (1996). Predicting the properties of bentonite-sand mixtures. *Clay Minerals* 31(2), 243-252.

Naghibi, M., Abuel-Naga, H. and Orense, R. (2016). Modified odometer cell to measure electrical resistivity of clays undergoing consolidation process. *Journal of Testing and Evaluation* 45(4), 1261-1269, DOI: 10.1520/JTE20160002.

Oh, M., Seo, M. W., Lee, S. and Park, J. (2008). Applicability of grid-net detection system for landfill leachate and diesel fuel release in the subsurface. *Journal of Contaminant Hydrology* 96(1-4), 69-82, DOI: 10.1016/j.jconhyd.2007.10.002.

Pandey, L.M.S. and Shukla, S.K. (2017). Detection of leachate contamination in Perth landfill base soil using electrical resistivity technique. *International Journal of Geotechnical Engineering*, 1-12, DOI: 10.1080/19386362.2017.1339763.

Pandey, L.M.S., Shukla, S.K. and Habibi, D. (2015). Electrical resistivity of sandy soil. *Geotechnique Letters* 5(3), 178-185, DOI: 10.1680/jgele.15.00066.

Panthulu, T.V., Krishnaiah, C. and Shirke, J.M. (2001). Detection of seepage paths in earth dams using self-potential and electrical resistivity methods. *Engineering Geology* 59(3-4), 281-295, DOI: 10.1016/S0013-7952(00)00082-X.

Parastar, F., Hejazi, S. M., Sheikhzadeh, M. and Alirezazadeh, A. (2017). A parametric study on hydraulic conductivity and self-healing properties of geotextile clay liners used in landfills. *Journal of Environmental Management* 202(1), 29-37, DOI: 10.1016/j.jenvman.2017.07.013.

Productivity Commission (2006). Waste Management-Productivity Commission Inquiry Report. Commonwealth of Australia, Canberra. https://www.pc.gov.au/__data/assets/pdf_file/0014/21614/waste.pdf. (Accessed 23 May 2018).

Sharma, H.D. and Reddy, K.R. (2004). Geoenvironmental engineering: site remediation, waste containment, and emerging waste management technologies. John Wiley & Sons, Inc.

Shukla, S.K. (2016). An Introduction to Geosynthetic Engineering, CRC Press, Taylor & Francis Group, Florida, USA.

Sirieix, C., Genelle, F., Barral, C., Touze-Foltz, N., Riss, J. and Bégassat, B., (2016). Characterizing the ageing of a geosynthetic clay liner through electrical resistivity. *Canadian Geotechnical Journal* 53(3), 423-430, DOI: 10.1139/cgj-2015-0111.

Sreedeep, S., Reshma, A.C. and Singh, D.N. (2004). Measuring soil electrical resistivity using a resistivity box and a resistivity probe. *Geotechnical Testing Journal* 27(4), 411–415.

Stewart, D.I., Cousens, T.W., Studds, P.G. and Tay, Y.Y. (1999). Design parameters for bentonite-enhanced sand as a landfill liner. *Proceeding of the Institution of Civil Engineers-Geotechnical Engineering 1999*, 137(4), 189 –195.

USEPA (United States Environmental Protection Agency) (2011). Exposure Factors Handbook 2011 Edition (Final Report). Washington, DC. https://cfpub.epa.gov/ncea/risk/recordisplay.cfm?deid=236252. (Accessed 06 June 2018).

Van Ree, C.C.D.F., Weststrate, F.A., Meskers, C.G. and Bremmer, C.N. (1992). Design aspects and permeability testing of natural clay and sand-bentonite liners. *Geotechnique* 42(1), 49-56.

CHAPTER 3

FIELD INVESTIGATION OF AUSTRALIAN WASTE MANAGEMENT AND LEAK DETECTION PRACTICES

This chapter is based on the paper submitted to the Journal of Cleaner Production, Elsevier, as listed in Section 1.6. The details presented here are the same, except some changes in the layout in order to maintain a consistency in the presentation throughout the thesis.

3.1 Introduction

Despite being the least favoured option for waste disposal, landfilling is still widely prevalent globally (Ministry for the Environment, New Zealand, 2001; Productivity Commission, 2006; EC, 2008; Hoornweg and Bhada-Tata, 2012; Lopes *et al.*, 2012; USEPA, 2012; Department of the Environment and Energy, Australia, 2013; Esteban-Altabella *et al.*, 2017; Geoscience Australia, 2017; Jovanov *et al.*, 2017). Every year 1.3 billion tonnes of municipal solid waste (MSW) are generated worldwide (Hoornweg and Bhada-Tata, 2012) and a majority of this ends up in landfills. Furthermore, globally, the rate of growth of MSW is greater than the rate of growth of urbanization. China has the fastest rate of MSW growth, followed by other parts of East Asia, parts of Eastern Europe, and the Middle East. Domestic households account for the major MSW production (55 to 65%). Commercial and institutional locations generate 35 to 45% of the total MSW. The contribution by industrial sector is comparatively small due to recycling, reuse, or self-disposal practiced by industrial waste landfills (USEPA, 2011). The waste production trend reported in Australia, also shows a similar pattern. As per the DEWHA (2010), the waste production registered an increase of 170% in the period of 1996-2015, at a compound growth rate of 7.8% per annum.

Figure 3.1 gives the various municipal solid waste (MSW) disposal techniques practiced globally (Hoornweg and Bhada-Tata, 2012). It can be noticed from the figure that the dumping of wastes to landfilling facilities is the principal method of waste disposal. Therefore, the issue of appropriate handling and management of wastes in landfilling facilities becomes extremely important.

Landfills often deal with very putrescible and at times, hazardous wastes. Hence, the leachates generated by the aerobic and anaerobic decomposition of these wastes consist of a variety of pollutants, and are hazardous for the environment (Aboyeji and Eigbokhan, 2016; Esteban-Altabella *et al.*, 2017). In fact, the landfill leachates are one of the most difficult wastes to handle due to variations in their composition and flow rates, seasonal variation in the amount of precipitation, type and age of the facility, and so on (Zolfaghari *et al.*, 2016; Brennan *et al.*, 2017). The landfills produce leachates during their active operation period and continue to do so for many years even after decommissioning (Brennan *et al.*, 2017). To address this problem, the Environmental Protection Authorities around the world have recommended that the lining systems used in landfilling facilities must be engineered, constructed and frequently monitored, such that the complete isolation of all contaminants from soil and groundwater can be ascertained over their design life (Shukla, 2016; Jovanov *et al.*, 2017; Parastar *et al.*, 2017). However, it is disturbing to note that developing countries still practice uninhibited waste disposal to non-engineered open dumps (Hoornweg and Bhada-Tata, 2012; Jovanov *et al.*, 2017). This is a highly unhygienic and non-sustainable practice which will lead to organic, inorganic and microbial pollution of soil and groundwater (Aboyeji and Eigbokhan, 2016). This necessitates that all landfills be constructed using suitable lining systems.

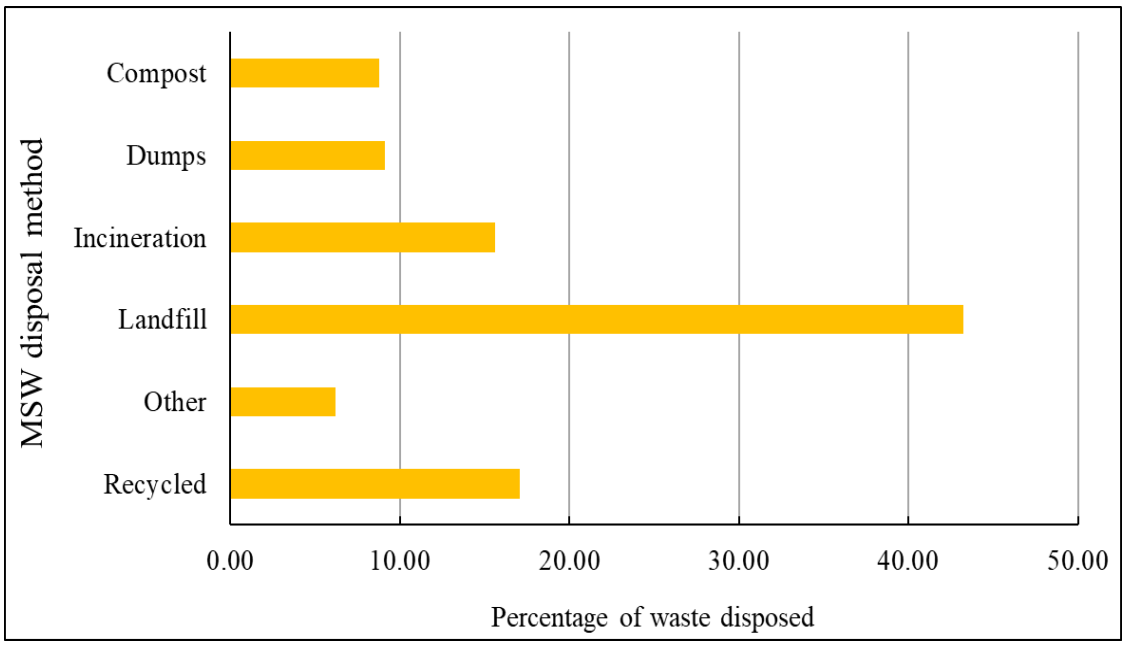

Figure 3.1: Municipal solid waste (MSW) disposal techniques practiced globally.

Interestingly, although the liners are constructed to be intact during their working life, severe operating conditions and poor placement assurance lead to the eventual failure of the lining systems. Their integrity is often compromised (Giroud, 1984) and consequently, the landfill leachates are found to leak, resulting in the contamination of underlying soil and groundwater (Oh *et al.*, 2008; Aboyeji and Eigbokhan, 2016). The extent of contamination and the adverse effects of leachate leakages on the surrounding environment, intensifies with passing time. Additionally, as time lapses, the cost of repair and remediation also increases manifold. Therefore, it becomes imperative to detect the leakage issues as soon as possible so that suitable remedial measures can be taken (Lopes *et al.*, 2012; Pandey *et al.*, 2017). Consequently, in an attempt to achieve timely detection of leakages, different landfilling facilities use various leak detection techniques for the control and management of contaminants.

It is critical that appropriate measures of waste handling and management should be practiced by all landfilling facilities. Government agencies and Environmental Protection Authorities around the world need to work in tandem to create and execute explicit regulation to achieve the same. It is also essential to generate an awareness about these issues among the general public so that the proper implementation of the rules and regulations can be ensured. Therefore, in the present work, an extensive study has been conducted to investigate the current state of landfilling in Australia with particular attention to the lining practices and leak detection methods currently in application. Table 3.1 lists the details of the landfilling facilities which participated in the study. This paper presents the complete details of the investigation. It also proposes a new method of leak detection by simulation of landfill liner, which is being developed and investigated by the Geotechnical and Geoenvironmental Research Group at Edith Cowan University with a view to its application in the design of lining systems for effective contamination control.

3.2 Waste Management Practices in Australia

Australia is an island continent with a population of nearly 25 million people occupying 7.692 million km² of land mass and a waste production of 2.2 tonnes per capita in 2010–11 alone. 60% of this generated waste was either recovered or recycled, with the rest 40% sent for disposal to landfills. The solid wastes consisted of commercial and industrial wastes (C & I, construction and demolition wastes (C & D) and municipal solid wastes (MSW). Out of all these, municipal solid wastes (MSW) has the lowest recovery rate among the three main waste streams. MSW generally consist of food scraps, composite products, paper and paperboard, wood, plastics, metals, textile, yard trimmings, glass, rubber, leather, miscellaneous inorganic

wastes, and mixed categories (USEPA, 2014). From the 14 million tonnes of MSW generated in 2010-11, 49% could not be recovered and was sent for disposal (DEWHA, 2010; DEE, 2013).

Table 3.1: Details of the participating landfill facilities.

Landfill number	State	Operator type	Name of the company (or operator)	Name and address of the landfill facility
L1	New South Wales	Public	Newcastle City Council	Summerhill Waste Management Centre, 141 Minmi Rd, Wallsend NSW 2287
L2	New South Wales	Private	SUEZ Australia	Lucas Heights Landfill (Sydney), New Illawarra Rd, Lucas Heights NSW 2234
L3	Victoria	Public	City of Greater Geelong	Drysdale landfill, Becks Rd, Drysdale VIC 3222
L4	Victoria	Private	SUEZ Australia	Hallam Road Landfill, 274 Hallam Rd, Hampton Park VIC 3976
L5	Western Australia	Public	City of Cockburn	Henderson Waste Recovery Park, 920 Rockingham Rd Henderson WA 6166
L6	Western Australia	Public	City of Armadale	Armadale Landfill and Recycling Facility, Lot 600 Hopkinson Road Hilbert WA 6112
L7	Western Australia	Public	Eastern Metropolitan Regional Council	Red Hill Waste Management Facility,

				1094 Toodyay Road, Red Hill WA 6056
L8	Western Australia	Private	SUEZ Recycling and Recovery	North Bannister Resource Recovery Park – 6364 Albany Hwy, North Bannister WA 6390

Figure 3.2 displays the different types of waste management facilities in Australia. For the municipal solid waste (MSW) management, most of these facilities follow the pattern of separation of waste, recycling, aerobic composting and landfilling. It can be observed that the majority of the waste ends up in landfilling facilities (Geoscience Australia, 2017).

It is interesting to note that more than 85% of the Australian population is currently living in urban areas. Even though Australia has a huge land mass, the habitable land area is only about 10% and the rest is deemed inhabitable for humans. Australia has 8 states and 8 federal territories. The majority of the population resides in the 8 capital cities of the 8 states (nearly 70%), which have a population density of 378 people per square kilometre. Among the 8 Australian territories, 2 are currently uninhabited and 3 do not have any waste management facility (DEE, 2010). The Norfolk Island has 3 landfilling facilities, while the Christmas Island and Cocos (Keeling) Islands have 1 landfilling facility each. As a result, most of the waste production is focused in the major urban areas.

Figure 3.3 shows the distribution of landfilling facilities in Australia by state (Geoscience Australia, 2017). It can be noticed that New South Wales (NSW) has the maximum number of landfill sites, followed by Western Australia (WA), Queensland (QLD) and Victoria (VIC) at 2nd, 3rd and 4th position, respectively. The Australian Capital Territory has the lowest number of landfill sites, specifically only two. Furthermore, it is interesting to observe that as per the Australian Bureau of Statistics (2017) report, ACT has the highest population density followed by Victoria and NSW. WA is at 7th position, followed by the Northern Territory (NT) at the last place. Considering the land area, WA is at the 1st place with 32.89% of Australia's land mass. Queensland, NT and South Australia (SA) are at 2nd, 3rd and 4th position, respectively, followed by NSW at 5th, Victoria at 6th and Tasmania (TAS) at the 7th position. ACT has the smallest land mass, only about 0.03% of Australia (Geoscience Australia, 2017).

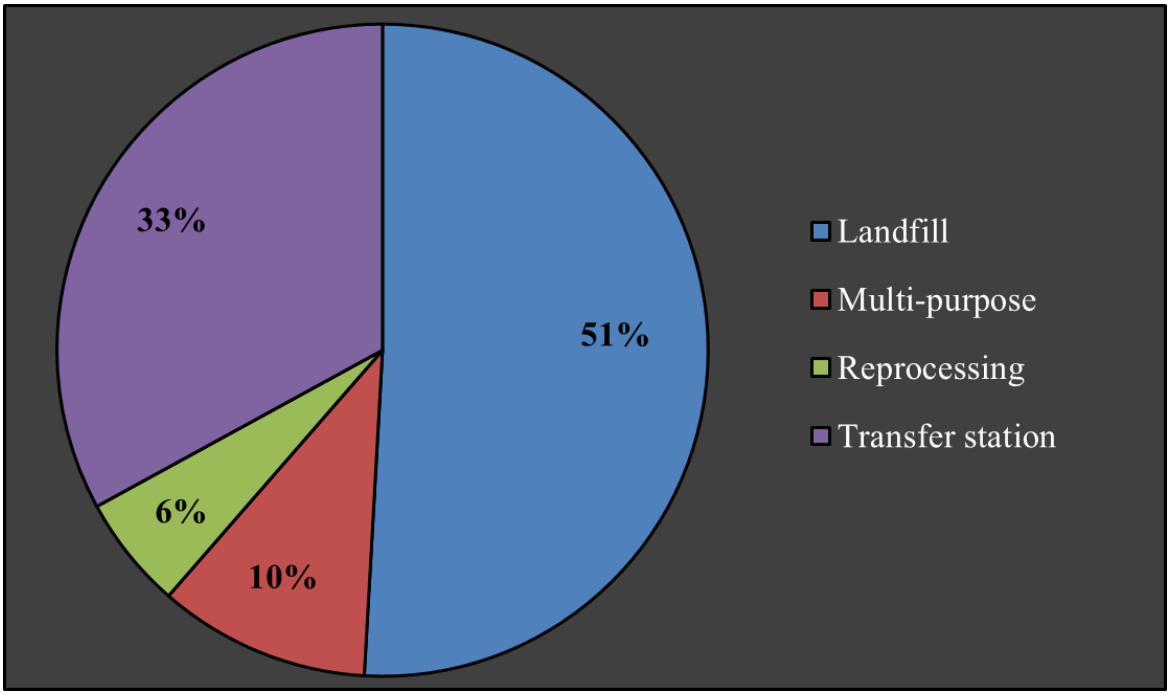

Figure 3.2: Different types of waste management facilities in Australia.

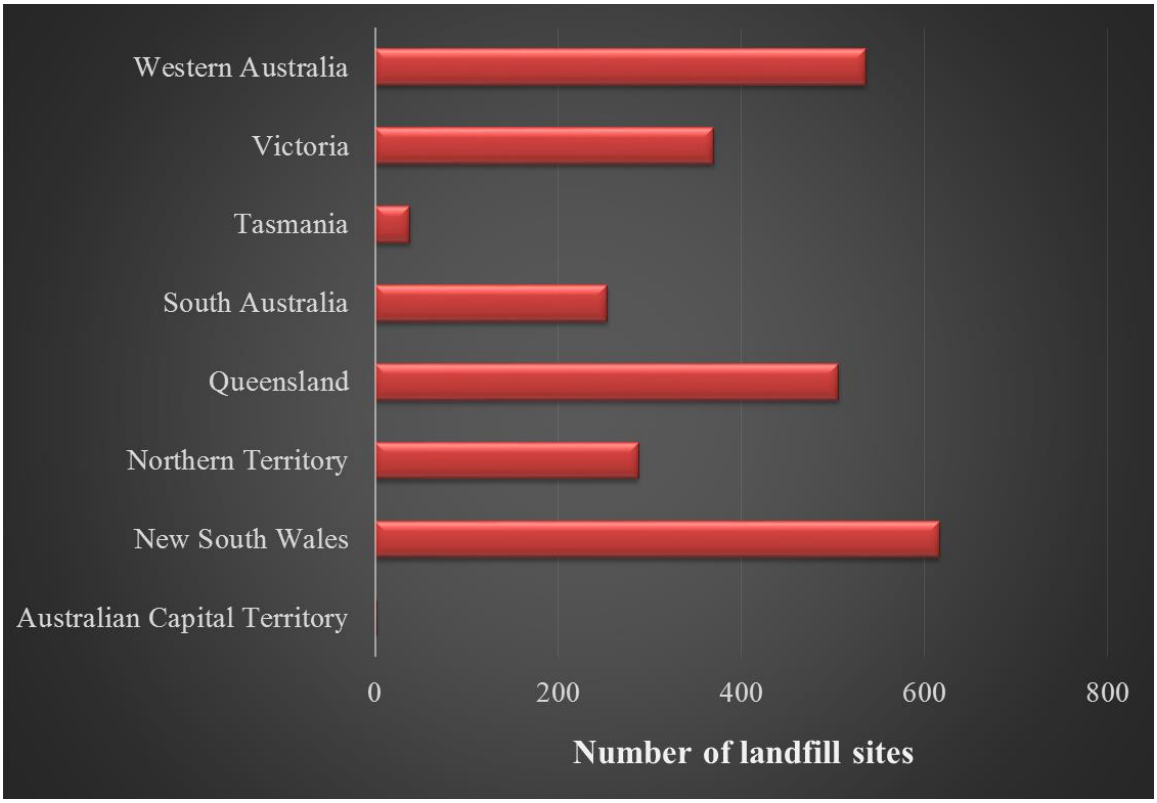

Figure 3.3: Distribution of landfilling facilities in Australia by state.

Construction of new landfill sites is time consuming due to several procedures such as siting, design and construction, planning and appeal processes, and so on. In addition, commencing new landfills is generally not supported by the local population. Therefore, Australian landfills are often developed in old quarries as it is a cost-effective method of rehabilitating used quarries. Additionally, more material is removed from quarries than the amount of waste generated to fill it. Hence, sufficient quarry space is available for use in landfilling. However, owing to geographical and geological constraints, difficulty in obtaining approval for a new site, etc., there is a scarcity of available space. Furthermore, if the landfills are situated far off from the metropolitan areas, the cost of transportation and disposal of wastes becomes extremely high. Hence, although Australia has a huge land mass, the siting, design, operation, and proper maintenance of landfilling facilities is a major concern (WMAA, 2013).

Figure 3.4 is the distribution of ownership for different waste management facilities. Public sector includes cities, counties/parishes, regional authorities, state governments, and the federal government owned landfills. Private sector entities are privately owned businesses ranging in size from very small to large (USEPA, 2014). A significant percentage of the landfill facilities as well as the transfer stations are operated by public owned companies (Figure 3.4). Comparatively, only a small portion of the landfill facilities and the transfer stations are managed by private companies (13% and 11%, respectively). In contrast, reprocessing facilities fall mostly under private ownership, specifically 87.4% (Geoscience Australia, 2017). Similar observation can be made from the Figure 5 which presents the ownership details of the participating landfill facilities. It can be seen that the majority of the landfills involved in the study are owned by the public entities. This appears to be a general trend in other major countries such as the USA as well. As per the USEPA (2014), 64 percent of MSW landfills were owned by public companies while 36 percent were owned privately in 2004. Keeping in mind the threat posed by landfilling facilities to the environment, the motivation behind the predominance of public entities' ownership of landfills could be the concern that privately-operated landfills might limit the community's degree of control over its operations.

Figure 3.6 has been developed from the research data and details the amount of waste generated at different landfill facilities. As per the Department of Environment and Conservation (1996), landfills are classified as small, medium or large based on the annual tonnage of waste received by them. A landfill is classified as small if the waste is less than 10,000 tpa. If the waste is greater than 100,000 tpa, the landfill is termed as large. For annual tonnage between 10,000 to 100,000 tpa, the landfill is classified as medium sized. Based on the above classification, 37.5% of the landfills are of medium size and 62.5% are large.

3.3 Lining Systems Practiced in Australian Landfills

Depending on the type of waste to be handled onsite, lining systems are constructed with a combination of different natural and man-made products (Rowe *et al.*, 2004; Shukla, 2016; Parastar *et al.*, 2017). Interestingly, different states in Australia have different landfill classifications (DEE, 2010). For example, in Western Australia, landfills are classified as Class I, II, III, IV or V depending on the type of waste that is permitted to be disposed to that particular landfill. The lining system to be uses is also varied accordingly.

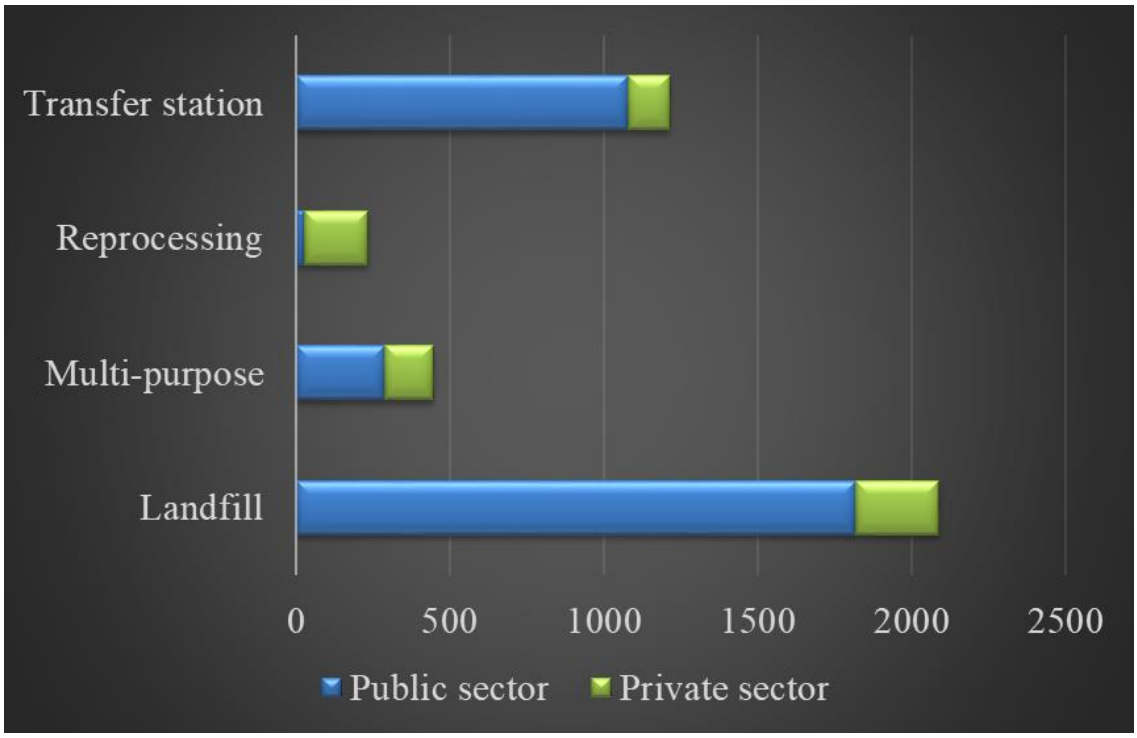

Figure 3.4: Distribution of ownership for different waste management facilities.

As per the classification given by DEC (1996), three of the participating landfills given in Figure 3.6, are classified as Class II (Putrescible landfill), four are Class III (Putrescible landfill) and one is a combination of Putrescible landfill (Class III) and Secure landfill (Class IV). Design of the lining system is determined based on the landfill classification.

Figure 3.7 gives a typical single composite liner system for waste containment facilities. A leak detection/recovery layer ($k \sim 10^{-1}$ m/s) forms the bottom, where k is the permeability of soil. It is overlain by a compacted clay layer ($k \sim 10^{-9}$ m/s) covered with high-density polyethylene (HDPE) geomembrane (GMB), and at the top is a leachate collection layer with high hydraulic conductivity ($k \sim 10^{-1}$ m/s). A GMB is a synthetic sheet with very low

permeability, used to control contaminant flow. Single (also referred to as simple), composite, or double liner can be used at landfill site, based on the type of waste to be stored (Shukla, 2016).

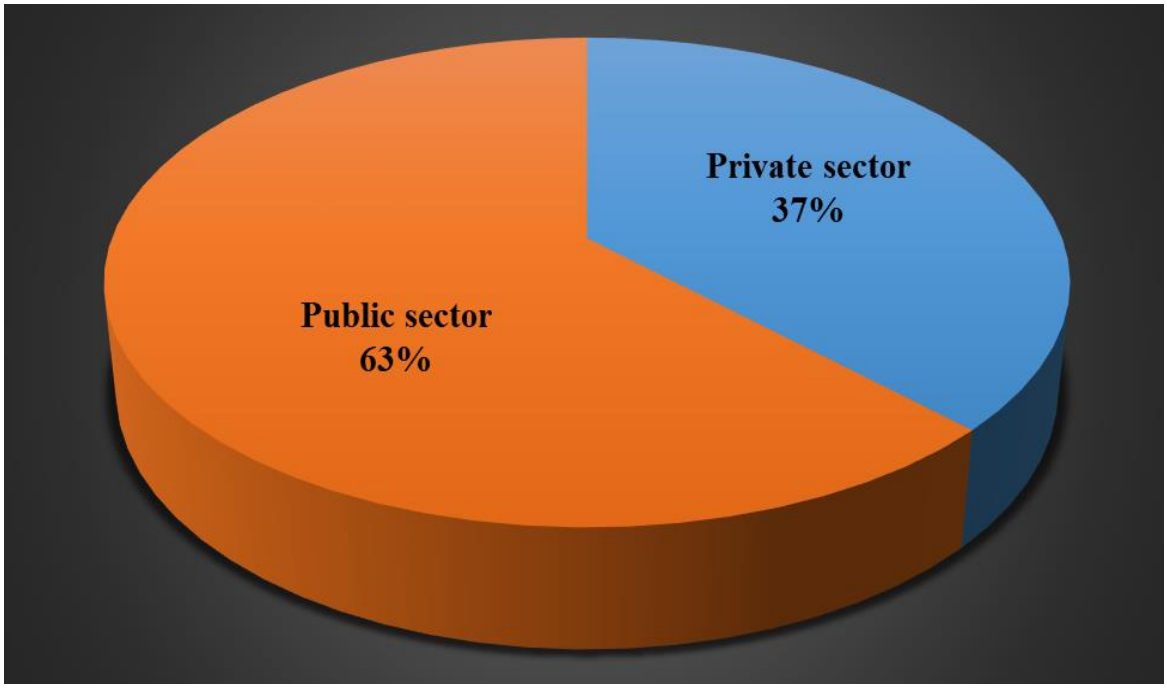

Figure 3.5: Ownership details of participating landfill facilities.

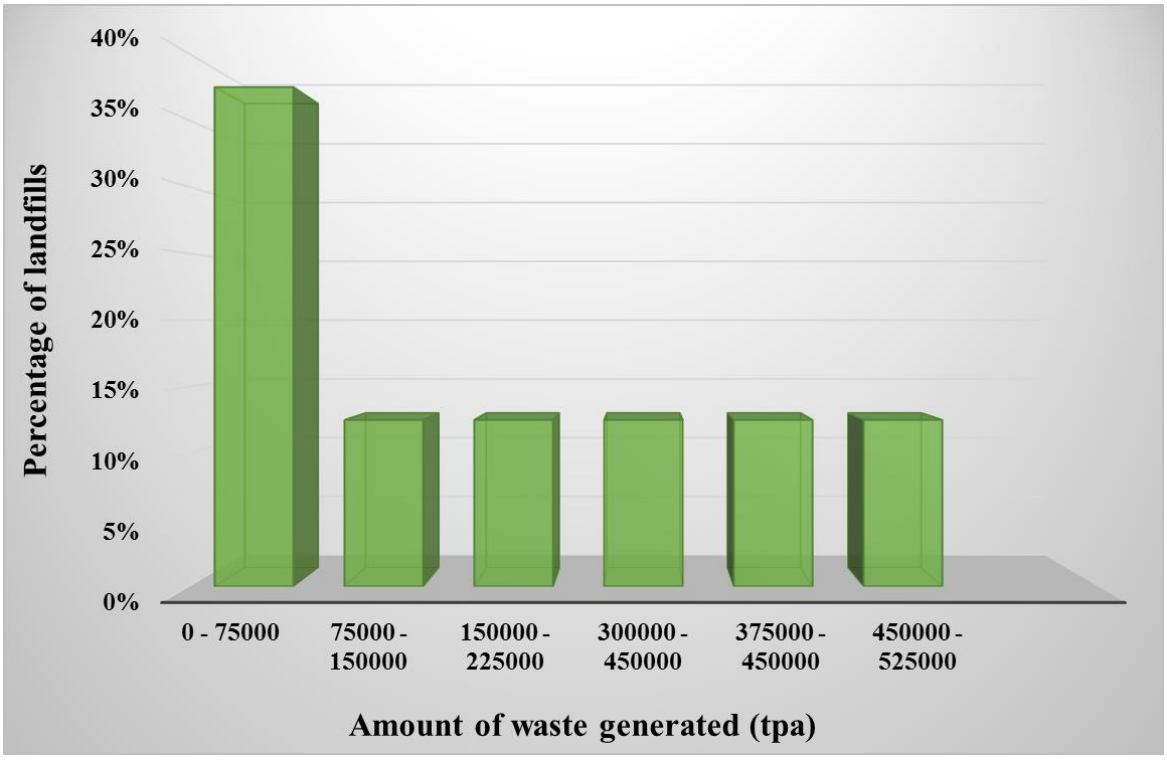

Figure 3.6: Amount of waste generated at various landfilling facilities.

Table 3.2 gives a list of the various leachate barrier systems currently used in Australia (Dixon, 2013). It can be observed that the Australian landfilling facilities generally consist of compacted clay and geomembrane (GMB) layers. Additionally, a geosynthetic clay liner (GCL) is also used. It is made by sandwiching a layer of clay between two geotextiles (Shukla, 2016).

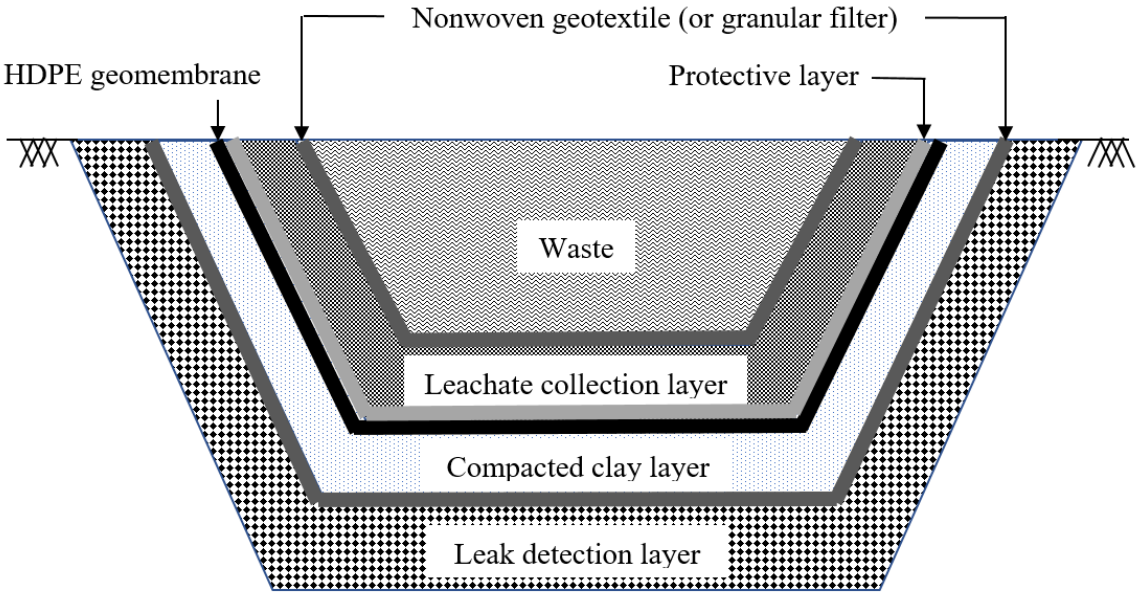

Figure 3.7: A typical single composite liner system for waste containment facilities.

Table 3.3 presents the details of various lining practices in the participating waste management facilities. It is interesting to note that while landfills in New South Wales and Victoria follow the guidelines laid down by their respective environmental protection agencies, the landfill sites in Western Australia do not comply with any one guideline unanimously. Similar discrepancy is observed for the implemented ground preparation methods. Most of the landfills are situated in old quarries and only basic ground preparation by compaction is followed (Table 3.3). There seems to be a lack of standardized methods in practice.

It can further be noticed from Table 3.3 that while all the landfill facilities use suitable lining systems for preparation of landfills, there are no set regulations or unifying code of practice. Different combinations of natural clay liners, compacted clay liners (CCL), HDPE geomembranes, geosynthetic clay liners (GCL), geotextiles and geonets are being used in the landfills. In general, the majority of large landfills have some form of lining while most of the

small landfills are constructed without any engineered lining system, Victoria being the only exception where all landfills have some sort of liner in place (DEE, 2010).

Table 3.2: Leachate barrier systems used in Australia.

State/Territory	Minimum requirements
New South Wales (NSW)	90 cm thick layer of compacted clay with permeability less than 10^{-9} m/s should be used. The compacted clay might be covered with geomembrane (GMB).
Northern Territory (NT)	A single liner of either clay, geomembrane (GMB) or geosynthetic clay liner (GCL) to be used. Composite liners should be used for municipal solid wastes (MSW) landfills. In case of hazardous wastes, double liners with leak detection system should be used.
Queensland (QLD)	The lining system to be used is determined by the risk assessment of the site.
South Australia (SA)	A composite liner with geomembrane (GMB) should be used.
Tasmania (TAS)	Engineered clay liner to be used for municipal solid wastes (MSW) landfills and geosynthetic clay liner (GCL) to be used for secure landfills.
Victoria (VIC)	Lining system should be engineered so that the seepage is less than 10 L/ha/day for municipal solid wastes (MSW) landfills and is less than 100 L/ha/day for secure landfills.

The Department of the Environment and Energy (2010) has reported that Tasmania, NSW and Victoria have the highest level of compliance with the design and construction requirements, in the given order. In comparison, WA demonstrates the poorest compliance. Ideally, there should be a unique set of laws and regulations for siting, design, operation and rehabilitation to govern all Australian landfill facilities.

Table 3.3: Lining practices in the participating waste management facilities.

Landfill number	Standards used	Ground preparation	Lining system	Lining system in use
L1	NSW EPA Solid Waste Landfill Guidelines	Geotechnical assessment is undertaken on the underlying strata and any engineered corrections or compensations are made. Batters are laid back to a minimum of 4:1 m gradient.	Yes	1-2 m thick CCL, 6 mm thick GCL, 2 mm thick HDPE, 4.5 mm thick Geotextile
L2	Site licence and NSW EPA Solid Waste Landfill Guidelines	-	Yes	Ground water drainage, 900 mm of engineered clay, 2.5 mm HDPE geomembrane, Geotextile
L3	EPA Victoria "Best Practice Environmental Management (BPEM) Siting, Design, Operation and Rehabilitation of Landfills, 2015.	Ground is compacted, and proof rolled	Yes	Compacted clay liner and HDPE plastic liner
L4	EPA Victoria "Best Practice Environmental Management (BPEM) Siting, Design, Operation and	-	Yes	Ground water drainage system, 500 mm engineered clay, GCL, 2

	Rehabilitation of Landfills, 2015.			mm HDPE, Geotextile
L5	Department of Environmental Regulation	Cells are constructed in a former limestone quarry. The base is excavated 8 m above the water table so the base is a compacted limestone material.	Yes	2 HDPE liners (2 mm thick) 1 Geotextile liner
L6	Licence conditions, groundwater monitoring and pest control	No new cells being developed	Yes	Natural clay lining
L7	EPA Victoria "Best Practice Environmental Management (BPEM) Siting, Design, Operation and Rehabilitation of Landfills, 2015.	Landfill cell and leachate pond foundation surfaces are cut with clean blades and shaped according to the design drawings. All foundation surfaces are maintained at the natural moisture content until covered. The foundation surfaces are compacted before the clay liner is constructed. If the construction of foundations involved thickness of more than 200 mm then the compaction is done by	Yes	500 mm of compacted clay, 1 has 1000 mm of CCL. 1-2 mm HDPE liner in 4. Geonet, geotextile and GCL in 1.

		lifts not exceeding 200 mm.		
L8	EPA Victoria "Best Practice Environmental Management (BPEM) Siting, Design, Operation and Rehabilitation of Landfills, 2015.	Prepared with survey set out and Civil equipment.	Yes	2 mm HDPE Membrane, GCL and clayey subgrade. 300 mm aggregate over the top.

Courtesy Sheen (2016) for L1, Jones (2017) for L2 and L4, Middleton (2016) for L3, Haynes (2016) for L5, Wallrodt (2017) for L6, Maslen (2017) for L7, Olman (2017) for L8.

3.4 Current Practices of Leakage Detection

As discussed in preceding sections, "all liners leak" (Giroud, 1984). Consequently, it is essential for landfill facilities to use proper leak detection systems to ensure adequate leachate containment. Different methods of leakage detection are practiced by landfilling sites, such as capacitance sensors, diffusion hoses, electro-chemical sensing cables, ground penetration radar (GPR), groundwater monitoring wells, lysimeters, resistivity cone penetration test (RCPT), tracers, time domain reflectometry (TDR), etc. (Hix, 1998; Oh *et al.* 2008; ASTM D6431-99(2010); Lopes *et al.*, 2012). Methods which involve on-site sampling and laboratory analysis are cost and time intensive. In addition, electrical leak detection methods, such as water puddle method (ASTM D7002 - 16), conductive geomembrane spark test (ASTM D7240 - 06(2011)), water lance method (ASTM D7703 - 16), arc testing method (ASTM D7953 - 14), electrode grid method (ASTM D6747 − 15), etc., are also used extensively because of low costs and ease of operation (Oh *et al.* 2008). These methods use the changes in the electrical properties of the liner subbase produced due to its leachate contamination, to detect lining system defects (Pandey and Shukla, 2017).

Table 3.4 details the leak detection techniques being practiced by landfills as recorded by the study. Except one landfill site in Victoria, all others are currently using some method of leak detection. The most popular method in practice is the use of groundwater monitoring wells to monitor the groundwater quality upstream and downstream of landfills. In fact, 87.5% of the facilities have monitoring wells onsite. This method detects leachate contamination of

groundwater to determine contaminant plumes, and thereby identifies leakage issues in liners. While this method has certain advantages such as low installation and operation costs, and ease of operation, it also has some major limitations. The use of this method does not prevent groundwater and soil contamination. Furthermore, it can only detect plumes that pass by the line of wells and the leak is detected after a considerable lapse of time (Hix, 1998; Oh *et al.*, 2008). Hence, the use of a permanent monitoring system which makes use of the electrical resistivity method, is highly desirable and is therefore, gaining more prevalence. However, it can be noticed from Table 4 that only one of the landfill facilities is currently using pre-laid sensor beds in seven landfill cells. One important reason behind this is that the electrode grid sensing system has high capital cost and can only be laid down in new landfill cells. It cannot be used for pre-existing cells. In spite of these drawbacks, the sensor beds are still a lucrative option because of their ease of operation, ability to constantly monitor lining system without onsite presence, and capability to detect leakage issues at the onset.

3.5 Proposed Method of Leakage Detection

It can be observed from Table 3.4 that among the various conventional methods of leakage detection, the monitoring wells are used most frequently. However, this method proves to be ineffective because by the time the leakage issue is detected, a substantial amount of soil and ground water is already contaminated (Hix *et al.*, 1998; Oh *et al.*, 2008; Pandey *et al.* 2017). For proper contamination control, it is important that the leak detection method used is both time and cost effective. It has been noted in previous research work that the use of electrical resistivity method for leakage detection is very prevalent owing to its operational and cost benefits (Oh *et al.* 2008; Pandey and Shukla, 2017). Specifically, the use of electrode grids below lining systems is highly desirable for newly constructed landfills, for the detection of leakages at their onset (ASTM D6747 – 15; Pandey *et al.*, 2017). However, such a method is limited by a thorough understanding of the parameters controlling the resistivity of that specific soil such as various soil parameters, the type of defects and the type of contaminants. Hence, to address these needs, the Geotechnical and Geoenvironmental research group at Edith Cowan University (ECU), Perth, Australia has been actively working in the direction of developing an innovative leak detection system, by simulating an actual lining system. The detailed design of this new technique has been presented by Pandey *et al.* (2017). Figure 3.8 gives the conceptual design of the experimental setup for the leak detection technique.

Table 3.4: Leak detection techniques being practiced by landfills.

Landfill number	Leak detection method used?	Current method of detection	Use of sensor beds
L1	Yes	Environmental Monitoring - including groundwater, surface water and leachate characterisation, undertaken on a quarterly basis.	No
L2	Yes	Ground water monitoring bores upstream and downstream of landfill	No
L3	No	None	No
L4	Yes	Ground water monitoring bores upstream and downstream of landfill	No
L5	Yes	Series of bores and nested wells (11) that are tested by an independent consultant as part of our landfill licence conditions on a 6-monthly basis.	No
L6	Yes	Groundwater monitoring reports	No (old site)
L7	Yes	7 cells use electronic leachate leakage detection systems. Quarterly groundwater monitoring, surface water monitoring, landfill gas surveying, odour monitoring, rehabilitation of closed cells. Conditions monitored around landfill cells as well as in and around the leachate ponds.	Yes. 7 cells
L8	Yes	Up and down gradient groundwater monitoring	No

Courtesy Sheen (2016) for L1, Jones (2017) for L2 and L4, Middleton (2016) for L3, Haynes (2016) for L5, Wallrodt (2017) for L6, Maslen (2017) for L7, Olman (2017) for L8.

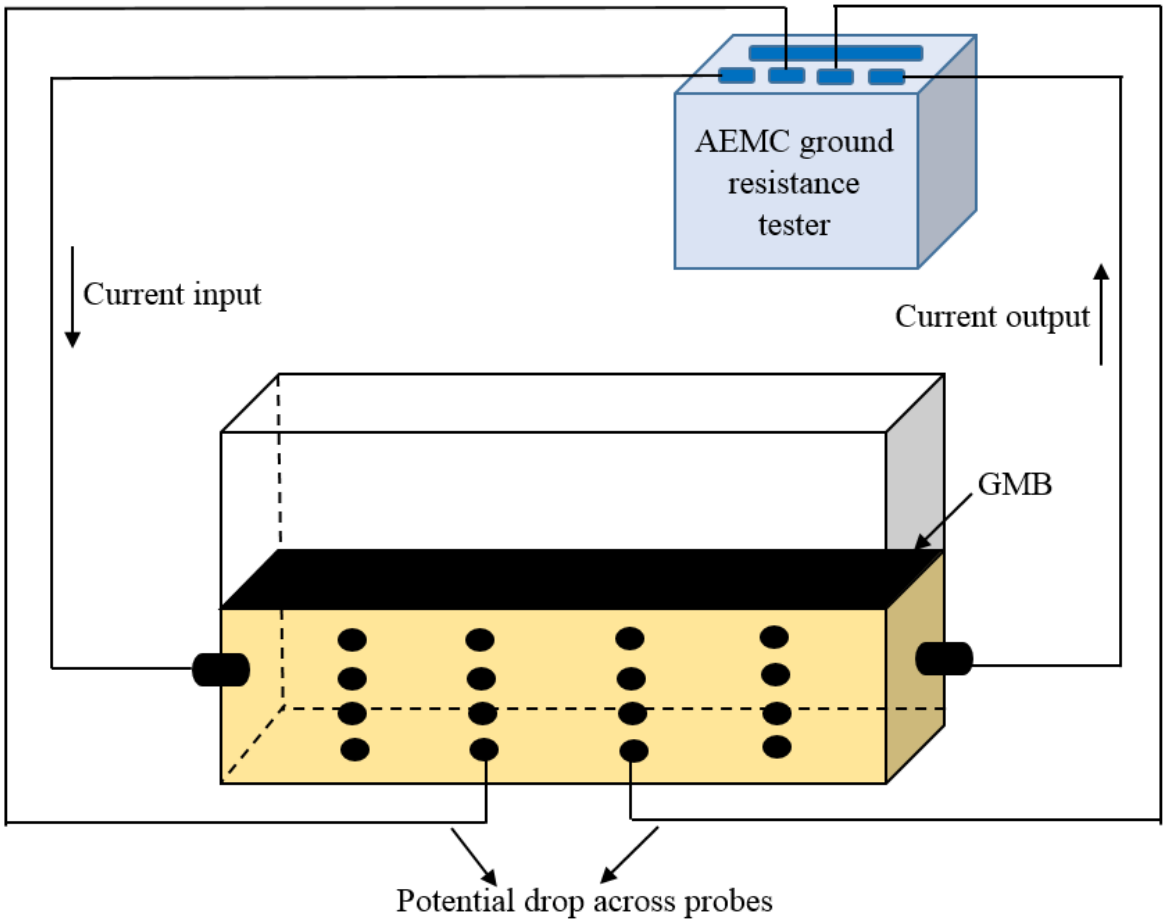

Figure 3.8: Conceptual design of leak detection developed at the Geotechnical and Geoenvironmental Research Group, School of Engineering, Edith Cowan University, Perth, Australia.

The test setup consists of a soil box filled with test specimen and covered with a geomembrane (GMB) liner, paired with an AEMC 6471 ground resistance testing machine. The GMB is covered with leachate. Leak is then intentionally introduced in the GMB and controlled leakage to the subbase soil, is allowed. The ground resistance tester is used at regular time intervals, to inject current across outer plate electrodes, and to measure the resultant potential drop across each pair of inner potential measuring probes. 12 resistance readings are obtained at each test interval for the soil specimen. Based on the variations in these readings, the location of the leak in the liner was determined. The developed technique was found to be effective in locating leachate leakages through liners. It is expected that the method will find a wide application in the design of monitoring systems for waste storage and handling facilities,

contamination detection, liner leak detection, development of sensors, numerical modeling for leak detection issues, and so on.

3.6 Conclusions

A review and quantitative comparison of the waste management in Australia, have been conducted to determine the current state of lining practices in landfills. Special emphasis has been given to liner design and leakage detection techniques. Based on the results and discussions presented, the following general conclusions can be made:

(1) Landfilling is the predominant method of waste disposal. Nearly 51% of the generated waste ends up in landfills. New South Wales has the highest number of landfill sites, followed by Western Australia.
(2) Majority of the landfill facilities are owned and operated by public sector entities such as cities, counties/parishes, regional authorities, state governments, and the federal government.
(3) Australians landfills generally consist of varying combinations of compacted clay and geomembrane liners. However, they do not follow any one unifying guideline for ground preparation, siting, design, operation, and rehabilitation.
(4) Groundwater monitoring wells were found to be the principal method of leakage detection practiced by the landfills. The use of pre-laid sensor beds based on electrical resistivity method was observed to be marginal.
(5) The study will be useful in generating awareness about the state of landfilling in Australia and will help governing bodies in making informed decisions for the development of rules and regulations for landfill facilities.
(6) The newly presented method can be a good starting point in the development of monitoring systems for landfill liners, subbase contamination detection, design of sensors, and so on.

References

Aboyeji, O.S. and Eigbokhan, S.F. (2016). Evaluations of groundwater contamination by leachates around Olusosun open dumpsite in Lagos metropolis, southwest Nigeria. *Journal of Environmental Management* 183(1), 333-341, DOI: 10.1016/j.jenvman.2016.09.002.

ABS (Australian Bureau of Statistics), 2017. 3101.0 - Australian Demographic Statistics. ABS, Canberra, ACT. http://www.abs.gov.au/ausstats/abs@.nsf/mf/3101.0. (Accessed 05 June 2018).

AS 1289.4.4.1 (1997). Methods of Testing Soils for Engineering Purposes Soil Chemical Tests - Determination of the Electrical Resistivity of a Soil - Method for Sands and Granular Materials. Standards Australia, Sydney, NSW, Australia.

ASTM D6431-99 (2010). Standard guide for using the direct current resistivity method for subsurface investigation. ASTM International, West Conshohocken, PA, USA.

ASTM D6747-15 (2015). Standard guide for selection of techniques for electrical leak location of leaks in geomembranes. ASTM International, West Conshohocken, PA, USA.

ASTM D7002-16 (2016). Standard practice for electrical leak location on exposed geomembranes using the water puddle method. ASTM International, West Conshohocken, PA, USA.

ASTM D7240-06 (2011). Standard practice for leak location using geomembranes with an insulating layer in intimate contact with a conductive layer via electrical capacitance technique (conductive geomembrane spark test). ASTM International, West Conshohocken, PA, USA.

ASTM D7703-16 (2016). Standard practice for electrical leak location on exposed geomembranes using the water lance method. ASTM International, West Conshohocken, PA, USA.

ASTM D7953-14 (2014). Standard practice for electrical leak location on exposed geomembranes using the arc testing method. ASTM International, West Conshohocken, PA, USA.

Brennan, R.B., Clifford, E., Devroedt, C., Morrison, L. and Healy, M.G. (2017). Treatment of landfill leachate in municipal wastewater treatment plants and impacts on effluent ammonium concentrations. *Journal of Environmental Management* 188(1), 64-72, DOI: 10.1016/j.jenvman.2016.11.055.

Daniel, D.E. (1993). Landfills and impoundments, Geotechnical Practice for Waste Disposal, Springer, USA, p. 97-112.

DEC (Department of Environment and Conservation) (1996). Landfill Waste Classification and Waste Definitions. DEC, Perth, WA, Australia. https://www.der.wa.gov.au/images/documents/our-services/approvals-and-licences/landfillwasteclassificationandwastedefinitions1996.pdf. (Accessed 05 June 2018).

DEE (Department of the Environment and Energy) (2010). Review of the application of landfill standards. DEE, ACT, Australia. http://www.environment.gov.au/protection/national-waste-policy/publications/review-application-landfill-standards. (Accessed 05 June 2018).

DEE (Department of the Environment and Energy) (2013). National Waste Report. DEE, ACT, Australia. http://www.environment.gov.au/protection/national-waste-policy/national-waste-reports/national-waste-report-2013. (Accessed 09 Nov 2017).

DEWHA (Department of the Environment, Water, Heritage and the Arts) (2010). National Waste Report. DEWHA, ACT, Australia. http://www.environment.gov.au/system/files/resources/af649966-5c11-4993-8390-ab300b081f65/files/national-waste-report-2010.pdf. (Accessed 24 May 2018).

Dixon, A. (2013). A critical review of Australian landfill guidelines. GHD, Sydney, Australia. http://www.wmaa.asn.au/event-documents/2015_cdlf/SpeakerPresentations/Session%20Three.%20Landfill%20Planning%20and%20Developments/anthony_dixon.pdf. (Accessed 10 Nov 2017).

EC (European Commission) (2008). Official Journal of the European Union. Waste Framework Directive. http://ec.europa.eu/environment/waste/framework/. (Accessed 22 April 2018).

Esteban-Altabella, J., Colomer-Mendoza, F.J. and Gallardo-Izquierdo, A. (2017). Simulation of the behavior of a refuse landfill on a laboratory scale. *Journal of Environmental Management* 204(1), 144-151, DOI: 10.1016/j.jenvman.2017.08.045.

Geoscience Australia (2017). Waste Management Facilities. Geoscience Australia, Australian Government, ACT, Australia. Available via DIALOG. https://data.gov.au/dataset/waste-management-facilities. (Accessed 10 Nov 2017).

Giroud, J.P. (1984). Impermeability: The myth and a rational approach. *Proceedings of the International Conference on Geomembranes*, Vol. 1, p. 157-162.

Haynes, M. (2016). Personal communication. Henderson Waste Recovery Park, WA, Australia.

Hix, K. (1998). Leak detection for landfill liners. National Network for Environmental Management Studies Report. National Service Center for Environmental Publications, USA. https://clu-in.org/download/studentpapers/leaklnfl.pdf. (Accessed 15 June 2018).

Hoornweg, D. and Bhada-Tata, P. (2012). What a Waste (1st Ed.). World Bank. Washington D.C., USA.

Jones, J. (2017). Personal communication. SUEZ Recycling and Recovery Australia, NSW, Australia.

Jovanov, D., Vujić, B. and Vujić, G. (2017). Optimization of the monitoring of landfill gas and leachate in closed methanogenic landfills. *Journal of Environmental Management* 216(0), 32-40, DOI: 10.1016/j.jenvman.2017.08.039.

Lopes, D.D., Silva, S.M., Fernandes, F., Teixeira, R.S., Celligoi, A. and Dall'Antônia, L.H. (2012). Geophysical technique and groundwater monitoring to detect leachate contamination in the surrounding area of a landfill–Londrina (PR–Brazil). *Journal of Environmental Management* 113(0), 481-487, DOI: 10.1016/j.jenvman.2012.05.028.

Maslen, G. (2017). Personal communication. Red Hill Landfill Facility, WA, Australia.

Middleton, S. (2016). Personal communication. City of Greater Geelong, Victoria, Australia.

Ministry of Environment (2001). A guide for the management of closing and closed landfills in New Zealand, ISBN 0-478-24021-X.

Oh, M., Seo, M. W., Lee, S. and Park, J. (2008). Applicability of grid-net detection system for landfill leachate and diesel fuel release in the subsurface. *Journal of Contaminant Hydrology* 96(1-4), 69-82, DOI: 10.1016/j.jconhyd.2007.10.002.

Olman, E. (2017). Personal communication. North Bannister Resource Recovery Park (NBRRP), SUEZ Australia, WA, Australia.

Pandey, L.M.S. and Shukla, S.K. (2017). Detection of leachate contamination in Perth landfill base soil using electrical resistivity technique. *International Journal of Geotechnical Engineering*, 1-12, DOI: 10.1080/19386362.2017.1339763.

Pandey, L.M.S., Shukla, S.K. and Habibi, D. (2017). Resistivity profiles of Perth soil in Australia in leak-detection test. *Geotechnical Research* 4(4), 214-221, DOI: 10.1680/jgere.17.00014.

Parastar, F., Hejazi, S. M., Sheikhzadeh, M. and Alirezazadeh, A. (2017). A parametric study on hydraulic conductivity and self-healing properties of geotextile clay liners used in landfills. *Journal of Environmental Management* 202(1), 29-37, DOI: 10.1016/j.jenvman.2017.07.013.

Productivity Commission (2006). Waste Management-Productivity Commission Inquiry Report. Commonwealth of Australia, Canberra. https://www.pc.gov.au/__data/assets/pdf_file/0014/21614/waste.pdf. (Accessed 23 May 2018).

Rowe, R.K., Quigley, R.M., Brachman, R.W. and Booker, J.R. (2004). Barrier systems for waste disposal facilities (No. Ed. 2), Spon Press, London, UK.

Sheen, A. (2016). Personal communication. Newcastle City Council, WA, Australia.

Shukla, S.K. (2016). An Introduction to Geosynthetic Engineering, CRC Press, Taylor & Francis Group, Florida, USA.

USEPA (United States Environmental Protection Agency) (2011). Exposure Factors Handbook 2011 Edition (Final Report). Washington, DC. https://cfpub.epa.gov/ncea/risk/recordisplay.cfm?deid=236252. (Accessed 06 June 2018).

USEPA (United States Environmental Protection Agency) (2012). Municipal Solid Waste Generation, Recycling, and Disposal in the United States, Tables and Figures for 2012. Washington, DC. https://www.epa.gov/sites/production/files/2015-09/documents/2012_msw_dat_tbls.pdf. (Accessed 21 May 2018).

USEPA (United States Environmental Protection Agency) (2014). Municipal Solid Waste Landfills, Economic Impact Analysis for the Proposed New Subpart to the New Source Performance Standards. Washington, DC. https://www3.epa.gov/ttn/ecas/docs/eia_ip/solid-waste_eia_nsps_proposal_07-2014.pdf. (Accessed 06 June 2018).

Wallrodt, S. (2017). Personal communication. Armadale Landfill and Recycling Facility, WA, Australia.

WMAA (Waste Management Association of Australia) (2013). Analysis of Landfill Survey Data, Final Report. Blue Environment Pty Ltd, VIC, Australia. http://www.environment.gov.au/system/files/resources/91763f0e-f453-48d0-b33e-22f905450c99/files/landfill-survey-data.pdf. (Accessed 04 June 2018).

Zolfaghari, M., Jardak, K., Drogui, P., Brar, S.K., Buelna, G. and Dubé, R. (2016). Landfill leachate treatment by sequential membrane bioreactor and electro-oxidation processes. *Journal of Environmental Management* 184(2), 318-326, DOI: 10.1016/j.jenvman.2016.10.010.

CHAPTER 4

CHARACTERISATION OF LINING MATERIALS USING ELECTRICAL RESISTIVITY METHOD

This chapter is based on the paper published in the Journal of Applied Geophysics, Elsevier, as listed in Section 1.6. The details presented here are the same, except some changes in the layout in order to maintain a consistency in the presentation throughout the thesis.

4.1 Introduction

Lining systems are used widely by waste storage and handling facilities to isolate contaminants and ensure that their effect on the environment is negligible (Fityus *et al.*, 1999; Rowe *et al.*, 2004; Rowe, 2012). The potential impact of the waste handled by a specific site determines the type of lining system to be employed (Shah, 2000). The liners are designed such that they have a very low hydraulic conductivity ($<10^{-9}$ m/s). Geosynthetics as the man-made materials, such as geomembranes, geotextiles, and geosynthetic clay liners (Shukla, 2016), or natural materials, such as compacted clays (Daniel, 1984; Harrop-Williams, 1985; Chapuis, 2002), silty soils (Holtz, 1985), mine tailings (Jessberger and Beine, 1981), and sand- bentonite mixtures (Chapuis, 1990), can be used to make liners. This paper focusses on the liners made from bentonite and sand-bentonite mixtures.

Undoubtedly, the integrity of liners over their intended lifespan is vital. To guarantee adequate performance of liners, it is essential to account for the fact that liners are subject to harsh operating conditions, and they are likely to develop defects (Daniel, 1984; Rowe, 2005; Oh *et al.*, 2008; Rowe, 2012; Shukla, 2016; Sirieix *et al.*, 2016; Baawain *et al.*, 2018). Consequently, the leachates are prone to leak out and contaminate underlying soil and groundwater. This necessitates the use of appropriate methods for the early detection of leakage and liner defect issues to ensure the timely control and mitigation of contamination. The electrical resistivity method, which is cost-effective and easy to use, can assist in solving this problem (Oh *et al.*, 2008; Bai *et al.*, 2013; Choo *et al.*, 2016; Merritt *et al.*, 2016; Sirieix *et al.*, 2016; Wang *et al.*, 2017; Baawain *et al.*, 2018; Chu *et al.*, 2018). This method is based on

detecting the changes in the electrical resistivity of geomaterials, produced due to the addition of even a small amount of contaminant (Darayan *et al.*, 1998; Yoon and Park, 2001; Pandey and Shukla, 2017). Furthermore, the electrical conductivity of soil depends on its properties (such as porosity, degree of saturation, composition of pore fluid, etc.), state of compaction, mineralogy, structure and temperature (Abu-Hassanein *et al.*, 1996; Mitchell and Soga, 2005; Bai *et al.*, 2013) as well as on the composition of the pore fluid (Fukue *et al.*, 1999; Cardoso and Dias, 2017).

Besides their use in liner leak detection, there are additional applications of soil resistivity studies in geotechnics and especially in earthworks, such as anomaly detection (Panthulu *et al.*, 2001), determination of soil state properties (Archie, 1942; McCarter, 1984; Kalinski and Kelly, 1993; Abu-Hassanein *et al.*, 1996; Shah and Singh, 2005; Long *et al.*, 2012; Kibria and Hossain, 2014; Choo *et al.*, 2016; Merritt *et al.*, 2016; Chu *et al.*, 2018), locating liner leakages (Darilek and Parra, 1989; Pandey *et al.*, 2017), soil contamination detection (Oh *et al.*, 2008; Pandey and Shukla, 2017), ground water contamination detection (Yochim, 2013), subsurface water profiling (Doolittle *et al.*, 2006; Mahmoudzadeh *et al.*, 2012), soil and conductivity studies (Rohini and Singh, 2004; Shamal *et al.*, 2016; Wang *et al.*, 2017), near surface soil characterisation (Islam and Chik, 2013), and so on. Hence, many previous researchers have focussed on developing correlations for electrical resistivity of various soils (Archie, 1942; McCarter, 1984; Fukue *et al.*, 1999; Shah and Singh, 2005; Kibria and Hossain, 2012; Yan *et al.*, 2012; Pandey *et al.*, 2015).

The parameters affecting the conductivity of various soil types, differ significantly. For the coarse fraction like sand, the conductivity depends on interconnected voids, conductivity of interstitial fluid, state of compaction and granular skeleton. However, for clayey soils, the conductivity is governed by pore fluid conductivity as well as surface charge of the clay mineral (Mitchell and Soga, 2005). Consequently, the bentonite content of soil is known to have a significant impact on its electrical resistivity (Abu-Hassanein *et al.*, 1996; Kumar and Yong, 2002; Kibria and Hossain, 2014). Although many researchers have previously developed the relationship between the geotechnical properties of soil and its electrical resistivity, there are a limited number of studies to analyse the effect of bentonite content of soil on its resistivity (Shah and Singh, 2005). Furthermore, it is well-known that both water content and the degree of compaction are essential criteria to determine resistivity of soil (McCarter, 1984; Kalinski and Kelly, 1993). Hence, there is a significant scope for the development of correlations for the resistivity of soils which incorporate the effect of the state of compaction on the electrical resistivity of sand-bentonite liner materials. Therefore, the purpose of this study is to

characterize the electrical resistivity of the bentonite and sand-bentonite soil liners, so that later, this property could be measured to estimate soil contamination.

In most research works carried out in the past on investigation of electrical resistivity of soils, the dry unit weight γ_d of soils have been kept constant and the effect of changing water content on the resistivity has been investigated (McCarter, 1984; Abu-Hassanein *et al.*, 1996; Kibria and Hossain, 2012; Bai *et al.*, 2013; Kibria and Hossain, 2014). In this research, the unit weight γ_d has been varied such that at each water content, the maximum compaction is achieved. The motivation behind this is to replicate actual lining materials, as used in practice. Furthermore, the effect of bentonite content of soil and its state of compaction have been scrutinized for Australian soils. The focus in this research is to investigate the variation of resistivity as a geophysical parameter with the state of compaction, because the soil in field projects related to roads, embankments, foundations, and other geotechnical structures in civil engineering are regularly compacted. Therefore, the developed figures may work as the design charts for practising geotechnical/civil engineers. The results as presented, are highly useful to predict the densification of liner based on the non-destructive test that uses the resistivity measurement. This new research development can help avoid disturbing the compacted liner material at the landfill site, and hence, prevent any disturbance that can increase the infiltration of landfill leachate.

The results obtained from this study will provide a baseline for the detection of liner leakage for application in Australia as well as in other parts of the world. In addition, newly developed correlations have also been proposed, aiming at their application in liquid impoundment facilities, waste storage and handling facilities, contamination detection, liner leak detection, development of sensors, soil and corrosion studies, and so on.

4.2 Materials and Methods

Sand obtained from quarries around Perth, Western Australia (WA) is used for the experiments. Table 4.1 gives its various physical properties. Figure 4.1 shows the particle-size distribution curve of sand and bentonite. As per the Unified Soil Classification System (USCS), the sand is classified as poorly graded (SP) sand, which is a good representation of soil in WA.

The bentonite specimen used in this study is powdered sodium bentonite, procured from Ebenezer mine site in Queensland, Australia. Its various properties are listed in Table 4.2, and is classified as the highly plastic clay, also called the fat clay (CH) as per the Unified Soil

Classification System (USCS). Table 4.3 shows the composition of the tap water which has been used in this study. The tap water has been used as a representation of the groundwater.

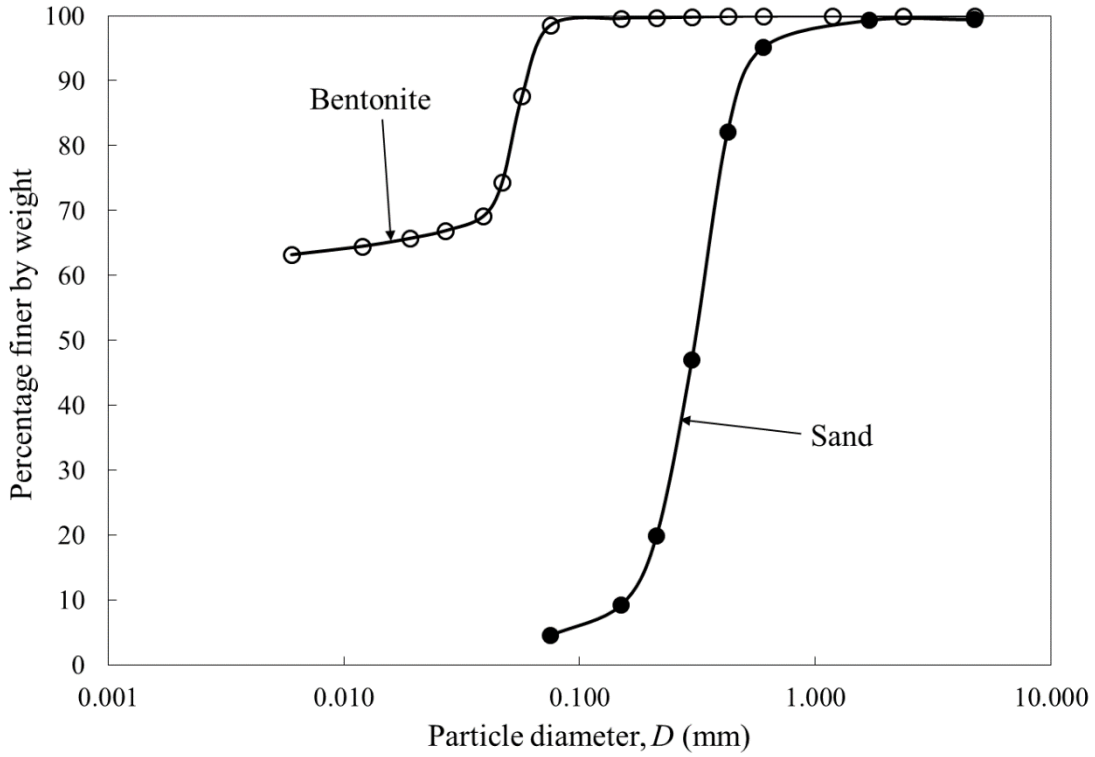

Figure 4.1: Particle-size distribution curve of sand and bentonite.

A total of five soil mixes were prepared for the study by mixing different amounts of oven-dried sand and bentonite, such that the bentonite in the soil mixtures was varied from 20 to 100% by weight. Standard Proctor compaction test was conducted for all soil mixtures, in accordance to the Australian Standard AS 1289.5.1.1–2003 (Standard Australia, 2003). It is an experimental method to determine the optimum water content at which a soil becomes most dense and achieves its maximum dry unit weight. The test is performed by compacting a soil at known water content into a cylindrical mould using a compaction effort of 596 kJ/m^3. The soil is compacted in three equal layers, each receiving 25 blows from a rammer. This process is repeated for various water contents and the dry unit weights are determined for each. The graph for the dry unit weight versus water content is then plotted to get the compaction curve. The maximum dry unit weight is obtained from the peak of the curve. The corresponding water content is known as the optimum water content.

Table 4.1: Physical properties of sand.

Property	Value	Unit
Specific gravity, G_s	2.68	Dimensionless
Coefficient of uniformity, C_u	2.27	Dimensionless
Coefficient of curvature, C_c	1.22	Dimensionless
Effective size, D_{10}	0.15	Mm
Minimum dry unit weight, $\gamma_{d\min}$	14.02	kN/m^3
Maximum dry unit weight, $\gamma_{d\max}$	15.56	kN/m^3
Soil classification as per USCS (Unified Soil Classification System)	Poorly graded sand (SP)	Dimensionless

Table 4.2: Physical properties of bentonite.

Property	Value	Unit
Specific gravity, G_s	2.66	dimensionless
Liquid limit, w_l	428	dimensionless
Plastic limit, w_p	51	dimensionless
Plasticity index, I_P	377	dimensionless
Free swell index	712.5	dimensionless
Maximum dry unit weight, $\gamma_{d\max}$	11.51	kN/m^3
Optimum water content, w_{opt}	30.5%	dimensionless
Soil classification as per USCS (Unified Soil Classification System)	Highly plastic clay (Fat clay) (CH)	dimensionless

A total of five soil mixes were prepared for the study by mixing different amounts of oven-dried sand and bentonite, such that the bentonite in the soil mixtures was varied from 20 to 100 percent by weight. Standard Proctor compaction test was conducted for all soil mixtures, in accordance to the Australian Standard AS 1289.5.1.1–2003 (Standard Australia, 2003). It is an

experimental method to determine the optimum water content at which a soil becomes most dense and achieves its maximum dry unit weight. The test is performed by compacting a soil at known water content into a cylindrical mould using a compaction effort of 596 kJ/m^3. The soil is compacted in three equal layers, each receiving 25 blows from a rammer. This process is repeated for various water contents and the dry unit weights are determined for each. The graph for the dry unit weight versus water content is then plotted to get the compaction curve. The maximum dry unit weight is obtained from the peak of the curve. The corresponding water content is known as the optimum water content.

Table 4.3: Water quality data for tap water (as per Water Corporation, WA).

Parameter	Value	Unit
Alkalinity as $CaCO_3$	95	mg/L
Aluminium	0.02	mg/L
Calcium	30.5	mg/L
Chloride	110	mg/L
Conductivity (at 25 $^{\circ}$C)	58.5	mS/ m
Hardness as $CaCO_3$	105	mg/L
Iron	0.006	mg/L
Magnesium	7.5	mg/L
Manganese	<0.002	mg/L
Nitrite plus nitrate as N	0.76	mg/L
pH	7.72	pH Units
Potassium	5.6	mg/L
Silicon as SiO_2	18	mg/L
Sodium	68	mg/L
Sulphate	19.5	mg/L
Total Dissolved Solids (TDS)	385	mg/L
True colour	<1	HU
Turbidity	<0.1	NTU

Based after Tyl E., Water Corporation, WA, Australia (Personal communication, 2016).

For each sand-bentonite mix, a known amount of soil was mixed with a specific amount of water to achieve the desired water content. The water content w was varied from 5% to 45%, based on the results reported by previous researchers (McCarter, 1984; Abu-Hassanein *et al.*, 1996; Kumar and Yong, 2002; Kibria and Hossain, 2014). Each specimen was covered and allowed to equilibrate in air-tight bags at room temperature (20 $^{\circ}$C) for 24 hours. The swelling time of 24 hours was chosen based on past research work (Elsharief and Sufian, 2018), as most of the swelling of soil specimen was found to occur within this duration. In this manner, several specimens were obtained by preparing each of the sand-bentonite mixes to achieve varying states of compaction.

4.2.1 Experimental set-up

The electrical resistivity tests were conducted as per the Australian Standard AS 1289.4.4.1–1997 (Standard Australia, 1997). A soil box (Figure 4.2) of 200 mm internal length, 40 mm internal width and 30 mm internal depth, was fabricated from 10-mm thick Perspex sheet. The box was fitted with two 10-mm thick brass plate electrodes, C_1 and C_2, of the same cross-sectional area as the box, and two brass potential measuring pins, P_1 and P_2. The diameter of the pins was 3 mm and the distance between their axes was 120 mm.

The four-terminal AEMC 6471 ground resistance testing machine (from AEMC instruments, USA) was used to measure the electrical resistivity of the soil mixture. Connections were made between the box and the AEMC tester as shown in Figure 4.2.

4.2.2 Test procedure

Figure 4.3 shows the compaction curves obtained for sand, bentonite and various sand-bentonite mixtures. The dry unit weight γ_d for each sand-bentonite mixture at a specific water content, was obtained from its respective compaction curve, as given by Figure 4.3. Using this γ_d value and known volume of soil box, the amount of specimen to be filled in the box, was calculated. The soil mass was filled into the box in three layers, to achieve homogeneity.

After the soil mixture was filled into the box, connections were made as shown in Figure 4.2. An AC voltage of 16 V at 128 Hz was applied to the outer electrode plates, C_1 and C_2, and the potential drop across the inner pins, P_1 and P_2, was measured to determine the resistance R. This specific input voltage was chosen based on the findings of Pandey *et al.* (2015).

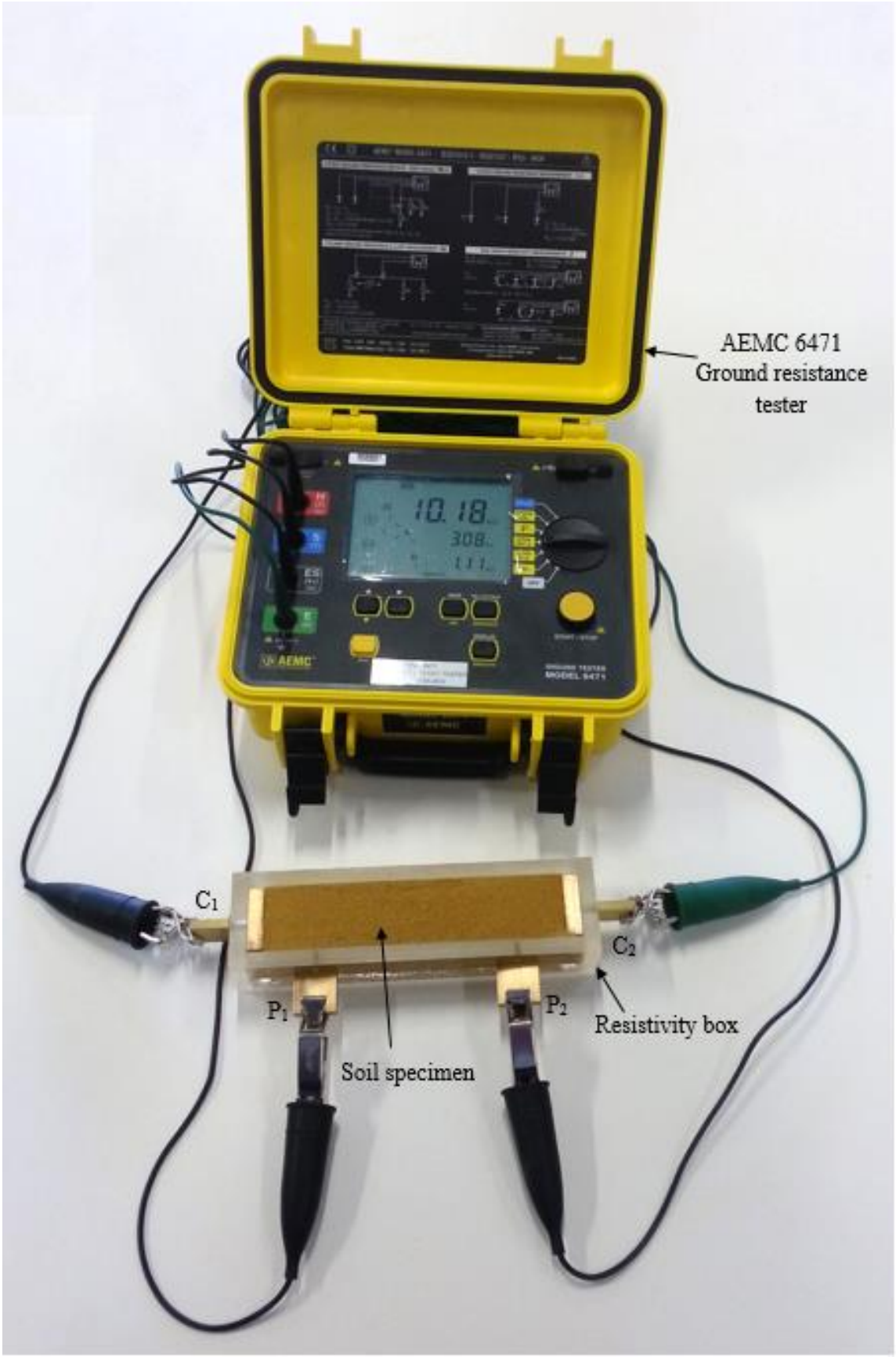

Figure 4.2: Experimental setup for the measurement of electrical resistivity as per AS 1289.4.4.1–1997.

The resistivity ρ is then obtained from the resistance R using the following equation:

$$\rho = \frac{AR}{L} \tag{4.1}$$

where A is the cross-sectional area and L is the length of the test specimen. In this instance, L is the distance between the inner potential measuring pins, P_1 and P_2. For this test, A = 1200 m^2 and L = 120 m. Hence, due to the specific geometry of the fabricated soil box (Standard Australia, 1997), the Eqn. (4.1) is modified as follows:

$$\rho = \frac{R}{100} \tag{4.2}$$

The room temperature was maintained at 20 °C to avoid the effect of its fluctuations on the electrical resistivity (Kalinski and Kelly, 1993; Bai *et al.*, 2013).

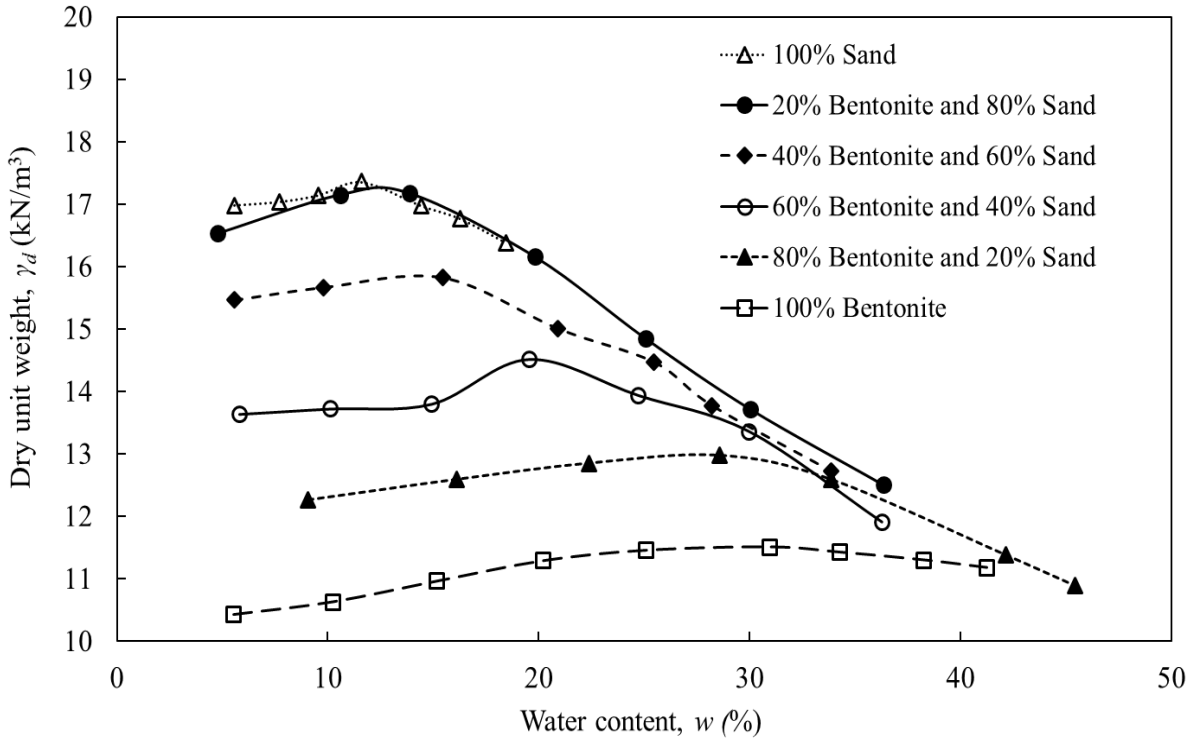

Figure 4.3: Compaction curves for all soil mixtures.

4.3 Results and Discussion

The compaction curves obtained for sand, bentonite and various sand-bentonite mixtures are shown in Figure 4.3. It can be observed that the dry unit weight γ_d first increases and then decreases, with increasing water content w. As the bentonite content in the soil mixture is decreased, the compaction curve shifts up and towards left. The maximum dry unit weight $\gamma_{d\max}$ increases and the w_{opt} decreases, with a decrease in bentonite content in the sand-bentonite mixture. With an increase in the bentonite content of the sand-bentonite mixture, the compaction behaviour of the soil mixture resembles that of bentonite more closely. Similarly, at lower bentonite contents, the compaction behaviour of the mixture is closer to that of sands. These observations are consistent with past research works, such as by Abramson *et al.* (1995), Kumar and Yong (2002), Shamal *et al.* (2016), Cardoso and Dias (2017), and so on.

Figures 4.5 through 4.8 give the variation of electrical resistivity with the state of compaction for different sand-bentonite mixtures. Figures 4.4 and 4.9 show the same for the sand and bentonite, respectively. The data for the electrical resistivity of the Perth sand has been developed after Pandey *et al.* (2015), for comparison.

The electrical resistivity value of clayey soils could not be determined at water content w below 8%. This has also been observed by previous researchers (McCarter, 1984; Abu-Hassanein *et al.*, 1996; Kumar and Yong, 2002; Kibria and Hossain, 2014). In contrast, resistivity readings could be obtained for water contents as low as 4% for sands. It can be explained by the well-established fact that the electrical resistivity of a soil is affected by the amount of interstitial pore fluid available in the soil (Yoon and Park, 2001; Cardoso and Dias, 2017). In case of sands, any liquid added to the soil is freely available in the interstices for electrical conduction. However, in a clayey soil, lesser amount of free interstitial water is available for conduction due to double layer of electric charges at the clay mineral surface resulting in adsorption (Mitchell and Soga, 2005; Cardoso and Dias, 2017).

Varied trends of the compaction curve and resistivity curve are observed (Figures 4.4 to 4.9) for sand-bentonite mixtures. The resistivity curve shows a decrease with increase in water content w, while the dry unit weight increases and then decreases with increasing w.

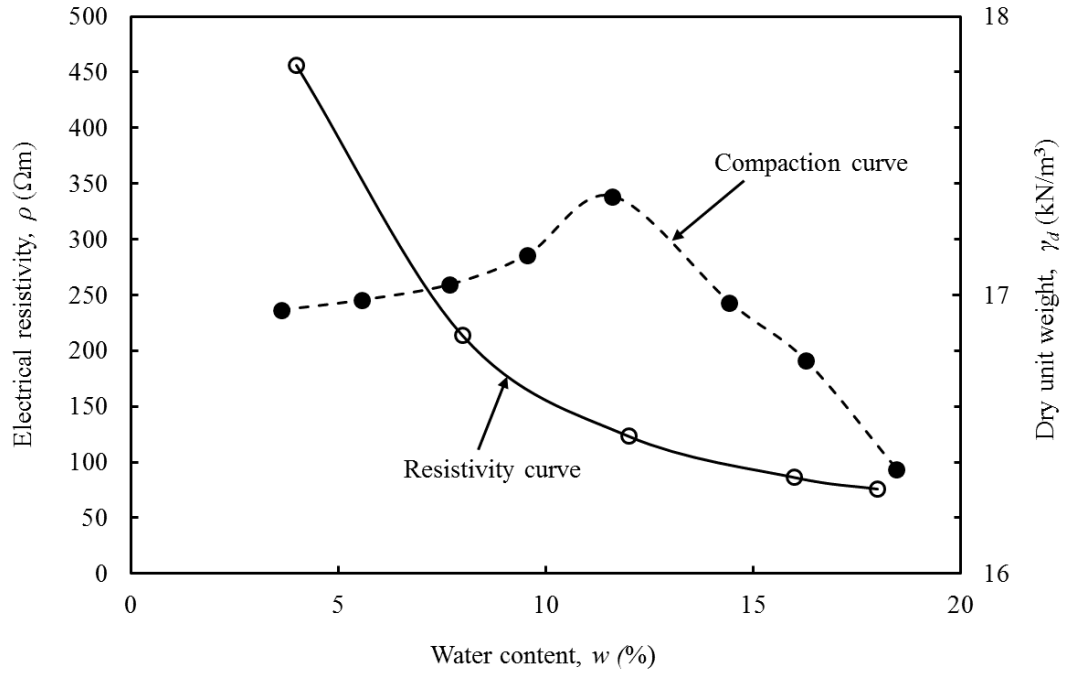

Figure 4.4: Electrical resistivity and compaction curves for sand.

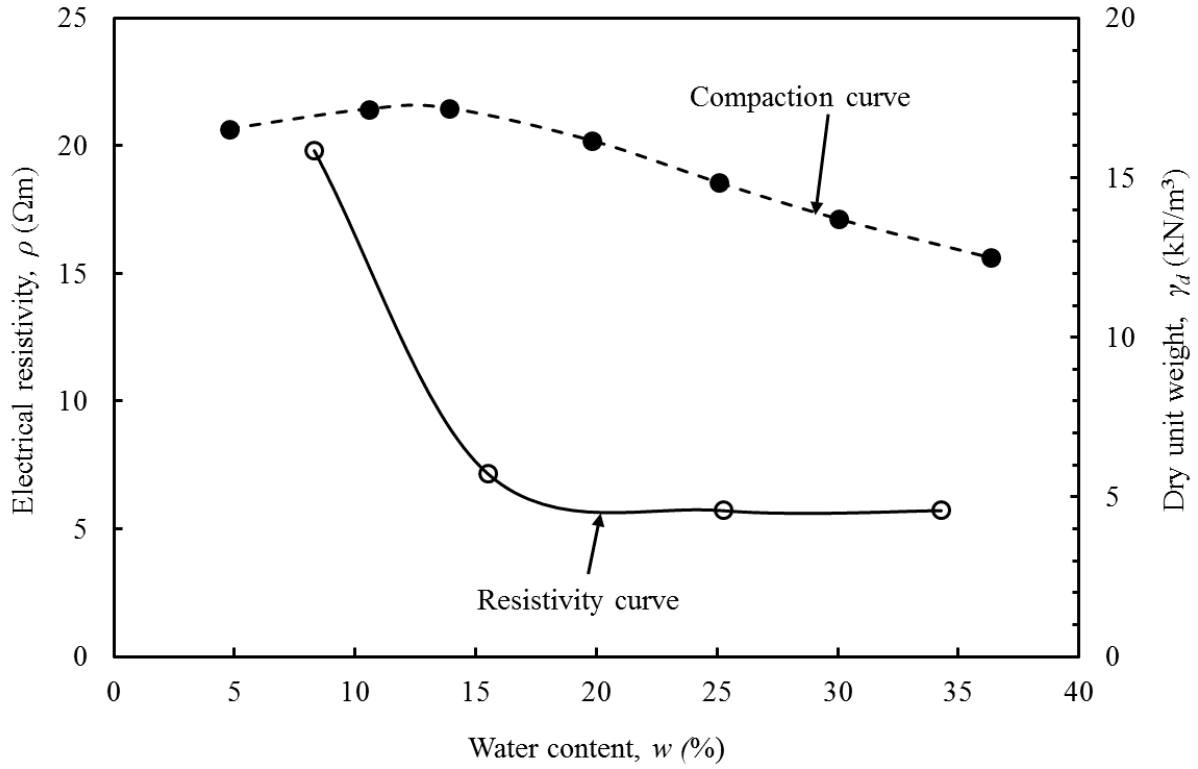

Figure 4.5: Electrical resistivity and compaction curves for a mixture of 20% bentonite and 80% sand.

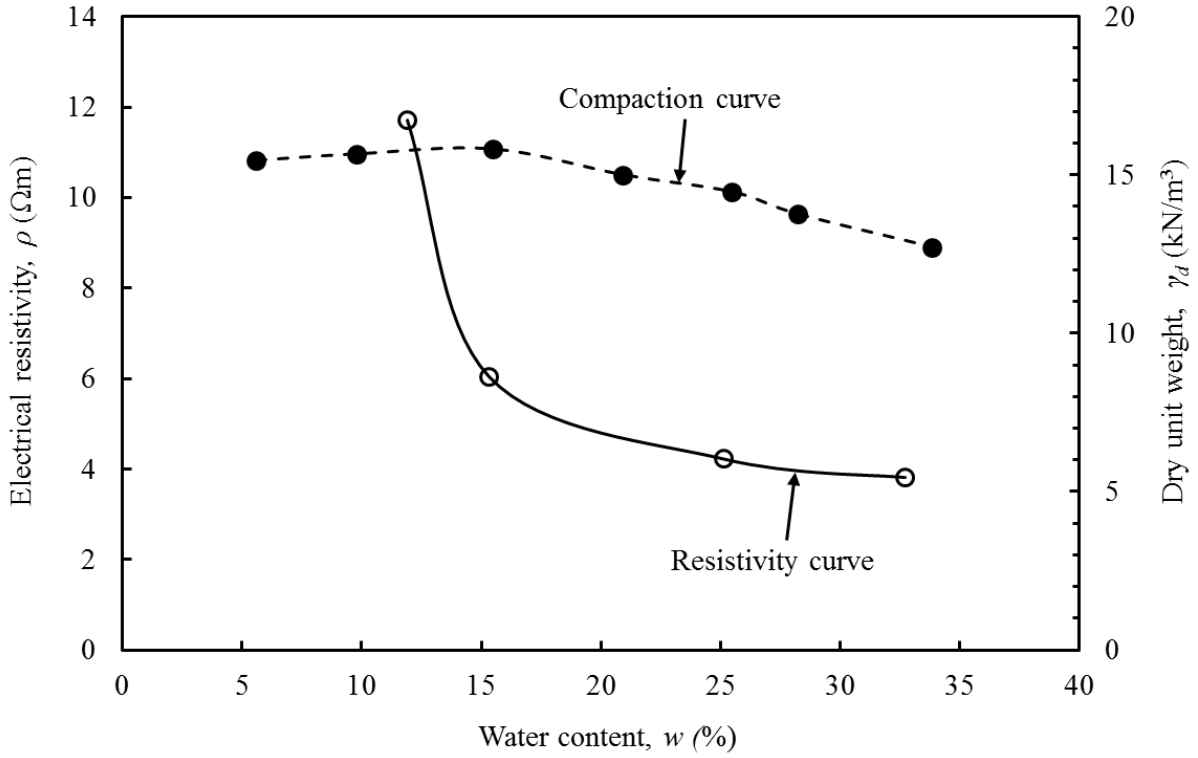

Figure 4.6: Electrical resistivity and compaction curves for a mixture of 40% bentonite and 60% sand.

It can be observed from Figures 4.4 through 4.9 that the electrical resistivity ρ decreases with an increase in the water content w. This decrease is rapid initially. However, the change in ρ becomes insignificant at higher w. Similar trends have been reported by other researchers for various soil specimens (McCarter, 1984; Abu-Hassanein *et al.*, 1996; Bai *et al.*, 2013). The water content value $w = w_T$, is the specific value of water content above which the decreasing trend of resistivity curve changes. The value of w_T was found to be different for each of the soil mixtures. It was also seen that w_T increased with increasing bentonite content for the sand-bentonite mixtures. From Figure 4.4, the w_T value for sand is observed to be about 10%. From Figures 4.5 to 4.8, w_T was found to be nearly 15, 17, 26 and 28% for 20, 40, 60 and 80% bentonite content, respectively. For the bentonite, w_T was observed to be approximately 19% (Figure 4.9). This observation can be explained by the swelling behaviour of clayey soils due to the adsorption of water (Mitchell and Soga, 2005).

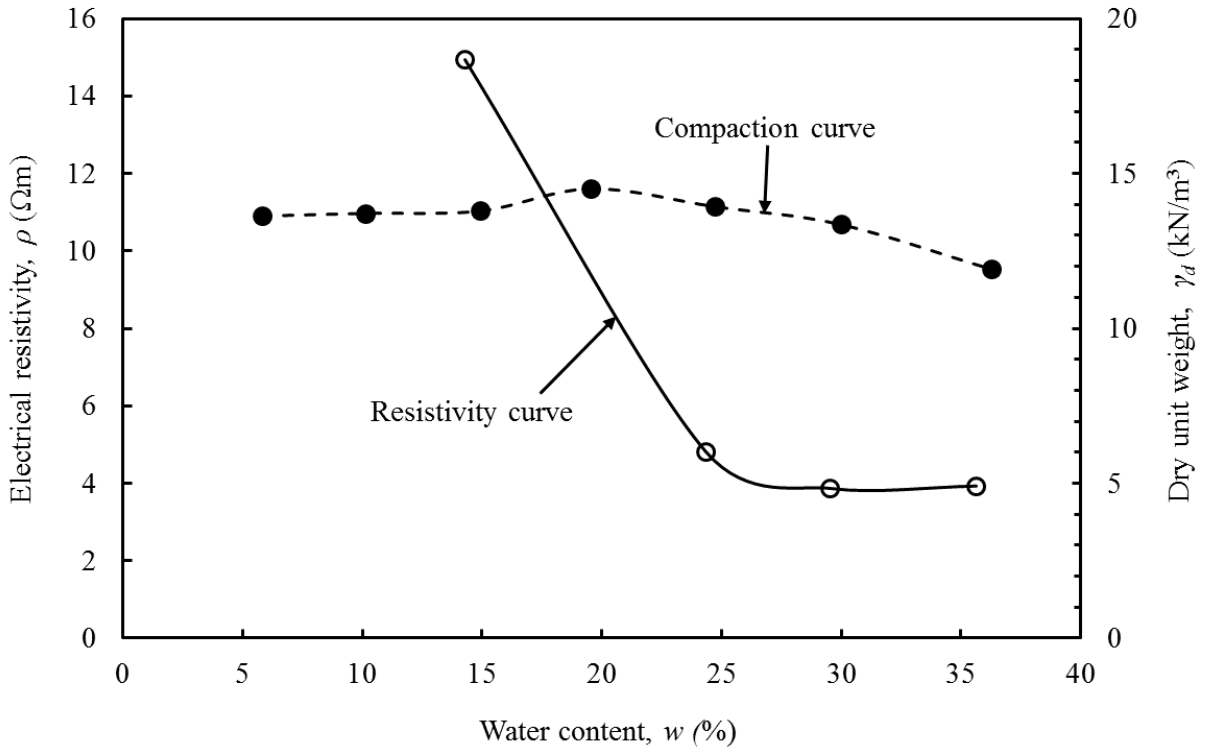

Figure 4.7: Electrical resistivity and compaction curves for a mixture of 60% bentonite and 40% sand.

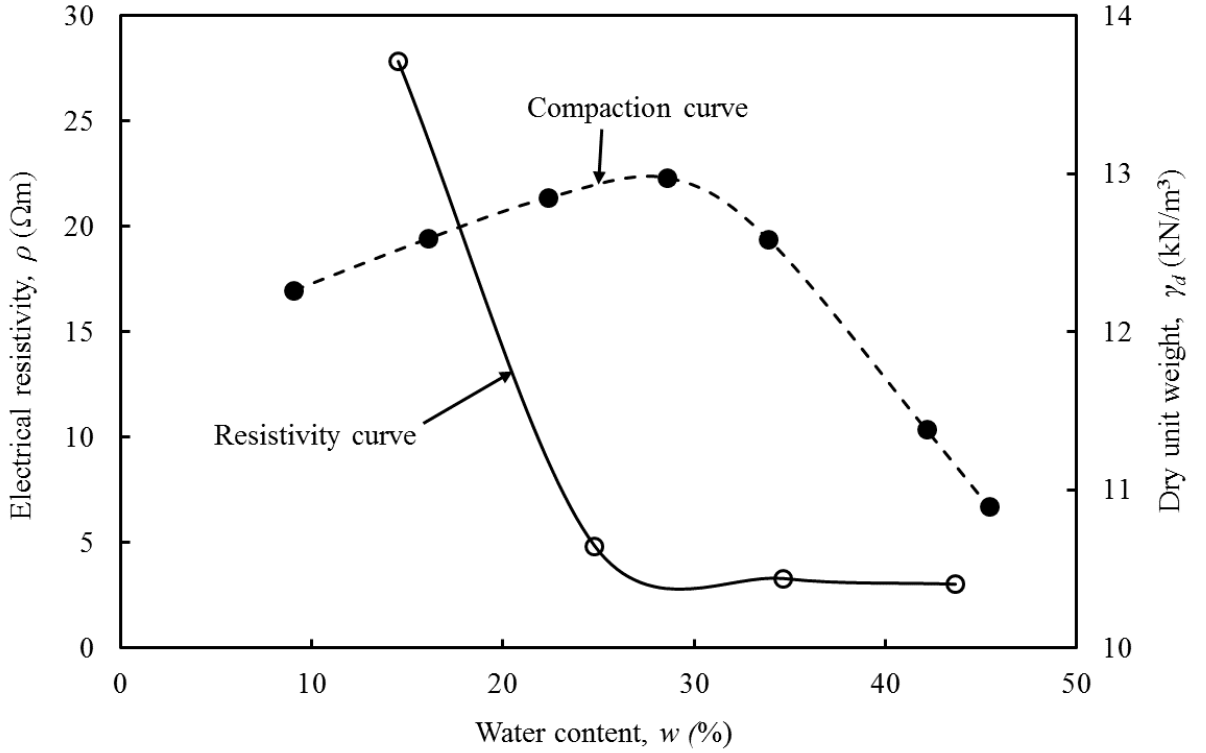

Figure 4.8: Electrical resistivity and compaction curves for a mixture of 80% bentonite and 20% sand.

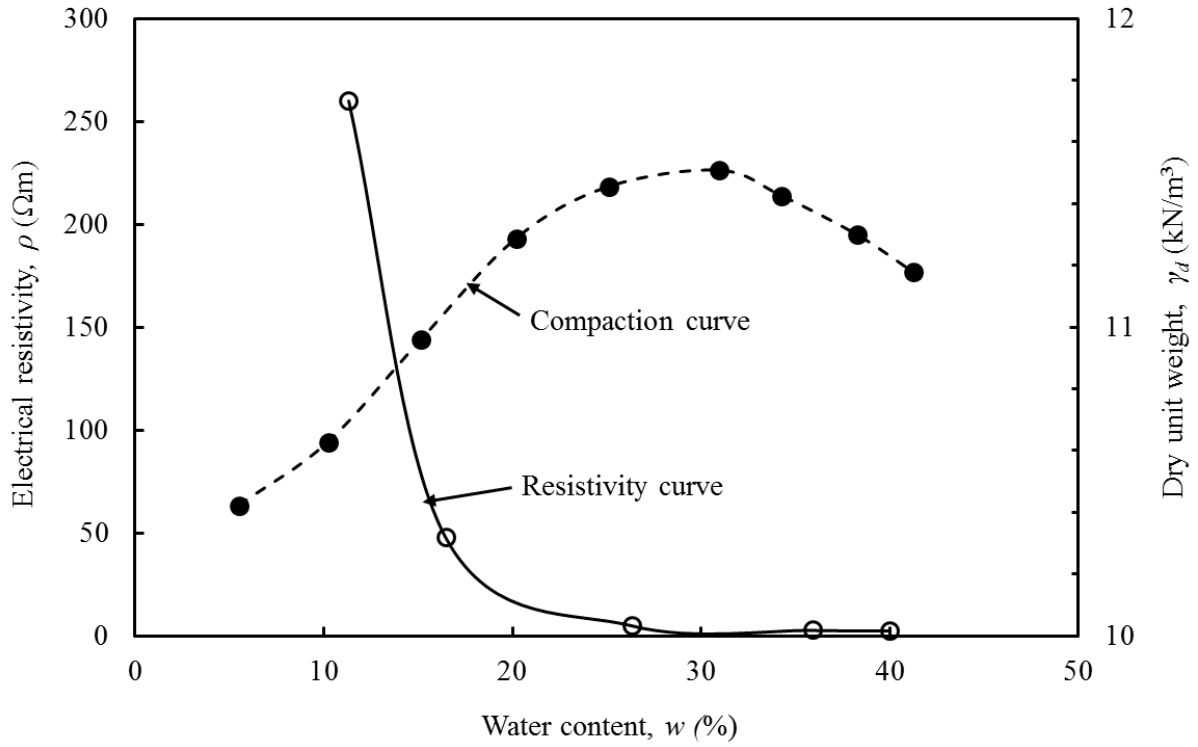

Figure 4.9: Electrical resistivity and compaction curves for bentonite.

It is interesting to note that w_T occurs on the wet-side of optimum for all sand-bentonite mixtures (Figures 4.5 through 4.8). Whereas, for the bentonite (Figure 4.9) and sand (Figure 4.4), w_T is on the dry-side of the optimum. For a sand-bentonite mix, the available porosity is less than that of bentonite or sand alone. As the resistivity of any soil is dependent on the amount of interstitial fluid and available porosity (Kibria and Hossain, 2012; Cardoso and Dias, 2017), hence, the above observation is made.

Figure 4.10 gives the comparison of the electrical resistivities of sand, bentonite and their mixtures for different water contents. It can be noticed that the effect of bentonite addition on the electrical resistivity of sand-bentonite mixture is most pronounced at 20%. Negligible impact on the resistivity is observed at bentonite contents >20%. A similar trend has been reported by Abu-Hassanein *et al.* (1996) and Kibria and Hossain (2014).

Interestingly, it can be noticed that the resistivity of sand is lower than the resistivity of bentonite at water content w below 15%. At w above 15%, the resistivity of the sand is greater than that of bentonite (Figure 4.10). These observations can be explained using the well-established fact that when less water is present in the clayey soil, the thickness of the double-layer of electric charges formed over the clay mineral surface, is less (Mitchell and Soga, 2005). The anions are strongly attracted to the clay particles and therefore, lesser ions are available

for the conduction of charge. In contrast, for sands, the conduction is dominated by available porosity and conductivity of interstitial fluid only. There is no surface conduction involved. Hence, at water contents below 15%, the resistivity of sand is observed to be lower compared to bentonite (Figure 4.10) due to availability of more ions for conduction in sand. However, at higher water content (>15%), for the clayey soils, double-layer thickness is greater. As a result, there are more ions available for conduction in bentonite. In addition to the pore fluid, the clay particles have surficial charges (Cardoso and Dias, 2017). Consequently, the resistivity of clay is observed to be lower than that of sand.

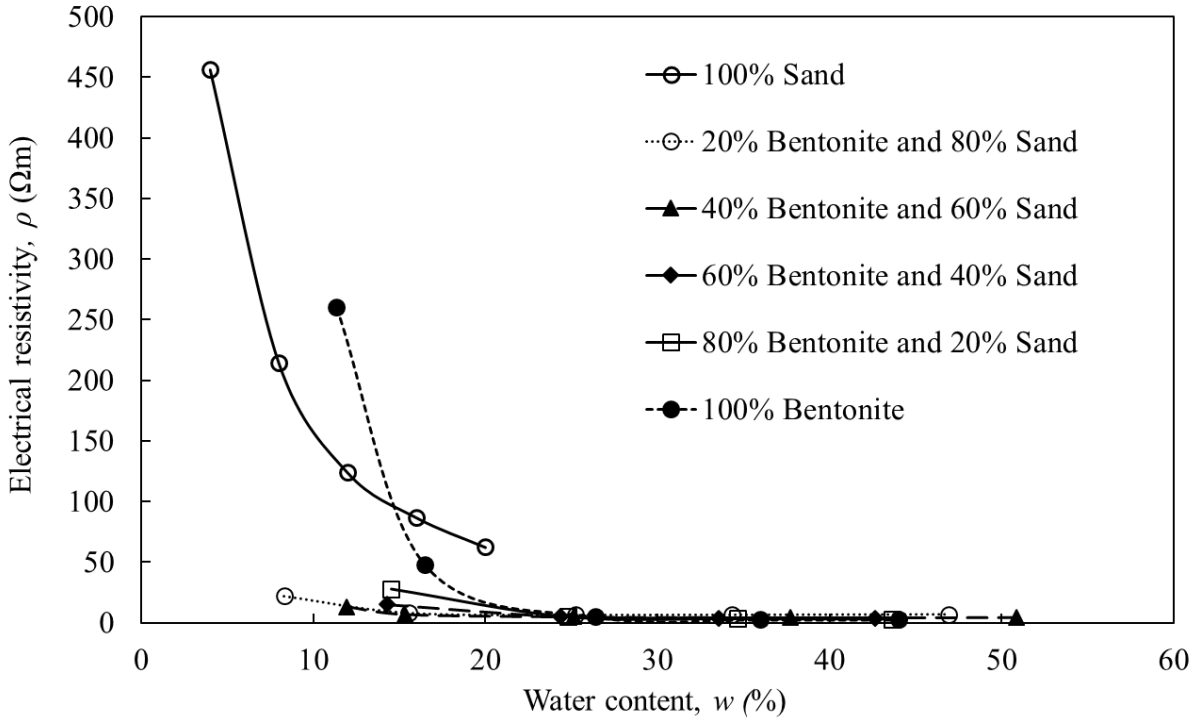

Figure 4.10: Comparison of electrical resistivities of sand, bentonite and their mixtures for different water contents.

It can also be noted that at any given value of water content, the resistivity values obtained for sand or bentonite alone, are greater than the resistivity of the sand-bentonite mixtures. This is as expected because when bentonite is added to sand, it occupies the interstitial pore voids, and it helps in conduction due to surficial charges.

The sand has greater resistivity compared to all other soil mixtures at $_w$ below 35% (Figures 4.4 to 4.9). Furthermore, the resistivity of bentonite is greater than resistivity of sand-bentonite mixtures at $_w$ below 20%. At higher water contents ($_w$>35% for sand and >20% for bentonite),

the effect of bentonite addition on the electrical resistivity of a soil mixture becomes insignificant.

Shah and Singh (2005) proposed the following generalized form of Archie's law (1942) for the bulk conductivity of soil σ for fine-grained soils in terms of its pore water conductivity σ_w, volumetric water content θ and percentage of clay fraction in soil p:

$$\sigma = c \times \sigma_w \times \theta^m \tag{4.3}$$

where, c and m are fitting parameters such that,

$c = 1.45$ when $p < 5\%$ and $c = 0.6 \times CL^{0.55}$ when $p \geq 5\%$

$m = 1.25$ when $p < 5\%$ and $m = 0.92 \times CL^{0.2}$ when $p \geq 5\%$

Furthermore, Yan *et al.* (2012) developed the following equation for resistivity ρ of soil in terms of volumetric water content θ:

$$\rho = 1828.4\, e^{-0.1214\theta} \tag{4.4}$$

Eqs. (4.3) and (4.4) were used to predict the electrical resistivity values corresponding to the sand-bentonite mixtures used in this study. The resistivity values predicted using Eqn. (4.4), were found to be closer to the experimentally obtained values compared to the resistivity values generated from Eqn. (4.3). The observed difference in resistivity values generated using Eqn. (4.4) and the actual values, could be because the equation does not consider the changes in the sand-bentonite composition. Therefore, there is a scope for the development of a correlation based on these past research works. It should be kept in mind, however, that Eqns. (4.3) and (4.4) (Shah and Singh, 2005; Yan *et al.*, 2012) have been developed for soils that are similar, but not the same as the soils used in this study.

Hence, based on past studies and using regression analysis, a generalized equation for the variation of resistivity ρ (Ωm), of a sand-bentonite mixture containing both sand and bentonite, with volumetric water content θ (dimensionless) can be given as:

$$\log \rho = a \times (\log \theta)^{-b} \tag{4.5}$$

where, a (Ωm) and b (dimensionless) are constants corresponding to a particular soil type and pore fluid. For the sand-bentonite mixtures used in this study, a and b in terms of bentonite content p_b (dimensionless) can be given as:

$$a = 49.91 p_b^{\,2} - 29.04 p_b + 4.05 \tag{4.6}$$

$$b = 5.22 p_b + 0.13 \tag{4.7}$$

Here, bentonite content is:

$$p_b = \left(\frac{m_b}{m_b + m_s} \right) \tag{4.8}$$

where, m_b (kg) is the mass of bentonite and m_s (kg) is the mass of sand.

4.4 Conclusions

The following conclusions summarise the observations made in this study:

- The compaction behaviour of the sand-bentonite mixture was found to resemble that of bentonite at higher bentonite contents.
- The electrical resistivity of each sand-bentonite mixture was found to decrease rapidly with an increase in water content. However, after a certain water content, this rate of decrease reduced significantly. This specific water content was found to be different for each of the sand-bentonite mixtures.
- At water content below 15%, the resistivity of bentonite was greater than that of sand. This reversed at water contents above 15%.
- The change in decreasing trend of resistivity occurred on the wet-side of the optimum for sand-bentonite mixtures and on the dry-side of the optimum for sand and bentonite.
- The effect of bentonite addition was negligible on the electrical resistivity of sand-bentonite mixture at bentonite contents over 20%.

It should be noted that the reported findings should be used for sand and bentonite types similar to those used in the present study. Further, the new concept as presented here can be used to develop correlations between compaction characteristics and resistivity of other lining materials.

References

Abramson, L.W., Lee, T.S., Sharma, S. and Boyce, G.M. (1995). Slope stability and stabilization methods. John Wiley and Sons, Inc. New York.

Abu-Hassanein, Z.S., Benson, C.H. and Blotz, L.R. (1996). Electrical resistivity of compacted clays. *Journal of Geotechnical Engineering* 122(5), 397-406, DOI: 10.1061/(ASCE)0733-9410(1996)122:5(397).

Archie, G.E. (1942). The electrical resistivity log as an aid in determining some reservoir characteristics. *Society of Petroleum Engineers* 146(01), 54-61, DOI: 10.2118/942054-G.

AS 1289.4.4.1 (1997). Methods of testing soils for engineering purposes. Standards Australia, Sydney, NSW, Australia.

AS 1289.5.1.1 (2003). Method for testing soils for engineering purposes-soil compaction and density tests-determination of the dry density/moisture content relation of a soil using standard compactive effort. Standards Australia, Sydney, NSW, Australia.

Baawain, M.S., Al-Futaisi, A.M., Ebrahimi, A. and Omidvarborna, H. (2018). Characterizing leachate contamination in a landfill site using TDEM (Time Domain Electromagnetic) imaging. *Journal of Applied Geophysics* 151(2018), 73-81, DOI: 10.1016/j.jappgeo.2018.02.002.

Bai, W., Kong, L. and Guo, A. (2013). Effects of physical properties on electrical conductivity of compacted lateritic soil. *Journal of Rock Mechanics and Geotechnical Engineering* 5(5), 406-411, DOI: 10.1016/j.jrmge.2013.07.003.

Cardoso, R. and Dias, A.S. (2017). Study of the electrical resistivity of compacted kaolin based on water potential. *Engineering Geology* 226(2017), 1-11, DOI: 10.1016/j.enggeo.2017.04.007.

Chapuis, R.P. (2002). The 2000 RM Hardy Lecture: Full-scale hydraulic performance of soil bentonite and compacted clay liners. *Canadian Geotechnical Journal* 39(2), 417-439, DOI: 10.1139/t01-092.

Chapuis, R.P. (1990). Sand-bentonite liners: predicting permeability from laboratory tests. *Canadian Geotechnical Journal* 27(1), 47-57, DOI:10.1139/t90-005.

Choo, H., Kim, J., Lee, W. and Lee, C. (2016). Relationship between hydraulic conductivity and formation factor of coarse-grained soils as a function of particle size. *Journal of Applied Geophysics* 127(2016), 91-101, DOI: 10.1016/j.jappgeo.2016.02.013.

Chu, Y., Liu, S., Bate, B. and Xu, L. (2018). Evaluation on expansive performance of the expansive soil using electrical responses. *Journal of Applied Geophysics* 148(2018), 265-271, DOI: 10.1016/j.jappgeo.2017.12.001.

Daniel, D.E. (1984). Predicting hydraulic conductivity of clay liners. *Journal of Geotechnical Engineering* 110(2), 285-300, DOI: 10.1061/(ASCE)0733-9410(1984)110:2(285)#sthash.g48WNynP.dpuf.

Darayan, S., Liu, C., Shen, L.C. and Shattuck, D. (1998). Measurement of electrical properties of contaminated soil. *Geophysical prospecting* 46(5), 477-488, DOI: 10.1046/j.1365-2478.1998.00104.x.

Darilek, G.T. and Parra, J.O. (1989). The electrical leak location method for geomembrane liners. *Journal of Hazardous Materials* 21(2), 177-187, DOI:10.1016/0304-3894(89)85008-3.

Doolittle, J.A., Jenkinson, B., Hopkins, D., Ulmer, M. and Tuttle, W. (2006). Hydropedological investigations with ground-penetrating radar (GPR): Estimating water-table depths and local ground-water flow pattern in areas of coarse-textured soils. *Geoderma* 131(3-4), 317-329, DOI: 10.1016/j.geoderma.2005.03.027.

Elsharief, A.M. and Sufian, M. (2018). Time rate of swelling of compacted highly plastic clay soil from Sudan. *Proceedings of Materials science, Engineering and Chemistry Web of Conferences*, EDP Sciences, France 149, pp. 1-5, DOI:10.1051/matecconf/201814902032.

Fityus, S.G., Smith, D.W. and Booker, J.R. (1999). Contaminant transport through an unsaturated soil liner beneath a landfill. *Canadian Geotechnical Journal* 36 (2), 330-354, DOI:10.1139/t98-112.

Fukue, M., Minato, T., Horibe, H. and Taya, N. (1999). The micro-structures of clay given by resistivity measurements. *Engineering Geology* 54(1-2), 43-53, DOI:10.1016/S0013-7952(99)00060-5.

Harrop-Williams, K. (1985). Clay liner permeability: evaluation and variation. Journal of *Geotechnical Engineering* 111(10), 1211-1225, DOI:10.1061/(ASCE)0733-410(1985)111:10(1211).

Holtz, W.G. (1985). Predicting hydraulic conductivity of clay liners: Discussion. *Journal of Geotechnical Engineering* 111, 1457-1459, DOI:10.1061/(ASCE)0733-9410(1984)110:2(285).

Islam, T. and Chik, Z. (2013). Improved near surface soil characterizations using a multilayer soil resistivity model. Geoderma 209, 136-142, DOI: 10.1016/j.geoderma.2013.06.015.

Jessberger, H.L. and Beine, R.A. (1981). Impermeabilisation of disposal sites by impervious blankets consisting of mine refuse. *Proceedings of l0th International Conference on Soil Mechanics and Foundation Engineering*, Stockholm 4, pp. 745-746.

Kalinski, R. and Kelly, W. (1993). Estimating water content of soils from electrical resistivity. *Geotechnical Testing Journal* 16(3), 323-32, DOI: 10.1520/GTJ10053J.

Kibria, G. and Hossain, M.S. (2012). Investigation of geotechnical parameters affecting electrical resistivity of compacted clays. *Journal of Geotechnical and Geoenvironmental Engineering* 138(12), 1520-1529, DOI:10.1061/(ASCE)GT.1943-5606.0000722.

Kibria, G. and Hossain, M.S. (2014). Effects of bentonite content on electrical resistivity of soils. *Proceedings of the Geo-Congress 2014: Geo-characterization and Modeling for Sustainability*, p. 2404-2413, DOI: 10.1061/9780784413272.233.

Kumar, S. and Yong, W.L. (2002). Effect of bentonite on compacted clay landfill barriers. *Soil and Sediment Contamination* 11(1), 71-89, DOI: 10.1080/20025891106709.

Long, M., Donohue, S., L'Heureux, J.S., Solberg, I.L., Rønning, J.S., Limacher, R. and Lecomte, I. (2012). Relationship between electrical resistivity and basic geotechnical parameters for marine clays. *Canadian Geotechnical Journal* 49(10), 1158-1168, DOI: 10.1139/t2012-080.

Mahmoudzadeh, M.R., Francés, A.P., Lubczynski, M. and Lambot, S. (2012). Using ground penetrating radar to investigate the water table depth in weathered granites—Sardon case study, Spain. *Journal of Applied Geophysics* 79(2012), 17-26, DOI: 10.1016/j.jappgeo.2011.12.009.

McCarter, W.J. (1984). The electrical resistivity characteristics of compacted clays. *Geotechnique* 34(2), 263-267, DOI: 10.1680/geot.1984.34.2.263.

Merritt, A.J., Chambers, J.E., Wilkinson, P.B., West, L.J., Murphy, W., Gunn, D. and Uhlemann, S. (2016). Measurement and modelling of moisture—electrical resistivity relationship of fine-grained unsaturated soils and electrical anisotropy. *Journal of Applied Geophysics* 124(2016), 155-165, DOI: 10.1016/j.jappgeo.2015.11.005.

Mitchell, J.K. and Soga, K. (2005). Fundamentals of Soil Behavior. John Wiley and Sons, Inc. New York.

Oh, M., Seo, M.W., Lee, S. and Park, J. (2008). Applicability of grid-net detection system for landfill leachate and diesel fuel release in the subsurface. *Journal of Contaminant Hydrology* 96(1-4), 69-82, DOI: 10.1016/j.jconhyd.2007.10.002.

Pandey, L.M.S. and Shukla, S.K. (2017). Detection of leachate contamination in Perth landfill base soil using electrical resistivity technique. *International Journal of Geotechnical Engineering*, 1-12, DOI: 10.1080/19386362.2017.1339763.

Pandey, L.M.S., Shukla, S.K. and Habibi, D. (2015). Electrical resistivity of sandy soil. *Geotechnique Letters* 5(3), 178–185, DOI: 10.1680/jgele.15.00066.

Pandey, L.M.S., Shukla, S.K. and Habibi, D. (2017). Resistivity profiles of Perth soil in Australia in leak-detection test. *Geotechnical Research* 4(4), 214-221, DOI: 10.1680/jgere.17.00014.

Panthulu, T.V., Krishnaiah, C. and Shirke, J.M. (2001). Detection of seepage paths in earth dams using self-potential and electrical resistivity methods. *Engineering Geology* 59(3-4), 281-295, DOI: 10.1016/S0013-7952(00)00082-X.

Rohini, K. and Singh, D.N. (2004). Methodology for determination of electrical properties of soils. *Journal of Testing and Evaluation* 32(1), 1-7, DOI:10.1520/JTE11884.

Rowe, R.K. (2005). Long-term performance of contaminant barrier systems. *Geotechnique* 55(9), 631-678, DOI:10.1680/geot.2005.55.9.631.

Rowe, R. K. (2012). Short-and long-term leakage through composite liners. The 7th Arthur Casagrande Lecture. *Proceedings of the 14th Pan-American Conference on Soil Mechanics and Geotechnical Engineering*, Toronto, Ont., October 2011. Canadian Geotechnical Journal 49, 141-169, DOI: 10.1139/t11-092.

Rowe, R.K., Quigley, R.M., Brachman, R.W., Booker, J.R. and Brachman, R. (2004). Barrier Systems for Waste Disposal Facilities (No. Ed. 2). London: Taylor and Francis (E and FN Spon Press).

Shah, K.L. (2000). Basics of Solid and Hazardous Waste Management Technology. Prentice Hall.

Shah, P.H. and Singh, D.N. (2005). Generalized Archie's law for estimation of soil electrical conductivity. *Journal of ASTM International* 2(5), 1-20, DOI: 10.1520/JAI13087.

Shamal, S.A.M., Alhwaimel, S.A. and Mouazen, A.M. (2016). Application of an on-line sensor to map soil packing density for site specific cultivation. *Soil and Tillage Research* 162, 78-86, DOI: 10.1016/j.still.2016.04.016.

Shukla, S. K. (2016). An Introduction to Geosynthetic Engineering, CRC Press, Taylor & Francis Group, Florida, USA.

Sirieix, C., Genelle, F., Barral, C., Touze-Foltz, N., Riss, J. and Bégassat, B., (2016). Characterizing the ageing of a geosynthetic clay liner through electrical resistivity. *Canadian Geotechnical Journal* 53(3), 423-430, DOI: 10.1139/cgj-2015-0111.

Wang, J., Zhang, X. and Du, L. (2017). A laboratory study of the correlation between the thermal conductivity and electrical resistivity of soil. *Journal of Applied Geophysics* 145, 12-16, DOI: 10.1016/j.jappgeo.2017.07.009.

Yan, M., Miao, L. and Cui, Y. (2012). Electrical resistivity features of compacted expansive soils. *Marine Georesources and Geotechnology* 30(2), 167-179, DOI: 10.1080/1064119X.2011.602384.

Yochim, A., Zytner, R.G., McBean, E.A., Endres, A.L. (2013). Estimating water content in an active landfill with the aid of GPR. *Waste Management* 33(10), 2015-2028, DOI: 10.1016/j.wasman.2013.05.020.

Yoon, G.L. and Park, J.B. (2001). Sensitivity of leachate and fine contents on electrical resistivity variations of sandy soils. *Journal of Hazardous Materials* 84(2-3), 147-161, DOI: 10.1016/S0304-3894(01)00197-2.

CHAPTER 5

DEVELOPMENT OF AN INNOVATIVE LINER LEAK DETECTION TECHNIQUE

This chapter is based on the published in Geotechnical Testing Journal, ASTM, as listed in Section 1.6. The details presented here are the same, except some changes in the layout in order to maintain a consistency in the presentation throughout the thesis.

5.1 Introduction

Lining systems are used in different waste storage and handling facilities, such as landfills, leachate collection ponds, underground storage tanks (USTs), sump wells, red mud ponds, tailing dams, etc., to control the migration of leachates generated from wastes, and the consequent environmental contamination (Bouazza and Impe, 1998). Different natural and man-made products are used to make liners (Rowe *et al.*, 2004; Shukla, 2016). The lining system is designed based on the type of waste that will be handled at the site (Daniel, 1993; Rowe, *et al.* 2004; Shukla and Yin, 2006). Figure 1 shows a typical landfill site in Perth metropolitan region (Western Australia, Australia), installed with a geosynthetic clay (GCL) liner.

Although the liners are engineered to be durable over their intended lifetime, harsh operating conditions, poor placement assurance and inadequate construction quality assurance (CQA), can result in the failure of the lining systems. This leads to soil and groundwater pollution due to leakage of leachates through the liners (Mohamed *et al.*, 2002; Rowe *et al.*, 2004; Oh *et al.*, 2008; Ben Othmen and Bouassida, 2013; Xie *et al.*, 2015a; Xie *et al.*, 2015b). As per Giroud (1984), “All liners leak.”. Hence, to control and minimize the resulting environmental pollution, all the lining systems must be monitored.

There are various methods for the detection of leakages, such as groundwater monitoring wells, lysimeters, diffusion hoses, capacitance sensors, tracers, electro-chemical sensing cables, resistivity cone penetration test (RCPT), ground penetration radar (GPR), time domain reflectometry (TDR), etc. (Oh *et al.*, 2008; ASTM D6431-99(2010)). Of these, the more

prevalent conventional monitoring method which is currently being practiced by different waste storage and handling facilities, is the use of monitoring wells. However, this method proves to be ineffective because by the time the leakage issue is detected, a substantial amount of soil and ground water is already contaminated (Mohamed *et al.*, 2002).

Figure 5.1: Geosynthetic liner at the Millar road landfill and recycling facility, Perth, WA, Australia.

Other field diagnostic techniques which have on-site sampling and laboratory analysis, prove to be time and cost intensive. Hence, the use of electrical leak detection methods such as water puddle method (ASTM D7002 - 16), conductive geomembrane spark test (ASTM D7240 - 06(2011)), water lance method (ASTM D7703 - 16), arc testing method (ASTM D7953 - 14), electrode grid method (ASTM D6747 − 15), etc., has gained prevalence because of their ease of installation and operation, and low operating costs (Oh *et al.*, 2008; Ben Othmen and Bouassida, 2013). These methods make use of subsurface contamination and electrical properties of the liners to detect defects. However, their extensive use is limited by high capital costs (Ben Othmen and Bouassida, 2013). Moreover, it is important to detect contamination issues as soon as they arise, so that the hazard to the environment can be mitigated early (Mohamed *et al.*, 2002). Furthermore, delays in defect detection also result in severe contamination issues and greater remediation costs. Hence, there is a significant scope for the

development of new diagnostic techniques which can investigate subsurface contamination at the onset and therefore, detect leaks across liners.

This paper gives a detailed overview of the development of an innovative system for the detection and localization of leaks in liners by simulating the field conditions, based on the electrical resistivity variations of base soil layer/leakage detection layer. This technique was developed with a view to its application in permanent monitoring systems for various waste impoundments in order to monitor the entire area below the liners in construction, operation and post-closure phases. Trial runs have been conducted and the system was found to be effective in ascertaining and locating liner leaks.

5.2 Principle of Operation

It is a well-established fact that all soils generally have very high electrical resistivity. In contrast, leachates generally possess low electrical resistivity. Hence, the addition of even a small of amount of contaminating fluid to the soil results in a sharp decrease in its resistivity. This change in resistivity can be easily measured to detect contamination of the soil layer (Oh *et al.,* 2008; Ben Othmen and Bouassida, 2013; Pandey and Shukla, 2017). This concept forms the basis for the development of the new leak detection system (LDS).

Figure 5.2 shows the schematic profile of a typical single liner system for waste containment facilities. The system consists of a leachate collection layer with high hydraulic conductivity (k ~10^{-1} m/s), a compacted clay layer (k ~10^{-9} m/s) covered with HDPE geomembrane, and a leak detection/recovery layer (k ~10^{-1} m/s). In case of development of a failure or defect in the lining system, leachates generated from the waste, contaminate the underlying soil of the leak detection layer. Therefore, the resistivity of this base soil layer is rapidly decreased. Alternatively, if the resistivity of the soil in the leak detection layer registers a sharp decrease, it can be deduced that these changes may have been produced due to leachate contamination. As a result, leakage issues through the liner can be easily determined.

It can be concluded from the preceding discussion that it is possible to establish a permanent monitoring system for liners in waste containment facilities using a suitable sensing technique, based on the electrical resistivity of soil, paired with on-line monitoring. Such a system can be highly effective in detecting liner defects at their onset, and will therefore aid in the timely mitigation of soil and groundwater contamination hazard.

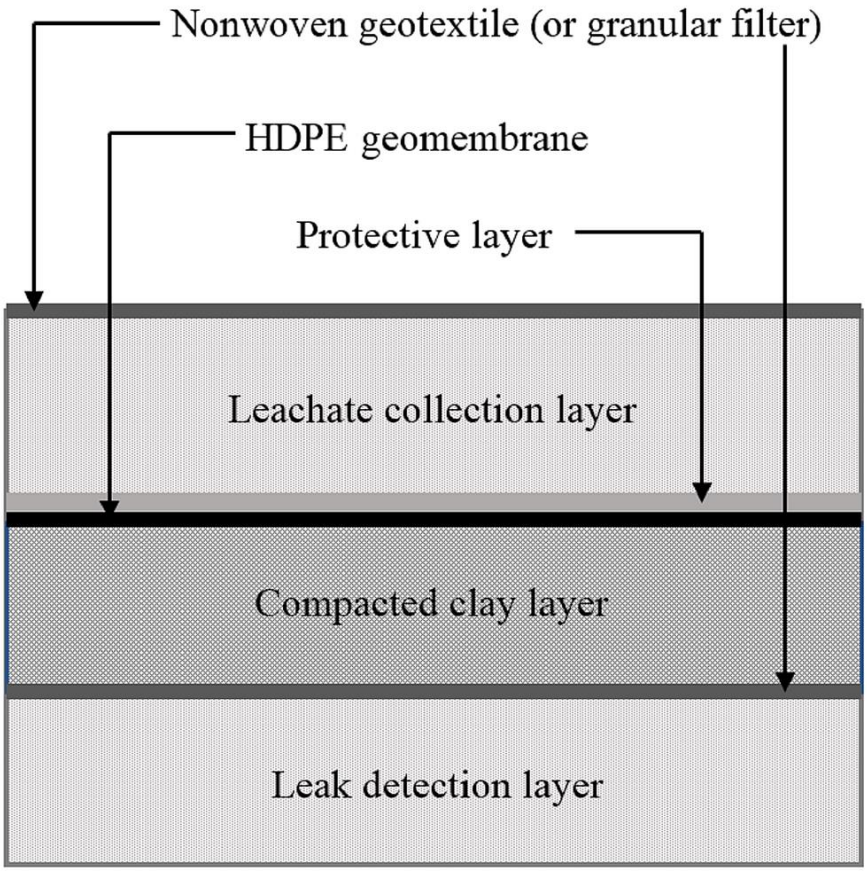

Figure 5.2: Schematic profile of a typical single liner system.

5.3 System Design

The design of the system makes use of the well-known principle of Ohm's law. The electrical resistivity (R in ohm (Ω)) of any soil is determined by providing a known current (i in ampere (A)) across a pair of electrodes and recording the subsequent voltage drop (V in volt (V)). The resistance is then computed as follows:

$$V = iR \tag{5.1}$$

However, resistance is not a true material property as it also depends on the dimensions of the sample being tested. Hence, it is used to calculate resistivity (ρ, Ωm), which is an intrinsic property of the material, using the following equation:

$$R = \frac{\rho L}{A} \tag{5.2}$$

where A is the cross-sectional area (m^2) and L is the length (m).

As previously discussed, it is relatively easy to obtain resistance readings for any soil specimen by passing a known current and recording the resulting voltage drop using any suitable device. However, to implement the electrical resistivity method into practice for the new leak detection system (LDS), a system geometry had to be devised which would enable the conversion of the recorded resistance to the resistivity of the soil. To address this problem, the Australian Standard AS 1289.4.4.1-1997 was chosen as a basis to develop the new technique.

The standard AS 1289.4.4.1-1997 describes the method for the testing of a soil specimen to determine its electrical resistivity using a four-electrode technique. A schematic diagram of the experimental setup, as recommended by AS 1289.4.4.1-1997, is shown in Figure 5.3. As per this method, a resistivity box with two outer plate electrodes, C_1 and C_2, and two inner potential measuring pin electrodes, P_1 and P_2, is used. Connections are made as shown in Figure 5.3. Current is injected through the outer plate electrodes and the resulting voltage drop is recorded across the inner potential measuring pins. Resistance is calculated using the Eqn. (5.1). Alternatively, the resistance reading can be directly obtained using any suitable four-point ground resistance testing machine such as AEMC 6471 tester. As the length and the area of the cross-sectional are known, Eqn. (5.2) can be used to calculate the resistivity of the soil specimen. This test method has been described in detail by Pandey and Shukla (2017).

Building on the guidelines put forth by the Australian Standard AS 1289.4.4.1-1997, the soil box for the leak detection system (LDS) was developed, as shown in Figure 5.4. The box was designed to represent an actual waste containment site with a geomembrane (GMB) liner placed on top of a soil layer (leakage detection layer). Leak was introduced intentionally in the GMB liner. Controlled leakage through the liner was then established to study the resistivity profile of the soil layer, in order to detect the liner leak.

The main concept behind the design was to detect contamination in the soil layer using resistivity method, and hence, to determine the liner leak at the beginning of its development. It was expected that as the depth or the distance from the introduced liner leak would increase, the obtained resistivity of the soil would decrease.

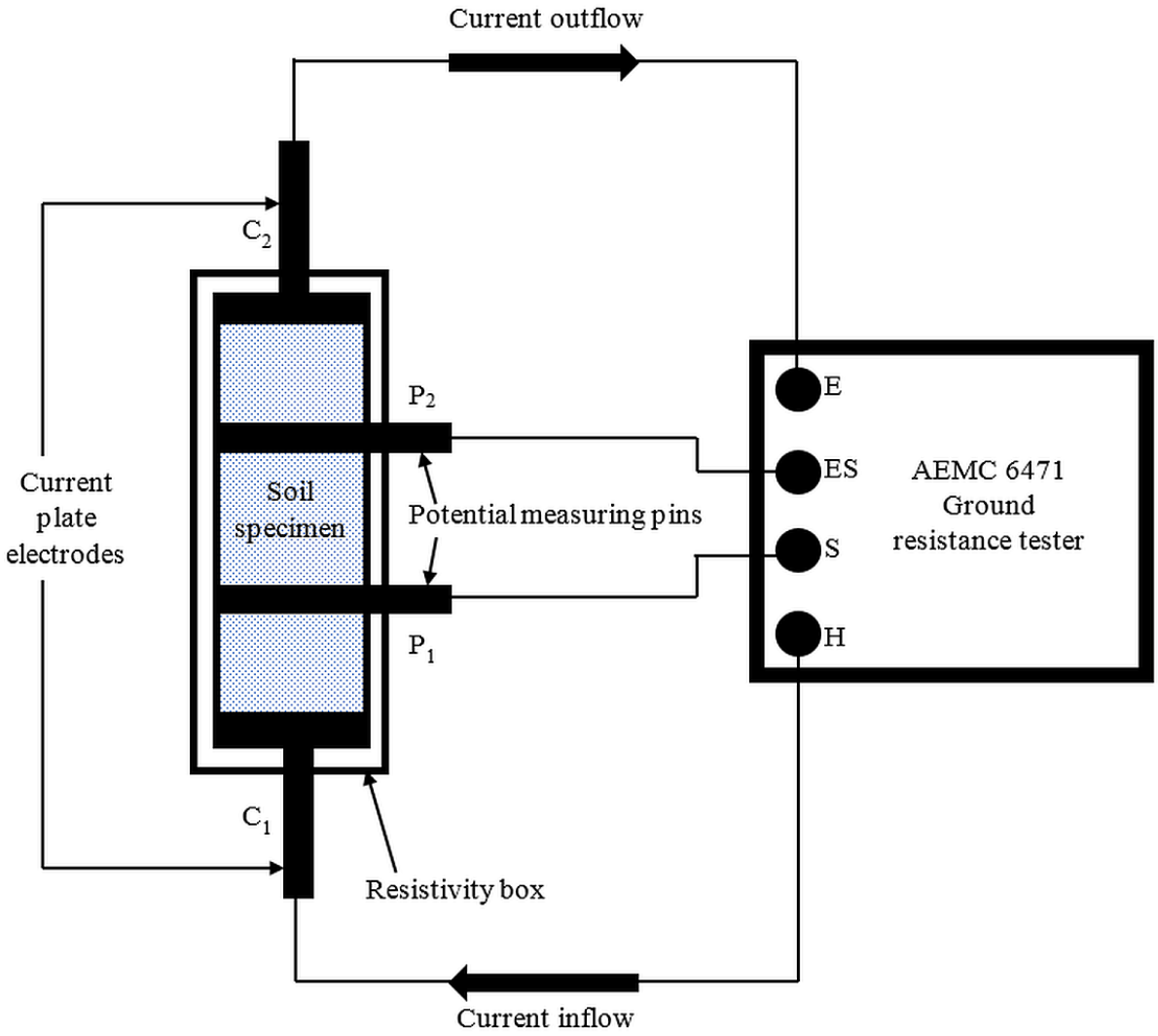

Figure 5.3: Schematic diagram of the experimental set-up for the measurement of electrical resistivity.

5.4 Materials and Methods

5.4.1 Laboratory setup

Figure 5.5 is a photograph of the soil box designed for the leak detection system (LDS). The box with internal dimensions of 500 mm length, 200 mm width and 400 mm height, was fabricated using 12-mm thick non-conducting perspex sheet. All joints were waterproofed.

Two brass current plate electrodes of dimensions 200 mm by 200 mm, and 16 brass potential measuring pins of 4 mm diameter, were installed in the box (Figure 5.5). On one side of the box, sixteen holes were made, through which the potential pin electrodes could be inserted into

the box after filling it with the soil specimen. Additionally, on the opposite side of the box, sixteen grooves were made corresponding to the centre of each of the pins.

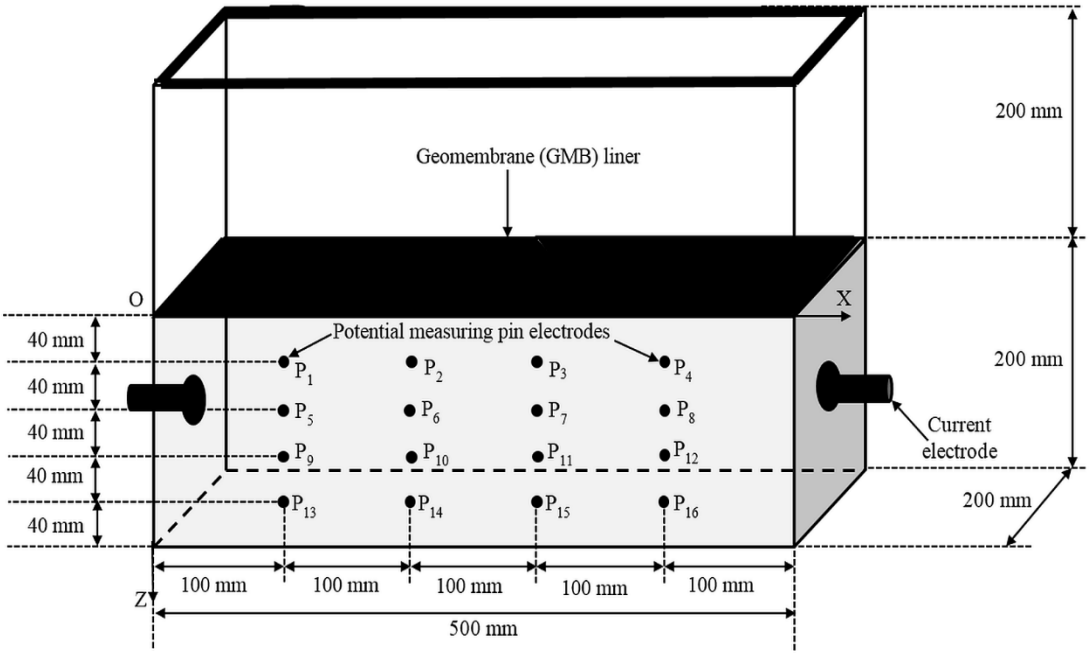

Figure 5.4: Isometric diagram of the soil box used for the leak detection system.

Figure 5.6 is a close-up of one of the sixteen potential measuring pin electrodes. Each pin was fabricated using a brass rod of 4 mm diameter. A piece of 218 mm length was cut from the rod. One end was shaped into a cone of 6 mm length, to enable the rod to be easily pushed into the compacted soil specimen. Furthermore, the pointed ends were intended to sit in one of the sixteen grooves made at the opposite end of the box to ensure that the rods were equispaced and remain immovable during the test. On the other end of the pre-cut rod, a knob was fixed, which was mounted with a rubber O-ring. This design ensures that no liquid will leak outside the soil box.

A groove of 8 mm diameter was made all around the box, with its centre at a height of 200 mm from the bottom. The purpose of this groove was to hold the geomembrane (GMB) in place over the soil layer. In addition, a gasket of 8 mm diameter was used to secure the GMB and therefore to achieve zero leakage.

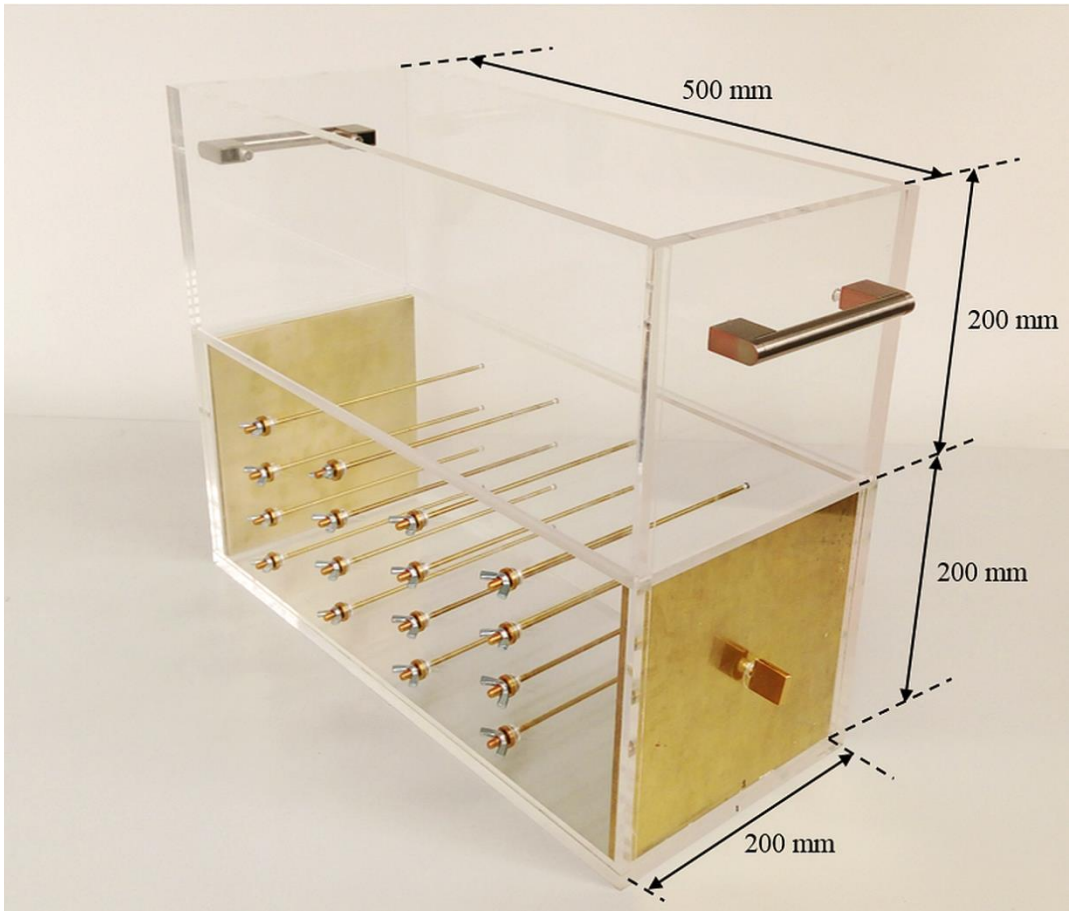

Figure 5.5: Photograph of the constructed soil box used for the leak detection system.

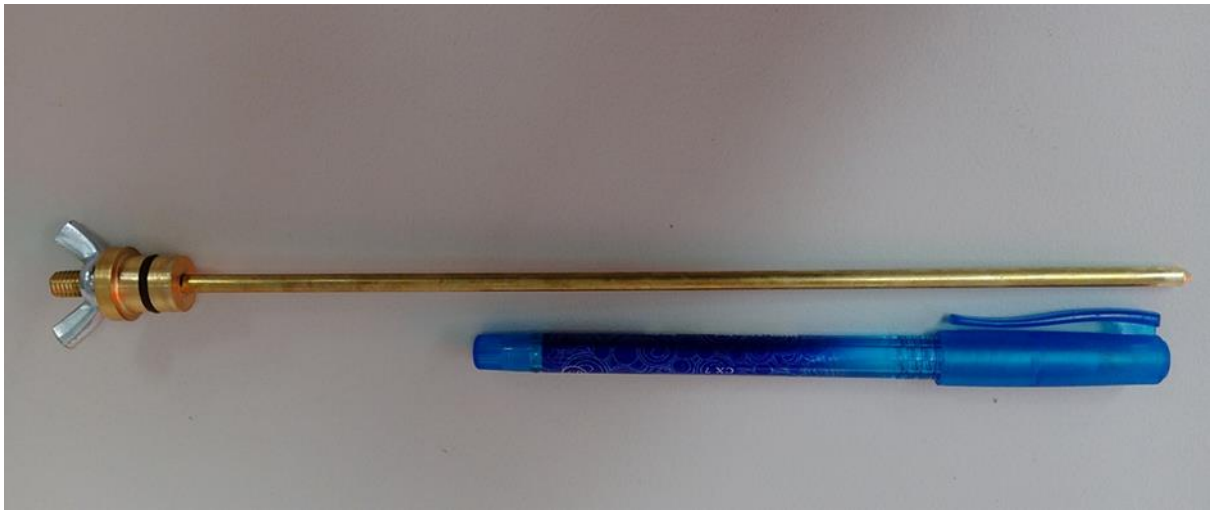

Figure 5.6: Close-up of one of the sixteen potential measuring pin electrodes.

5.4.2 Sample preparation

As a representation of the leakage detection layer (Figure 5.2), sandy soil was chosen for this study. It is widely available in Western Australia, and is extensively used in Perth metropolitan areas for various civil engineering projects. The properties of this poorly graded soil (SP) are detailed in Table 5.1.

5.4.3 Testing procedure

The soil was oven dried overnight at 110 ˚C. A relative density, of D_r = 100% was chosen for the test, to represent a real-life leakage detection layer of a lining system, as used in practice. The mass of oven dried soil to be filled in, was calculated using D_r and the known box dimensions. This sand was then filled into the soil box in five layers to ensure homogeneity.

Table 5.1: Physical properties of Perth sandy soil.

Properties	Values
Specific gravity of soil solids, G_s	2.68
Coefficient of uniformity, C_u	2.27
Coefficient of curvature, C_c	1.22
Effective size, D_{10} (mm)	0.15
Minimum dry unit weight, $\gamma_{d\min}$ (kN/m^3)	14.02
Maximum dry unit weight, $\gamma_{d\max}$ (kN/m^3)	15.56
Soil classification as per USCS (Unified Soil Classification System)	Poorly graded sand (SP)

A 220µ thick geomembrane (GMB) piece, of 550 mm length and 250 mm width, was used in this test. A puncture defect was intentionally made in the centre of the GMB with an angular gravel-size particle to replicate actual lining conditions. Figure 5.7 shows the pre-cut GMB and the gravel-size particle which was used to make the puncture defect at the centre of the GMB. The defect was covered initially with a piece of tape and uncovered at the beginning of the test,

that is, at time t = 0. Here, the leakage duration, $_t$ (min) is the duration for which the leakage through GMB was allowed. It is also the time at which the resistivity of the soil was recorded.

Then, the prepared leakage detection layer was covered with the pre-cut GMB layer to simulate a liner (Figure 5.8). As mentioned before, a rubber gasket (8 mm diameter) was fitted into the groove over the GMB layer to hold it in place and to ensure that there are no leakages, apart from the leakage through the intentionally introduced defect.

Figure 5.7: Pre-cut geomembrane (GMB) liner along with the gravel-size particle used to intentionally introduce defect.

A constant head of 100 mm of water, was maintained over the geomembrane for the test. After the water was filled in the box over the GMB liner, the tape which covered the defect was removed with a pair of tongs and the water was allowed to leak to the underlying soil layer. This time was recorded as t = 0.

The electrical resistance of soil (R) was obtained at regular time intervals using AEMC 6471 ground resistance testing machine. Current was injected through the outer plate electrodes

and the resulting potential drop across each pair of pin electrodes was measured to obtain the resistance, as shown in Figure 6.8. The resistivity, ρ was then calculated using Eqn. (5.2).

Figure 5.9 is a representation of the soil box used in this study. Here, X (mm) is the distance and Z (mm) is the depth of the mid-point of each pair of electrodes, respectively, as indicated in Figure 5.4. Twelve resistivity readings were obtained as shown in Figure 5.9. Resistivity between each electrode pair was assumed to be situated at the mid-point of the two electrodes, for simplicity in the analysis of results.

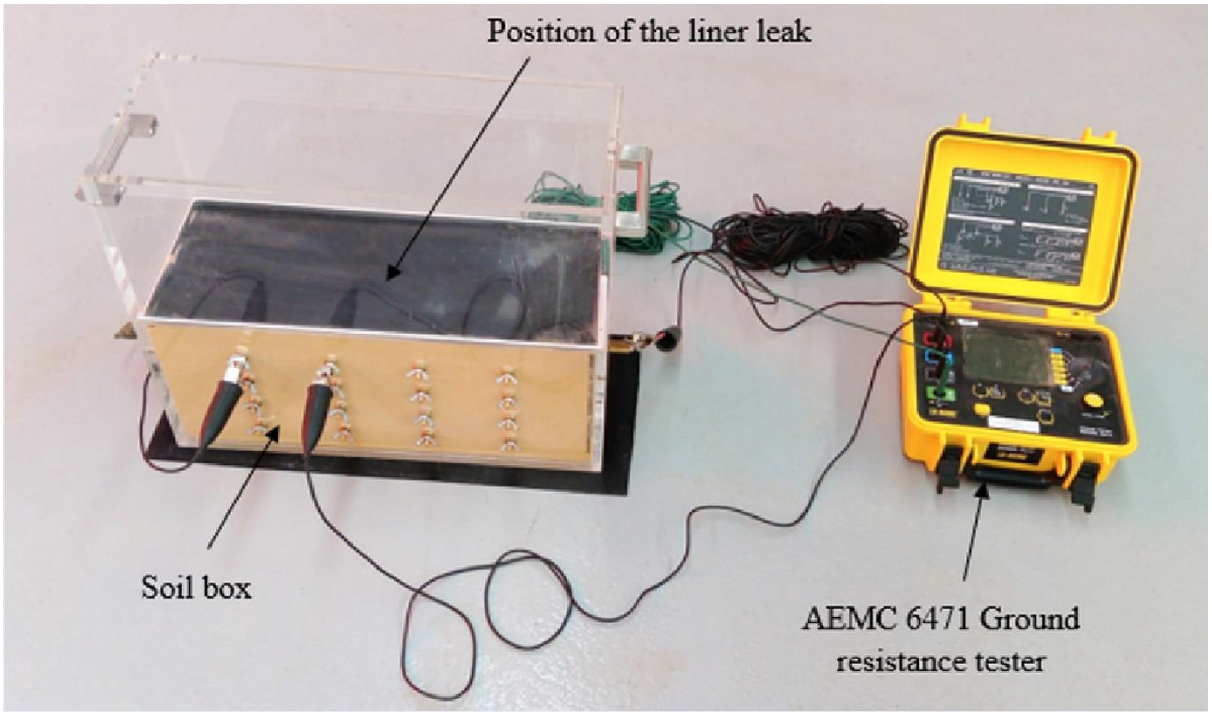

Figure 5.8: Experimental setup designed for liner leak detection.

5.5 Experimental Demonstration

To demonstrate the efficacy of the system in detecting leaks through liners, sample tests were conducted using tap water and municipal solid waste (MSW) landfill leachate as the leaching liquids. The properties of the tap water used in this study have been summarised in Table 5.2, while Table 5.3 provides the various properties of the landfill leachate used. As can be noticed from Table 5.3, in practice, the leachate composition is always a mix of both organic and inorganic components at most MSW landfills. As an example, the results obtained at the time duration, t = 30 min, have been presented in this paper (Figures 5.10 and 5.11).

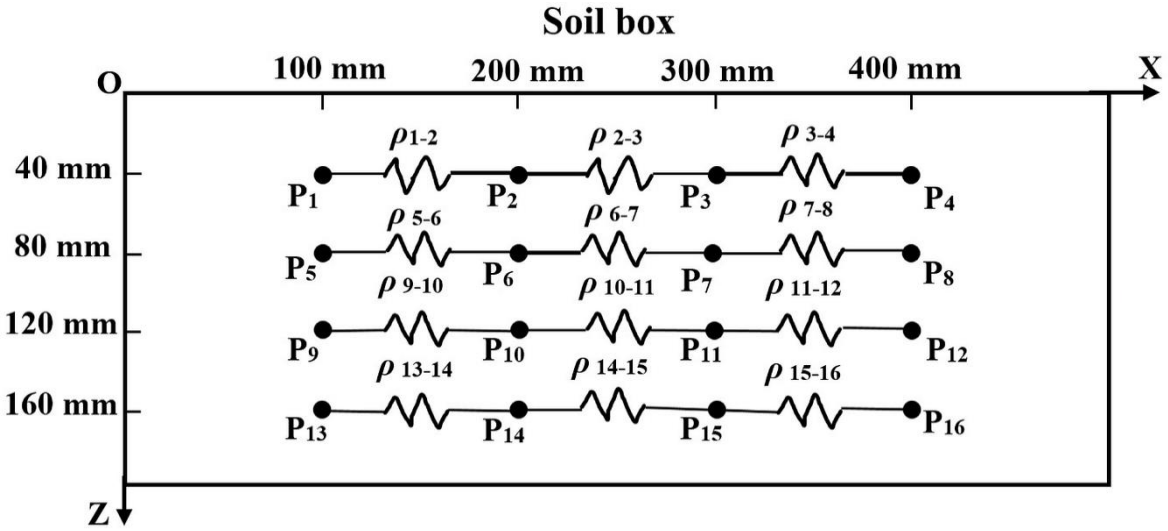

Figure 5.9: Representation of the soil box and associated resistivities.

5.6 Results and Discussion

Figures 5.10 and 5.11 give the resistivity profile for the leakage duration t = 30 min for the tap water and the landfill leachate, respectively. It can be observed that at a depth (z) of 40 mm, the resistivity first decreases and then increases with an increase in the distance (x) of the mid-point of electrode pair. This observation has been as per the expectation. The hole in the geomembrane (GMB) liner was positioned directly above the potential measuring electrodes, P_2 and P_3. Hence, the amount of water from the liner leakage between P_2 and P_3, would be greater than the amount of water between the other adjacent electrode pairs. Therefore, ρ_{2-3} was expected to be lower than ρ_{1-2} and ρ_{3-4}. Similar observations were made for the resistivities at a depth of 80 mm from the GMB liner.

It can be seen from Figures 5.10 and 5.11 that for a given x, the soil resistivity increases with an increase in the depth z. This observation also complies with the expectation that with an increase in z, the amount of water in soil would decrease, and consequently the resistivity would increase. However, at the depths of 120 and 160 mm, the variation of resistivity with x and z was found to be insignificant. This observation might differ with increase in the leakage duration t.

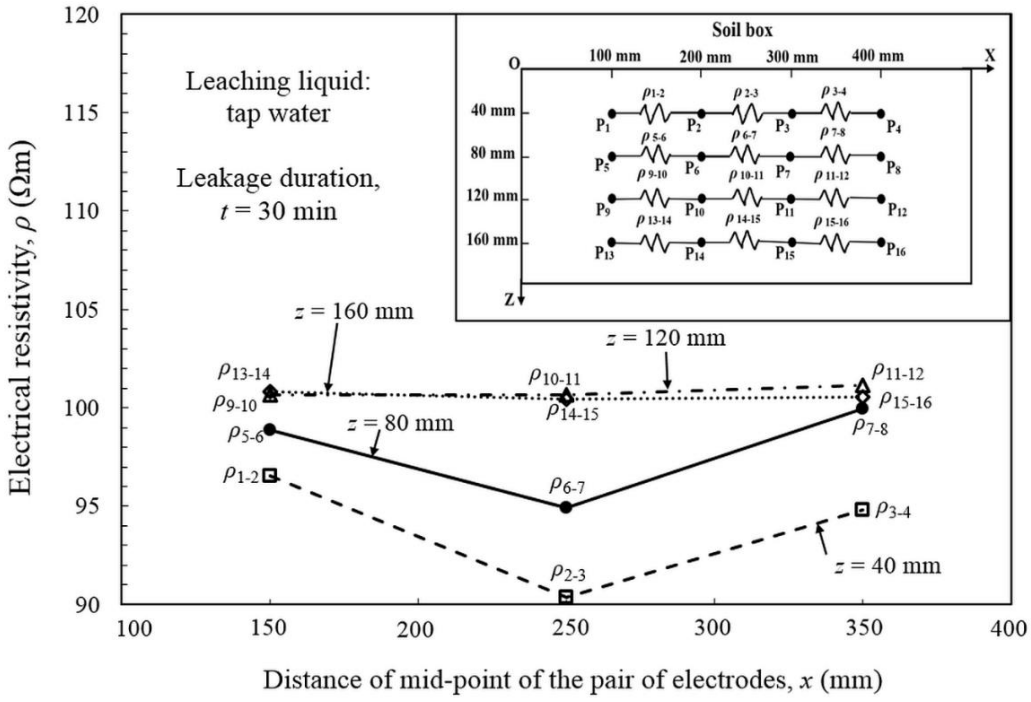

Figure 5.10: Resistivity profile of the leak detection system using tap water.

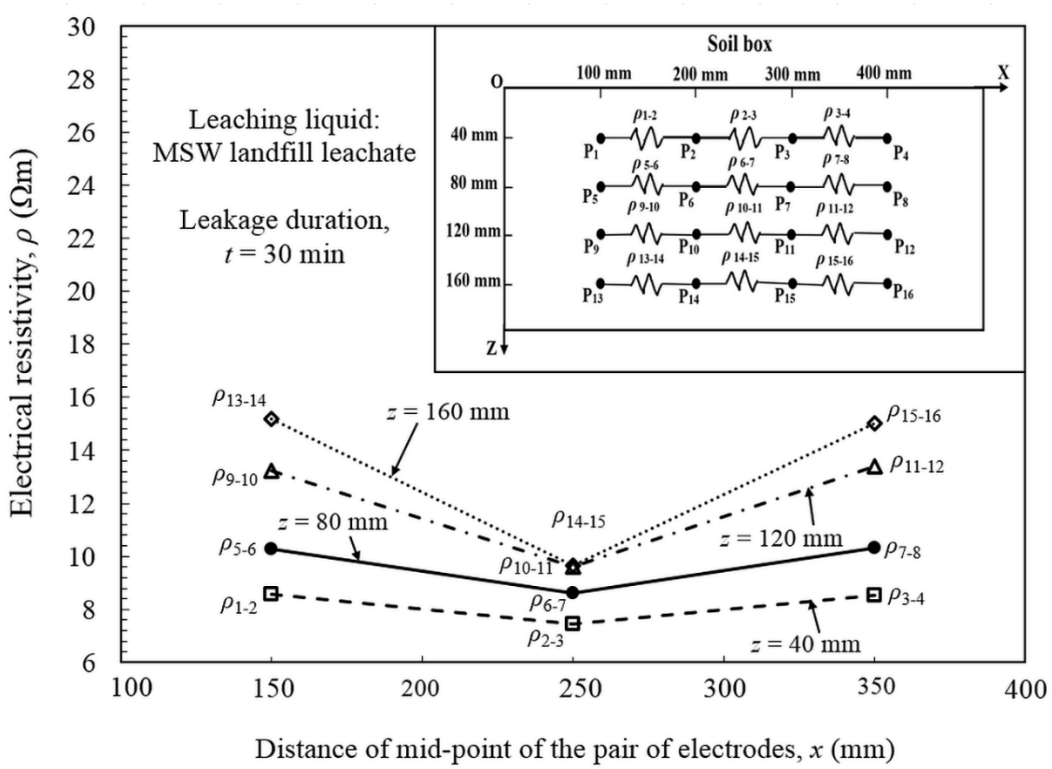

Figure 5.11: Resistivity profile of the leak detection system using MSW landfill leachate.

Table 5.2: Water quality data for tap water.

Properties	Units	Values
Alkalinity as $CaCO_3$	mg/L	95
Aluminium	mg/L	0.02
Calcium	mg/L	30.5
Chloride	mg/L	110
Conductivity (at 25 $^{\circ}$C)	mS/ m	58.5
Hardness as $CaCO_3$	mg/L	105
Iron	mg/L	0.006
Magnesium	mg/L	7.5
Manganese	mg/L	<0.002
Nitrite plus nitrate as N	mg/L	0.76
pH	pH Units	7.72
Potassium	mg/L	5.6
Silicon as SiO_2	mg/L	18
Sodium	mg/L	68
Sulphate	mg/L	19.5
Total Dissolved Solids (TDS)	mg/L	385
True colour	HU	<1
Turbidity	NTU	<0.1

Based after Tyl (2016).

It can be noticed that from Figure 5.11 that for the case where MSW landfill leachate is used as the leaching liquid, at a given depth, there is a decrease in resistivity with increase in the distance from the leak point. This decrease in resistivity becomes more pronounced with increase in depth from 40 mm to 160 mm. Similarly, for the case when tap water is used as the leaching liquid (Figure 5.10), at a given depth, there is a decrease in resistivity with increase in distance. However, this decrease in resistivity is less significant with increase in the depth. This observation can be explained using the well-known fact that with an increase in the distance from the leak point, the amount of leaching liquid decreases, and as a result, the electrical resistivity is expected to increase. Furthermore, it is known that the resistivity of soil at any given point depends upon the amount of leaching liquid at that point, as well as the resistivity

of the leaching liquid. The resistivity of the tap water is greater than the resistivity of MSW leachate, hence, there is a disparity in the resistivity values observed using tap water and MSW leachate as the leaching liquids.

Table 5.3: Chemical composition of the landfill leachate.

Chemical group	Chemical name	Unit	Value
Total Organic Carbon (TOC)	TOC	mg/L	1200
Inorganics	COD	mg/L	7300
Acidity and Alkalinity	Alkalinity (total as $CaCO_3$)	mg/L	5900
Metals	Arsenic	mg/L	0.21
	Chromium (III+VI) (Filtered)	mg/L	0.37
	Iron	mg/L	10
	Manganese (Filtered)	mg/L	0.11
	Nickel (Filtered)	mg/L	0.17
	Zinc (Filtered)	mg/L	0.1
Major Ions	Calcium	mg/L	41
	Chloride	mg/L	3800
	Magnesium	mg/L	31
	Potassium	mg/L	890
	Sodium	mg/L	1800
	Sulphate	mg/L	22
Nutrients	Ammonia as N	mg/L	1600
	Total Kjeldahl Nitrogen	mg/L	1900
	Nitrogen (Total)	mg/L	1900
	Phosphate total (P)	µg/L	3600

Based after Widenbar (2017).

It can be noticed that with an increase in the distance x or the depth z from the hole, the resistivity of the soil ρ generally shows an increase. Therefore, the location of the liner leak can be ascertained based on the resistivity profile of the soil obtained from the designed system as presented in this paper. In addition, it can be concluded that the newly developed leak

detection technique is reasonably effective for detecting and locating leakages through liners by simulating actual field conditions.

It should also be noted that although different soil types have different resistivities, the resistivity of any dry soil is generally higher than that of any contaminating fluids. Hence, the leak detection technique would be effective for the detection of liner defects, irrespective of the soil type.

5.7 Conclusions

Based on the well-established fact that the investigation of the electrical resistivity of the liner base soil is very useful in detecting leakage issues in liners, an innovative leak detection system has been developed to determine the electrical resistivity behaviour of soils as a result of leachate contamination. The details of this system and its design were presented in this paper. Results were also given for the experimental demonstration of the leak detection test for a leakage duration of 30 min using the tap water and the MSW landfill leachate. It was found that the resistivity of the soil increased with an increase in the depth or the distance, of the mid-point of the pair of electrodes, from the liner leak. The effect of distance and depth was found to be negligible at greater depths, for the leakage duration of 30 min. From these observations, it can be concluded that the newly developed system can be used to effectively detect and locate leakages in liners. This innovative diagnostic technique can find several applications in designing the monitoring systems for waste storage and handling facilities, contamination detection, liner leak detection, and development of sensors. Furthermore, the research work can also be useful in various numerical modeling applications for liner leakage issues.

References

AS 1289.4.4.1 (1997). Methods of testing soils for engineering purposes soil chemical tests - determination of the electrical resistivity of a soil - method for sands and granular materials, Standards Australia, Sydney, NSW, Australia.

ASTM D6431-99 (2010). Standard guide for using the direct current resistivity method for subsurface investigation, ASTM International, West Conshohocken, PA, USA.

ASTM D6747-15 (2015). Standard guide for selection of techniques for electrical leak location of leaks in geomembranes, ASTM International, West Conshohocken, PA, USA.

ASTM D7002-16 (2016). Standard practice for electrical leak location on exposed geomembranes using the water puddle method, ASTM International, West Conshohocken, PA, USA.

ASTM D7240-06 (2011). Standard practice for leak location using geomembranes with an insulating layer in intimate contact with a conductive layer via electrical capacitance technique (conductive geomembrane spark test), ASTM International, West Conshohocken, PA, USA.

ASTM D7703-16 (2016). Standard practice for electrical leak location on exposed geomembranes using the water lance method, ASTM International, West Conshohocken, PA, USA.

ASTM D7953-14 (2014). Standard practice for electrical leak location on exposed geomembranes using the arc testing method, ASTM International, West Conshohocken, PA, USA.

Ben Othmen, A. and Bouassida, M. (2013). Detecting defects in geomembranes of landfill liner systems: durable electrical method. *International Journal of Geotechnical Engineering* 7(2), 130-135, DOI: 10.1179/1938636213Z.00000000013.

Bouazza, A. and Van Impe, W.F. (1998). Liner design for waste disposal sites. *Environmental Geology* 35(1), 41-54, DOI: 10.1007/s002540050291.

Daniel, D.E. (1993). Landfills and Impoundments. Geotechnical Practice for Waste Disposal, Springer, USA, p. 97-112.

Giroud, J.P. (1984). Impermeability: The myth and a rational approach. *Proceedings of the International Conference on Geomembranes*, Vol. 1, p. 157-162.

Mohamed, A.M.O., Said, R.A., and Al-Shawawreh, N.K. (2002). Development of a methodology for evaluating subsurface concentrations of pollutants using electrical polarization technique. *Geotechnical Testing Journal* 25(2), 157–167, DOI: 10.1520/GTJ11359J.

Naghibi, M., Abuel-Naga, H. and Orense, R. (2016). Modified odometer cell to measure electrical resistivity of clays undergoing consolidation process. *Journal of Testing and Evaluation* 45(4), 1261-1269, DOI: 10.1520/JTE20160002.

Oh, M., Seo, M.W., Lee, S. and Park, J. (2008). Applicability of grid-net detection system for landfill leachate and diesel fuel release in the subsurface. *Journal of Contaminant Hydrology* 96(1-4), 69-82, DOI: 10.1016/j.jconhyd.2007.10.002.

Pandey, L.M.S. and Shukla, S.K. (2017). Detection of leachate contamination in Perth landfill base soil using electrical resistivity technique. *International Journal of Geotechnical Engineering*, 1-12., DOI: 10.1080/19386362.2017.1339763.

Rowe, R.K., Quigley, R.M., Brachman, R.W. and Booker, J.R. (2004). Barrier Systems for Waste Disposal Facilities (No. Ed. 2), Spon Press, London, UK.

Shukla, S.K. (2016). An Introduction to Geosynthetic Engineering, CRC Press, Taylor & Francis Group, Florida, USA.

Shukla, S.K. and Yin, J.H. (2006). Fundamentals of Geosynthetic Engineering, Taylor & Francis, UK.

Tyl, E. (2016). Personal Communication, Water Corporation, WA, Australia.

Widenbar, T. (2017). Personal communication, North Bannister Resource Recovery Facility, SUEZ, WA, Australia.

Xie, H., Jiang, Y., Zhang, C. and Feng, S. (2015). An analytical model for volatile organic compound transport through a composite liner consisting of a geomembrane, a GCL, and a soil liner. *Environmental Science and Pollution Research* 22(4), 2824-2836., DOI: 10.1007/s11356-014-3565-5.

Xie, H., Zhang, C., Sedighi, M., Thomas, H.R. and Chen, Y. (2015). An analytical model for diffusion of chemicals under thermal effects in semi-infinite porous media. *Computers and Geotechnics* 69(2015), 329-337, DOI: 10.1016/j.compgeo.2015.06.012.

CHAPTER 6

RESISTIVITY PROFILES OF LINER BASE WITH WATER AS LEACHATE

This chapter is based on the paper published in the Geotechnical Research, ICE; as listed in Section 1.6. The details presented here are the same, except some changes in the layout in order to maintain a consistency in the presentation throughout the thesis.

6.1 Introduction

The global population generates a huge amount of waste every year. The World Bank has estimated that the amount of municipal solid waste (MSW) generated worldwide will be doubled in the period 2012-2025 (Hoornweg and Bhada-Tata, 2012). In Australia alone, waste generation increased by 170% in the period of 1996-2015 at a compound growth rate of 7.8% per annum (DEWHA, 2010). About 42% of this waste went to landfills, while the rest was diverted to resource recovery centres. Specifically, in Western Australia (WA), landfilling is the usual method of waste disposal (Schollum, 2010). In 2014-15, 58% of the total waste generated in WA was sent to landfills (Waste Authority, 2016). These solid wastes consisted of commercial and industrial wastes, construction and demolition wastes and MSWs (Goldsworthy, 2010; Perryman and Green, 2017). The leachates produced by these wastes, contain multiple pollutants (O'Kelly, 2016), which can prove to be potentially harmful to the environment (Daniel, 1993; Bouazza and Van Impe, 1998). Therefore, the problems of safe handling, storage and disposal of wastes becomes very daunting challenges faced by landfills (Hoyos *et al.*, 2015), as well as the other waste containment facilities such as tailing dams, leachate collection ponds, sump wells, underground storage tanks, etc. (Sharma and Reddy, 2004; Shukla and Yin, 2006; Rowe, 2012). To counter these issues, most containment facilities use engineered lining systems (Seymour, 1992; Sharma and Reddy, 2004; Rowe, 2012). These lining systems are designed to create a barrier for the control of leachate contamination of soil and groundwater (Reddy *et al.*, 1996; Shukla, 2016).

The type of lining system for the landfill facility is chosen based on the probable hazards of the wastes handled by that particular site. Liners can be single (also referred to as simple), composite or double (Shah, 2000; Rowe, 2012; Shukla, 2016). Furthermore, the liners might be artificial or natural, such as compacted clays (Daniel, 1984; Harrop-Williams, 1985), silty soils (Holtz, 1985), mine tailings (Jessberger and Beine, 1981), or sand bentonite mixtures (Chapuis, 1990). Figure 6.1 shows the schematic profile of a typical single-liner system which consists of a leachate collection layer (k ~10^{-1} m/s), a compacted clay layer (k ~10^{-9} m/s) covered with high-density polyethylene (HDPE) geomembrane (GMB), and a leak detection/recovery layer (k ~10^{-1} m/s), where k is the hydraulic conductivity (Shukla and Yin, 2006).

While the liners are expected to be intact over their operating lifespan, due to various factors such as poor placement assurance, insufficient quality control and harsh conditions of operation, it is observed that the integrity of these liners is often compromised (Giroud, 1984; Giroud and Bonaparte, 1989; Buss *et al.*, 1995; Hoyos *et al.*, 2015). Defects frequently develop in liners, resulting in leachate leakages and consequent contamination issues (Ben Othmen and Bouassida, 2013). Figure 6.2 shows the photograph of a typical empty leachate collection pond, lined with geosynthetic clay liner (GCL). Leaks have developed in the liner, consequently resulting in the leakage of leachates to the soil and groundwater.

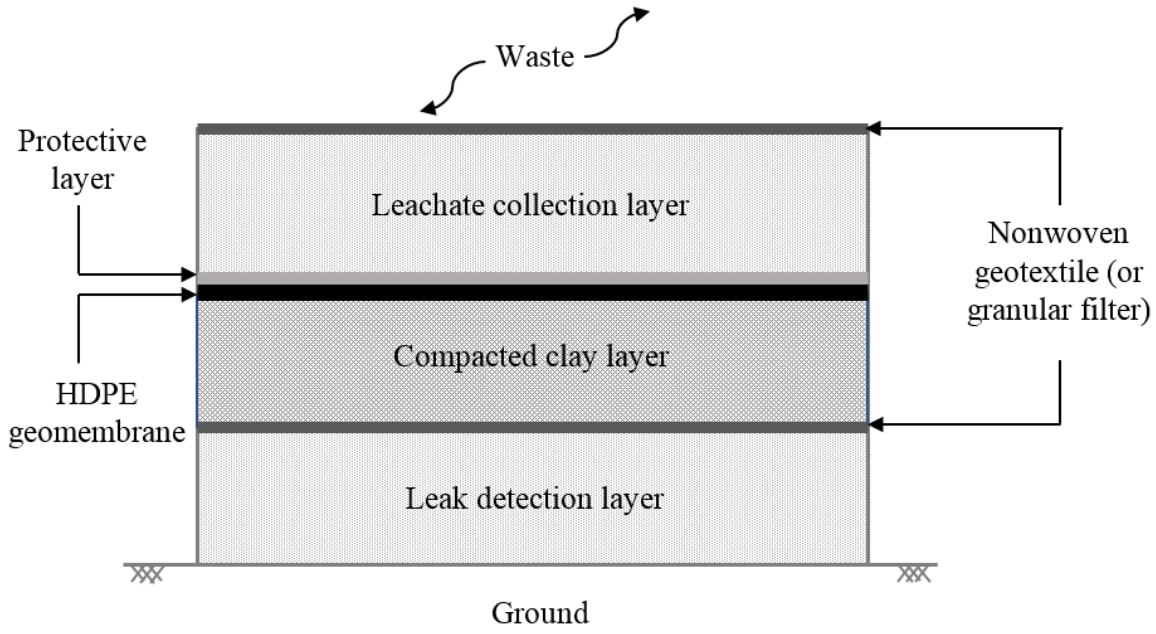

Figure 6.1: Schematic diagram profile of a single liner system.

In order to prevent the hazardous impacts of leachate contamination from getting magnified, it is essential to detect leakages timely and to execute adequate mitigation measures (Oh *et al.*, 2008; Pandey and Shukla, 2017). Therefore, various methods of leak detection are practiced by different waste containment facilities. Table 6.1 lists some of the methods used for the detection of leakages through liners. Some conventional methods of leak detection are groundwater monitoring wells, lysimeter, diffusion hoses, capacitance sensors, tracers, and so on (Hix, 1998; Oh *et al.*, 2008). The geophysical methods used are resistivity cone penetration test (RCPT), ground penetration radar (GPR), time domain reflectometry (TDR), etc. (Oh *et al.* 2008; ASTM D6431-99(2010)). Most of these methods are cost and time intensive, and hence, prove ineffective (Mohamed *et al.,* 2002). In addition, it is essential to detect leakage issues as soon as they arise so that the impact to the environment and the associated costs for remediation, can be minimized. Hence, the use of the electrical resistivity method for leak detection is widely prevalent for early leakage detection (ASTM D6747 – 15; ASTM D7002 – 16; ASTM D7240 - 06(2011); ASTM D7703 – 16; ASTM D7953 – 14), because of its ease of installation and operation, and relatively low expenditures (Oh *et al.,* 2008; Ben Othmen and Bouassida, 2013). This method is based on the electrical resistivity changes produced in soil due to its contamination by leachates.

In this method, a known current (i) is passed through a soil specimen. The resulting potential drop (V) is recorded. The resistance (R) of the soil is then obtained using the Ohm's law, as given below:

$$V = iR \tag{6.1}$$

It is a well-known fact that although different soil types have different resistivity values, all dry soils generally possess resistivity much higher than that of any contaminating fluid, such as leachate. Therefore, the addition of even a small amount of leaching liquid to the soil, results in a sharp decrease in its resistivity (Fukue *et al.*, 1999; Mitchell and Soga, 2005; Munoz-Castelblanco *et al.*, 2012; Pandey *et al.*, 2015; Naghibi *et al.*, 2016). These changes can be detected easily to determine soil contamination, and therefore, to detect leakage issues (Mitchell and Soga, 2005; Ben Othmen and Bouassida, 2013; Pandey and Shukla, 2017).

Figure 6.2: A typical leachate collection pond lined with GCL.

Based on the electrical resistivity method, an innovative leak detection system was developed by with a view to its application in the location of leaks in liners, at their onset. This system was demonstrated to be effective in leak determination. However, this technique is in a relatively nascent stage, and gaps exist in the understanding of the system. There is a significant scope for further investigation into the influence of various parameters, such as leakage duration and sensor location, on the resistivity profile of soil subjected to leak detection testing. Therefore, an attempt has been made in this paper to present an insightful knowledge about the same. This work will assist the practising engineers in the development of an online monitoring system for the timely detection and location of leaks in liners.

Table 6.1: Leak detection methods.

Leak detection methods	Advantages	Disadvantages
Groundwater monitoring wells	Detects contaminant plumes	Time consuming, expensive, localised
Lysimeter	Detects contamination	Laboratory testing required, high operating cost, cannot identify leak point
Diffusion hoses	Readily available components, automatic, low operating cost	Only useful for leachates with vapour
Capacitance sensors	Readily available, automatic	Detects any moisture
Tracers	Effective at any stage of landfilling, unaffected by leachate composition	High operating cost, does not locate exact leak point
Electro-chemical sensing cables	Widely available	Detects only some contaminants, site specific, must be pre-installed
Geophysical methods	Effective in locating contaminated zones	Not easy to operate, depends on detection of post contamination plume
Two electrode methods	Useful for detecting leaks in pre-existing landfills	Only indicates existence of a leak, cannot be used for active landfills
Electrode grid method	Easy to install and operate, low operating cost	High capital cost

6.2 Materials and Methods

Perth and its surrounding regions comprise mainly of sandy soil (Stephenson & Hepburn, 1955). The soil used in this study is a good representation of Perth soil. It is extensively available throughout Western Australia (WA) and is used widely by practicing Civil engineers. The properties of this soil have been presented in Table 6.2. Figure 6.3 gives the scanning electron microscopy (SEM) image of this soil. It is classified as a poorly graded sand (SP) and

is the foundation material for most waste impoundment systems in Perth metropolitan region. It has been used to create the leak detection layer in the designed leak detection system.

Tap water was used in this study as the leachate. This would enable us to test the system in extreme conditions, as any leaching liquid is expected to have conductivity higher than that of water (Pandey *et al.*, 2015). So, if water can be detected by the leak detection testing equipment, then the system can be demonstrated to have adequate sensitivity to detect leachate contaminations. The properties of the tap water used in this study, have been summarised in Table 6.3.

In addition, a 220 μm-thick geomembrane (GMB) liner was used for the test. A piece of 550 mm length and 250 mm width was pre-cut from the GMB. A leak was intentionally introduced in the centre of the GMB piece using a gravel-size particle to simulate a real-life puncture defect. Figure 6.4 shows a photograph of the pre-cut GMB beside the gravel-size particle, as used in this study.

Table 6.2: Physical properties of Perth sandy soil.

Properties	Values
Specific gravity of soil solids, G_s	2.68
Coefficient of uniformity, C_u	2.27
Coefficient of curvature, C_c	1.22
Effective size, D_{10} (mm)	0.15
Minimum dry unit weight, $\gamma_{d\min}$ (kN/m^3)	14.02
Maximum dry unit weight, $\gamma_{d\max}$ (kN/m^3)	15.56
Soil classification as per USCS (Unified Soil Classification System)	Poorly graded sand (SP)

6.2.1 Laboratory setup

Figure 6.5 shows the soil box used in the leak detection system to represent the lining system. Its design has been based on the four-point soil resistance test method given by the Australian standard AS 1289.4.4.1 (Standards Australia, 1997). A waterproof box with internal

dimensions of 500 mm length, 200 mm width and 400 mm height, was fabricated from 12 mm thick non-conductive perspex sheet. A groove of 8 mm diameter was made in the soil box at the height of 200 mm from the bottom. This groove was introduced with the intention to use it for securing the geomembrane (GMB) liner over the soil layer.

Two brass current plate electrodes with dimensions 200 mm by 200 mm, were fitted on either side of the soil box. Gaskets were used to waterproof the connections. Sixteen potential measuring point electrodes of 4 mm diameter were also fitted in the box, as shown in Figure 6.5. The experimental design of the leak detection setup is being reported separately in more detail.

Table 6.3: Water quality data for tap water.

Properties	Units	Values
Alkalinity as $CaCO_3$	mg/L	95
Conductivity (at 25 $^{\circ}$C)	mS/ m	58.5
Hardness as $CaCO_3$	mg/L	105
pH	pH Units	7.72
Total Dissolved Solids (TDS)	mg/L	385
True colour	HU	<1
Turbidity	NTU	<0.1
Sodium	mg/L	68
Calcium	mg/L	30.5
Magnesium	mg/L	7.5
Potassium	mg/L	5.6
Aluminium	mg/L	0.02
Manganese	mg/L	<0.002
Silicon as SiO_2	mg/L	18
Chloride	mg/L	110
Sulphate	mg/L	19.5
Nitrite plus nitrate as N	mg/L	0.76

Based after Tyl (2016).

6.2.2 Sample preparation

The soil was oven dried overnight at 110 ˚C. This soil was then used to fill the box up to a height of 200 mm, to achieve a relative density, D_r of 100%. The purpose of maintaining $D_r = 100\%$ was to simulate a real-life leak detection layer as used in any lining system. The box was filled using five lifts/layers to ensure homogeneity. After compacting soil in the first layer, four point electrodes were fitted laterally in the box. Then the second soil layer was poured in, and so on. Finally, after the fifth layer was placed in, the soil layer was levelled using a wooden float before placement of the geomembrane.

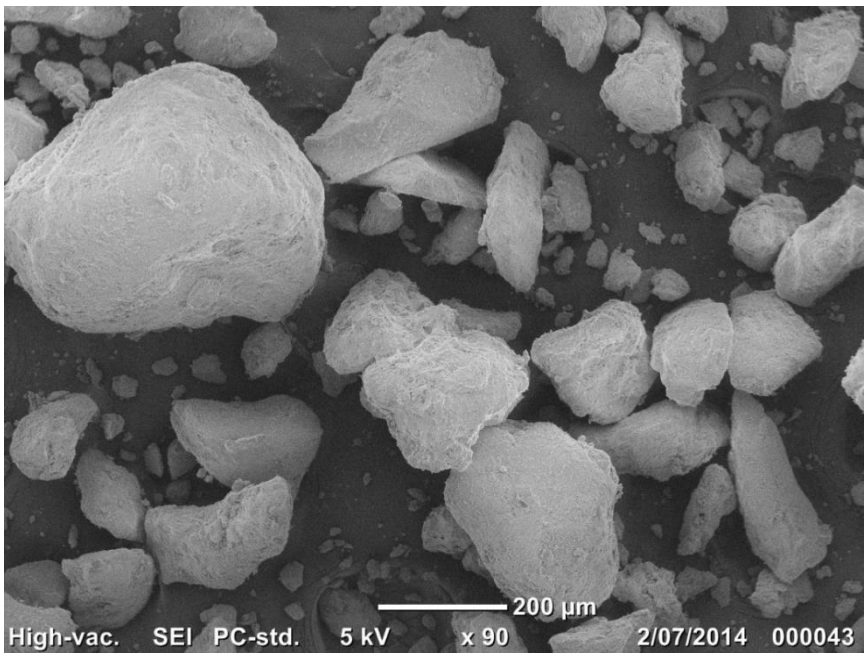

Figure 6.3: Scanning electron microscopy image of Perth soil.

The 550 mm by 250 mm pre-cut geomembrane (GMB) with the puncture defect (Figure 8.4), was kept over the soil. It was then secured over the soil layer using an 8-mm rubber gasket fitted into the 8-mm groove. This was done to ascertain that there would be no leakages apart from the leak from the intentional puncture defect. This defect was covered initially, while the water was filled over the GMB, and then uncovered at the beginning of the test at $t = 0$. Here, t is the duration for which the leakage was allowed. It is also the time at which the resistance was recorded.

Figure 6.4: Photograph of the pre-cut GMB liner and the gravel-size particle used to make puncture defect.

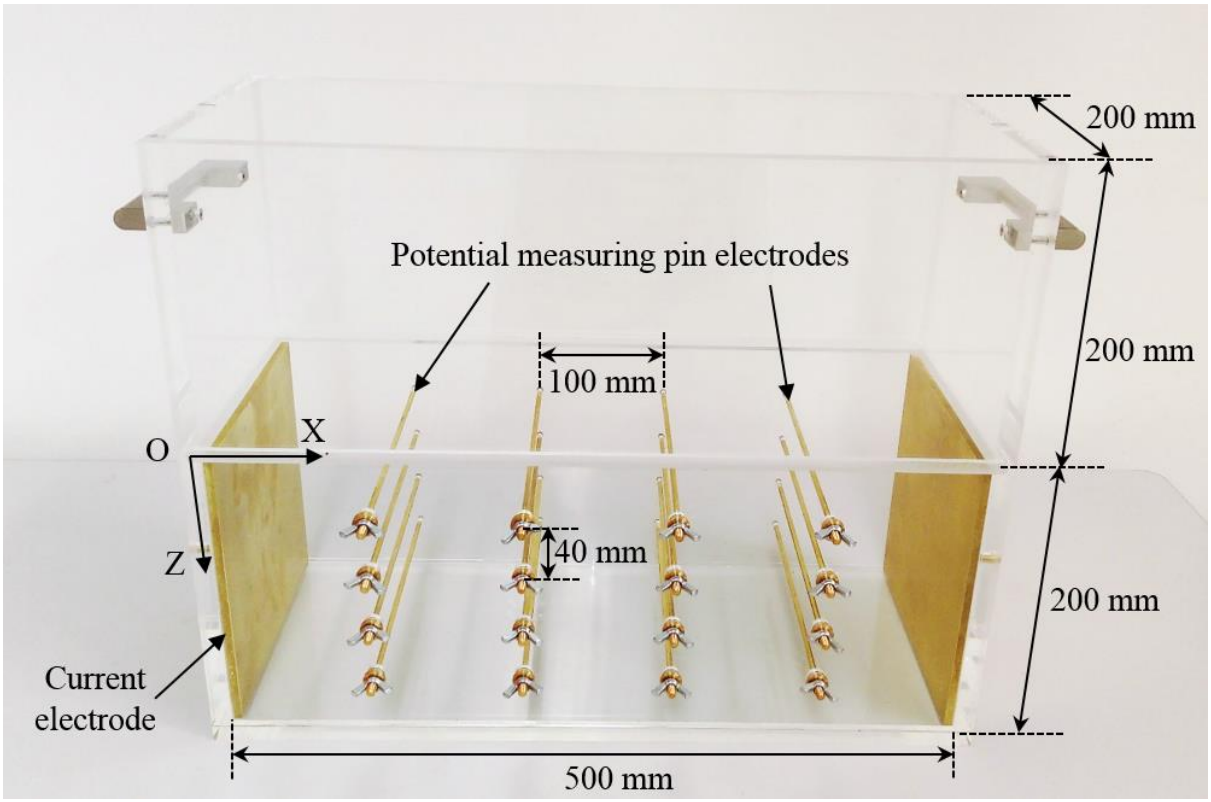

Figure 6.5: Soil box used in the leak-detection system.

6.2.3 Testing procedure

Figure 6.6 shows the experimental setup used in this study. It consists of the filled soil box, used to represent the lining system, and the AEMC 6471 machine for the resistance measurement. The AEMC 6471 is a standard four-point ground resistance tester. The connections were made as indicated in the figure.

A constant head of 100 mm of water was maintained over the geomembrane for the entire test. At the time of the commencement of experimentation, i.e. at $t = 0$, the tape which covered the GMB defect was removed. As a result, the water started leaking through the liner to the underlying soil.

The electrical resistance of soil (R) was obtained at 10 min time intervals using AEMC 6471 ground resistance testing machine. The test was concluded at $t = 60\,\text{min}$, as the soil was observed to reach near saturation condition around this time.

A current of AC-input voltage 16 V and AC-input frequency 128 Hz, was injected through the outer plate electrodes and the resulting potential drop across each pair of point electrodes was measured (Figure 6.6). Hence, twelve resistance readings were obtained for each leakage duration $_t$. The resistivity (ρ) was then calculated as per AS 1289.4.4.1 (Standards Australia, 1997), using the following equation:

$$R = \frac{\rho L}{A} \tag{6.2}$$

where A is the cross-sectional area (m^2) and L is the length (m) of the test specimen. It may be noted that the use of Eqn. (6.2) is justified, because the voltage drop is measured between different set of electrodes independently while the area of the plate electrodes remains the same, as considered in the derivation of Eqn. (6.2).

Figure 6.7 is a representation of the soil box. Here, the potential measuring point electrodes, P_1 through P_{16}, have been indicated along with the associated resistivities. In this figure, $_x$ (mm) is the distance and $_z$ (mm) is the depth of the mid-point of each pair of electrodes, respectively. For the ease of analysis, the soil resistivity obtained between a pair of electrodes, was assumed to be situated at the mid-point of that electrode pair.

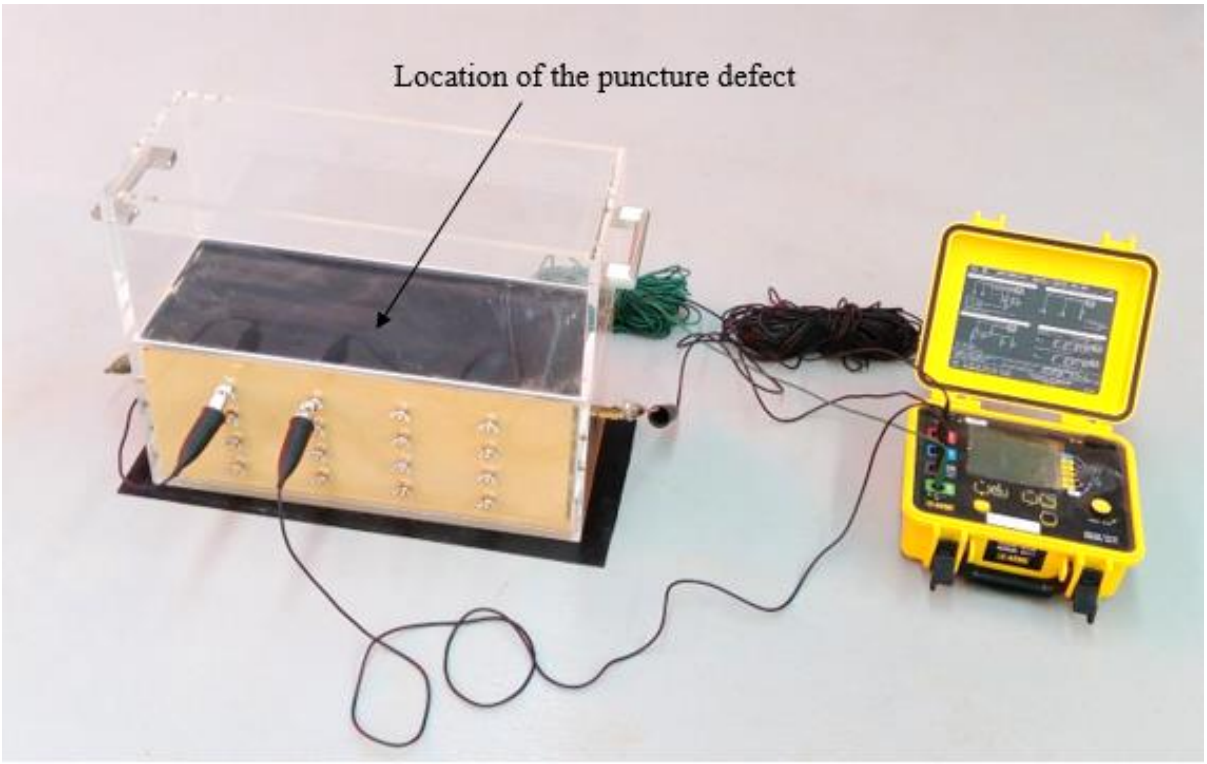

Figure 6.6: Experimental set-up of the leak-detection system.

6.3 Results and Discussion

Figure 6.8(a) gives the variation of the resistivity with leakage duration, for the electrode pairs with their mid-points located at the depth $z = 40$ mm. Figures 6.8(b) through 6.8(d) show the same variation at $z = 80$, 120 and 160 mm, respectively. The purpose was to observe the impact of leakage duration (t) as well as the influence of distance (x) of the mid-point of electrode pair. It was found that steady readings for the electrical resistance were not obtained at leakage durations less than 30 min. This can be explained using the fact that the resistivity of dry sand is extremely high. Fukue *et al.* (1999) obtained about 10^5 Ωm electrical resistivity for dry sands. Another study reported electrical resistivity values from 10^{10} to 10^{14} Ωm for silicates (Munoz-Castelblanco *et al.*, 2012). As the standard ground resistance testing equipment used in actual field testing generally has a range of 10^1 to 10^6 Ωm, readings for the resistance of the soil specimen were recorded at $t \geq 30$ min.

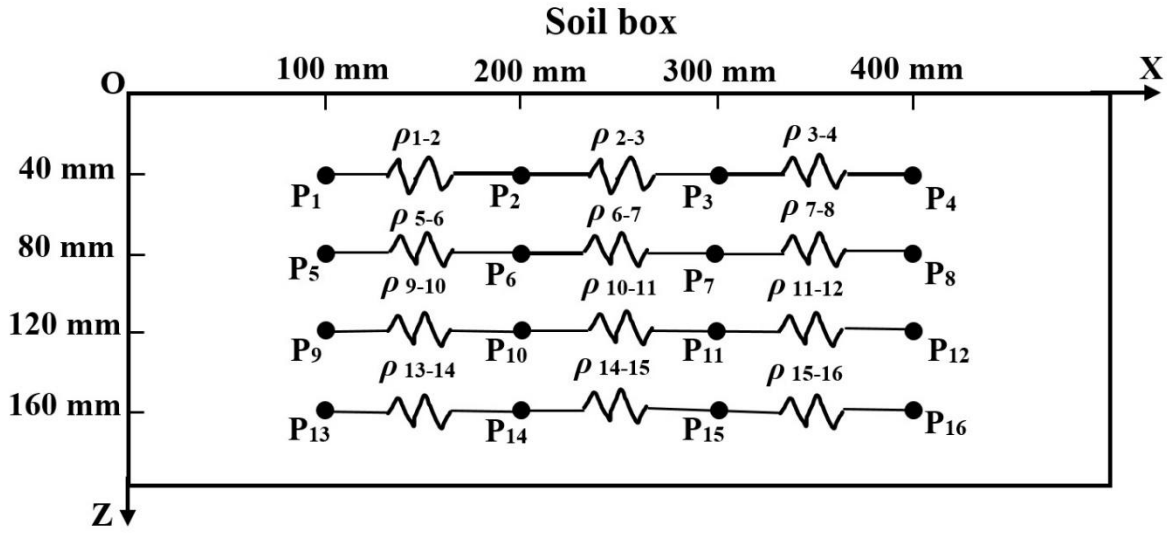

Figure 6.7: Representation of the soil box showing potential measuring point electrodes and associated resistivities.

It can be observed from Figure 6.8(a) that the three resistivities, ρ_{1-2}, ρ_{2-3} and ρ_{3-4}, show a decrease with an increase in the leakage duration, t. This is as expected, because with an increase in t, the amount of water leaked to the soil layer would also increase. Therefore, the resistivity would decrease. It is also interesting to note that at any leakage duration (t), the resistivity ρ_{2-3} is lower than ρ_{1-2} and ρ_{3-4}. This indicates that the highest amount of water from leakage is accumulated in the soil between the inner two electrodes, P_2 and P_3. This experimental finding is consistent with expectations, as it is known that the leak is situated directly above the mid-point of P_2 and P_3. As a result, it is possible to locate the leak in liner at any time using this technique. Furthermore, it can be noticed that ρ_{1-2} and ρ_{3-4} are nearly same at any t as they are equidistant from the introduced leak.

Similar observations were made for Figure 6.8(b). Resistivity was found to decrease with an increase in leakage duration. ρ_{6-7} is lesser than ρ_{5-6} and ρ_{7-8} for any t. However, this difference was seen to be more apparent at $t = 30\,\text{min}$. For $t \geq 40\,\text{min}$, insignificant difference is observed.

From Figures 6.8(c) and 6.8(d), while the resistivities were generally found to register a decrease with increase in t, in contrast, the effect of changing x was negligible. The electrodes at the depth, $z = 40\,\text{mm}$ are most sensitive to the leakage detection. These observations

indicate that the greater is the proximity of the electrode sensing system to the liner, the better is the leakage detection capacity. As the depth z increases, the effect of distance x and leakage duration t is found to be negligible.

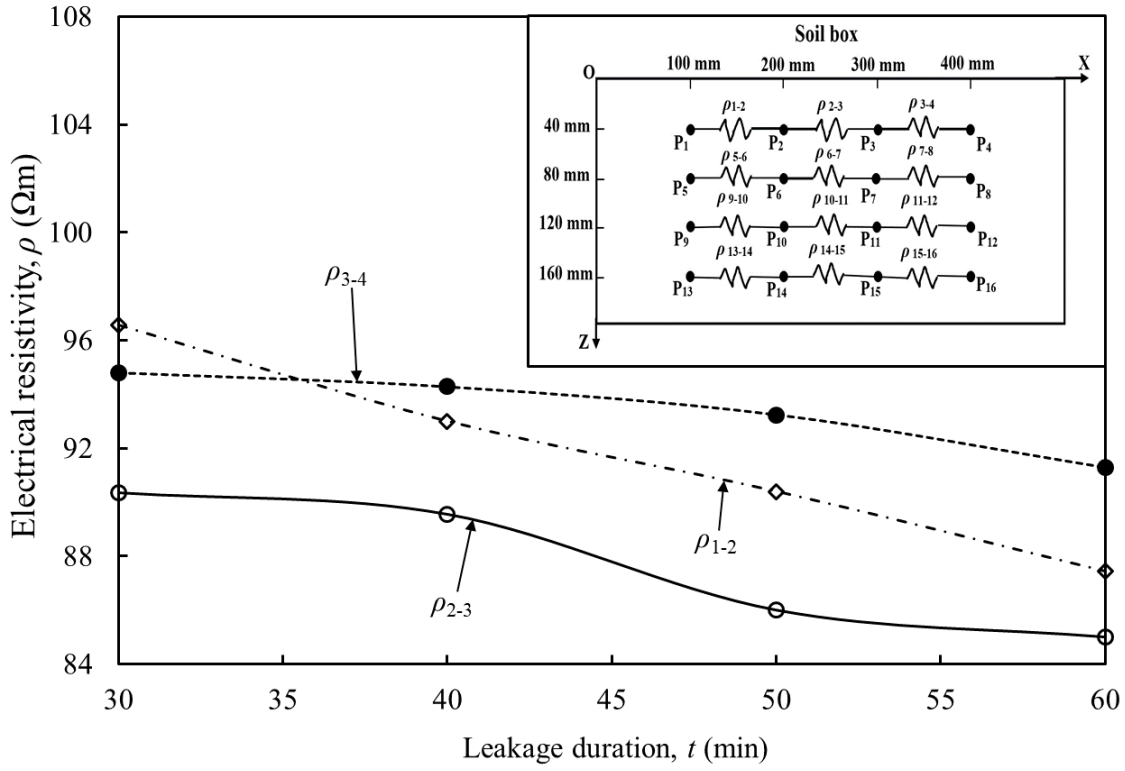

(a)

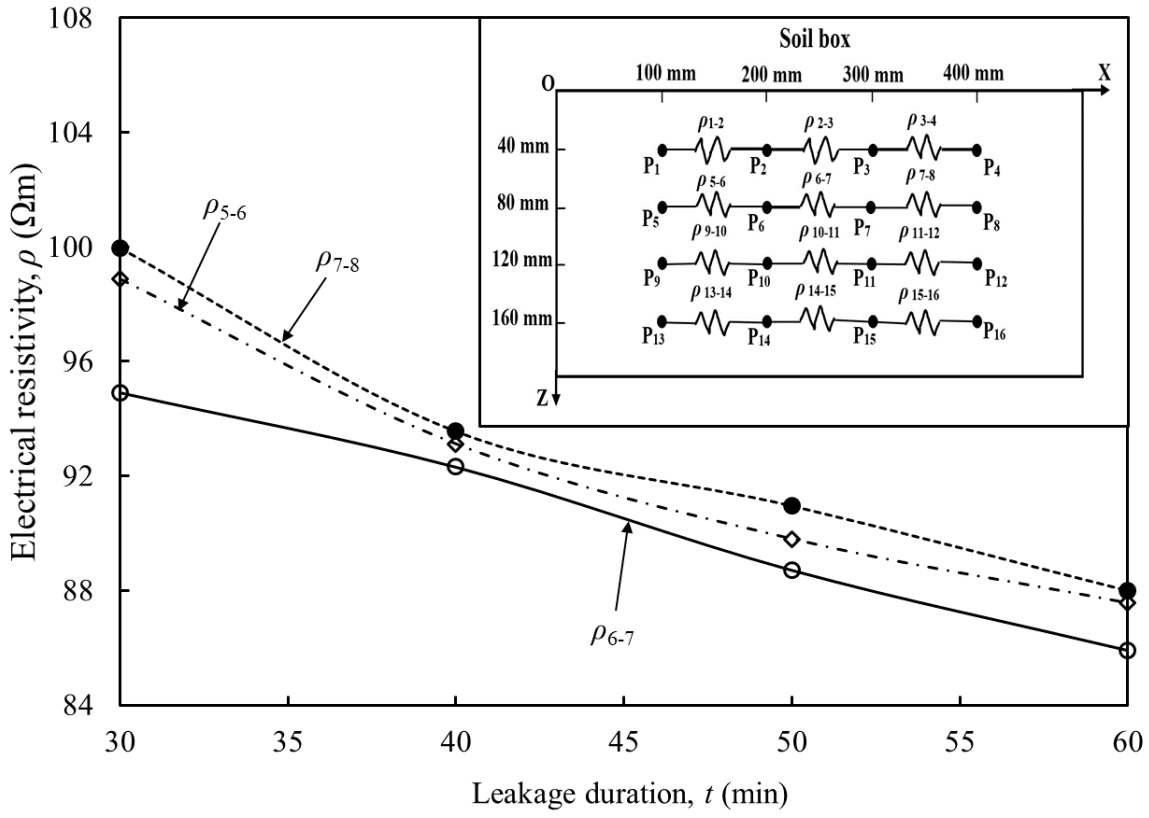
Soil box
100 mm
200 mm
300 mm
400 mm
X
O
Z
40 mm
80 mm
120 mm
160 mm
ρ_{1-2} ρ_{2-3} ρ_{3-4}
P_1 P_2 P_3 P_4
ρ_{5-6} ρ_{6-7} ρ_{7-8}
P_5 P_6 P_7 P_8
ρ_{9-10} ρ_{10-11} ρ_{11-12}
P_9 P_{10} P_{11} P_{12}
ρ_{13-14} ρ_{14-15} ρ_{15-16}
P_{13} P_{14} P_{15} P_{16}
ρ_{5-6}
ρ_{7-8}
ρ_{6-7}
Electrical resistivity, ρ (Ωm)
Leakage duration, t (min)
108
104
100
96
92
88
84
30
35
40
45
50
55
60

(b)

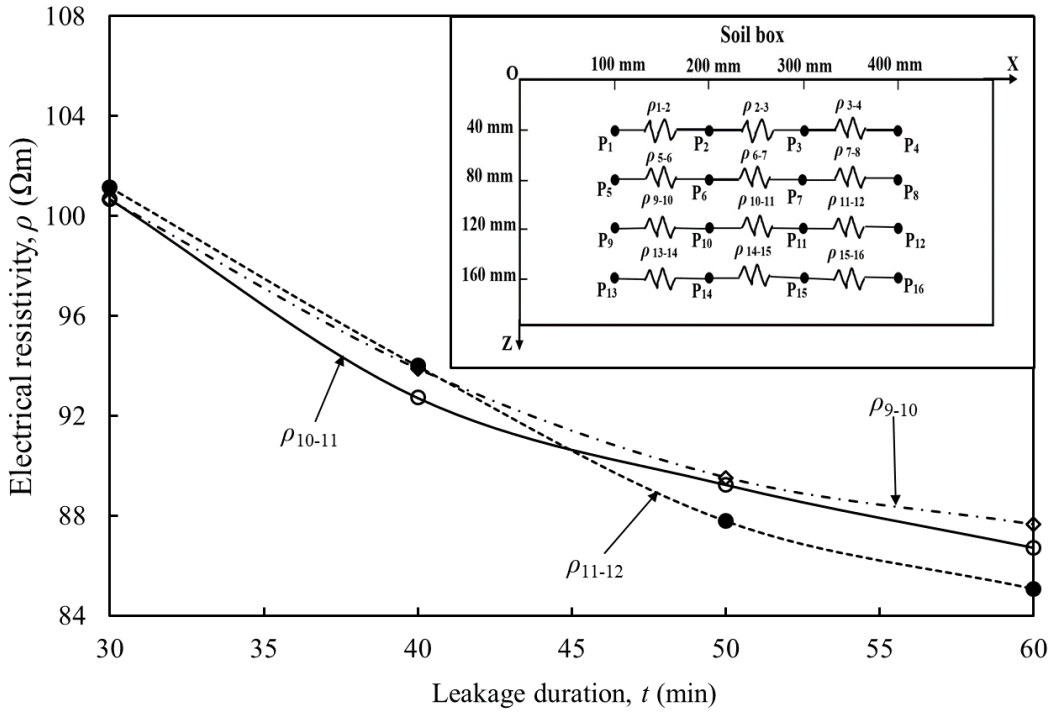
Soil box
100 mm
200 mm
300 mm
400 mm
X
O
Z
40 mm
80 mm
120 mm
160 mm
ρ_{1-2} ρ_{2-3} ρ_{3-4}
P_1 P_2 P_3 P_4
ρ_{5-6} ρ_{6-7} ρ_{7-8}
P_5 P_6 P_7 P_8
ρ_{9-10} ρ_{10-11} ρ_{11-12}
P_9 P_{10} P_{11} P_{12}
ρ_{13-14} ρ_{14-15} ρ_{15-16}
P_{13} P_{14} P_{15} P_{16}
ρ_{10-11}
ρ_{9-10}
ρ_{11-12}
Electrical resistivity, ρ (Ωm)
Leakage duration, t (min)
108
104
100
96
92
88
84
30
35
40
45
50
55
60

(c)

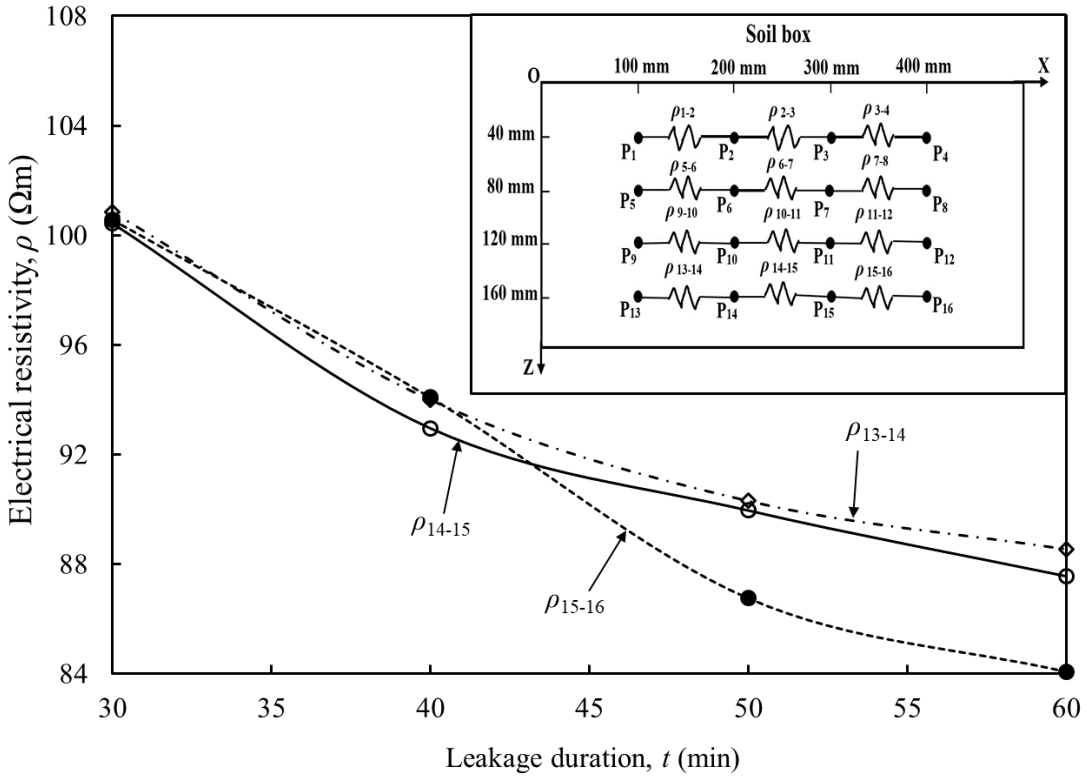

(d)

Figure 6.8: Resistivity profiles of electrode pairs located below the GMB liner at depths of (a) 40, (b) 80, (c) 120 and (d) 160 mm.

Figures 6.9(a) through 6.9(c) depict the resistivity profile of the soil specimen with variations in the distance of the mid-point of the electrode pairs, $_x$ = 150, 250 and 350 mm. It can be seen that the resistivity for any particular electrode pair, exhibits a decrease with an increase in the leakage duration (t). Moreover, it was noticed that the resistivity was lowest at $z = 40\,\text{mm}$, irrespective of $_x$. This observed trend is more pronounced at $t = 30\,\text{min}$. However, for $t \geq 40\,\text{min}$, the variations are less pronounced. This can be attributed to the fact that although attempts have been made to fill the soil box homogeneously, the soil is inherently neither homogeneous, nor isotropic.

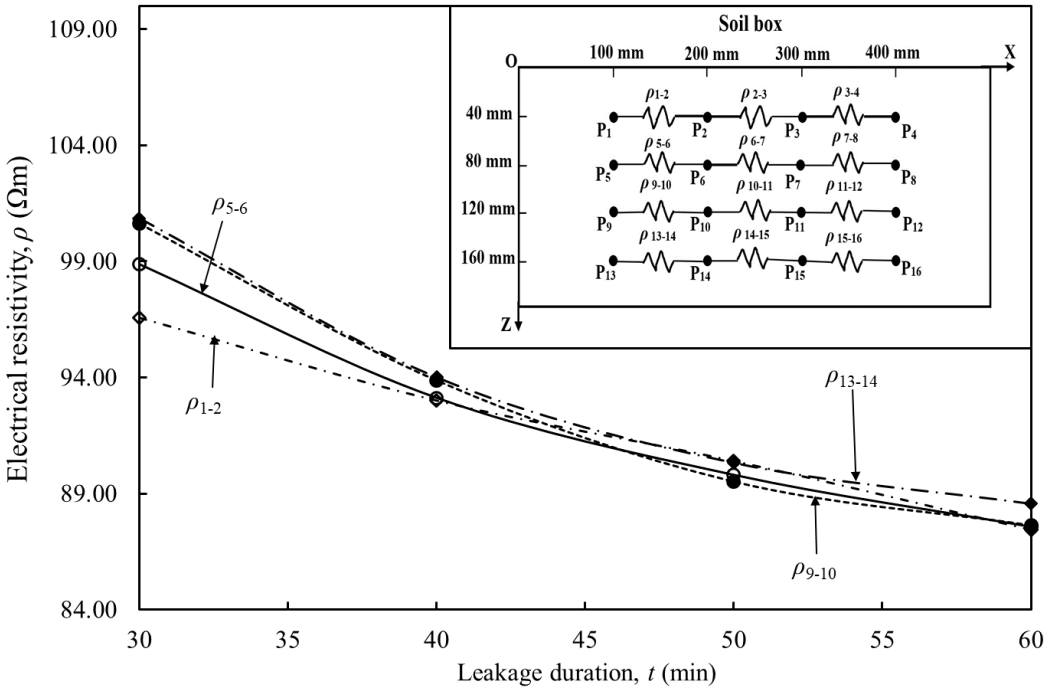
Soil box
O
100 mm
200 mm
300 mm
400 mm
X
Z
40 mm
80 mm
120 mm
160 mm
ρ1-2
ρ2-3
ρ3-4
ρ5-6
ρ6-7
ρ7-8
ρ9-10
ρ10-11
ρ11-12
ρ13-14
ρ14-15
ρ15-16
P1
P2
P3
P4
P5
P6
P7
P8
P9
P10
P11
P12
P13
P14
P15
P16
Electrical resistivity, ρ (Ωm)
109.00
104.00
99.00
94.00
89.00
84.00
30
35
40
45
50
55
60
Leakage duration, t (min)
ρ5-6
ρ1-2
ρ13-14
ρ9-10

(a)

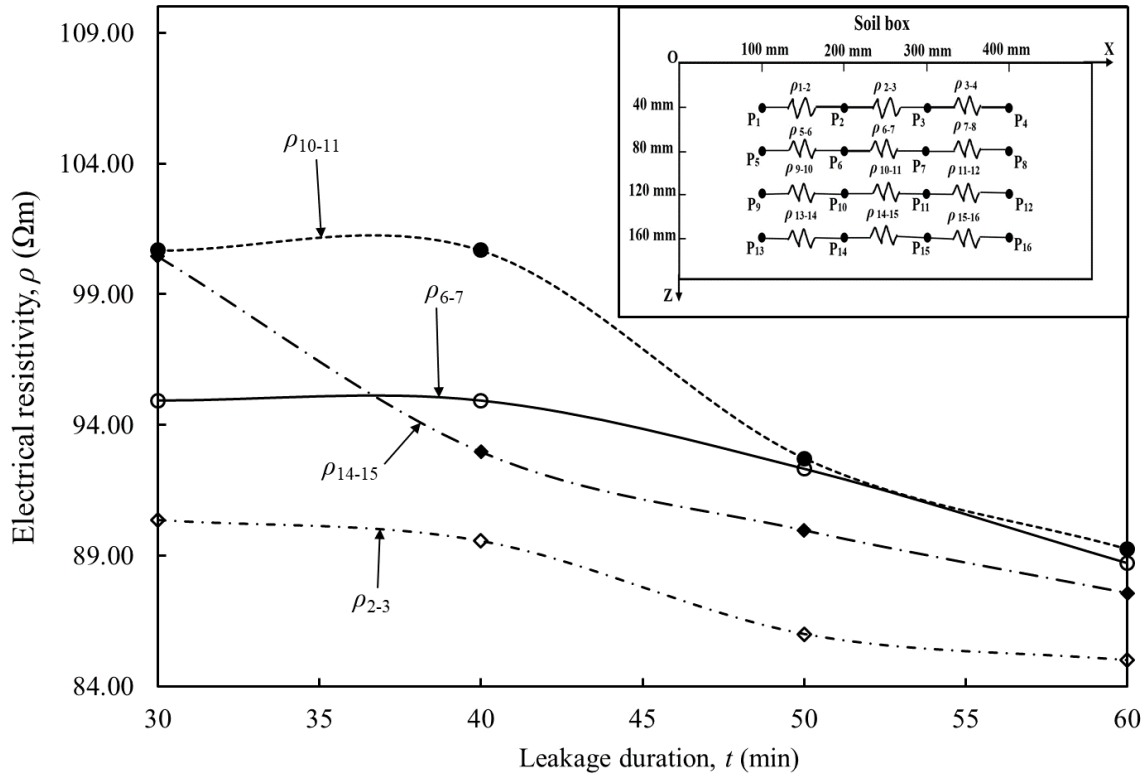

(b)

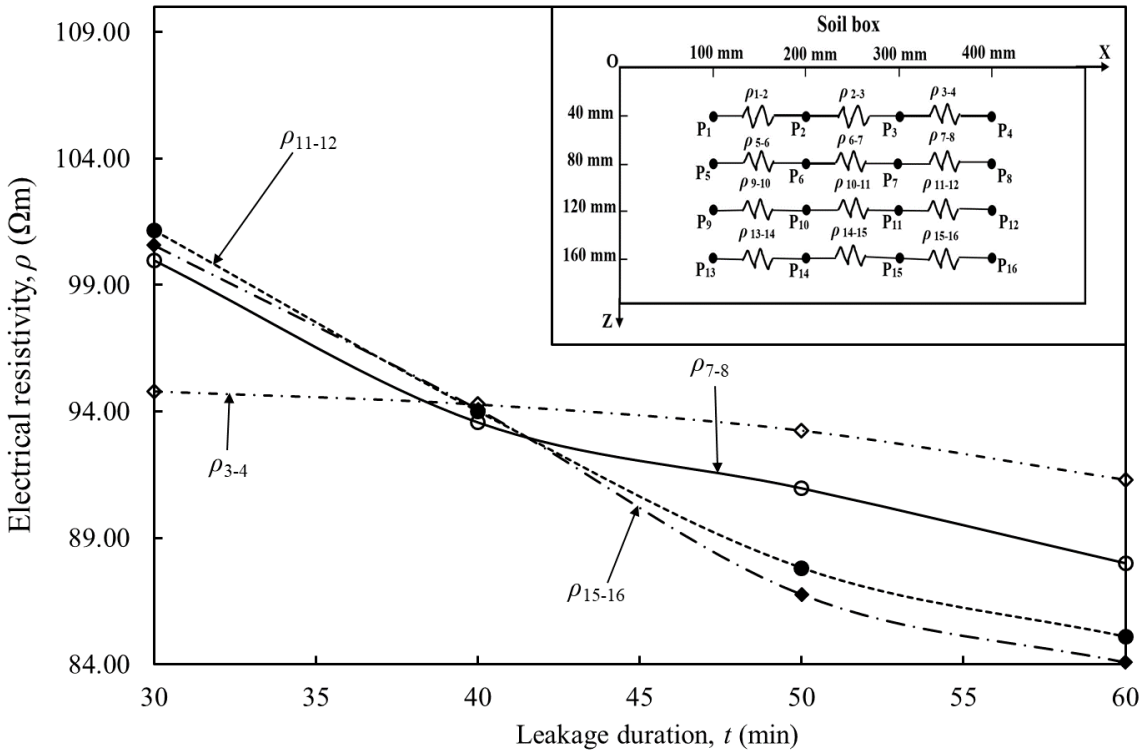

(c)

Figure 6.9: Resistivity profile of electrode pairs with their midpoint at distances of (a) 150, (b) 250 and (c) 350 mm.

6.4 Conclusions

Based on the results and discussion presented, the following general conclusions can be made:

- The leak detection system was found to be effective in determining leakage in the liner, irrespective of the leakage duration.
- Leaks could be located as early as 30 min within the commencement of leakage.
- The electrical resistivity across all electrode pairs was found to decrease with increasing leakage duration.
- The resistivity increased with an increase in the distance/depth from the leak point.
- Electrode sensing system which is closest to the liner has the better ability to detect leakage. The resistivities recorded using sensors at the depth of 120 mm and above, showed insignificant variation with distance and leakage duration.
- The findings reported here should not be extrapolated to soil types which differ significantly from the soil used in this study.
- It may be noted that the leak detection system will not be able to detect leakages in the liner if the soil is completely saturated.

References

AS 1289.4.4.1 (1997). Methods of Testing Soils for Engineering Purposes Soil Chemical Tests - Determination of the Electrical Resistivity of a Soil - Method for Sands and Granular Materials. Standards Australia, Sydney, NSW, Australia.

ASTM D6431-99 (2010). Standard guide for using the direct current resistivity method for subsurface investigation. ASTM International, West Conshohocken, PA, USA.

ASTM D6747-15 (2015). Standard guide for selection of techniques for electrical leak location of leaks in geomembranes. ASTM International, West Conshohocken, PA, USA.

ASTM D7002-16 (2016). Standard practice for electrical leak location on exposed geomembranes using the water puddle method. ASTM International, West Conshohocken, PA, USA.

ASTM D7240-06 (2011). Standard practice for leak location using geomembranes with an insulating layer in intimate contact with a conductive layer via electrical capacitance

technique (conductive geomembrane spark test), ASTM International, West Conshohocken, PA, USA.

ASTM D7703-16 (2016). Standard practice for electrical leak location on exposed geomembranes using the water lance method, ASTM International, West Conshohocken, PA, USA.

ASTM D7953-14 (2014). Standard practice for electrical leak location on exposed geomembranes using the arc testing method, ASTM International, West Conshohocken, PA, USA.

Ben Othmen, A. and Bouassida, M. (2013). Detecting defects in geomembranes of landfill liner systems: durable electrical method. *International Journal of Geotechnical Engineering* 7(2), 130-135, DOI: 10.1179/1938636213Z.00000000013.

Bouazza, A. and Van Impe, W.F. (1998). Liner design for waste disposal sites. *Environmental Geology* 35(1): 41-54, DOI: 10.1007/s002540050291.

Buss, S.E., Butler, A.P., Sollars, C.J., Perry, R. and Johnston, P.M. (1995). Mechanisms of leakage through synthetic landfill liner materials. *Water and Environment Journal* 9(4), 353-359, DOI: 10.1111/j.1747-6593.1995.tb00952.x.

Chapuis, R.P. (1990). Sand–bentonite liners: predicting permeability from laboratory tests. *Canadian Geotechnical Journal* 27(1), 47-57, DOI: 10.1139/t90-005.

Daniel, D.E. (1984). Predicting hydraulic conductivity of clay liners. *Journal of Geotechnical Engineering* 110(2), 285-300, DOI: 10.1061/(ASCE)0733-9410(1984)110:2(285)#sthash.g48WNynP.dpuf.

Daniel, D.E. (1993). Landfills and impoundments. Geotechnical practice for waste disposal, Springer, USA, pp. 97-112.

DEWHA (Department of the Environment, Water, Heritage and the Arts) (2010). National Waste Report. DEWHA, ACT, Australia. http://www.environment.gov.au/system/files/resources/af649966-5c11-4993-8390-ab300b081f65/files/national-waste-report-2010.pdf. (Accessed 26 September 2017).

Fukue, M., Minato, T., Horibe, H. and Taya, N. (1999). The micro-structures of clay given by resistivity measurements. *Engineering Geology* 54(1), 43-53, DOI: 10.1016/S0013-7952(99)00060-5.

Giroud, J.P. (1984). Impermeability: The myth and a rational approach. *Proceedings of the International Conference on Geomembranes*, Vol. 1, p. 157-162.

Giroud, J.P. and Bonaparte, R. (1989). Leakage through liners constructed with geomembranes—Part I. *Geomembrane liners. Geotextiles and Geomembranes* 8(1), 27-67, DOI: 10.1016/0266-1144(89)90009-5.

Goldsworthy, K. (2010). Waste recycling activity in Western Australia. Western Australia Waste Authority, Perth, WA, Australia.

Harrop-Williams, K. (1985). Clay liner permeability: evaluation and variation. *Journal of Geotechnical Engineering* 111(10), 1211-1225, DOI: 10.1061/(ASCE)0733-410(1985)111:10(1211).

Hix, K. (1998). Leak detection for landfill liners. National Network for Environmental Management Studies Report. National Service Center for Environmental Publications, USA. https://clu-in.org/download/studentpapers/leaklnfl.pdf. (Accessed online on 15 June 2017).

Holtz, W.G. (1985). Predicting hydraulic conductivity of clay liners: Discussion. *Journal of Geotechnical Engineering* 111(12), 1457-1459, DOI: 10.1061/(ASCE)0733-9410(1984)110:2(285).

Hoornweg, D. and Bhada-Tata, P. (2012). What a Waste (1st Ed.). World Bank. Washington D.C., USA.

Hoyos, L.R., DeJong, J.T., McCartney, J.S., Puppala, A.J., Reddy, K.R. and Zekkos, D. (2015). Environmental geotechnics in the US region: a brief overview. *Environmental Geotechnics* 2(6), 319-325, DOI: 10.1680/envgeo.14.00024.

Jessberger, H.L. and Beine, R.A. (1981). Impermeabilisation of disposal sites by impervious blankets consisting of mine refuse. *Proceedings of l0th International Conference on Soil Mechanics and Foundation Engineering*, StockholmI, Vol. 4, p. 745-746.

Mitchell, J.K. and Soga, K. (2005). Fundamentals of soil behaviour (3rd Ed.). John Wiley & Sons, Inc., New Jersey, USA.

Mohamed, A.M.O., Said, R.A. and Al-Shawawreh, N.K. (2002). Development of a methodology for evaluating subsurface concentrations of pollutants using electrical polarization technique. *Geotechnical Testing Journal* 25(2), 157–167, DOI: 10.1520/GTJ11359J.

Munoz-Castelblanco, J.A., Pereira, J.M., Delage, P. and Cui, Y.J. (2011). The influence of changes in water content on the electrical resistivity of a natural unsaturated loess. *Geotechnical Testing Journal* 35(1), 11-17, DOI: 10.1520/GTJ103587.

Naghibi, M., Abuel-Naga, H. and Orense, R. (2016). Modified odometer cell to measure electrical resistivity of clays undergoing consolidation process. *Journal of Testing and Evaluation* 45(4), 1261-1269, DOI: 10.1520/JTE20160002.

O'Kelly, B.C. (2016). Geotechnics of municipal sludges and residues for landfilling. *Geotechnical Research* 3(4), 148-179, DOI: 10.1680/jgere.16.00013.

Oh, M., Seo, M. W., Lee, S. and Park, J. (2008). Applicability of grid-net detection system for landfill leachate and diesel fuel release in the subsurface. *Journal of Contaminant Hydrology* 96(1-4), 69-82, DOI: 10.1016/j.jconhyd.2007.10.002.

Pandey, L.M.S., Shukla, S.K. and Habibi, D. (2015). Electrical resistivity of sandy soil. *Geotechnique Letters* 5(3), 178–185, DOI: 10.1680/jgele.15.00066.

Pandey, L.M.S. and Shukla, S.K. (2017). Detection of leachate contamination in Perth landfill base soil using electrical resistivity technique. *International Journal of Geotechnical Engineering*, 1-12, DOI: 10.1080/19386362.2017.1339763.

Perryman, G. and Green, S. (2017). Waste recycling activity in Western Australia. Western Australia Waste Authority, Perth, WA, Australia.

Reddy, K.R., Kosgi, S. and Motan, E.S. (1996). Interface shear behavior of landfill composite liner systems: a finite element analysis. *Geosynthetics International* 3(2), 247-275, DOI: 10.1680/gein.3.0062.

Rowe, R.K. (2012). Geotechnical and Geoenvironmental Engineering Handbook. Springer Science & Business Media, Berlin, Germany.

Schollum, P. (2010). Evaluation of the social optimum for the landfill levy in WA. Report prepared for the Waste Authority, The Government of Western Australia, Australia.

Seymour, K.J. (1992). Landfill lining for leachate containment. *Water and Environment Journal* 6(5), 389-396, DOI: 10.1111/j.1747-6593.1992.tb00768.x.

Shah, K.L. (2000). Basics of solid and hazardous waste management technology. Prentice Hall.

Sharma, H.D. and Reddy, K.R. (2004). Geoenvironmental engineering: site remediation, waste containment, and emerging waste management technologies. John Wiley & Sons, Inc., New Jersey, USA.

Shukla, S.K. (2016). An introduction to geosynthetic engineering. CRC Press, Taylor & Francis Group, Florida, USA.

Shukla, S.K. and Yin, J.H. (2006). Fundamentals of geosynthetic engineering. Taylor & Francis, UK.

Stephenson, G. and Hepburn, J.A. (1955). Plan for the metropolitan region of Perth and Fremantle, Western Australia: an atlas prepared for the government of Western

Australia (plate 4). Perth, Western Australia: Government Printing Office. Retrieved from http://www.planning.wa.gov.au/dop_pub_pdf/plate4.pdf.

Tyl, E. (2016). Personal communication. Water Corporation, WA, Australia.

Waste Authority (2016). Recycling activity in Western Australia. Perth, Western Australia. http://www.wasteauthority.wa.gov.au/publications/recycling-activity-2014-15. (Accessed 27 September 2017).

CHAPTER 7

RESISTIVITY PROFILES OF LINER BASE WITH MSW LANDFILL LEACHATE

This chapter is based on a section of the paper submitted to Surveys in Geophysics, Springer, as listed in Section 1.6. The details presented here for this part of the paper are the same, except some changes in the layout in order to maintain a consistency in the presentation throughout the thesis.

7.1 Introduction

Municipal solid waste (MSW) landfills generally make use of lining systems as the barriers to control the migration of leachate contaminants to underlying soil and groundwater (Koerner, Koerner and Martin, 1994; Giroud and Bonaparte, 2001; Misra and Pandey, 2005; Arora *et al.*, 2007; Shukla, 2016). Figure 7.1 is the photograph of a typical leachate collection pond at a landfilling facility in Perth, lined with a geosynthetic clay (GCL) liner.

The lining systems are engineered to be intact over the lifespan of the landfill. However, due to various factors, such as inappropriate seaming practices, puncture defects, aging, harsh operating conditions, ultraviolet lights, radiation effects, etc., liners often fail (Giroud and Bonaparte, 1989; Shukla, 2016). The liner defects lead to subsequent contamination issues. Hence, it is imperative to detect these leaks at the onset, repair them timely, and prevent the hazardous impact of the contamination from intensifying (Oh *et al.*, 2008; Pandey and Shukla, 2017). Therefore, the landfilling facilities currently adopt various leak detection methods for the proper management of contaminants (Chen and Wang, 1997; Mohamed *et al.*, 2002; Praharaj *et al.*, 2002; Arora *et al.*, 2007; Oh *et al.*, 2008; Ben Othman and Bouassida, 2013; Teng *et al.*, 2014; Pandey *et al.*, 2017; Pandey and Shukla, 2018).

Among the various detection methods, the use of the electrical resistivity technique for leak detection is most extensive due to its easy operation and low expenses (Oh *et al.*, 2008; Ben Othmen and Bouassida, 2013). This method detects the changes in the resistivity of soil below the liner, produced due to its contamination with leachate, to determine the liner failures (Mohamed *et al.*, 2002; Munoz-Castelblanco *et al.*, 2012; Pandey *et al.*, 2015; Pandey and

Shukla, 2017). It is furthermore essential that the leak should be determined at the earliest. Hence, there is a significant scope for a leak detection technique based on the electrical resistivity method, which can be installed below the lining systems as a real-time monitoring technique in landfilling facilities (Pandey *et al.*, 2017; Pandey and Shukla, 2018; Pandey and Shukla, 2019).

Figure 7.1: A typical leachate collection pond lined with geosynthetic clay liner (Red Hill Waste Management Facility, Eastern Metropolitan Regional Council, Western Australia).

Though a new technique has been developed by Pandey and Shukla (2019) and has been shown to work with water as the leaching liquid, it has not been used to verify how the system works with the field leachates. Such a study would be particularly useful for the design of suitable monitoring system for a specific landfill site. Further, the results will also serve as a baseline, and assist in the detection of leakage using an online monitoring system, for predetermined leachate properties. Hence, this paper focuses on the investigation of the leakage of field leachates through liners using the innovative leak detection technique, as developed

earlier. In the experimental investigation, tests have been conducted by simulating an actual liner leak situation. The resulting leachate leakage was ascertained by detecting the changes produced in the soil electrical resistivity. Newly developed empirical correlations and analytical modelling have also been presented as one of the objectives of the work. An understanding of these correlations and models will help practicing engineers to detect contamination and liner leakage issues, design and placement of sensor systems, numerical modelling, and so on.

7.2 Materials and Methods

The soil used for this study is a good representation of the foundation soil in Western Australia (WA) and was used extensively throughout Perth metropolitan region. The properties of this soil are listed in Table 7.1. Figure 7.2 shows the scanning electron microscopy (SEM) image and Figure 7.3 is the SEM energy dispersive spectroscopy (EDS) overlay of Perth sandy soil. It can be observed that the main constituents of the soil are carbon, silicon, oxygen and aluminium. The Leachate #1 used for the experimentation was procured from the North Bannister Resource Recovery Facility, SUEZ Australia, and the Leachate #2 was procured from Red Hill Landfill Facility. Tables 7.2 and 7.3 give the chemical compositions of the leachate specimens.

Table 7.1: Physical properties of Perth soil.

Properties	Values
Specific gravity of soil solids, G_s	2.68
Coefficient of uniformity, C_u	2.27
Coefficient of curvature, C_c	1.22
Effective size, D_{10} (mm)	0.15
Minimum dry unit weight, $\gamma_{d\min}$ (kN/m^3)	14.02
Maximum dry unit weight, $\gamma_{d\max}$ (kN/m^3)	15.56
Soil classification as per USCS (Unified Soil Classification System)	Poorly graded sand (SP)

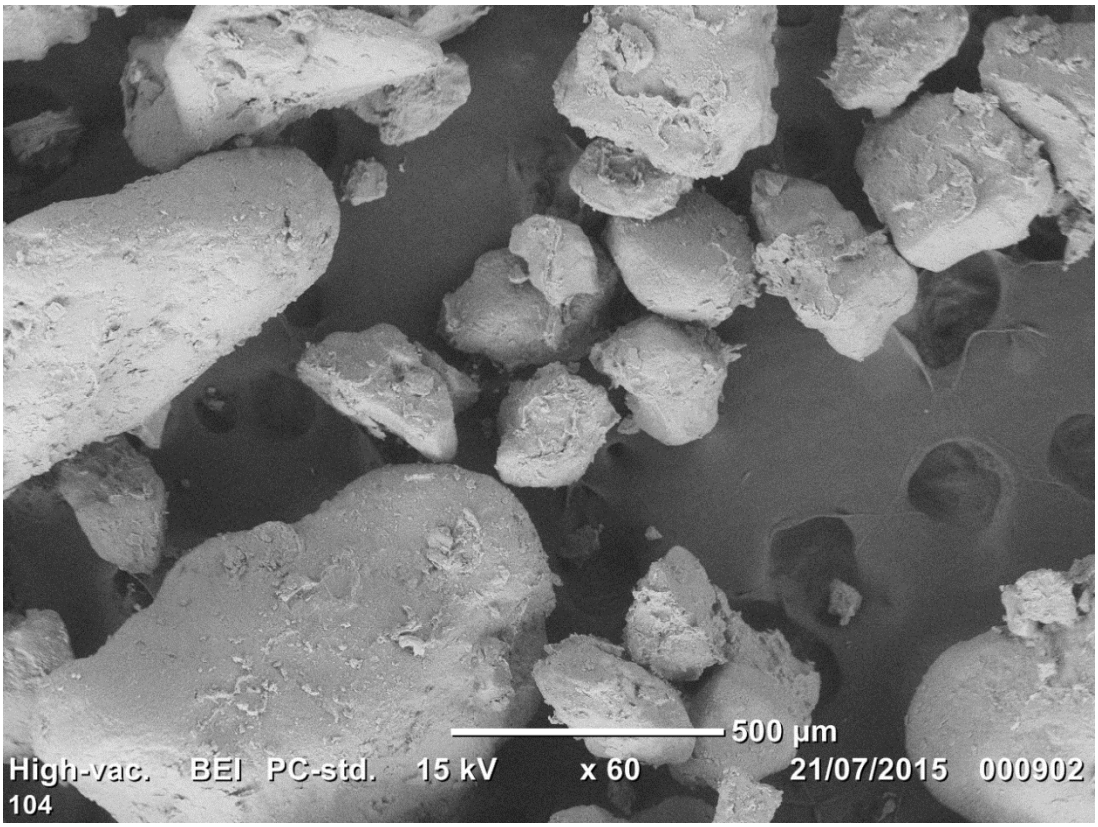

Figure 7.2: Scanning electron microscopy (SEM) image of soil.

A 220 µ thick geomembrane (GMB) liner was used for this test. A 550-mm long and 250-mm wide GMB piece was cut and a leak was intentionally introduced in its centre using a gravel-size particle.

Figure 7.4 shows the soil box used in this study. It was used to replicate an actual lining system as used by landfilling facilities. It was fabricated from 12-mm thick non-conducting perspex sheet. The inner dimensions of the box were 500-mm length, 200-mm width and 400-mm height. It was fitted with two brass current plate electrodes (C_1 and C_2) of 200-mm length and 200-mm width, as shown in the figure. In addition, sixteen brass potential measuring pins (P_1 through P_{16}) were also installed in the box. Furthermore, a groove of 8-mm diameter was made in the soil box at a height of 200-mm from the bottom. This groove was used to secure the GMB over the soil. The system design is presented with complete details by Pandey and Shukla (2018b).

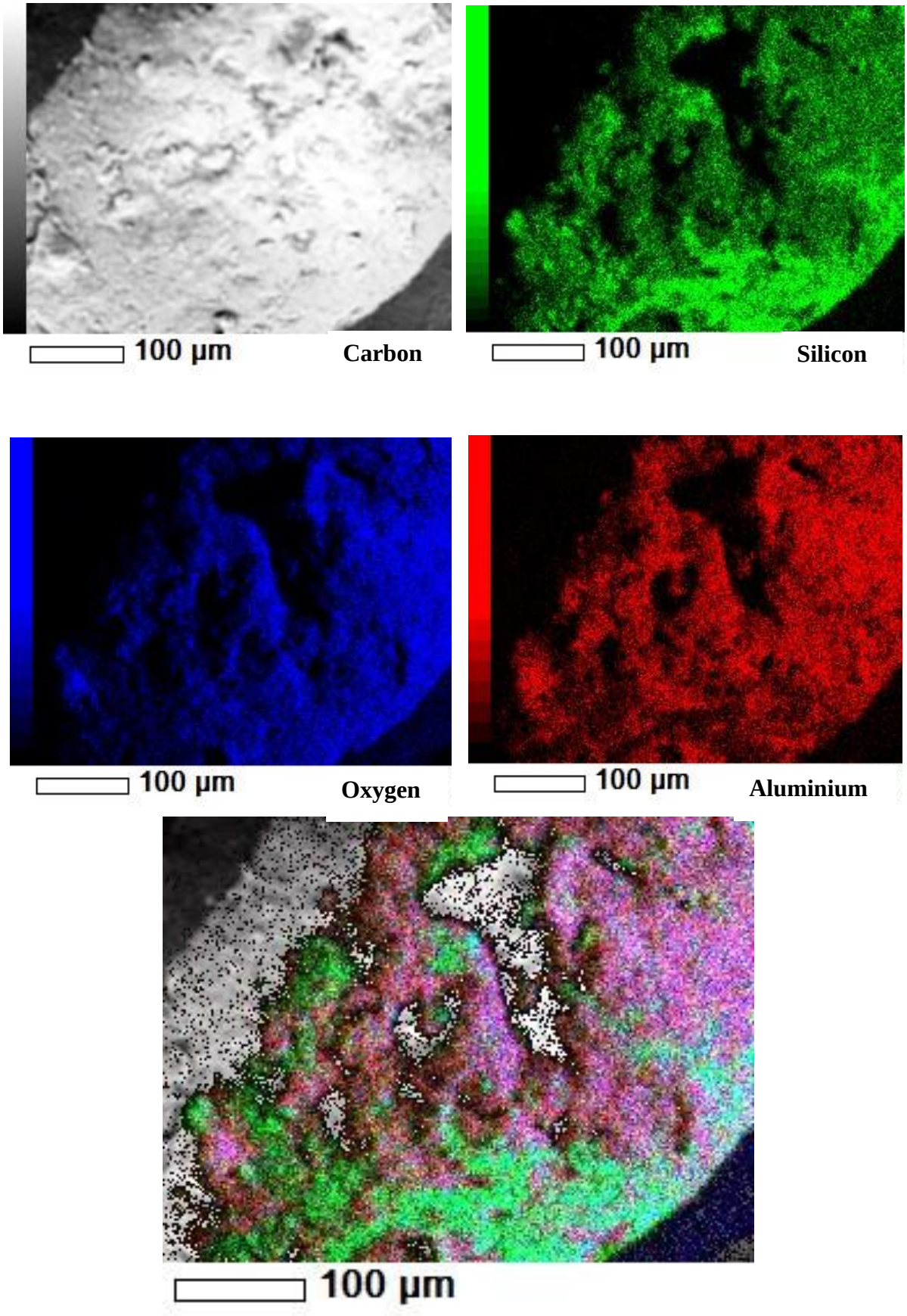

Figure 7.3: SEM energy dispersive spectroscopy (EDS) overlay of Perth sandy soil.

Table 7.2: Chemical composition of the Leachate #1.

Chemical group	Chemical name	Unit	Value
BTEXN	Benzene	µg/L	<40
	Toluene	µg/L	100
	Ethylbenzene	µg/L	150
	Xylene (o)	µg/L	120
	Xylene (m & p)	µg/L	220
	Xylene Total	µg/L	340
Total Organic Carbon (TOC)	TOC	mg/L	1200
Inorganics	COD	mg/L	7300
	Nitrate and Nitrite (as N)	mg/L	<5
Metals	Arsenic	mg/L	0.21
	Cadmium (Filtered)	mg/L	<0.001
	Chromium (III+VI) (Filtered)	mg/L	0.37
	Copper (Filtered)	mg/L	<0.005
	Iron	mg/L	10
	Lead (Filtered)	mg/L	<0.005
	Manganese (Filtered)	mg/L	0.11
	Mercury (Filtered)	mg/L	<0.0005
	Molybdenum (Filtered)	mg/L	<0.025
	Nickel (Filtered)	mg/L	0.17
	Selenium (Filtered)	mg/L	<0.005
	Zinc (Filtered)	mg/L	0.1
Polycyclic aromatic hydrocarbon (PAH)	PAHs (Sum of total)	µg/L	14
Acidity and alkalinity	Alkalinity (Carbonate as $CaCO_3$)	mg/L	<10
	Alkalinity (Hydroxide as $CaCO_3$)	mg/L	<10
	Alkalinity (total as $CaCO_3$)	mg/L	5900

	Bicarbonate Alkalinity as $CaCO_3$	mg/L	5900
Major ions	Calcium	mg/L	41
	Chloride	mg/L	3800
	Magnesium	mg/L	31
	Potassium	mg/L	890
	Sodium	mg/L	1800
	Sulphate	mg/L	22
Nutrients	Ammonia as N	mg/L	1600
	Total Kjeldahl Nitrogen	mg/L	1900
	Nitrate (as N)	mg/L	<2
	Nitrite (as N)	mg/L	<2
	Nitrogen (Total)	mg/L	1900
	Phosphate total (P)	µg/L	3600

Based after Widenbar (2017).

Table 7.3: Chemical composition of the Leachate #2.

Chemical group	Chemical name	Unit	Value
Physical Parameters	pH (lab)	-	7.6
	Conductivity @ 25°C	µS/cm	2600
	$CaCO_3$ (unfiltered hardness)	mg/L	490
	TDS	mg/L	850
	TSS	mg/L	32
	BOD	mg/L	120
Major Cations and Anions	Potassium	mg/L	69.7
	Chloride	mg/L	128
	Sodium	mg/L	92.7
	Magnesium	mg/L	25.9

	Calcium	mg/L	152
	Sulphate	mg/L	<1
Nutrients	Total Nitrogen	mg/L	210
	Nitrate	mg/L	1.5
	Nitrite	mg/L	1.5
	Ammonia	mg/L	180
	Total Phosphorous	mg/L	1.9
	Reactive Phosphorus	mg/L	0.54
Metals	Aluminium	mg/L	0.058
	Arsenic	mg/L	0.004
	Cadmium	mg/L	<0.0001
	Chromium	mg/L	0.006
	Copper	mg/L	0.0009
	Iron	mg/L	3.6
	Lead	mg/L	0.0004
	Manganese	mg/L	0.13
	Mercury	mg/L	<0.0001
	Nickel	mg/L	0.026
	Zinc	mg/L	0.08
Polycyclic aromatic hydrocarbon (PAH)	Naphthalene	µg/L	<1
	Acenaphthene	µg/L	<1
	Anthracene	µg/L	<1
	Fluoranthene	µg/L	<1
	Pyrene	µg/L	<1

	Benzo(a) pyrene	µg/L	<1
Organochlorine Pesticides	Chlordane	µg/L	<0.01
	Trans (g-) Chlordane	µg/L	<0.01
	Oxychlordane	µg/L	<0.01
	gamma BHC (lindane)	µg/L	<0.01
	Heptachlor	µg/L	<0.01
	Heptachlor epoxide	µg/L	<0.01
	DDT	µg/L	<0.01
	DDD	µg/L	<0.01
	DDE	µg/L	<0.01
	Aldrin	µg/L	<0.01
	Dieldrin	µg/L	<0.01
	HCB	µg/L	<0.01
Organophosphate Pesticides	Chlorpyrifos	µg/L	<0.01
	Diazinon	µg/L	<0.01
	Dimethoate	µg/L	<0.05
	Fenamiphos	µg/L	<0.05
	Fenthion	µg/L	<0.05
	Malathion	µg/L	<0.01
	Parathion	µg/L	<0.01
	Demeton-S-methyl	µg/L	<0.05
Triazine Herbicides	Atrazine	µg/L	<0.1
	Prometryn	µg/L	<0.1
	Terbutryn	µg/L	<0.1
BTEXN	Benzene	µg/L	<1

	Toluene	µg/L	2
	Ethyl benzene	µg/L	<1
	m/p - Xylenes	µg/L	<2
	o-Xylenes	µg/L	<1
Total Recoverable Hydrocarbons	TRH C6-C10	µg/L	300
	TRH C10-C16	µg/L	5700
	TRH C16-C34	µg/L	2600
	TRH C34-C40	µg/L	290
Other Organic Compounds	Chlorobenzene	µg/L	<1.0
	1,2 - Dichloro benzene	µg/L	<1.0
	Simazine	µg/L	<0.1
	Molinate	µg/L	<0.1
	2, 4-D	µg/L	<1
	2,4,5-T	µg/L	<1
Total Recoverable Hydrocarbons with Silica Gel Cleanup	TRH C6-C10 Silica	-	
	TRH >C10-C16 Silica	-	2500
	TRH >C16-C34 Silica	-	400
	TRH >C36-C40 Silica	-	<100
Radionuclide Testing	Gross Alpha	mBq/L	130
	Gross Beta	mBq/L	170
	Radium-228	-	
	Radium-226	-	
	K40	mBq/L	1900
PFAS	PFOS	µg/L	0.09
	PFHxS	µg/L	0.11
	PFOA	µg/L	0.34
	6:2FTS	-	0.77
	8:2FTS	-	<0.001

	PFBA	-	0.091
	PFBS	-	0.15
	PFHpA	-	0.11
	PFHxA	-	0.21
	PFPeA	-	0.081
Other Metals	Beryllium	mg/L	<0.0001
	Cobalt	mg/L	0.0042
	Antimony	mg/L	0.0009
	Titanium	mg/L	<0.002
	Thallium	mg/L	<0.0001
	Vanadium	mg/L	0.003

Based after Maslen (2018).

In Figure 7.4, x and z axes are shown to report the horizontal distance $_x$ (mm) of the electrodes and the vertical distance/depth distance $_z$ (mm) of the mid-point of each pair of electrodes. For the analysis, the soil resistivity obtained between a pair of electrodes was assumed to be at the mid-point of that electrode pair.

7.3 Experimental Procedure

Oven dried soil was filled in the soil box up to a height of 200 mm, such that a relative density (D_r) of 100% was achieved. The box was filled in five layers to ensure homogeneity. The pre-cut geomembrane (GMB) liner with the leak in its centre (Figure 7.5), was installed over this soil layer. It was secured using an 8-mm diameter rubber gasket, fixed into the 8-mm groove to ensure that the leakage only takes place from the leak which was introduced intentionally. The leak in the centre of the GMB was initially kept covered with tape.

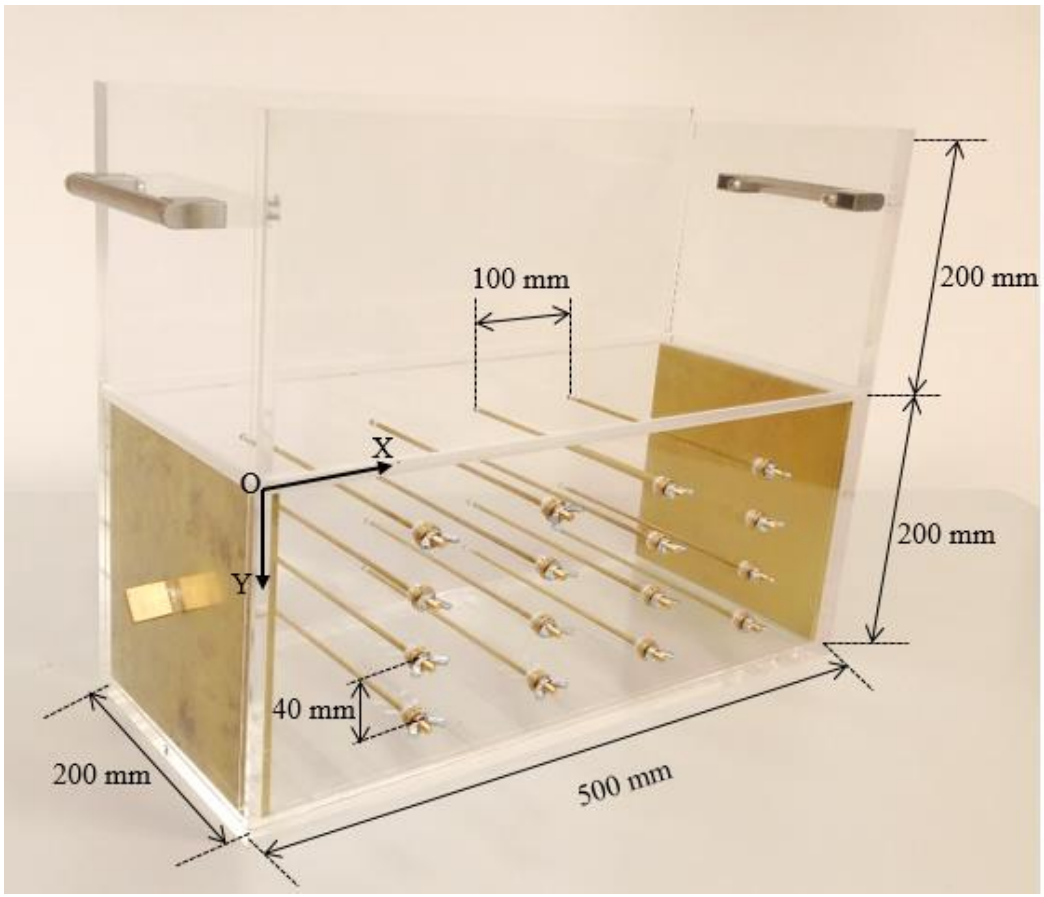

Figure 7.4: Soil box used in the leak detection technique.

Figure 7.5: Geomembrane liner with leak point.

A constant head of 100 mm of the leachate was maintained over the GMB liner. The duration for which the leakage was permitted through the liner defect, was denoted as t. At the commencement of the test, the leak was uncovered and the time was recorded as $t = 0$. The AEMC 6471 ground resistance testing machine was used to measure the resistance of the soil. The connections between the soil box and the resistance tester were made as shown in Figure 7.6. A known current was input through the outer current electrodes and the resulting voltage drop across a pair of potential measuring pins was measured to obtain the soil resistance. This resistance was then used to compute the resistivity (ρ , Ωm) of the soil specimen (Pandey *et al.*, 2017, Pandey and Shukla, 2018b) using Eqn. (7.1). Here, A is the cross-sectional area (m^2) and L is the length (m) of the test specimen. Twelve resistivity values were obtained at each 10-min time interval. The test run was stopped when the soil was observed to be near saturation condition.

$$R = \frac{\rho L}{A} \tag{7.1}$$

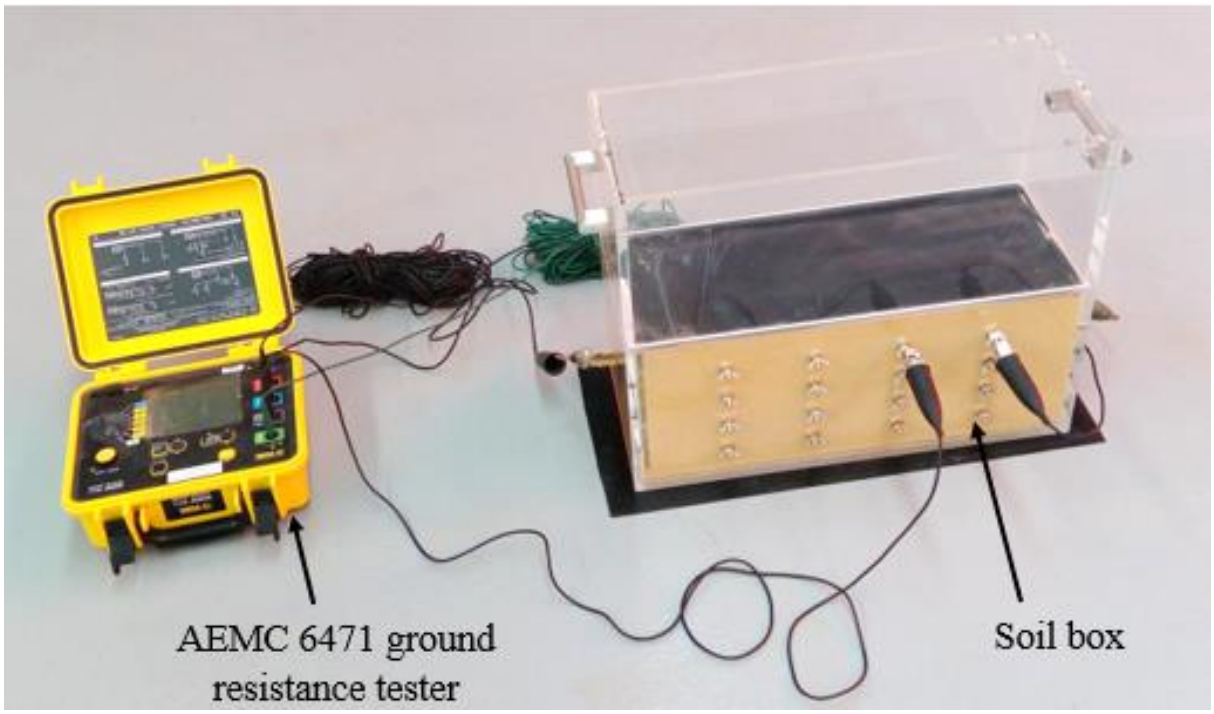

Figure 7.6: Leak detection system.

A test environment of 20℃ was maintained for the duration of the leak detection test. This was done to eliminate the effect of temperature fluctuations on the resistivity of the soil (Pandey *et al.*, 2015).

7.4 Results and Discussion

Figures 7.7(a) through 7.8(d) show the variation of the electrical resistivity (ρ) of the soil with an increase in the leakage duration (t), for the electrode pairs with their mid-points located at the depth z = 40, 80, 120 and 160 mm, respectively. Figures 7.7(a) through 7.7(d) give the results for the Leachate #1 while the Figures 7.8(a) through 7.8(d) present the results for Leachate #2. It was observed that the resistivity of the soil decreased with an increase in the leakage duration, irrespective of the depth (z). This is as per the expectation, because the resistivity of leachate is much lower than that of the soil. Hence, as the amount of leachate infiltrated through the soil increases, soil resistivity should decrease. In other words, the decrease in soil resistivity points to an increase in the leachate content of soil, and therefore, indicates the development of liner leaks. Consequently, this method was noticed to be effective in ascertaining the presence of liner leakages.

Furthermore, the following relationship is known for permeability of soil medium (k) (Das, 2013; Shukla, 2014):

$$k = \frac{\gamma_l}{\eta} K \tag{2}$$

where k = coefficient of permeability of soil (m/s), η = viscosity of leachate (Pas or Ns/m^2), γ_l = unit weight of leachate (kN/m^3), and K = absolute permeability of soil (m^2).

Here, k depends on properties of both soil and leachate while K is independent of the properties of the leachate. This relationship can be used to explain the observed disparity between the resistivity values for leakage tests conducted with both the leachates (Figures 7.7(a) through 7.8(d)). As per Eqn. (7.2), permeability (k) is inversely proportional to the viscosity of the leachate (η). Therefore, the leachate with higher η will have lower k, and hence, the observed difference in resistivity readings for the leachate specimens is noted. Consequently, it may be inferred that Leachate #1 has higher viscosity as compared to Leachate #2.

In addition, it is seen from Figures 7.7(a) through 7.8(d) that for any given z, the resistivity ρ of the central pair of electrodes was lesser than that of the adjacent pairs, irrespective of the leakage duration t. For example, ρ_{2-3} is lower than ρ_{1-2} and ρ_{3-4}, for any leachate duration

(Figure 7.7(a)). Moreover, it is interesting to note that the leak was positioned directly above the mid-point of electrodes with resistivity ρ_{2-3}. As a result, the soil between these two electrodes is expected to have more leachate content than the soil between the adjacent pairs at the same depth, and hence, ρ_{2-3} is expected to be lesser than ρ_{1-2} and ρ_{3-4}. Based on the observations from Figures 7.7(a) through 7.8(d), the system can be shown to be effective in determining the location of the leak timely.

Further, it is noted from Figure 7.7(a) that although ρ_{1-2} and ρ_{3-4} were equidistant from the leak, their readings at a given leakage duration (t) were not same. For example, for Leachate #1 at $t = 40\,\text{min}$, ρ_{1-2} is $7.92\,\Omega\text{m}$, while ρ_{3-4} is $7.38\,\Omega\text{m}$ (Figure 7.7(a)). However, this disparity becomes negligible as the leakage duration increases. Similar observations are made from Figures 7.7(b) through 7.7(d). This can be explained by considering the fact that although attempts were made to fill the soil box uniformly, the soil was non-homogeneous and anisotropic medium.

It is interesting to note that the resistivity of soil was not obtained at leakage durations less than 30 min for Leachate #1 and less than 130 min for Leachate #2. This observation can be accounted for using the well-established fact that the resistivity of dry soils is extremely high (Munoz-Castelblanco *et al.*, 2012; Pandey and Shukla, 2017) and hence, generally beyond the range of standard ground resistance testing equipment used in the field (Pandey *et al.*, 2017; Pandey and Shukla, 2018; Pandey and Shukla, 2019). For instance, the AEMC 6471 tester has a resistivity range of 10^1 to $10^6\,\Omega\text{m}$. The addition of leachate lowers the resistivity of the soil, and therefore, readings can be obtained when resistivity falls within the range of the test equipment.

Figures 7.9(a) through 7.10(c) give the resistivity profiles of the soil with variations in the distance of the mid-point of the electrode pairs, x = 150, 250 and 350 mm, respectively. Figures 7.9(a) through 7.9(c) are for the readings obtained for Leachate #1 while Figures 7.10(a) through 7.10(c) give the results for Leachate #2. The soil resistivity demonstrated a sharp decrease with an increase in the leakage duration, irrespective of the position of the potential measuring electrode pair.

Moreover, it may be noticed from Figures 7.9(a) through 7.10(c) that at any given leakage duration (t), the resistivity of the soil increased with an increase in the depth of the electrodes. However, the resistivity profiles obtained for z = 120 and 160 mm, exhibit negligible variance, irrespective of t.

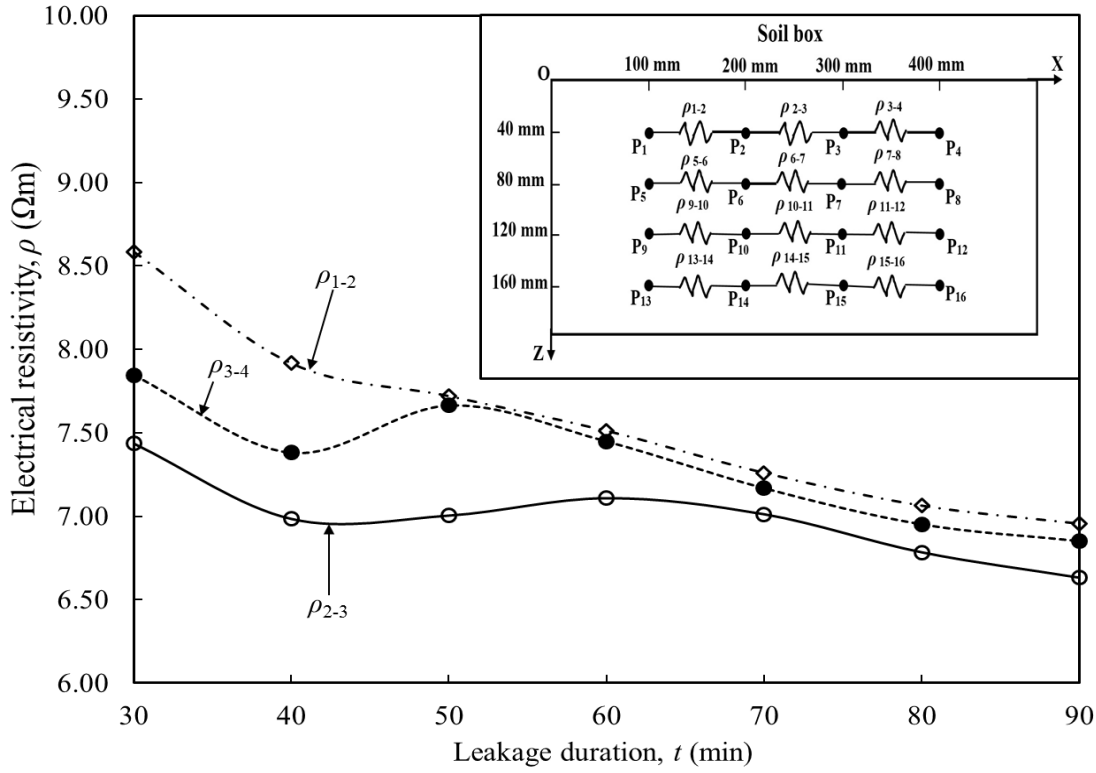
Soil box
100 mm
200 mm
300 mm
400 mm
O
X
Z
40 mm
80 mm
120 mm
160 mm
ρ_{1-2}
ρ_{2-3}
ρ_{3-4}
ρ_{5-6}
ρ_{6-7}
ρ_{7-8}
ρ_{9-10}
ρ_{10-11}
ρ_{11-12}
ρ_{13-14}
ρ_{14-15}
ρ_{15-16}
P1 P2 P3 P4
P5 P6 P7 P8
P9 P10 P11 P12
P13 P14 P15 P16
Electrical resistivity, ρ (Ωm)
Leakage duration, t (min)
10.00
9.50
9.00
8.50
8.00
7.50
7.00
6.50
6.00
30
40
50
60
70
80
90

(a)

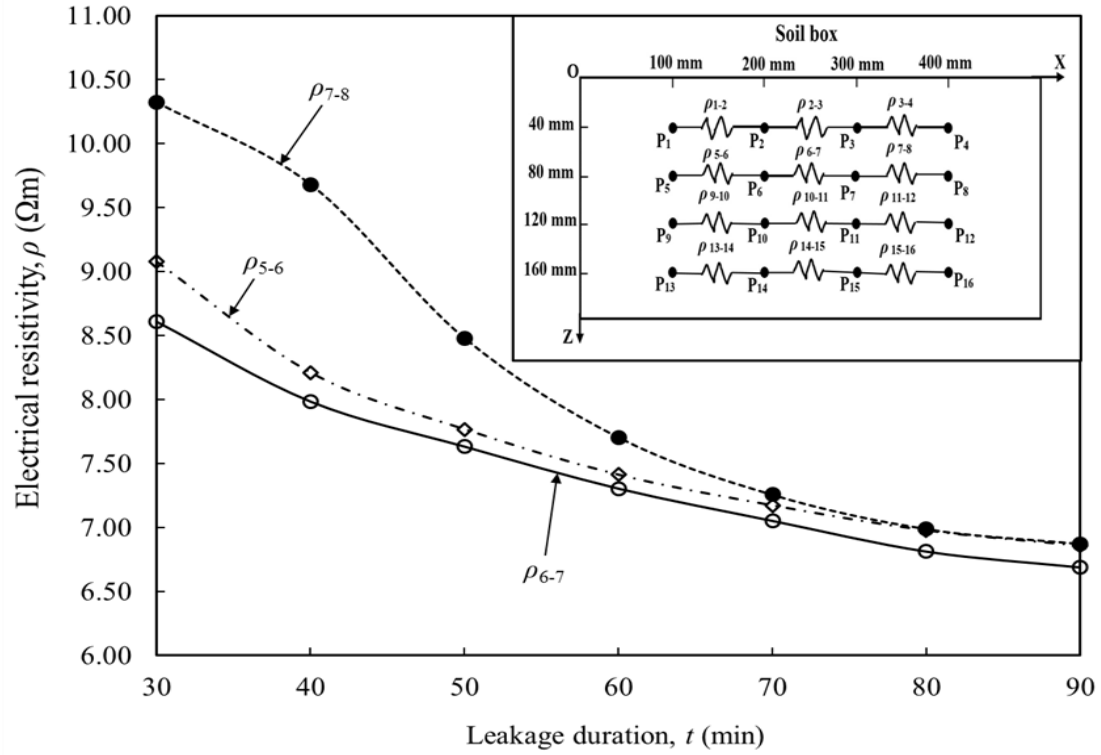
Soil box
100 mm
200 mm
300 mm
400 mm
O
X
Z
40 mm
80 mm
120 mm
160 mm
ρ_{1-2}
ρ_{2-3}
ρ_{3-4}
ρ_{5-6}
ρ_{6-7}
ρ_{7-8}
ρ_{9-10}
ρ_{10-11}
ρ_{11-12}
ρ_{13-14}
ρ_{14-15}
ρ_{15-16}
P1 P2 P3 P4
P5 P6 P7 P8
P9 P10 P11 P12
P13 P14 P15 P16
Electrical resistivity, ρ (Ωm)
Leakage duration, t (min)
11.00
10.50
10.00
9.50
9.00
8.50
8.00
7.50
7.00
6.50
6.00
30
40
50
60
70
80
90

(b)

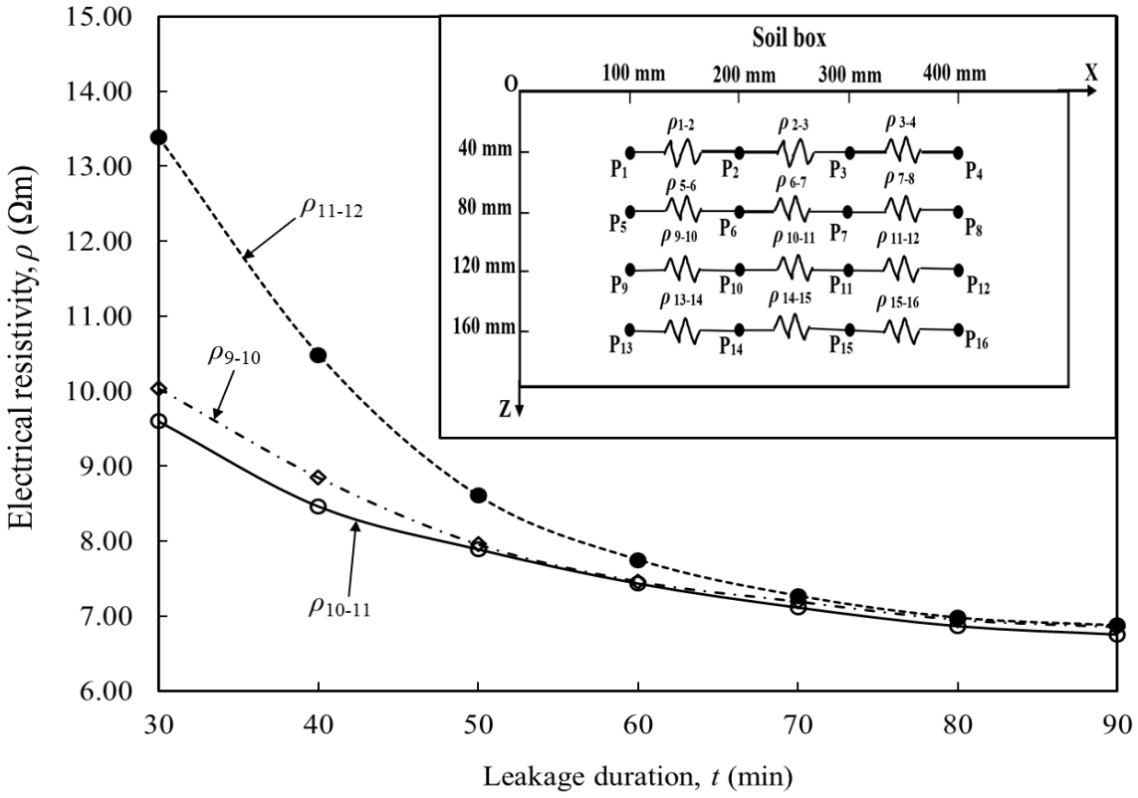

(c)

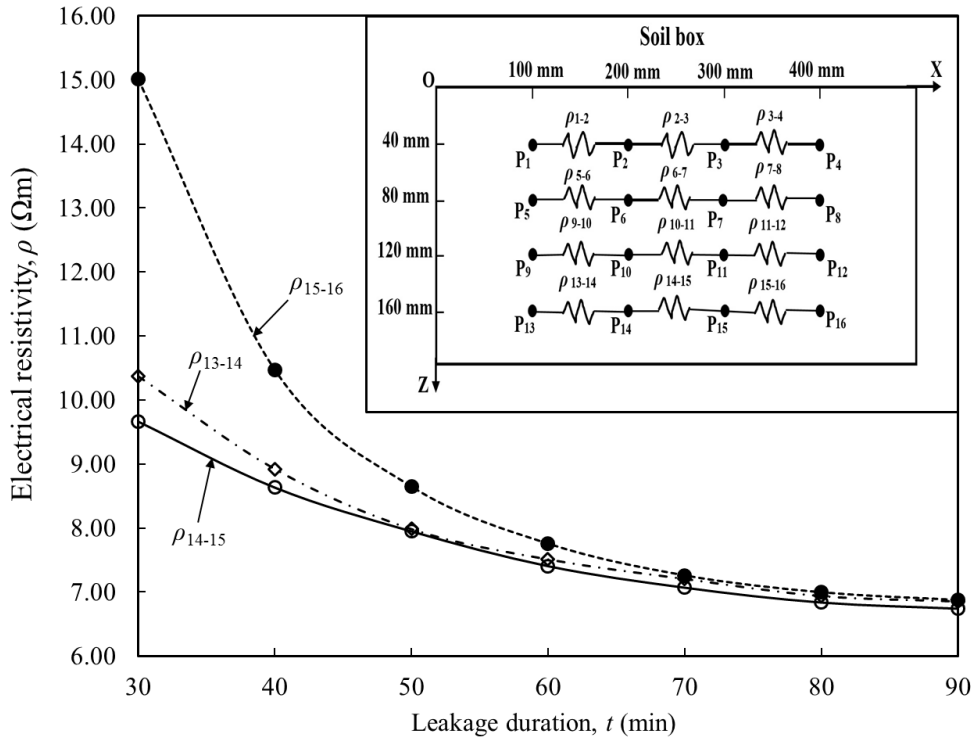

(d)

Figure 7.7: Resistivity profiles of electrode pairs located below geomembrane liner at the depth of: (a) 40 mm; (b) 80 mm; (c) 120 mm; and (d) 160 mm using Leachate #1.

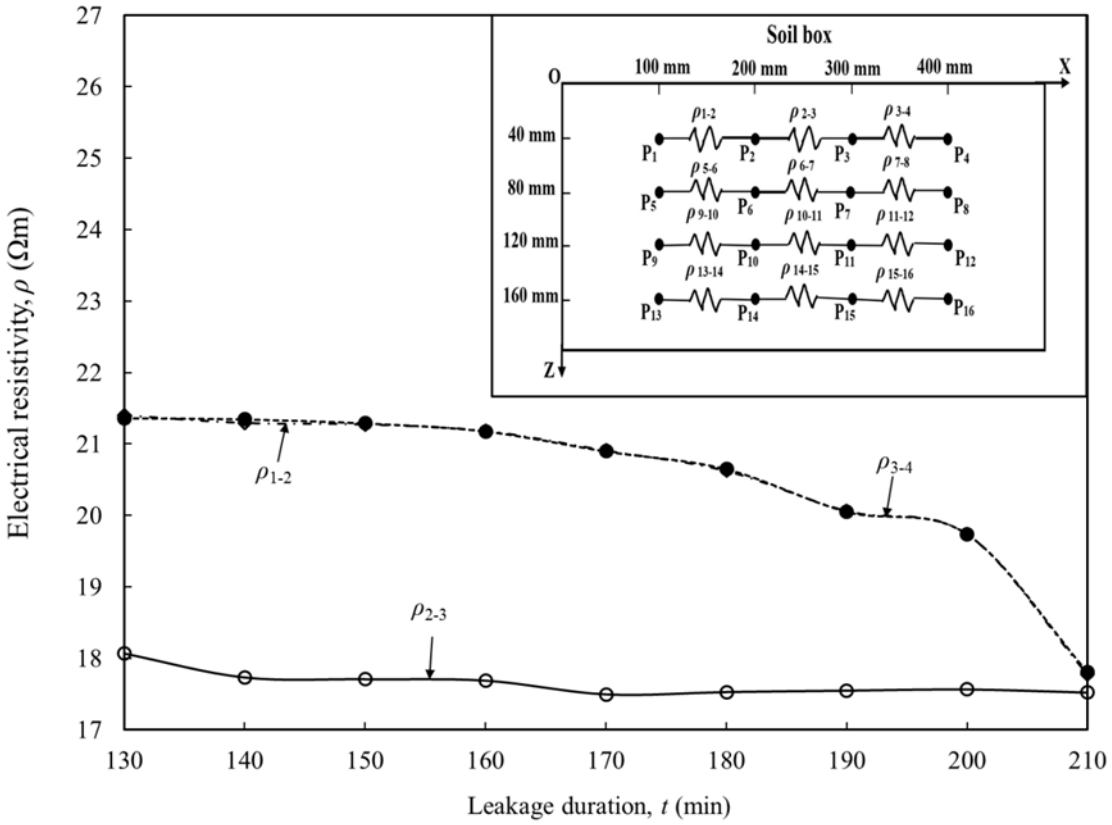
Soil box
100 mm
200 mm
300 mm
400 mm
O
X
Z
40 mm
80 mm
120 mm
160 mm
P1
P2
P3
P4
P5
P6
P7
P8
P9
P10
P11
P12
P13
P14
P15
P16
ρ1-2
ρ2-3
ρ3-4
ρ5-6
ρ6-7
ρ7-8
ρ9-10
ρ10-11
ρ11-12
ρ13-14
ρ14-15
ρ15-16
Electrical resistivity, ρ (Ωm)
Leakage duration, t (min)

(a)

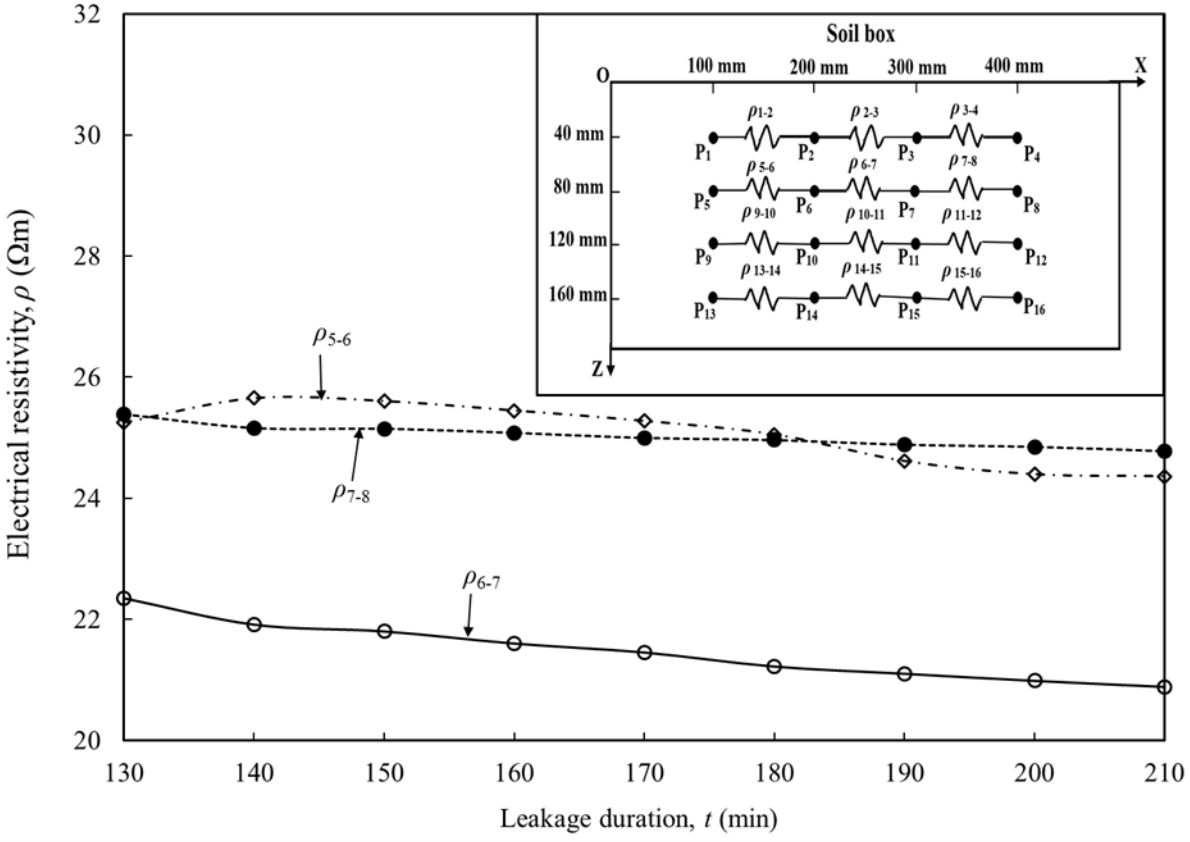
Soil box
100 mm
200 mm
300 mm
400 mm
O
X
Z
40 mm
80 mm
120 mm
160 mm
P1
P2
P3
P4
P5
P6
P7
P8
P9
P10
P11
P12
P13
P14
P15
P16
ρ1-2
ρ2-3
ρ3-4
ρ5-6
ρ6-7
ρ7-8
ρ9-10
ρ10-11
ρ11-12
ρ13-14
ρ14-15
ρ15-16
Electrical resistivity, ρ (Ωm)
Leakage duration, t (min)

(b)

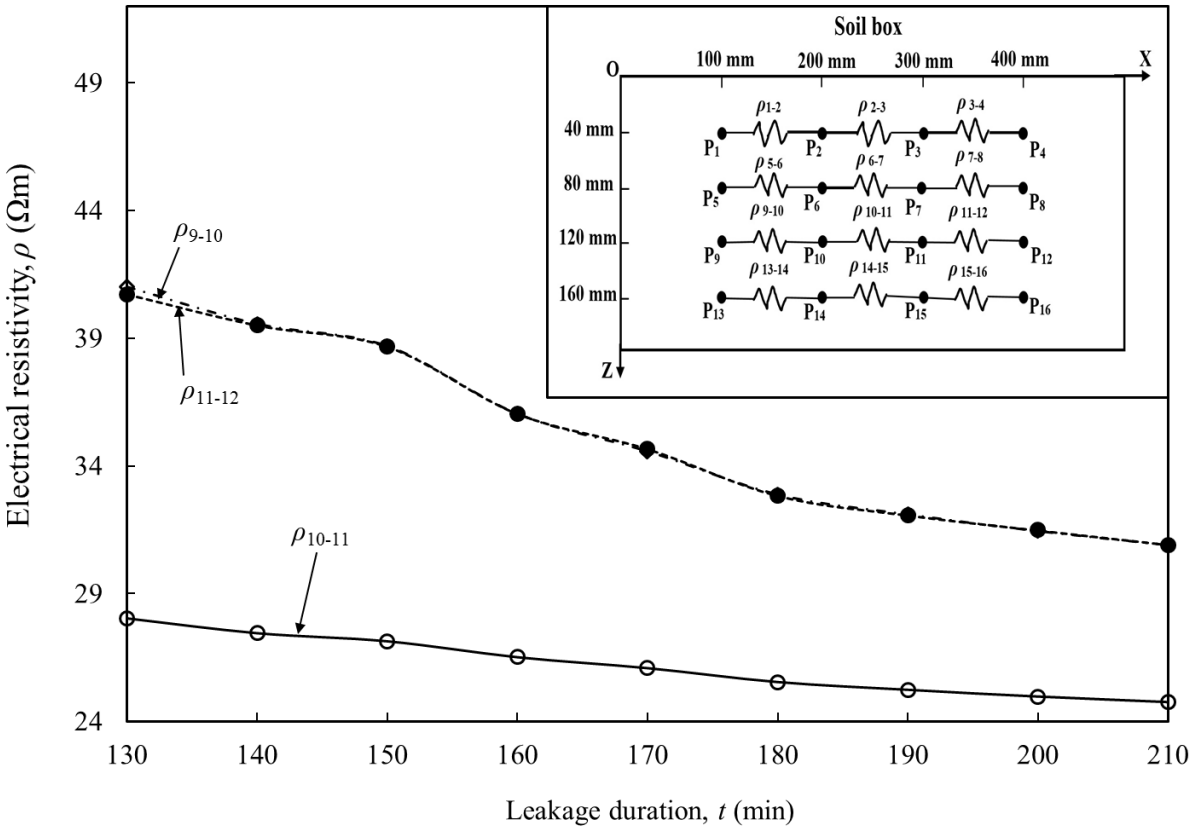

(c)

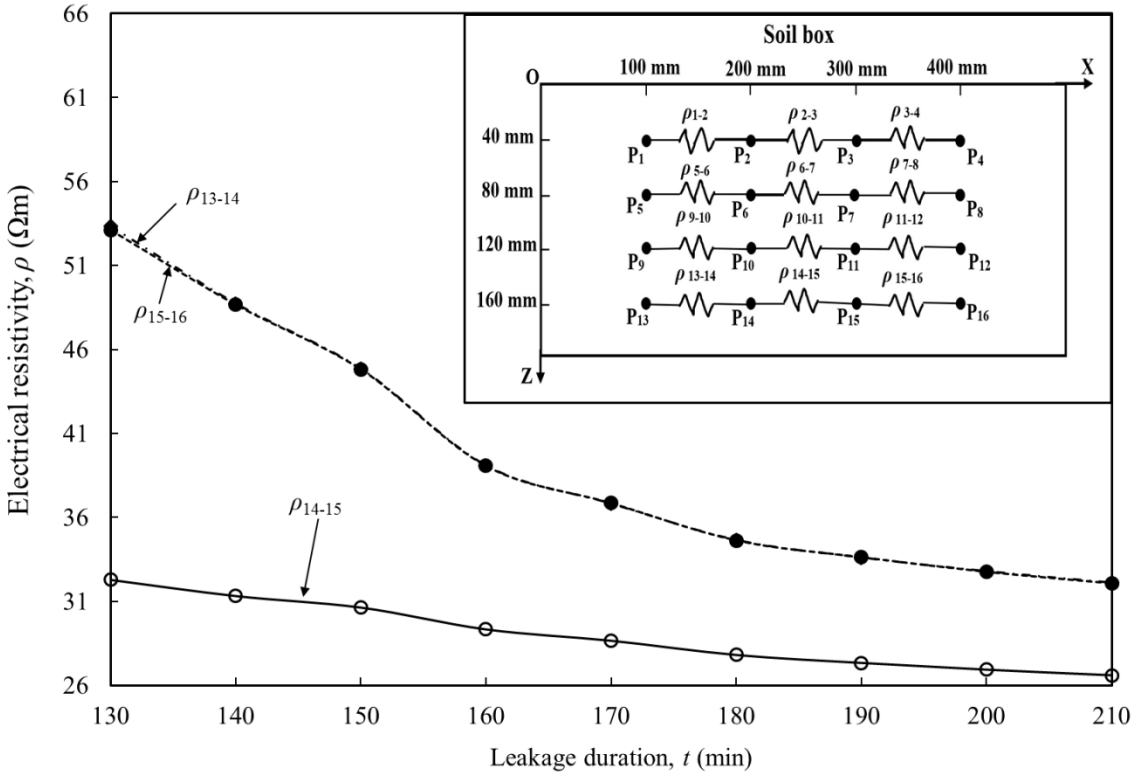

(d)

Figure 7.8: Resistivity profiles of electrode pairs located below geomembrane liner at the depth of: (a) 40 mm; (b) 80 mm; (c) 120 mm; and (d) 160 mm using Leachate #2.

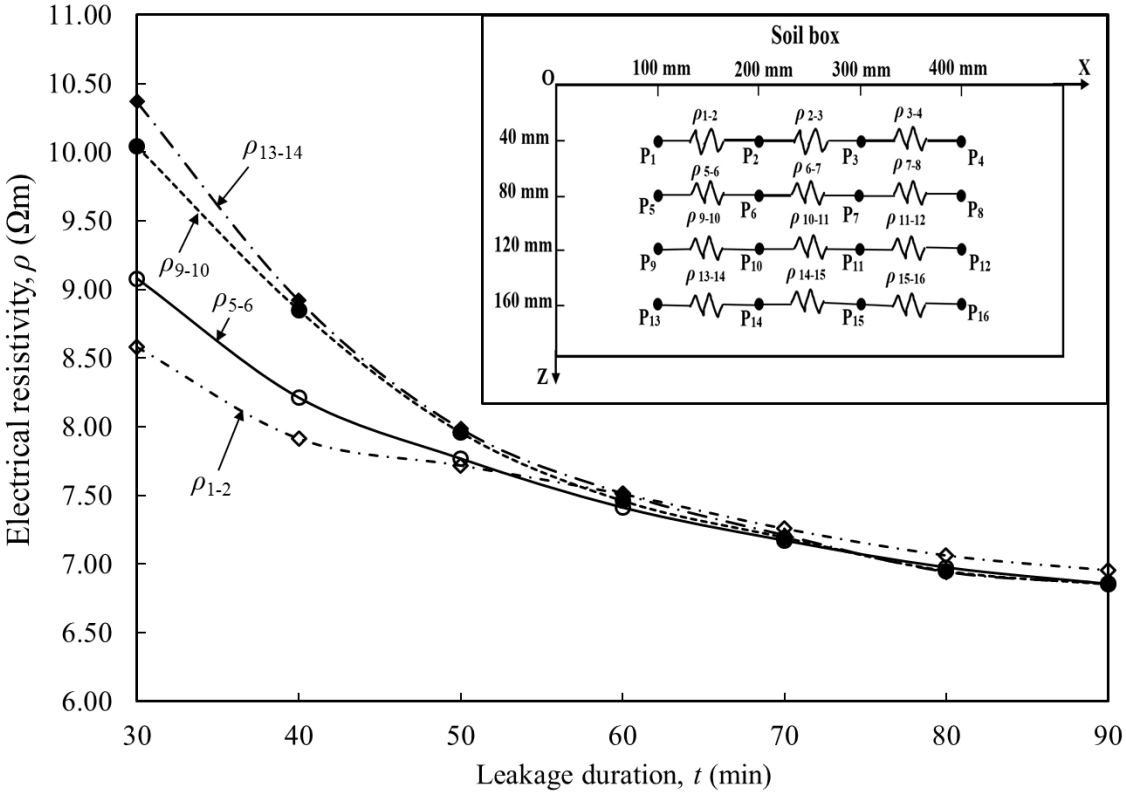
Soil box
100 mm
200 mm
300 mm
400 mm
X
O
Z
40 mm
80 mm
120 mm
160 mm
ρ_{1-2}
ρ_{2-3}
ρ_{3-4}
ρ_{5-6}
ρ_{6-7}
ρ_{7-8}
ρ_{9-10}
ρ_{10-11}
ρ_{11-12}
ρ_{13-14}
ρ_{14-15}
ρ_{15-16}
P1
P2
P3
P4
P5
P6
P7
P8
P9
P10
P11
P12
P13
P14
P15
P16
ρ_{13-14}
ρ_{9-10}
ρ_{5-6}
ρ_{1-2}
Electrical resistivity, ρ (Ωm)
Leakage duration, t (min)
11.00
10.50
10.00
9.50
9.00
8.50
8.00
7.50
7.00
6.50
6.00
30
40
50
60
70
80
90

(a)

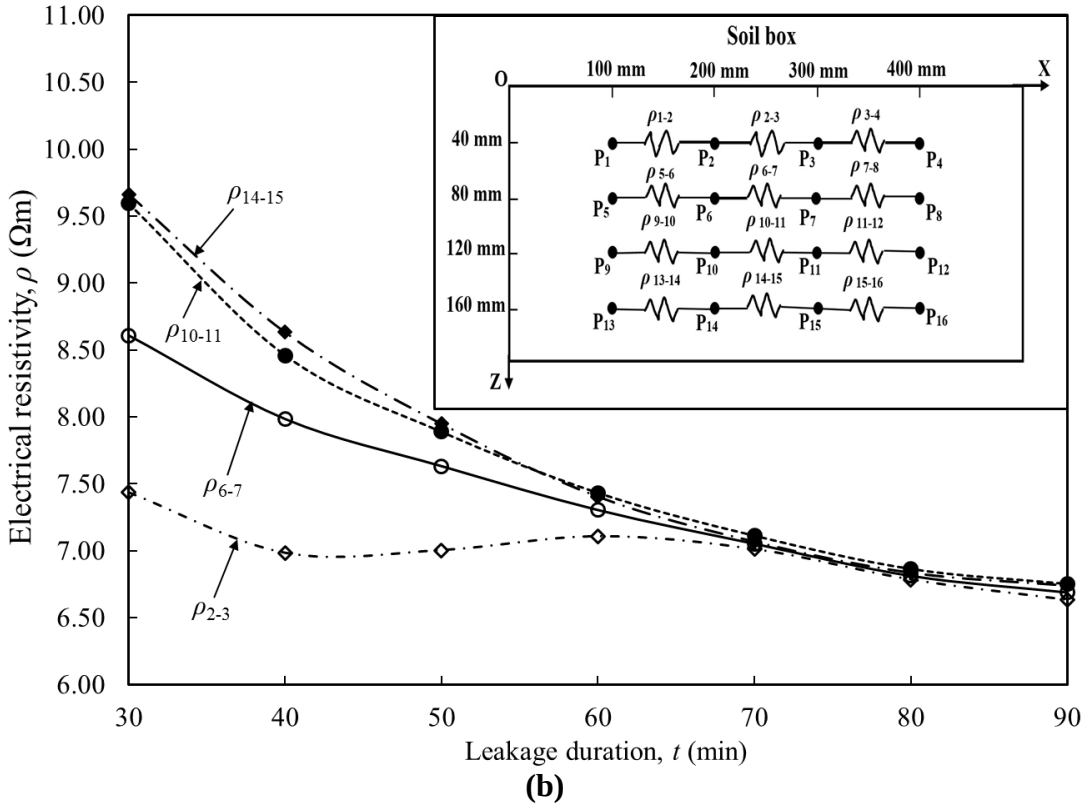
Soil box
100 mm
200 mm
300 mm
400 mm
X
O
Z
40 mm
80 mm
120 mm
160 mm
ρ_{1-2}
ρ_{2-3}
ρ_{3-4}
ρ_{5-6}
ρ_{6-7}
ρ_{7-8}
ρ_{9-10}
ρ_{10-11}
ρ_{11-12}
ρ_{13-14}
ρ_{14-15}
ρ_{15-16}
P1
P2
P3
P4
P5
P6
P7
P8
P9
P10
P11
P12
P13
P14
P15
P16
ρ_{14-15}
ρ_{10-11}
ρ_{6-7}
ρ_{2-3}
Electrical resistivity, ρ (Ωm)
Leakage duration, t (min)
11.00
10.50
10.00
9.50
9.00
8.50
8.00
7.50
7.00
6.50
6.00
30
40
50
60
70
80
90

(b)

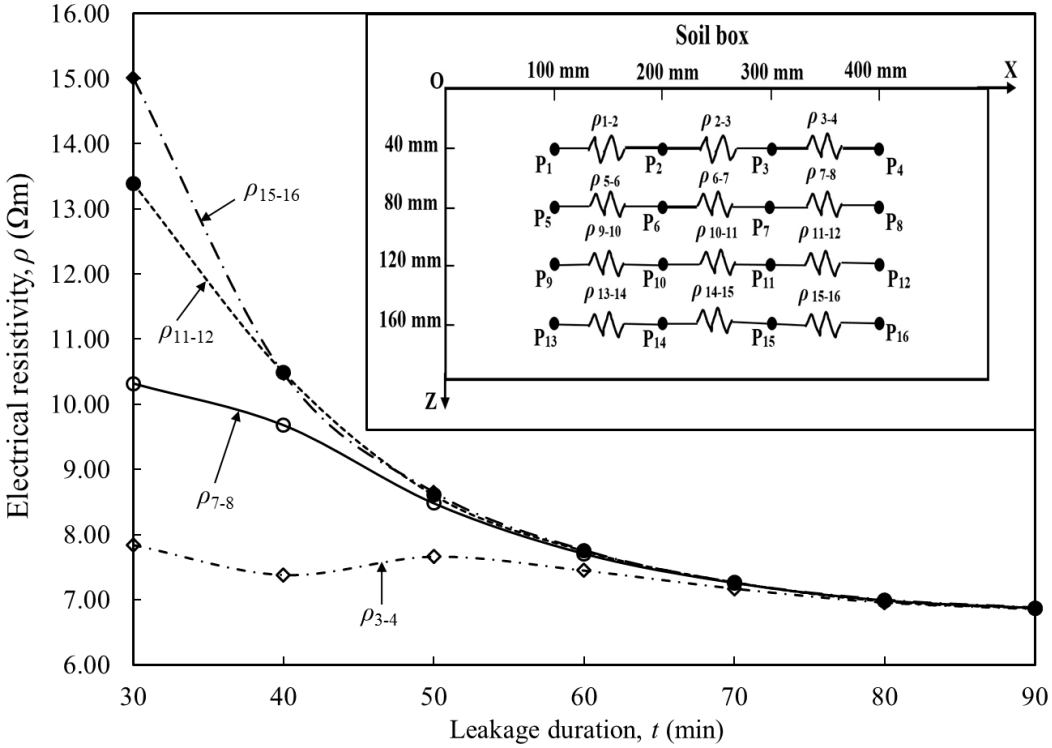

(c)

Figure 7.9: Resistivity profile of electrode pairs with their mid-point at the distance of: (a) 150 mm; (b) 250 mm; (c) 350 mm using Leachate #1.

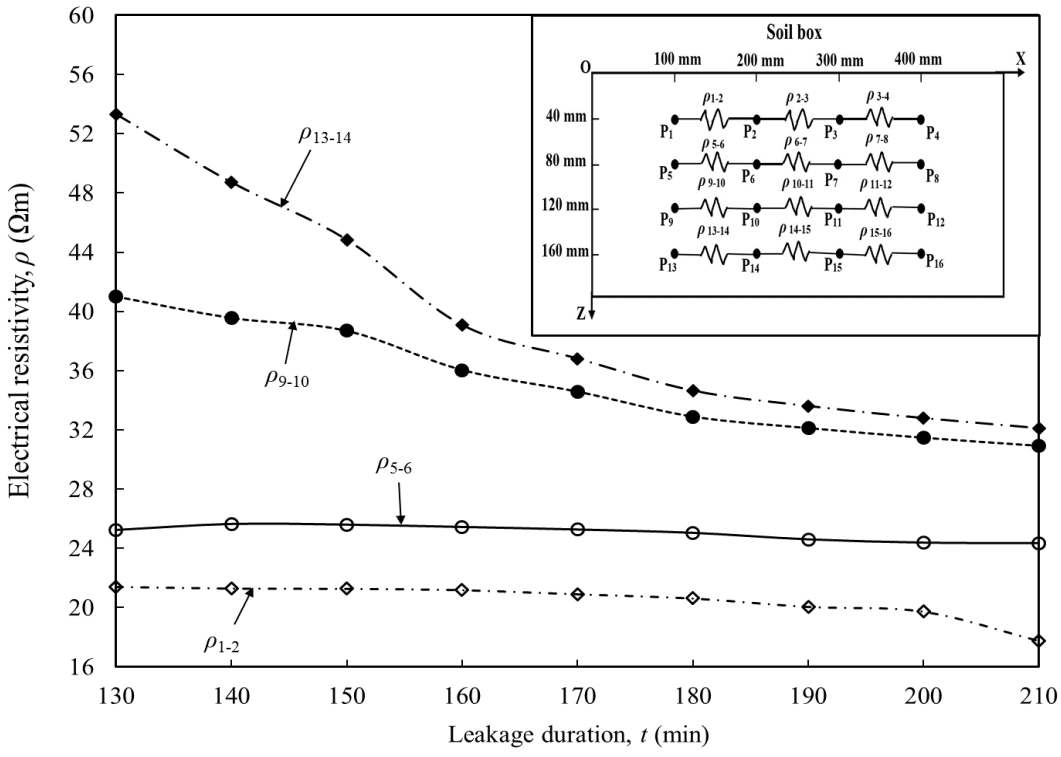

(a)

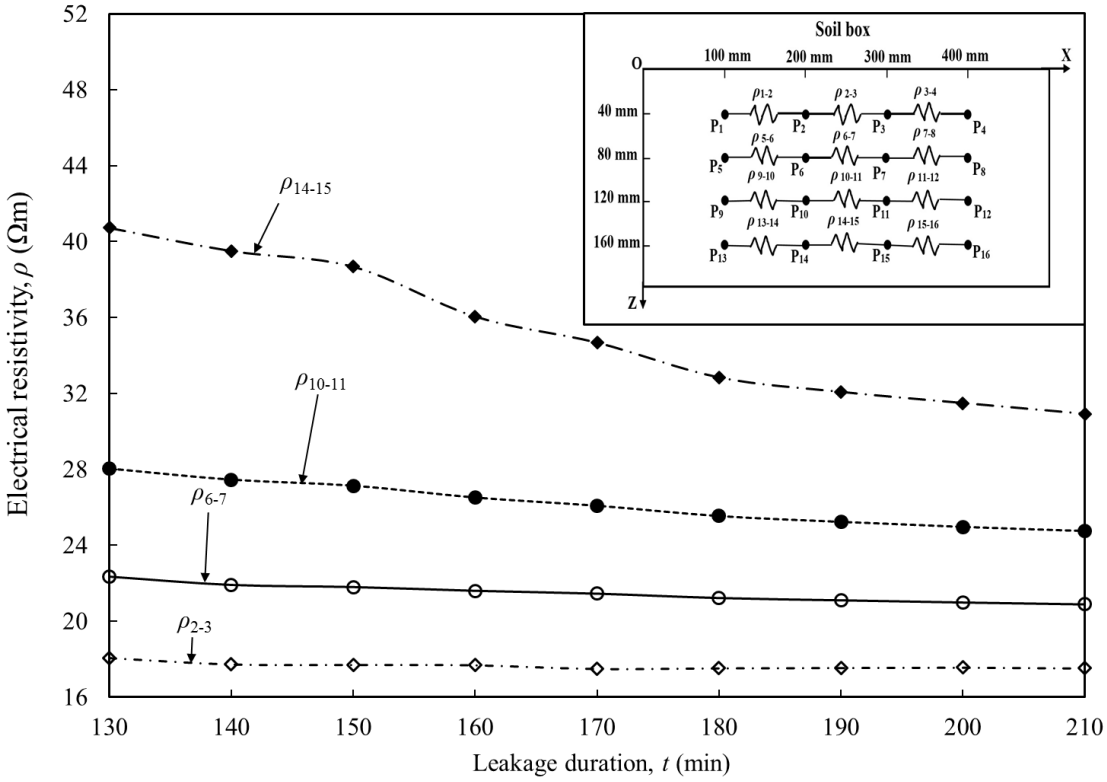

(b)

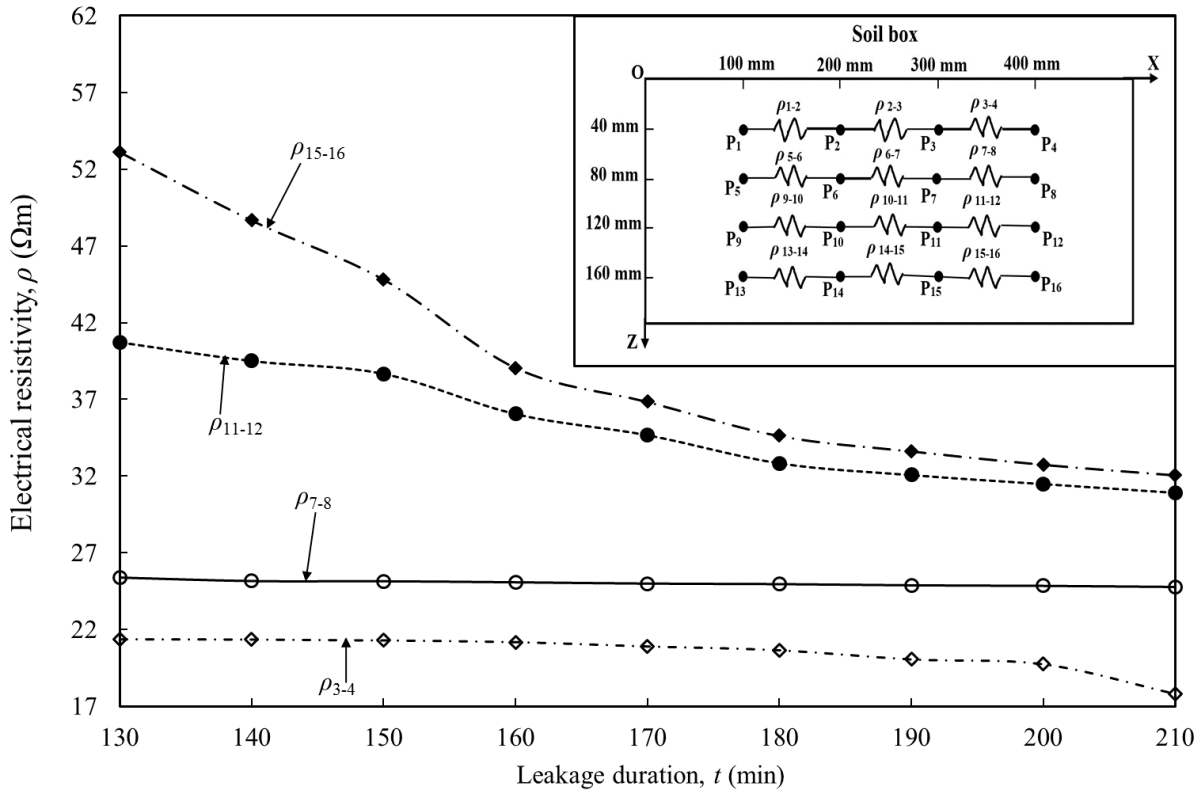

(c)

Figure 7.10: Resistivity profile of electrode pairs with their mid-point at the distance of: (a) 150 mm; (b) 250 mm; (c) 350 mm using Leachate #2.

From Figures 7.9(a) through 7.10(c), it can be noticed that the effect of locations in X and Z directions on the soil resistivity is negligible at t greater than 60 min for Leachate #1 and 160 min for Leachate #2. This can be accounted for from the observation that the soil specimen was near saturation condition at this time.

Additionally, it can be observed that with an increase in x and z, the resistivity of soil also increased. Hence, it can be inferred that the resistivity of soil increases with an increase in the proximity of the measuring electrodes to the liner leak. Consequently, this observation can be used in-field to determine and locate leakages.

Pandey *et al.* (2017) summarized the results of leak detection test using the tap water in lieu of groundwater as the leaching liquid. Similar resistivity profiles were observed for the leakage of tap water and leachate. However, it was noted that the resistivity values obtained with tap water was much greater than the values observed with landfill leachate as the leaching liquid. As an example, at $t = 30\,\text{min}$, ρ_{6-7} is 94.92 Ωm and 8.61 Ωm, for tap water and Leachate #1, respectively. This observation can be used during the real-life monitoring to detect whether the soil below liner has been infiltrated by groundwater or contaminated by leachates.

7.5 Conclusions

Based on the results and discussion presented previously, the following can be concluded:

- Resistivity of the soil decreased rapidly with an increase in the leakage duration.
- The soil resistivity was found to increase with an increase in the depth/distance from the liner leak. This observation can be used to localize the leak position in the liner.
- The innovative leak detection technique was effective in detecting and locating leaks in liners, irrespective of the leakage duration.
- The use of this innovative technique for the monitoring of lining systems can significantly aid landfilling facilities to manage and control contamination due to leachate migration.
- The findings reported here should not be extrapolated to soil and leachate types which differ significantly from the soil used in this study.

References

Arora, T., Linde, N., Revil, A. and Castermant, J. (2007). Non-intrusive characterization of the redox potential of landfill leachate plumes from self-potential data. *Journal of Contaminant Hydrology* 92(3), 274-292, DOI: 10.1016/j.jconhyd.2007.01.018.

Ben Othmen, A. and Bouassida, M. (2013). Detecting defects in geomembranes of landfill liner systems: durable electrical method. *International Journal of Geotechnical Engineering* 7(2), 130-135, DOI: 10.1179/1938636213Z.00000000013.

Chen, P.H. and Wang, C.Y. (1997). Investigation into municipal waste leachate in the unsaturated zone of red soil. *Environment International* 23(2), 237-245, DOI: 10.1016/S0160-4120(97)00010-X.

Das, B.M. (2013). Fundamentals of geotechnical engineering, 4th edition, Cengage Learning, Stamford.

Giroud, J.P. and Bonaparte, R. (1989). Leakage through liners constructed with geomembranes—Part I. Geomembrane liners. *Geotextiles and Geomembranes* 8(1), 27-67, DOI: 10.1016/0266-1144(89)90009-5.

Giroud, J.P. and Bonaparte, R. (2001). Geosynthetics in liquid-containing structures. Geotechnical and Geoenvironmental Engineering Handbook (pp. 789-824). Springer, Boston, MA.

Koerner, G.R., Koerner, R.M. and Martin, J.P. (1994). Design of landfill leachate-collection filters. *Journal of Geotechnical Engineering* 120(10), 1792-1803, DOI: 10.1061/(ASCE)0733-9410(1994)120:10(1792).

Maslen, G. (2018). Personal communication. Red Hill Landfill Facility, WA, Australia.

Misra, V. and Pandey, S.D. (2005). Hazardous waste, impact on health and environment for development of better waste management strategies in future in India. *Environment International* 31(3), 417-431, DOI: 10.1016/j.envint.2004.08.005.

Mohamed, A.M.O., Said, R.A. and Al-Shawawreh, N.K. (2002). Development of a methodology for evaluating subsurface concentrations of pollutants using electrical polarization technique. *Geotechnical Testing Journal* 25, 157–167, DOI: 10.1520/GTJ11359J.

Munoz-Castelblanco, J.A., Pereira, J.M., Delage, P. and Cui, Y.J. (2012). The influence of changes in water content on the electrical resistivity of a natural unsaturated loess. *Geotechnical Testing Journal* 35(1), 11–17, DOI: 10.1520/GTJ103587.

Oh, M., Seo, M.W., Lee, S. and Park, J. (2008). Applicability of grid-net detection system for landfill leachate and diesel fuel release in the subsurface. *Journal of Contaminant Hydrology* 96(1-4), 69-82, DOI: 10.1016/j.jconhyd.2007.10.002.

Pandey, L.M.S. and Shukla, S.K. (2017). Detection of leachate contamination in Perth landfill base soil using electrical resistivity technique. *International Journal of Geotechnical Engineering*, 1-12, DOI: 10.1080/19386362.2017.1339763.

Pandey, L.M.S. and Shukla, S.K. (2018). Effect of state of compaction on the electrical resistivity of sand-bentonite lining materials. *Journal of Applied Geophysics* 155, 208-216, DOI: 10.1016/j.jappgeo.2018.06.016.

Pandey, L.M.S. and Shukla, S.K. (2019). Development of an innovative liner leak detection technique. *Geotechnical Testing Journal* 42(5), DOI: 10.1520/GTJ20170292.

Pandey, L.M.S., Shukla, S.K. and Habibi, D. (2015). Electrical resistivity of sandy soil. *Géotechnique Letters* 5(3), 178-185, DOI: 10.1680/jgele.15.00066.

Pandey, L.M.S., Shukla, S.K. and Habibi, D. (2017). Resistivity profiles of Perth soil in Australia in leak-detection test. *Geotechnical Research* 4(4), 214-221, DOI: 10.1680/jgere.17.00014.

Praharaj, T., Swain, S.P., Powell, M.A., Hart, B.R. and Tripathy, S. (2002). Delineation of groundwater contamination around an ash pond: geochemical and GIS approach. *Environment International* 27(8), 631-638, DOI: 10.1016/S0160-4120(01)00121-0.

Shukla, S.K. (2014). Core Principles of Soil Mechanics. ICE Publishing, London, UK.

Shukla, S.K. (2016). An introduction to geosynthetic engineering. CRC Press, Taylor & Francis Group, Florida, USA.

Teng, Y., Wu, J., Lu, S., Wang, Y., Jiao, X. and Song, L. (2014). Soil and soil environmental quality monitoring in China: a review. *Environment International* 69, 177-199, DOI: 10.1016/j.envint.2014.04.014.

Widenbar, T. (2017). Personal communication. North Bannister Resource Recovery Facility, SUEZ, WA, Australia.

CHAPTER 8

RESISTIVITY PROFILES OF LINER BASE WITH BAYER LIQUOR AS LEACHATE

This chapter is based on the conference proceedings of the international conference Sustainable Waste Management Through Design, 2-3 November 2018, Ludhiana, Punjab, India*; as mentioned in Section 1.6. The details presented here are the same, except some changes in the layout in order to maintain a consistency in the presentation throughout the thesis.*

8.1 Introduction

The Australian aluminium industry is a significant contributor to the national economy for over 50 years. This industry consists of 5 bauxite mines, 6 alumina refineries and 4 aluminium smelters. Australia is the world's second largest producer and exporter of alumina, accounting for 22% of the global production (Australian Aluminium Council, 2018). As per the Australian Aluminium Council (2011), 19.1 million tonnes of metallurgical alumina and nearly 0.5 million tonnes of chemical grade alumina, were produced domestically.

Alumina is extracted from bauxite by digesting it in a severely caustic solution, at high temperature and pressure. This process is known as the Bayer process and the liquid effluent generated from this process is called the Bayer liquor. Bayer liquors are challenging leachates due to their high dissolved aluminium, sodium carbonate, sodium chloride, sodium sulphate, and sodium oxalate content (Bouchard *et al.*, 2009; Busetti *et al.*, 2014).

Due to the high concentration of contaminants in the Bayer liquor and the threat it poses to the environment, its proper handling and storage are of critical importance. In an effort to prevent soil and groundwater contamination, highly engineered lining systems are used by aluminium manufacturing companies for the containment of Bayer liquor. Although the integrity of these liners should ideally not be compromised during their operating period, however, due to various factors, the liners often develop defects and tend to fail. Figure 8.1 is a photograph of one such liner failure. This leads to subsequent soil and groundwater

contamination issues (Pandey *et al.*, 2017). Therefore, the lining systems need to be proactively monitored to ensure the early detection of liner defects so that adequate hazard mitigation measures can be taken (Pandey and Shukla, 2018).

Figure 8.1: A typical liner failure (*Courtesy of Iluka Resources, WA, Australia*).

Pandey and Shukla (2018) have developed and presented an innovative method for the detection of leakages through liners by simulating actual lining systems. This system was further tested and found to be effective in detecting leakages across liners when municipal solid waste (MSW) landfill leachate was used as the leaching liquid (Pandey *et al.*, 2017). However, the efficacy of this system in detecting leakage issues when Bayer liquor is the leachate, has not been examined yet. The current study aims to fill this gap in knowledge by conducting leak detection tests in the setup developed by Pandey and Shukla (2018), using the Bayer liquor leachate procured from an actual aluminium manufacturing company in Perth, Western Australia (WA), Australia. Based on the results from this study, the effectiveness of the use of this innovative leak detection technique in Bayer liquor containment systems in the aluminium industries can be adjudged. The understanding developed by this study will assist practicing

engineers in Australia as well as internationally to detect contamination and liner leakage issues, design and placement of sensor systems, numerical modelling, and so on.

8.2 Materials Used

Sandy soil was used for this study. This soil is a good representation of Perth, WA, Australia, and is widely used for engineering works. The properties of this poorly graded sand are presented in Table 8.1.

Bayer liquor was used as the leaching liquid for this test. It was procured from Alcoa, WA, Australia. The composition of the liquor is given in Table 8.2. Its pH is 13.8 and the specific gravity is 1.25.

A 220 μm thick geomembrane (GMB) liner was used for the test. A piece of 550 mm length and 250 mm width was pre-cut, and a leak was intentionally introduced in the centre of the GMB piece using a gravel-size particle, to simulate an actual puncture defect as observed in practice.

Table 8.1: Physical properties of sand.

Property	**Unit**	**Value**
Specific gravity	dimensionless	2.68
Coefficient of uniformity	dimensionless	2.27
Coefficient of curvature	dimensionless	1.22
Effective size	mm	0.15
Minimum dry unit weight	kN/m^3	14.02
Maximum dry unit weight	kN/m^3	15.56
Soil classification as per USCS (Unified Soil Classification System)	dimensionless	Poorly graded sand (SP)

8.3 Test Methodology

The experiments were conducted using the innovative leak detection technique developed by Pandey and Shukla (2018). This technique is based on the electrical resistivity. The electrical

resistivity of soil below liner is very high. As soon as leakage occurs, the leachate tends to contaminate this soil. Generally, leachates possess much lower resistivity than any soil. Hence, in case of even mild leachate contamination, the soil resistivity decreases significantly. This change can be easily detected to determine the leakage issue (Pandey *et al.*, 2015, Pandey, 2017, 2019). Based on this well-established fact, a new leak detection technique was developed and presented (Pandey *et al.*, 2017; Pandey and Shukla, 2018).

Table 8.2: Composition of Bayer liquor (*Courtesy of Alcoa, WA, Australia*).

Chemical	**Percentage by weight**
Sodium aluminate	5-20
Sodium hydroxide	2-9
Sodium carbonate	<4
Sodium oxalate	<3.5
Sodium sulphate	<3
Sodium chloride	<2
Water	64-90

As per this method, a resistivity box as shown in Figure 8.2, was filled with the soil specimen and covered with the punctured geomembrane (GMB) liner. Initially the leak was kept covered. The Bayer liquor was then filled over this GMB layer and the leak was uncovered to allow leakage to the underlying soil. Resistance readings were then taken at various leakage durations (t) using the electrodes fitted on the resistivity box using a four-point resistance testing machine. Resistivity was obtained between each pair of electrodes. The resistivity profile was then generated to locate the leak in the GMB liner. This method has been discussed in greater detail by Pandey *et al.* (2017) and Pandey and Shukla (2018).

8.4 Results and Discussion

Figures 8.3 and 8.4 give the resistivity profiles for the leakage durations, t = 80 min and 90 min, respectively, for the Bayer liquor as the leachate.

It can be observed that at any depth (z), the resistivity first decreases and then increases with an increase in the distance (x) of the mid-point of electrode pair. The hole in the geomembrane

(GMB) liner was positioned directly above the mid-point of the electrodes, P_2 and P_3, as given in Figure 10.2. Hence, the amount of leachate between these electrodes would be greater than the amount of leachate between the adjacent electrode pairs. Therefore, this observation was as expected.

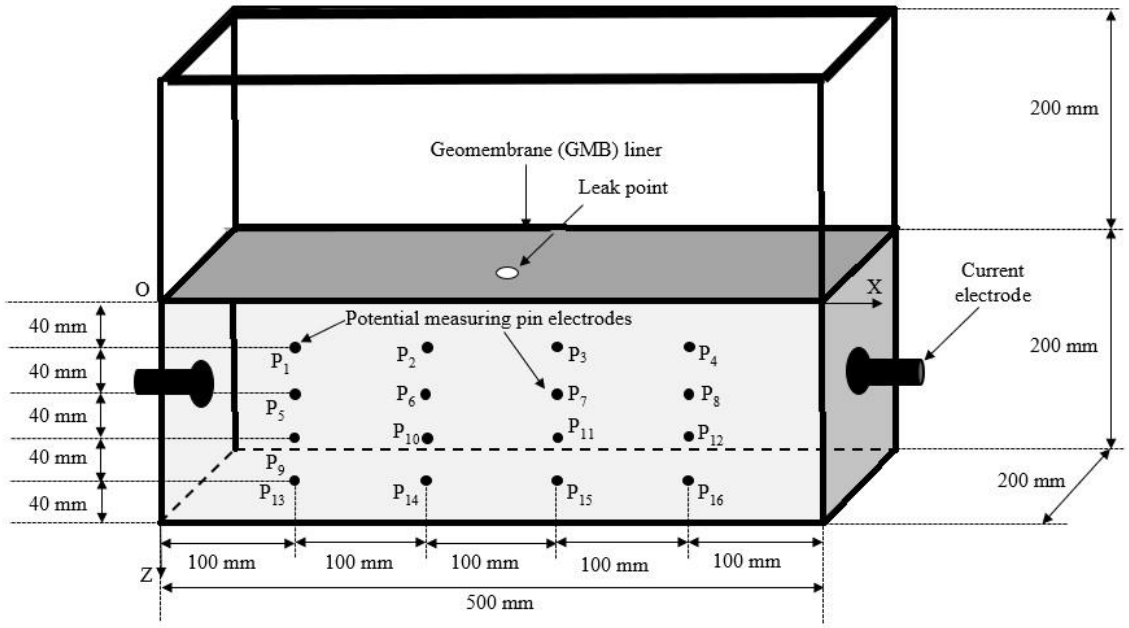

Figure 8.2: Schematic diagram of the resistivity box used in the leak detection test (*Adapted from Pandey and Shukla (2018)*).

It can be seen from Figures 8.3 and 8.4 that at any given *x*, soil resistivity decreases with a decrease in the depth *z*. This observation also complies with the expectation that with a decrease in *z*, the amount of leachate in soil would increase, and consequently resistivity would decrease.

It can be observed from Figures 8.3 and 8.4 that with an increase in the distance/depth from the leak, the resistivity of the soil shows an increase. Therefore, the location of the liner leak can be determined based on the resistivity profile of the soil.

In addition, it is interesting to note that the resistivity profiles show a similar trend, irrespective of the leakage duration. This indicates that the leakage can be located at any leakage duration, using the resistivity profile.

Based on these observations, it can be concluded that the leak detection technique is reasonably effective for detecting and locating leakages through lining systems used in the Bayer liquor containment facilities of aluminium manufacturing industry.

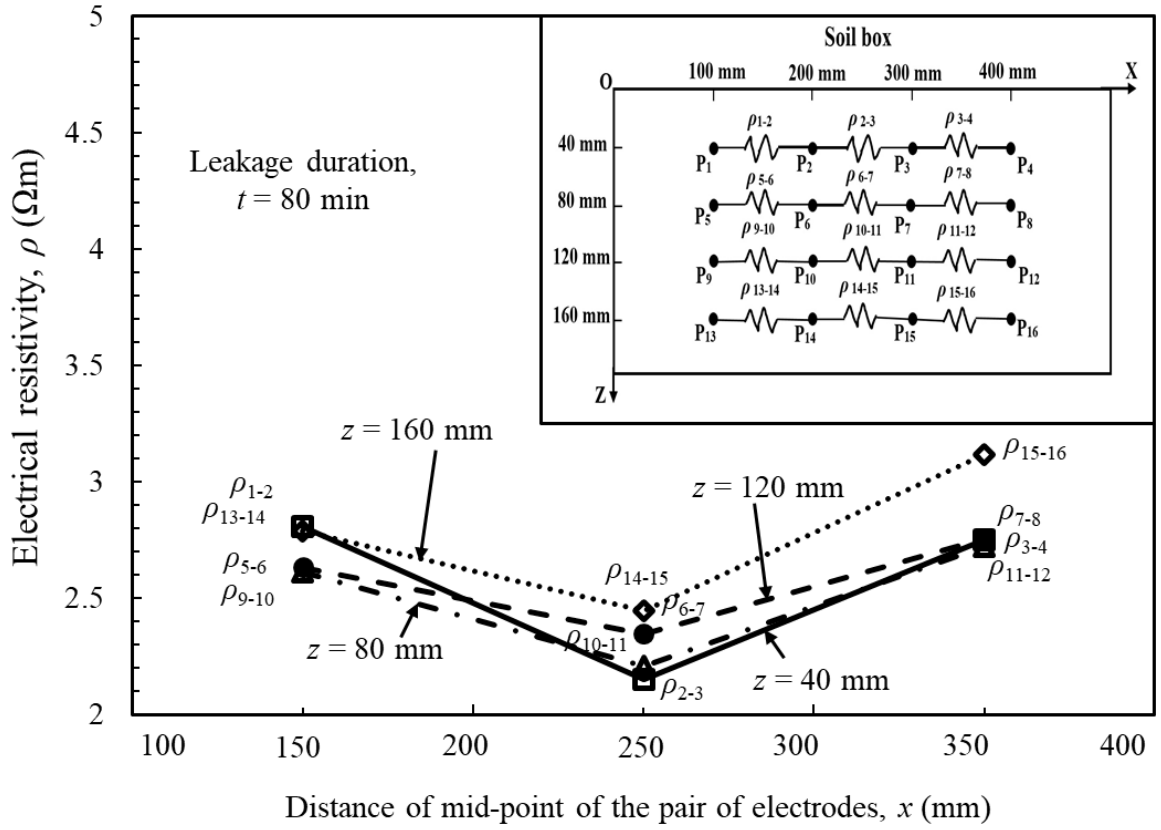

Figure 8.3: Resistivity profiles at the leakage duration of 80 min.

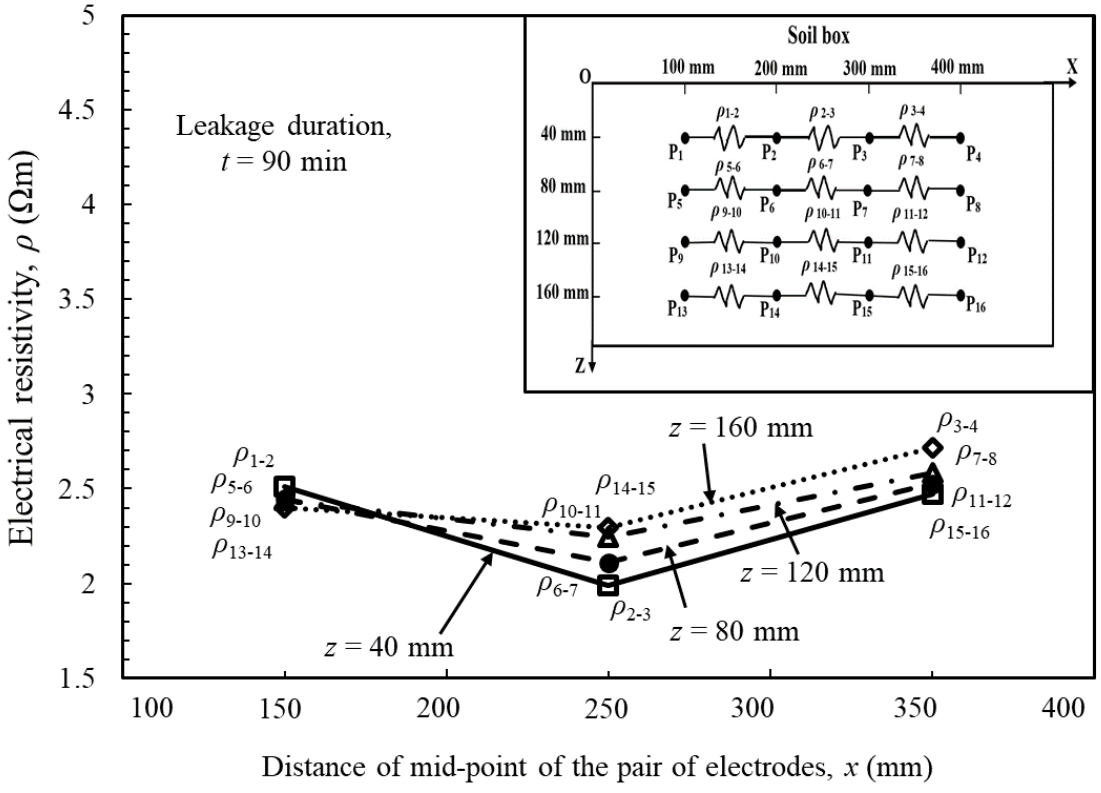

Figure 8.4: Resistivity profiles at the leakage duration of 90 min.

8.5 Conclusions

Results have been given for the leak detection test conducted using Bayer liquor from aluminium manufacturing process, for the leakage durations of 80 min and 90 min. The resistivity of the soil increased with an increase in the depth/distance, of the mid-point of the pair of electrodes, from the liner leak, irrespective of the leakage duration. It was observed that the newly developed system can be used by containment systems in aluminium industry to effectively detect and locate leakages in liners. Additionally, the system can help the practicing engineers in the design and placement of sensors, numerical modelling, leakage detection, and so on.

References

Australian Aluminium Council (2011). Australian Industry. https://aluminium.org.au/australian-industry/. (Accessed online 29 July 2018.)

Australian Aluminium Council (2018). Australian Alumina. https://aluminium.org.au/australian-industry/industry-description/australian-alumina/. (Accessed online 29 July 2018.)

Bouchard, P., Larner, B., Nunes, M. and Sabsabi, M. (2009). Laser-induced breakdown spectroscopy (LIBS) of elements in Bayer liquor. Research Disclosure Journal. https://nparc.nrc-cnrc.gc.ca/fra/voir/objet/?id=0ed9826b-d160-434b-ac9c-c8e29e7be443. (Accessed online 30 July 2018.)

Busetti, F., Berwick, L., McDonald, S., Heitz, A., Joll, C. A., Loh, J. and Power, G. (2014). Physicochemical characterization of organic matter in Bayer liquor. *Industrial & Engineering Chemistry Research* 53(15), 6544-6553, DOI: 10.1021/ie4028268.

Pandey, L.M.S. and Shukla, S.K. (2017). Detection of leachate contamination in Perth landfill base soil using electrical resistivity technique. *International Journal of Geotechnical Engineering*, 1-12, DOI: 10.1080/19386362.2017.1339763.

Pandey, L.M.S. and Shukla, S.K. (2018). Effect of state of compaction on the electrical resistivity of sand-bentonite lining materials. *Journal of Applied Geophysics* 155, 208-216, DOI: 10.1016/j.jappgeo.2018.06.016.

Pandey, L.M.S. and Shukla, S.K. (2019). Development of an innovative liner leak detection technique. *Geotechnical Testing Journal* 42(5), DOI: 10.1520/GTJ20170292.

Pandey, L.M.S., Shukla, S.K. and Habibi, D. (2015). Electrical resistivity of sandy soil. *Géotechnique Letters* 5(3), 178-185, DOI: 10.1680/jgele.15.00066.

Pandey, L.M.S., Shukla, S.K. and Habibi, D. (2017). Resistivity profiles of Perth soil in Australia in leak-detection test. *Geotechnical Research* 4(4), 214-221, DOI: 10.1680/jgere.17.00014.

CHAPTER 9

ANALYTICAL AND NUMERICAL MODELLING FOR ELECTRICAL RESISTIVITY OF LINER BASE

A part of this chapter is based on a section of the paper submitted to Surveys in Geophysics, Springer; as listed in Section 1.6. The details presented here for this part of the paper are the same, except some changes in the layout in order to maintain a consistency in the presentation throughout the thesis.

9.1 Introduction

Geotechnical properties of soil have been demonstrated by previous researchers, such as Archie (1942), Gupta and Hanks (1972), Kalinski and Kelly (1993), Pandey *et al.* (2015), Pandey and Shukla (2017), Pandey and Shukla (2018a), and so on, to show a close relationship with its electrical resistivity. These studies have also developed and presented correlations for the relationship between resistivity of soil and its various properties. Such relationships are particularly useful for the design and placement of sensor systems for liner leak detection techniques using electrical resistivity method (Oh *et al.*, 2008). Therefore, an attempt has been made in this chapter to develop similar analytical and numerical models for electrical resistivity of liner base which can be used by practicing design engineers in waste containment facilities.

Based on the leak detection test results presented by Pandey *et al.* (2017) (see Chapter 6), Pandey and Shukla (2019) (see Chapter 5), and Pandey and Shukla (2018b) (see Chapter 7), empirical correlations and analytical modelling have been developed. New empirical correlations have also been presented for the relationship between resistivity, leakage duration and distance/depth. These can be used to generate a resistivity profile for any specific soil type and leachate, in the leak detection test. Further, new equations have been given to predict the flow velocity of leachate at any point within a soil specimen, if the resistivity is measured at a given time.

A few illustrative examples are also shown in this chapter, to demonstrate the application of the newly developed equations. Furthermore, a numerical model for the seepage analysis of

the leak detection test, has been developed using GeoStudio SEEP/W. The data obtained from this model has been used in conjunction with the new correlations to generate resistivity profiles. It was noted that the obtained resistivity trends were similar to the trends reported in experimental observations. Therefore, these correlations can be particularly useful for practicing engineers in the design of lining systems, as well as for various numerical modelling applications in waste containment facilities. Depending on availability, any other suitable seepage analysis software, such as DC-Infilt, GFLOW, GGU-3D-TRANSIENT, GGU-SEEP, GGU-SS-FLOW2D, GGU-SS-FLOW3D, GGU-TRANSIENT, GGU-UPLIFT, GWDivide, Seepage Analysis, SVFlux, etc., can be used by practicing engineers to predict resistivity and to obtain resistivity profiles.

9.2 Development of Empirical Correlations and Analytical Modelling

Permeability of a soil (k) is an important parameter. It signifies the ease of flow of a leaching liquid through the soil. It depends on the properties of the leachate as well as the soil. The following relationship is known for the permeability of soil medium (Das, 2013; Shukla, 2014):

$$k = \frac{\gamma_l}{\eta} K \tag{9.1}$$

where k = coefficient of permeability of soil (m/s), η = viscosity of leachate (Pas or Ns/m^2), γ_l = unit weight of leachate (kN/m^3), and K = absolute permeability of soil (m^2).

Here, k depends on properties of both soil and leachate while K is independent of the properties of the leachate.

From the resistivity profiles obtained in Chapters 6 and 7 (Pandey *et al.*, 2017; Pandey and Shukla, 2018b), it can be observed that the resistivity (ρ, Ωm) of the soil decreases with an increase in the leakage duration (t, min). Furthermore, it is expected that at $t = 0$ min, $\rho \to \infty$; hence, the following relationship holds true:

$$\rho \propto a_1 t^{-b_1} \tag{9.2}$$

where a_1 and b_1 are positive constants which depend upon the properties of the soil and the leachate composition. It is also known that resistivity of soil decreases with an increase in distance/depth from the leak position in the liner. If the soil is assumed to be homogeneous, the

flow in all directions will be uniform. Therefore, to implement the simplification, a parameter r, which is the radial distance of the mid-point of any electrode pair from the leak position, is defined as follows:

$$r = \sqrt{(x - x_l)^2 + (z - z_l)^2} \tag{9.3}$$

Here x is the distance of the mid-point of a pair of electrodes (mm) and z is the depth of the mid-point of a pair of electrodes (mm). Note that (x_l, z_l) are the coordinates of the leak position. In this case $x_l = 250$ mm and $z_l = 0$ mm.

From the resistivity profiles presented in Chapters 6 and 7 (Pandey *et al.*, 2017; Pandey and Shukla, 2018b), the following relationship was observed for the resistivity (ρ, Ωm) of the soil measured between an electrode pair with the radial distance (r, mm) from the leak position:

$$\rho = a_2 r^{b_2} \tag{9.4}$$

where a_2 and b_2 are positive constants which depend upon the properties of the soil and the leachate composition. Using curve fitting and regression analysis, the following equation was developed for the resistivity (ρ, Ωm) of the soil in terms of the leakage duration (t, min) and the radial distance of the mid-point of any electrode pair from the leak position (r, mm):

$$\rho = a t^{-b} r^{c} \tag{9.5}$$

where a, b and c are positive constants which depend upon the soil properties (such as porosity, mineralogy, structure, etc.), the leachate composition and the test environment.

For the use of the innovative leak detection system for any specific soil type and leachate, a, b and c can be defined using a specimen with known values of ρ, t and r, so that later the developed equation can be used to generate a resistivity profile. Further Eqn. (9.5) can be used by practicing engineers to detect contamination and liner leakage issues. This correlation can also be useful for engineers in the design and placement of sensor systems.

The velocity (v, m/s) of flow of leachate is defined in terms of the rate (Q, m^3/s) of leachate migration through a geomembrane defect and the area (A_l, m^2) through which the leachate flows:

$$v = \frac{Q}{A_l} \tag{9.6}$$

As the soil is assumed to be homogeneous, the flow takes place through a hemispherical surface, hence, the following equation holds true:

$$A_l = 2\pi\left(\frac{r}{1000}\right)^2 \tag{9.7}$$

where r (mm) is the radial distance of the mid-point of any electrode pair from the leak position.

From Eqns. (9.6) and (9.7),

$$v = \frac{10^6 \times Q}{2\pi r^2} \tag{9.8}$$

As per Giroud *et al.* (1989) and Giroud and Bonaparte (2001), an intimate or good contact is important between the liner and the underlying base soil. In the experimental demonstration presented by Pandey *et al.* (2017), Pandey and Shukla (2018b), and Pandey and Shukla (2019), the soil bed has been prepared in a manner so that a good contact can be assumed to exist between the geomembrane (GMB) liner and the soil. Hence, the rate of flow Q of leachate through a circular defect can be given by (Forchheimer, 1930; Giroud and Bonaparte, 2001):

$$Q = 4R'hk \tag{9.9}$$

for an ideal case, where R' = radius of geomembrane defect (m), h = head of leachate on top of the liner (m), and k = coefficient of permeability of soil (m/s).

On replacing Q using Eqn. (9.9), Eqn. (9.8) reduces to

$$v = \frac{2 \times 10^6 \times R' hk}{\pi r^2} \tag{9.10}$$

Additionally, from Eqn. (9.5),

$$r = \left(\frac{\rho}{at^{-b}} \right)^{\frac{1}{c}} \tag{9.11}$$

Using Eqns. (9.10) and (9.11),

$$v = \frac{2 \times 10^6 \times R' hk}{\pi \left(\frac{\rho}{at^{-b}} \right)^{\frac{2}{c}}} \tag{9.12}$$

Eqn. (9.12) can further be simplified to

$$v = \frac{2 \times 10^6 \times a^{\frac{2}{c}} R' hk}{\pi \rho^{\frac{2}{c}} t^{\frac{2b}{c}}} \tag{9.13}$$

Furthermore, k can be replaced using Eqn. (9.1) so that Eqn. (9.13) becomes,

$$v = \frac{2 \times 10^6 \times a^{\frac{2}{c}} R' h \gamma_l K}{\pi \rho^{\frac{2}{c}} t^{\frac{2b}{c}} \eta}$$

or,

$$v = 6.37 \times 10^5 \times \left(\frac{a^{\frac{2}{c}} R' h \gamma_l K}{\rho^{\frac{2}{c}} t^{\frac{2b}{c}} \eta} \right) \tag{9.14}$$

Let us consider the leak detection tests conducted with Leachate #1 and Leachate #2, as presented in Chapter 7. Since the soil specimen is same for both cases, the absolute permeability (K) is same for both. Eqn. (9.1) changes to:

$$k_1 = \frac{\gamma_{l1}}{\eta_1} K \tag{9.15}$$

for Leachate #1, and,

$$k_2 = \frac{\gamma_{l2}}{\eta_2} K \tag{9.16}$$

for Leachate #2. Here k_1 = coefficient of permeability of soil using Leachate #1 (m/s), k_2 = coefficient of permeability of soil using Leachate #2 (m/s), γ_{l1} = unit weight of Leachate #1 (kN/m^3), γ_{l2} = unit weight of Leachate #2 (kN/m^3), η_1 = viscosity of Leachate #1 (Pas or Ns/m^2), and η_2 = viscosity of Leachate #2 (Pas or Ns/m^2).

Considering similar circular defects in the geomembrane for leak detection tests with Leachates #1 and #2, radius of geomembrane defect (R') is same. Furthermore, the head of leachate on top of the liner (h) was kept constant for all the tests. Therefore, Eqn. (9.10) changes to the following:

$$v_1 = \frac{2 \times 10^6 \times R' h k_1}{\pi r^2} \tag{9.17}$$

for Leachate #1, and,

$$v_2 = \frac{2 \times 10^6 \times R' h k_2}{\pi r^2} \tag{9.18}$$

for Leachate #2, where v_1= velocity of flow of Leachate #1 (m/s), and v_2 = velocity of flow of Leachate #2 (m/s).

From Eqns. (9.17) and (9.18), the following relationship results:

$$\frac{v_1}{v_2} = \frac{k_1}{k_2} \tag{9.19}$$

Substituting values from Eqns. (9.15) and (9.16) into Eqn. (9.19),

$$\frac{v_1}{v_2} = \frac{\gamma_{l1}\eta_2}{\gamma_{l2}\eta_1} \tag{9.20}$$

9.3 Illustrative Examples

Consider the leak detection tests conducted with Leachate #1. It is known that $k = 10^{-4}$ m/s, $a = 9.42$, $b = 0.3$, and $c = 0.1$. Determine the resistivity (ρ) and the velocity of flow of leachate ($_v$), for the following conditions:

a) $x = 150$ mm, $z = 40$ mm, and $t = 30$ min

b) $x = 250$ mm, $z = 80$ mm, and $t = 60$ min

Assume $R' = 0.5 \times 10^{-3}$ m, and $h = 0.1$ m.

Solutions

a) With $x = 150$ mm, $z = 40$ mm, and $t = 30$ min.

From Eqn. (9.4),

$$r = \sqrt{(150-250)^2 + (40-0)^2} = 107.703$$

Further, from Eqn. (9.6), for $a = 9.42$, $b = 0.3$, and $c = 0.1$,

$$\rho = 9.42 \times 30^{-0.3} \times 107.703^{0.1} = 5.422 \ \Omega\text{m}$$

Substituting values into Eqn. (9.14),

$$v = 6.37 \times 10^5 \times \left(\frac{9.42^{\frac{2}{0.1}} \times 0.5 \times 10^{-3} \times 0.1 \times 10^{-4}}{5.422^{\frac{2}{0.1}} \times 30^{\frac{2\times 0.3}{0.1}}} \right) = 2.743 \times 10^{-7} \text{ m/s}$$

b) With $x = 250$ mm, $z = 80$ mm, and $t = 60$ min.

From Eqn. (9.4),

$$r = \sqrt{(250-250)^2 + (40-80)^2} = 40$$

From Eqn. (9.6), using $a = 9.42$, $b = 0.3$, and $c = 0.1$,

$$\rho = 9.42 \times 60^{-0.3} \times 40^{0.1} = 3.989\ \Omega\text{m}$$

Putting values in Eqn. (9.14),

$$v = 6.37 \times 10^5 \times \left(\frac{9.42^{\frac{2}{0.1}} \times 0.5 \times 10^{-3} \times 0.1 \times 10^{-4}}{3.989^{\frac{2}{0.1}} \times 60^{\frac{2 \times 0.3}{0.1}}} \right) = 1.986 \times 10^{-6}\ \text{m/s}$$

Hence, for a particular soil, if the resistivity (ρ, Ωm) is measured at a given time (t, min), the velocity of flow of leachate (v, m/s) at any point within a soil specimen, can be predicted using Eqn. (9.14). Furthermore, the developed correlations can be used with any software that deals with seepage analysis and provides the velocity vector at different locations, to predict expected resistivity values. As an example, an attempt has been made to develop a numerical model using GeoStudio SEEP/W, as presented in the Sections 9.4 and 9.5. The magnitude of the *xy*-velocity vector obtained from the model was then replaced in Eqn. (9.14) to generate resistivity values.

9.4 Development of the Numerical Model

GeoStudio SEEP/W 2007, which is a well-accepted and widely used software, was adopted for creating a model to simulate the newly developed leak detection test. The leakage of the leachate through geomembrane (GMB) liner and the resulting seepage into the underlying soil layer keeps changing with passage of time. Hence, a transient flow pattern was selected for the model (Geo-Slope International Ltd., 2012). The leak in the GMB was assumed to be circular, and hence, an axisymmetric analysis was chosen. The leakage duration was kept as 90 mins, with 10 minute time intervals. The next step was to define material properties.

9.4.1 Volumetric water content function for Perth sandy soil

For the Perth sandy soil, firstly the volumetric water content function was defined. Then based on the volumetric water content function, the hydraulic conductivity function was developed to completely define the properties of the soil (Geo-Slope International Ltd., 2012).

To define the volumetric water content function of the sand, the data-point function was chosen, and the grain-size data obtained through experiments were used. The data-point function was selected as it is most suitable for the soil type being used in the leak detection test, which is a poorly graded sand (Geo-Slope International Ltd., 2012). For Perth soil case, $D_{10} = 0.15\,\text{mm}$ and $D_{60} = 0.34\,\text{mm}$.

Relative density (D_r) is related to the void ratio (e) of soil, maximum void ratio ($e_{\max}$) and minimum void ratio ($e_{\min}$) as follows (Shukla, 2014):

$$D_r = \left(\frac{e_{\max} - e}{e_{\max} - e_{\min}} \right) \times 100 \tag{9.21}$$

For the leak detection test, relative density, $D_r = 100\%$. Putting this value into Eqn. (9.21),

$$e = e_{\min} \tag{9.22}$$

Further, the following relationship is known for minimum dry unit weight ($\gamma_{d\min}$), unit weight of water (γ_w), specific gravity of sand particles (G_s) and minimum void ratio:

$$\gamma_{d\min} = \frac{G_s \gamma_w}{1 + e_{\min}} \tag{9.23}$$

Using Eqns. (9.22) and (9.23),

$$e = \left(\frac{G_s \gamma_w}{\gamma_{d\min}} - 1 \right) \tag{9.24}$$

For the leak detection test with water, G_s is 2.68, γ_w is 9.81 kN/m^3 and $\gamma_{d\min}$ is 14.02 kN/m^3. Putting these values into Eqn. (9.24), $e = 0.875$. Further,

$$\theta_w = nS \tag{9.25}$$

where θ_w = volumetric water content, n = porosity, and S = degree of saturation (Geo-Slope International Ltd., 2012). In addition,

$$n = \frac{e}{1+e} \tag{9.26}$$

Using Eqns. (9.25) and (9.26), $\theta_w = 0.47$ at 100% saturation. On inputting these values, the volumetric water content function for Perth sandy soil was obtained, which is shown in Figure 9.1.

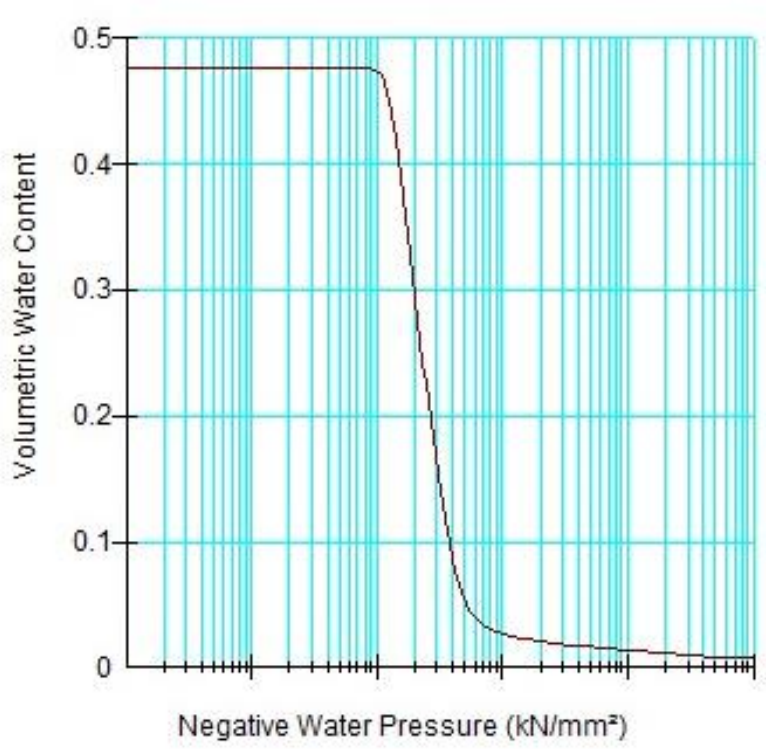

Figure 9.1: Volumetric water content function for Perth sandy soil.

9.4.2 Hydraulic conductivity function for Perth sandy soil

Once the volumetric content function is obtained, the next step is to create the hydraulic conductivity function for the soil medium.

A conductivity ratio of 1 was selected as the prepared soil is assumed to be homogeneous and hence, the hydraulic conductivity would be same in the X and Y directions. The conductivity direction was chosen as 0° as the model has been created using the default X and Y axes itself. The conductivity at saturation (k_{sat}) was assumed to be 10^{-4} m/s and the residual water content was kept 5%. Using Van Genuchten model, the hydraulic conductivity function for Perth sandy soil, as shown in Figure 9.2, was obtained.

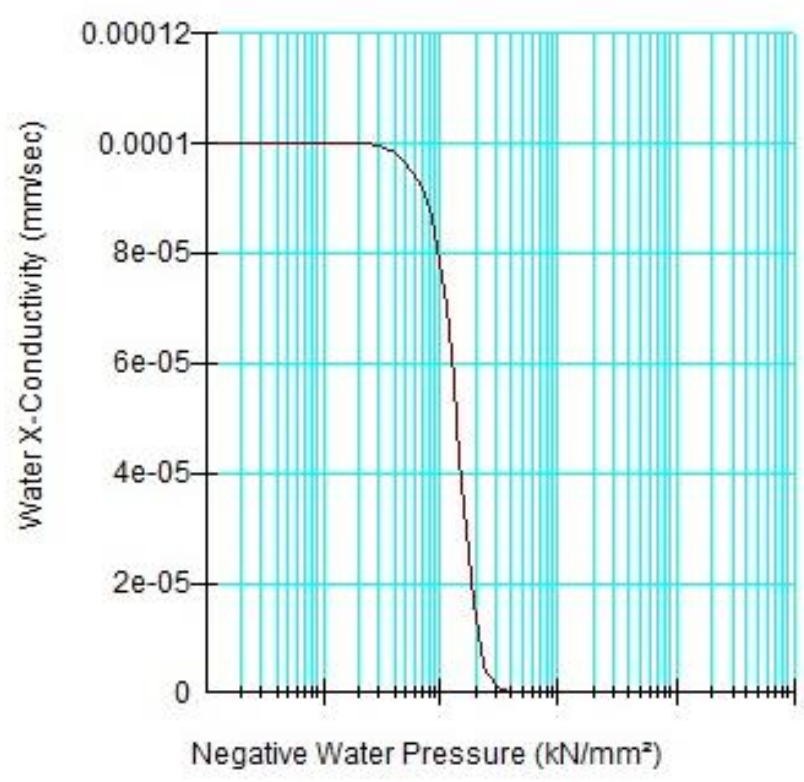

Figure 9.2: Hydraulic conductivity function for Perth sandy soil.

9.4.3 Defining material properties for geomembrane liner

The geomembrane (GMB) liner was taken as two straight lines divided by a gap for the leak, and assigned the material model of interface. As the liner is nearly impermeable (Giroud and

Bonaparte, 2001), the tangential conductivity as well as normal conductivity is assigned the value of 0 m/s.

9.4.4 Boundary conditions

A hydraulic boundary condition was created at the leak position. As the water over GMB has been kept constant for the test duration, a constant head was defined as the hydraulic boundary (Pandey *et al.*, 2017; Pandey and Shukla, 2018b, 2019).

Figure 9.3 shows the model developed after leak detection test. The model was then executed to achieve several contour curves.

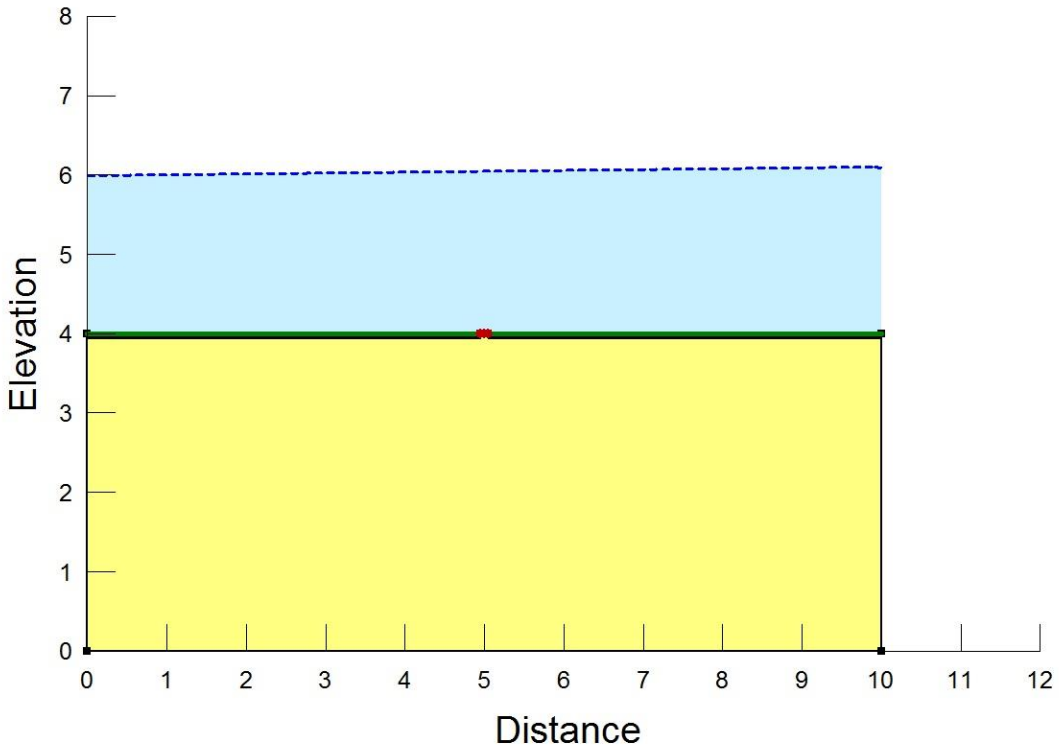

Figure 9.3: Model developed after leak detection test method.

9.5 Application of developed model for resistivity prediction

Figures 9.4 through 9.13 give the contour profiles for pore-water pressure, obtained using the developed model in GeoStudio SEEP/W. The arrows in the figures depict not only the direction, but the magnitudes of the velocity vectors as well. The direction of arrow head shows where the flow is occuring, while the length of each arrow is a visual representation of the magnitude of the actual velocity (Geo-Slope International Ltd., 2012).

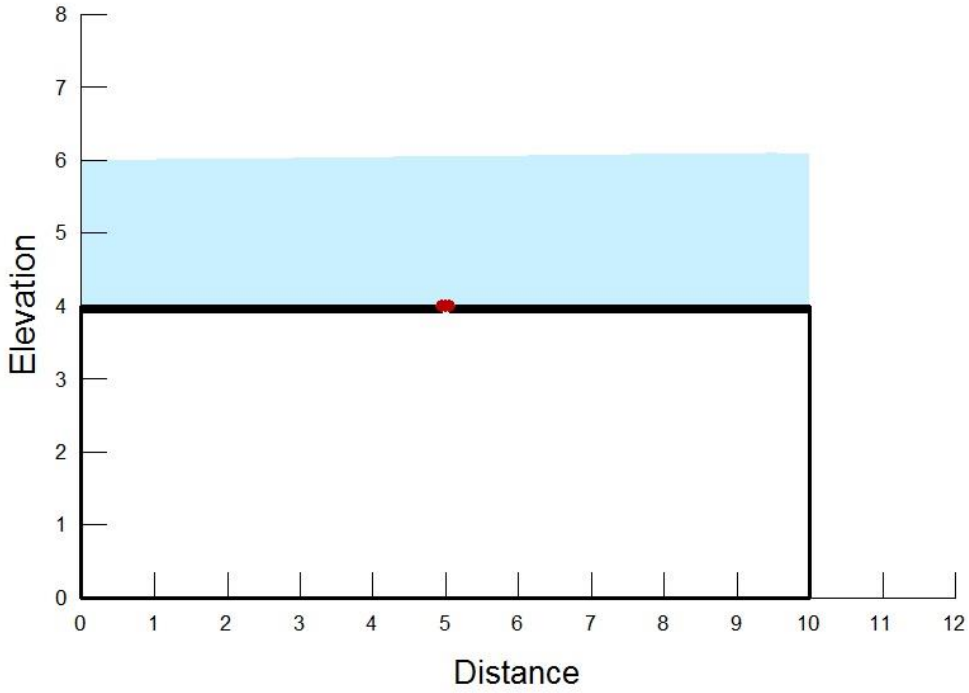

Figure 9.4: Water flow at 0 min.

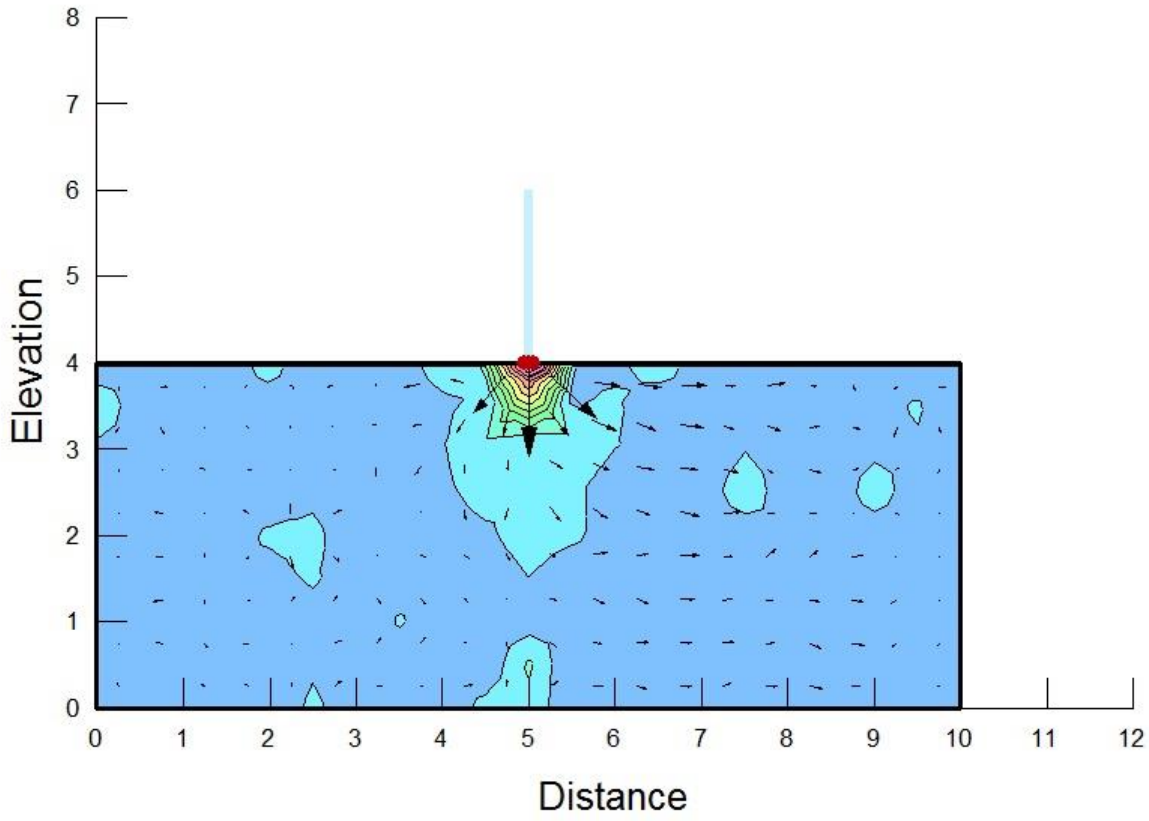

Figure 9.5: Water flow at 10 min.

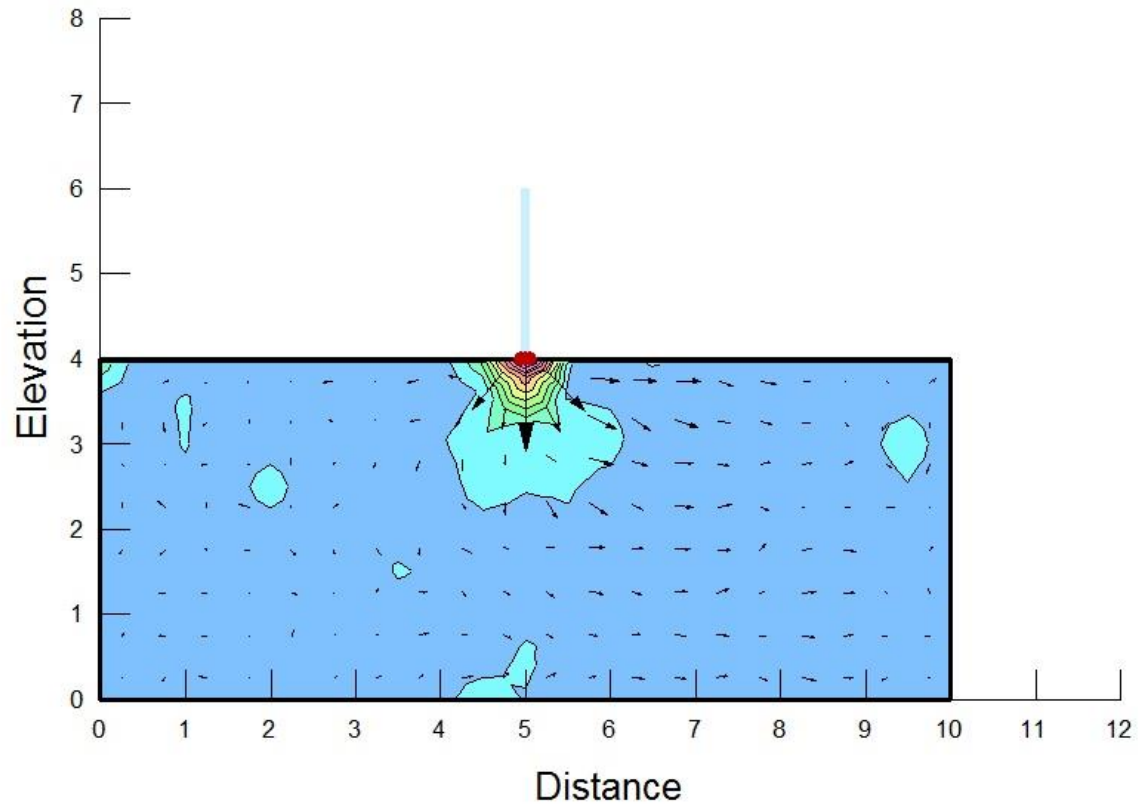

Figure 9.6: Water flow at 20 min.

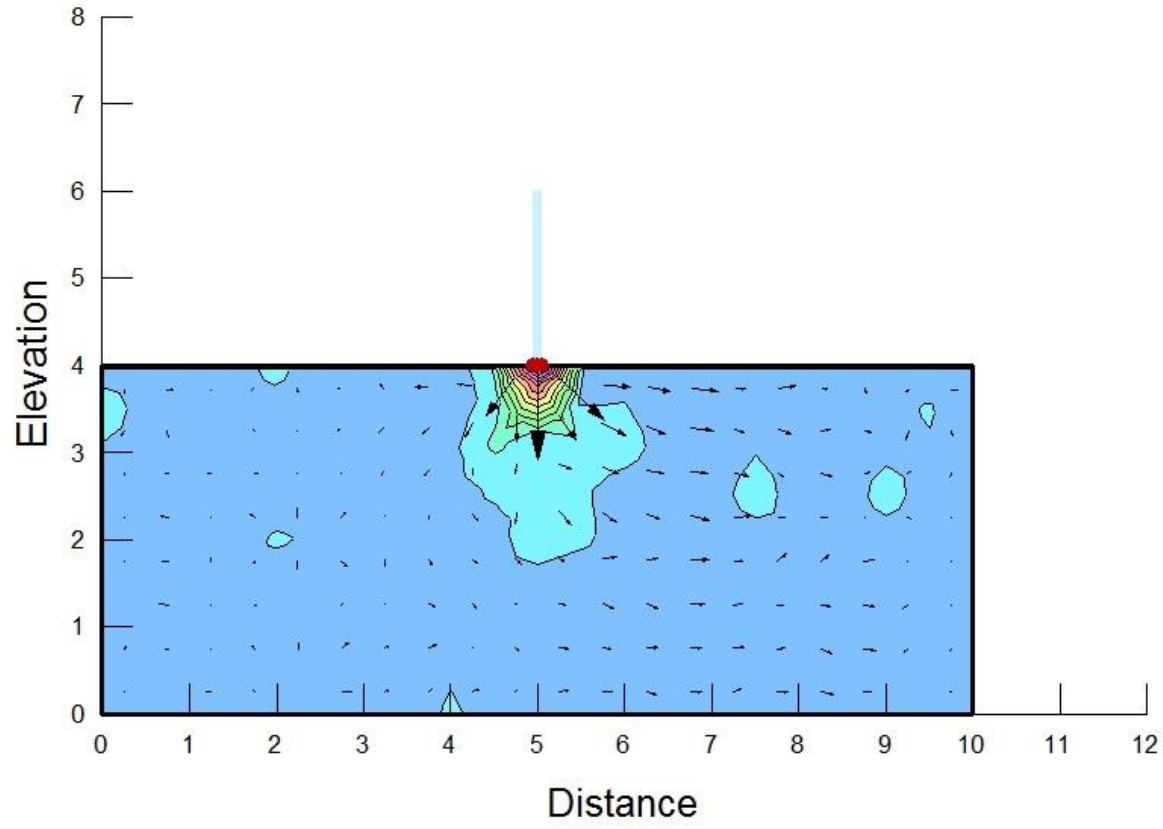

Figure 9.7: Water flow at 30 min.

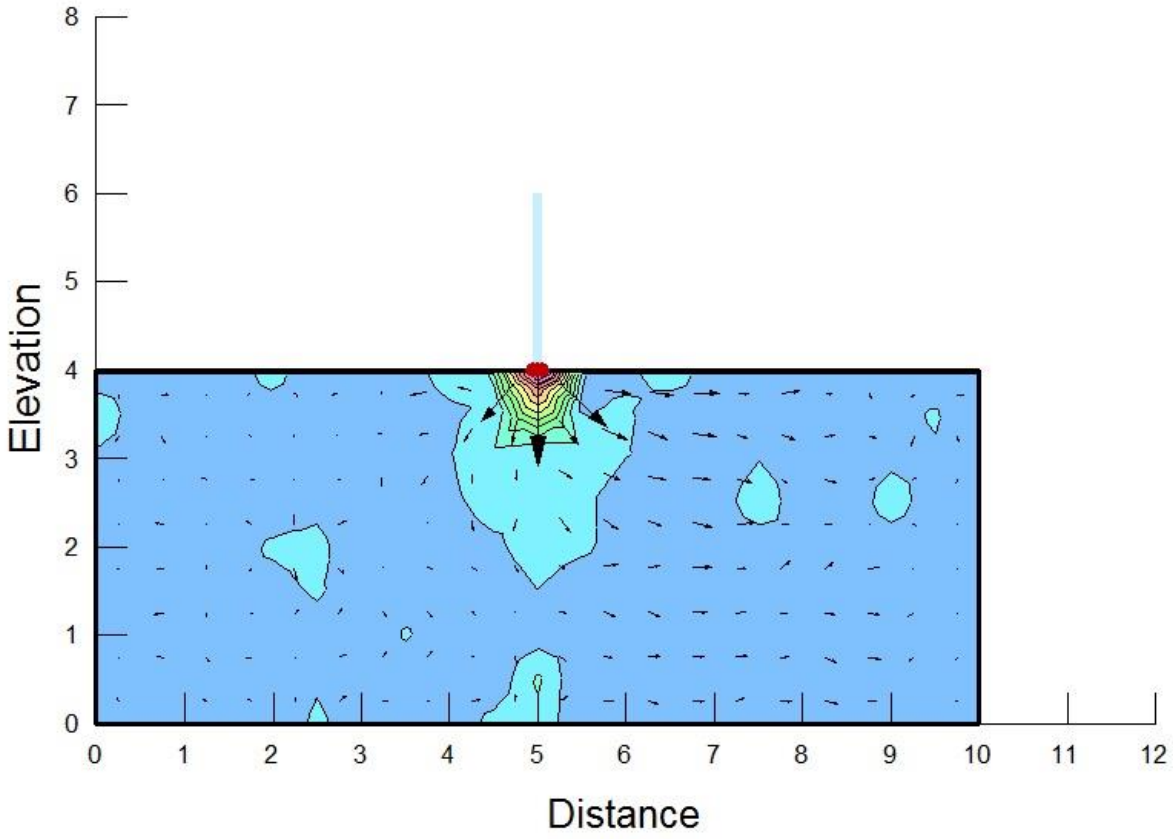

Figure 9.8: Water flow at 40 min.

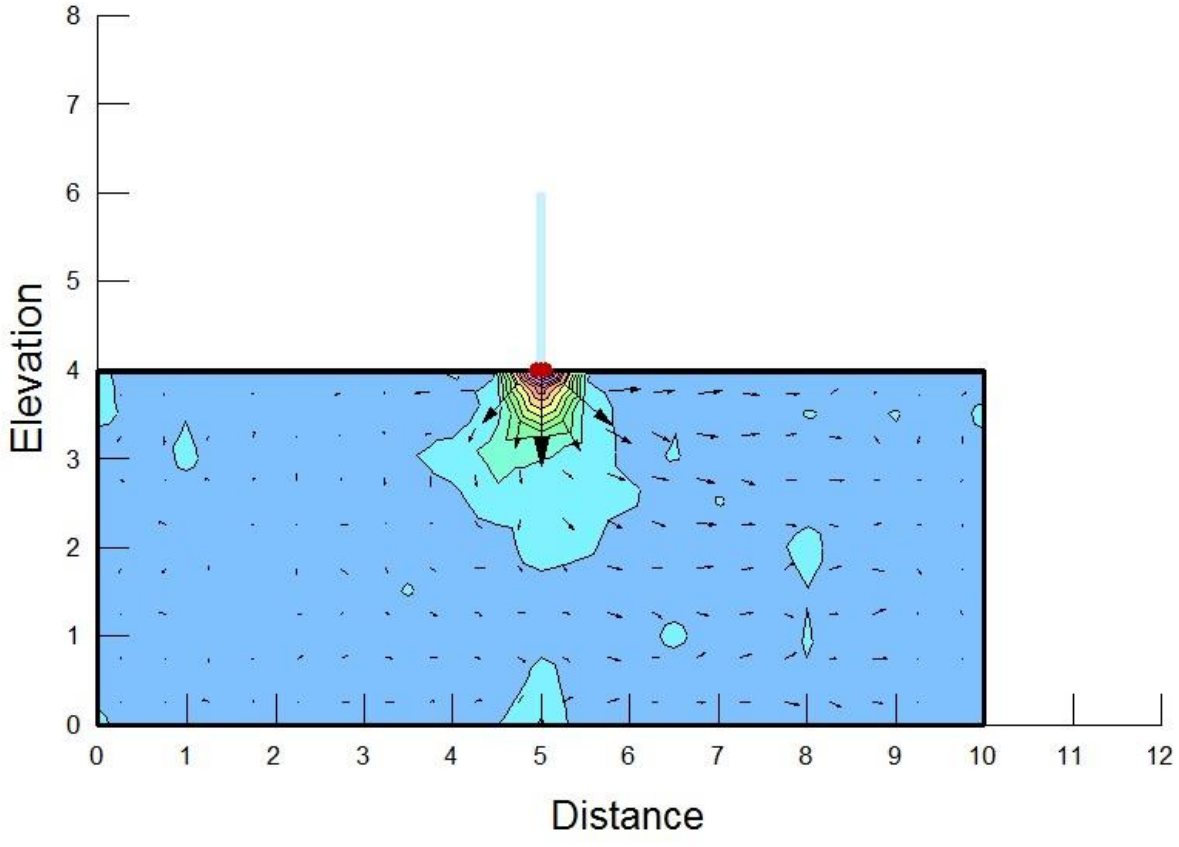

Figure 9.9: Water flow at 50 min.

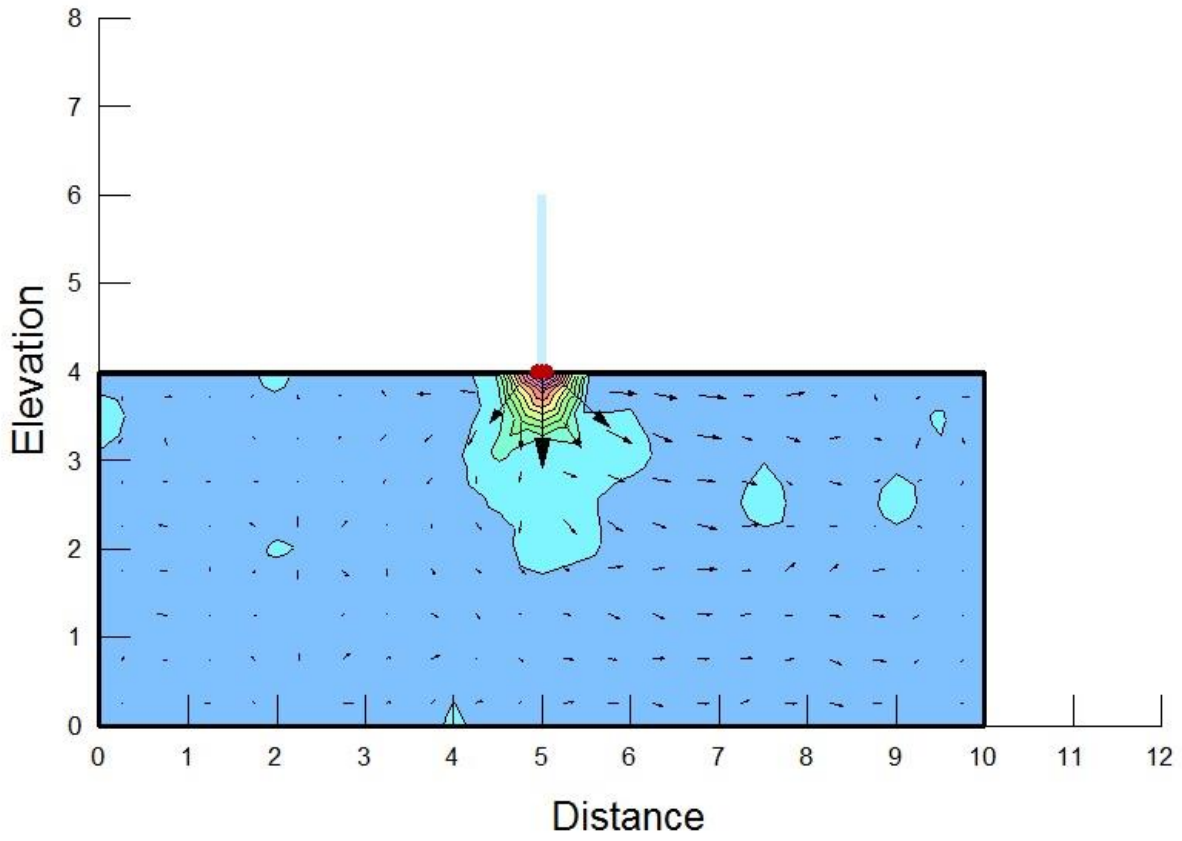

Figure 9.10: Water flow at 60 min.

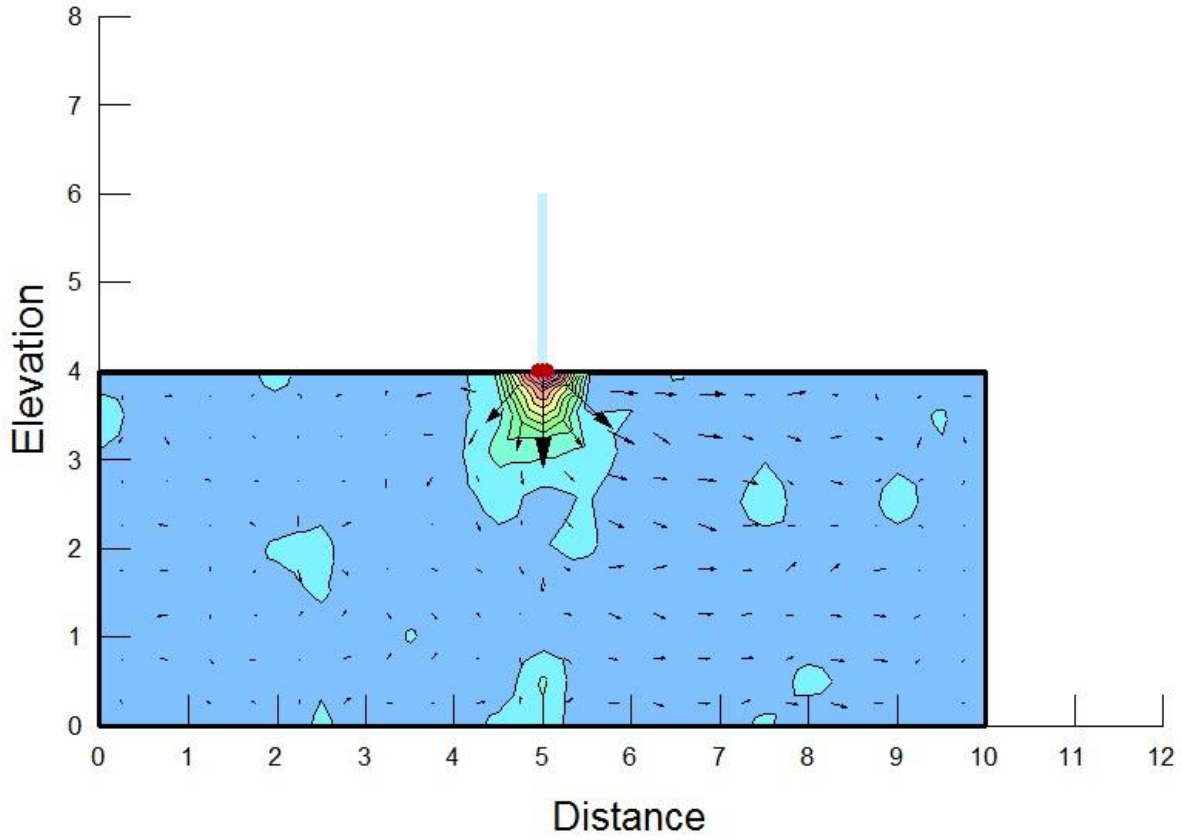

Figure 9.11: Water flow at 70 min.

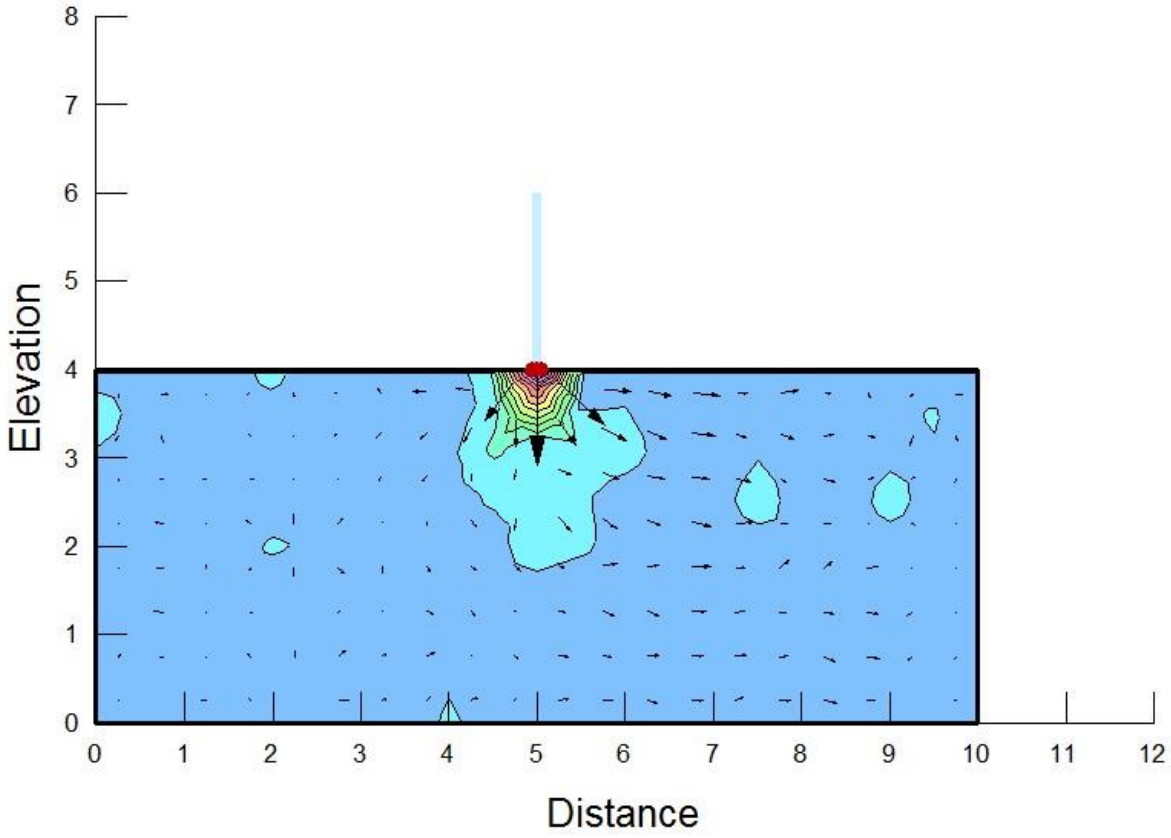

Figure 9.12: Water flow at 80 min.

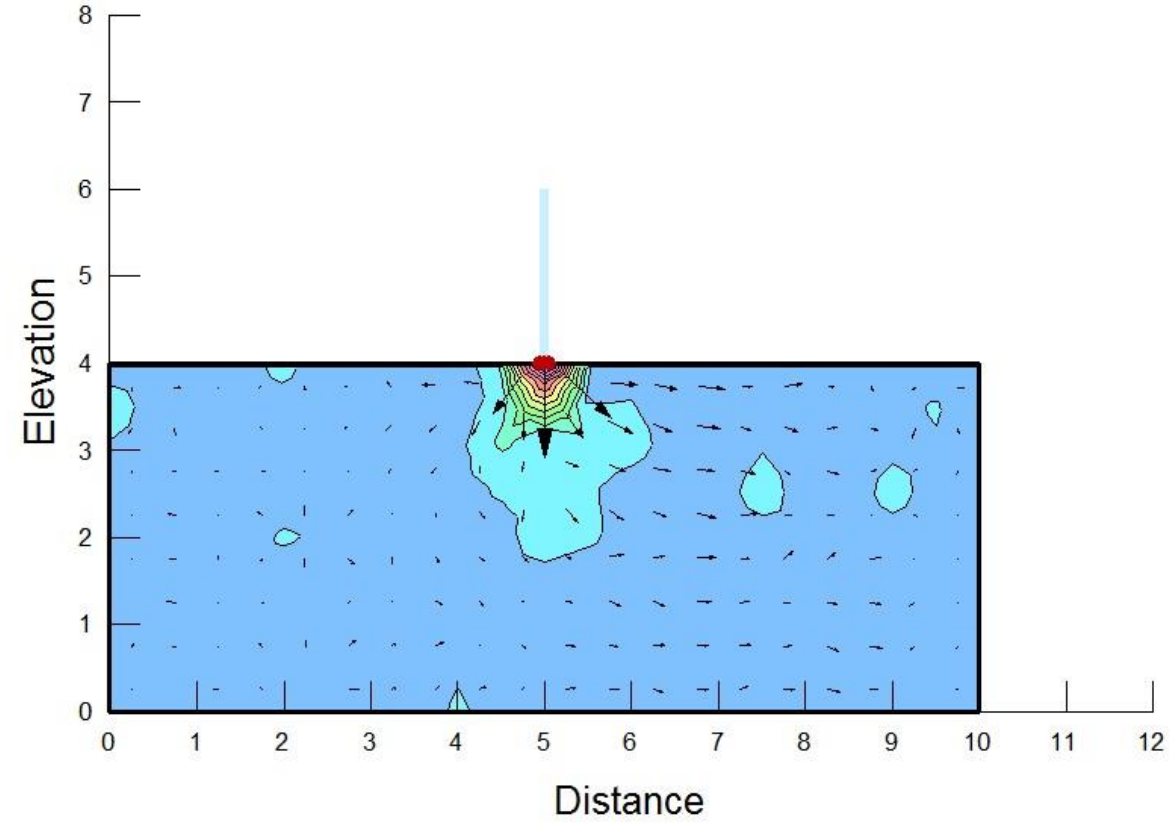

Figure 9.13: Water flow at 90 min.

Using the developed model, the velocity vector (v) was obtained at specific Gauss points, for different leakage durations (t). This velocity value was then substituted into Eqn. (9.14) to predict the electrical resistivity (ρ). The resistivity values at different Gauss points were plotted in graphs to obtain resistivity profiles for the soil.

To determine the variation of resistivity with leakage duration and distance (x), three points were selected in the developed model with coordinates as P_1 (2.5 m, 3 m), P_2 (5 m, 3 m) and P_3 (7.5 m, 3 m). It should be noted that the centre of the leak was positioned directly above P_2, at (5 m, 4 m). The *xy*-velocity magnitude at each of these points was obtained at different leakage durations, with 10 min intervals (Figures 9.3 through 9.13). Figure 9.14 shows the resistivity variations with time, generated for each of the three points.

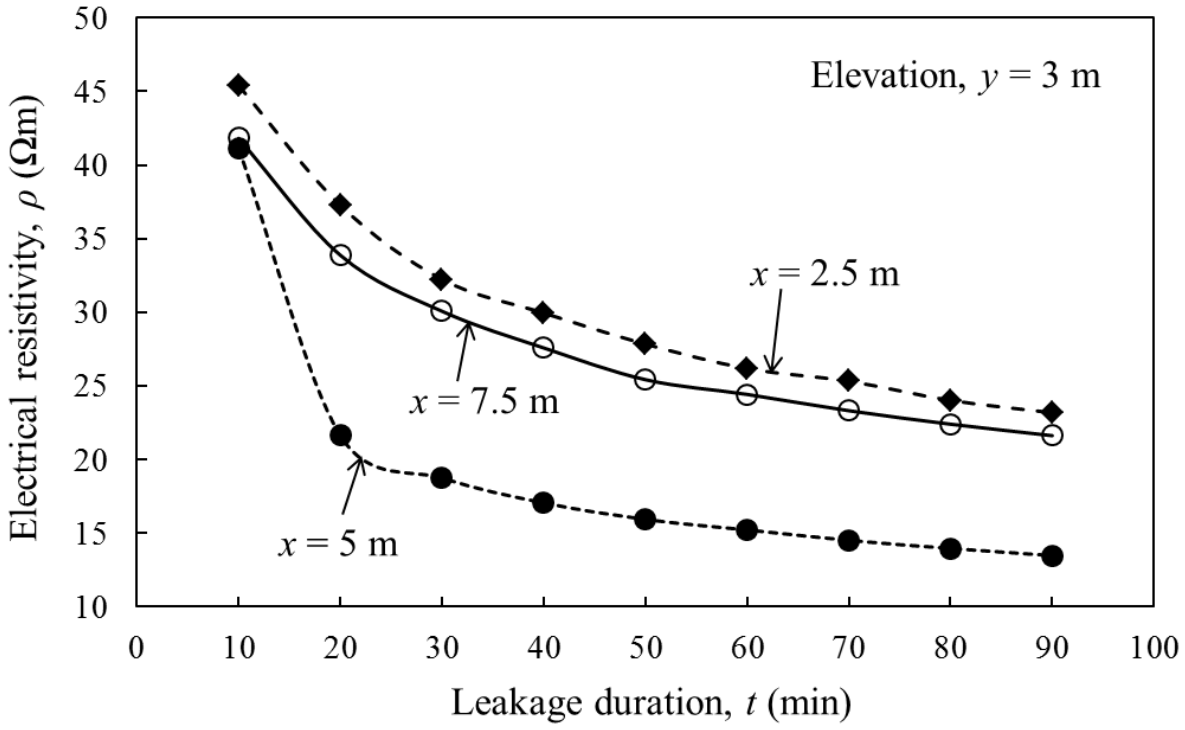

Figure 9.14: Resistivity profiles generated using the developed model at y = 3 m.

From Figure 9.14, it can be observed that the resistivity shows a decrease with an increase in the leakage duration. This observation complies with the expectation that with an increase in t, the amount of water in soil due to leakage would increase, and consequently resistivity would decrease.

The rate of decrease of resistivity with leakage duration is rapid intially. However, this rate of decrease reduces significantly at leakage durations greater than 35 mins. Furthermore, it can

be seen that at any given leakage duration, the resistivities obtained at P_1 and P_3 are higher than the resistivity at P_2. This observation is as per the expectation as the hole in the geomembrane (GMB) liner was positioned directly above resistance at (5 m. 4 m). Hence, the amount of water at P_1 and P_3 would be greater than the amount of water at P_2. Therefore, resistivity at P_2 was expected to be lower than resistiivty at P_1 and P_3.

A similar analysis was conducted to determine the variation of resistivity with leakage duration and elevation (y). Three points were selected in the developed model with coordinates as P_2 (5 m, 3 m), P_4 (5 m, 2 m) and P_5 (5 m, 1 m). Figure 9.15 shows the resistivity profiles obtained for P_2 , P_4 and P_5 using the developed model.

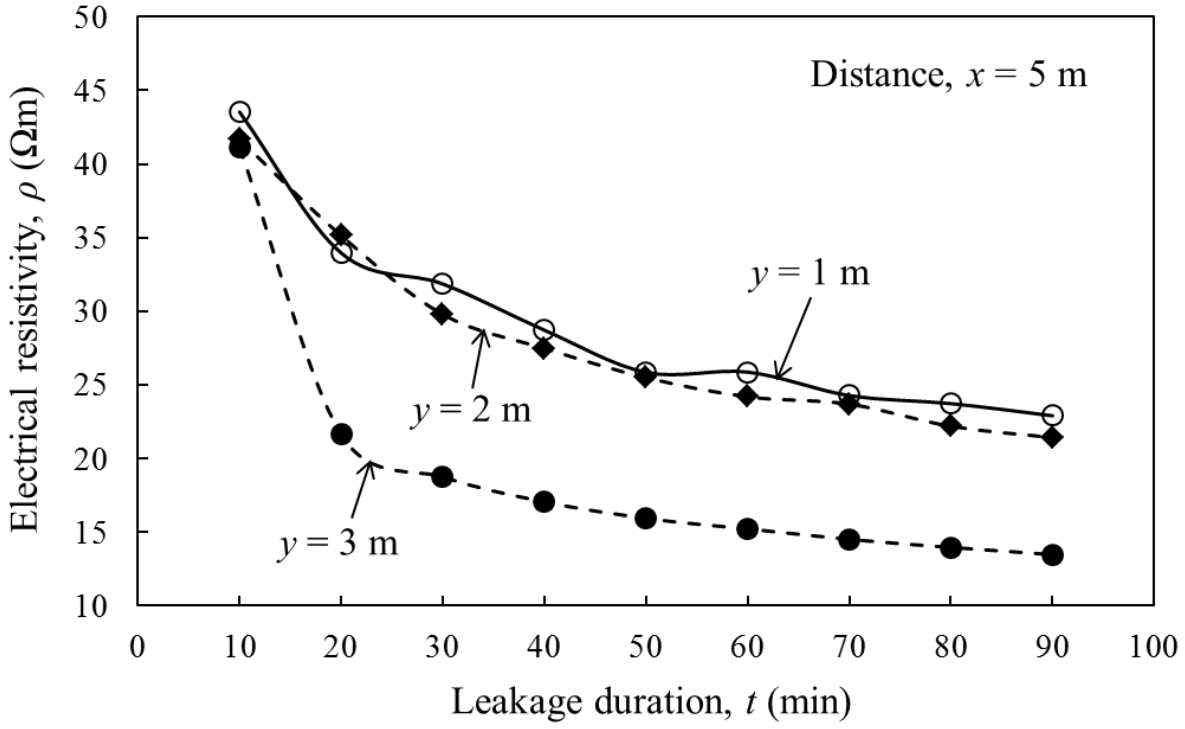

Figure 9.15: Resistivity profiles generated using developed model at x = 5 m.

The electrical resistivity demonstrates a decrease with an increase in the leakage duration, irrespective of the position of the point of measurement (Figure 9.15). It can be seen that the resistivity increases with an increase in the distance from the leak point. This is as expected, and can be attributed to the decrease in water content with increase in distance from leak.

Hence, it can be concluded that with an increase in the distance/depth from the hole, the resistance of the soil shows an increase. Therefore, the location of the liner leak can be ascertained based on the resistance profile of the soil.

Figure 9.16 shows the variation of the resistance generated using the developed model, for leakage durations, t = 30, 60 and 90 min, at the points P_1 (2.5 m, 3 m), P_2 (5 m, 3 m) and P_3 (7.5 m, 3 m). It can be noticed that the resistivity first decreased and then increased with an increase in the distance of the point of measurement.

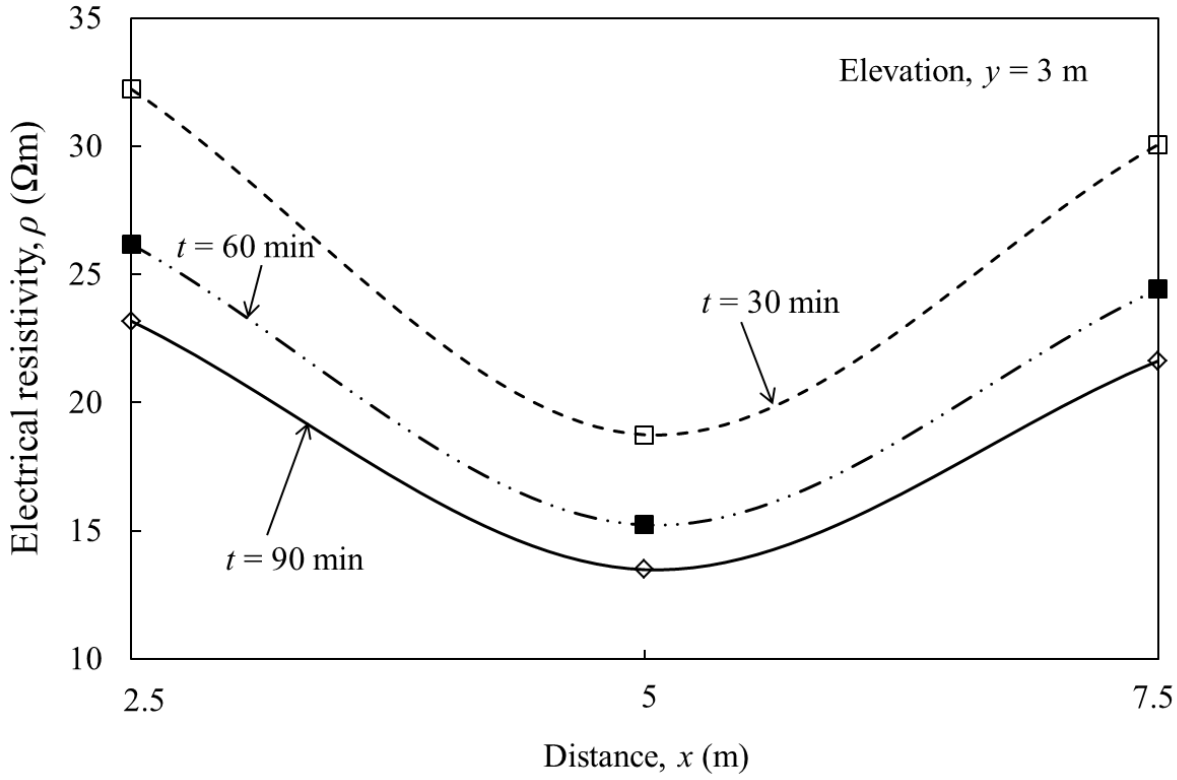

Figure 9.16: Variation of resistivity generated using the developed model.

It is interesting to note that the trend in the resistivity obtained from the developed model, is the same as the trend observed in the experimental demonstrations. Therefore, it can be concluded that the developed correlations can be used in conjunction with any seepage analysis software that provides the velocity vector at different locations in order to predict expected resistivity values, and subsequently, to generate resistivity profiles for use by design engineers.

9.6 Conclusions

New empirical correlations have been developed and presented for the relationship between resistivity, leakage duration and distance/depth. In addition, the equations have also been given to predict the flow velocity of leachate at any point within a soil specimen, for known resistivity at a given time. These correlations can be used with any software that deals with seepage analysis and provides the velocity vector at different locations, to predict expected resistivity

values. The application of these new relationships has been demonstrated by developing a numerical model for seepage analysis using the SEEP/W software. Then, the velocity vector generated from this numerical model has been replaced in the developed correlations to obtain electrical resistivity. Therefore, the newly developed correlations were demonstrated to be useful for practicing engineers in the design of lining systems as well as for various numerical modelling applications in the waste containment facilities.

References

Archie, G.E. (1942). The electrical resistivity log as an aid in determining some reservoir characteristics. *Society of Petroleum Engineers* 146(1), 54–61, DOI: 10.2118/942054-G.

Das, B.M. (2013). Fundamentals of geotechnical engineering, 4th edition, Cengage Learning, Stamford.

Forchheimer, P. (1930). Hydraulik, 3rd Edn, B.G. Teubner, Leipzig, Berlin, Germany.

Geo-Slope International Ltd. (2012). Seepage modeling with SEEP/W: An Engineering Methodology, July 2012 Edition. GEO-SLOPE International Ltd. Calgary, Alberta, Canada.

Giroud, J.P. and Bonaparte, R. (2001). Geosynthetics in liquid-containing structures. Geotechnical and Geoenvironmental Engineering Handbook (pp. 789-824). Springer, Boston, MA.

Giroud, J.P., Khatami, A. and Badu-Tweneboah, K. (1989). Evaluation of the rate of leakage through composite liners. *Geotextiles and Geomembranes* 8(4), 337-340, DOI: https://doi.org/10.1016/0266-1144(89)90016-2.

Gupta, S.C. and Hanks, R.J. (1972). Influence of water content on electrical conductivity of the soil. *Soil Science Society of America* 36(6), 855–857, DOI: 10.2136/sssaj1972.03615995003600060011x.

Kalinski, R. and Kelly, W. (1993). Estimating water content of soils from electrical resistivity. *Geotechnical Testing Journal* 16(3), 323-32, DOI: 10.1520/GTJ10053J.

Oh, M., Seo, M. W., Lee, S. and Park, J. (2008). Applicability of grid-net detection system for landfill leachate and diesel fuel release in the subsurface. *Journal of Contaminant Hydrology* 96(1-4), 69-82, DOI: 10.1016/j.jconhyd.2007.10.002.

Pandey, L.M.S. and Shukla, S.K. (2017). Detection of leachate contamination in Perth landfill base soil using electrical resistivity technique. *International Journal of Geotechnical Engineering*, 1-12, DOI: 10.1080/19386362.2017.1339763.

Pandey, L.M.S. and Shukla, S.K. (2018a). Effect of state of compaction on the electrical resistivity of sand-bentonite lining materials. *Journal of Applied Geophysics* 155, 208-216, DOI: 10.1016/j.jappgeo.2018.06.016.

Pandey, L.M.S. and Shukla, S.K. (2018b). Detection of leakage of MSW landfill leachates through a liner defect. *Surveys in Geophysics* (under review).

Pandey, L.M.S. and Shukla, S.K. (2019). Development of an innovative liner leak detection technique. *Geotechnical Testing Journal* 42(5), DOI: 10.1520/GTJ20170292.

Pandey, L.M.S., Shukla, S.K. and Habibi, D. (2015). Electrical resistivity of sandy soil. *Géotechnique Letters* 5(3), 178-185, DOI: 10.1680/jgele.15.00066.

Pandey, L.M.S., Shukla, S.K. and Habibi, D. (2017). Resistivity profiles of Perth soil in Australia in leak-detection test. *Geotechnical Research* 4(4), 214-221, DOI: 10.1680/jgere.17.00014.

Shukla, S.K. (2014). Core Principles of Soil Mechanics. ICE Publishing, London, UK.

CHAPTER 10

SUMMARY AND CONCLUSIONS

This chapter summarises briefly the problem being addressed and outlines the methodology that was used. Though conclusions have been given at the end of each chapter, the overall key findings have been presented in this chapter. It goes further to point out the main novel findingsas this research has produced. Finally, it makes some recommendations for future research trajectories based on the experience from this research.

10.1 Summary

Every year large quantities of waste are generated, handled and disposed, worldwide. The leachates generated from the disintegration and decomposition of these wastes are potentially harmful to the environment. Therefore, it is critical for waste management facilities such as, landfills, leachate ponds, tailing dams, red mud ponds, sump wells, etc., to follow proper waste handling and management practices. This includes the use of suitable engineered lining systems for waste containment, and the implementation of efficient leakage monitoring and detection systems by waste impounding facilities to prevent the soil and groundwater contamination.

The liners used in various lining systems are designed to be intact over their operating life. However, defects are often found to develop in liners due to the use of inappropriate placement practices or severe conditions of operation. Hence, their performance tends to get compromised over the intended design life. Subsequent environmental pollution ensues because of such defects. Therefore, it becomes critical to detect leakage issues as soon as they arise. These defects if not detected timely, can lead to severe environmental pollution. Furthermore, the early leak detection of leakage is of vital importance for timely and economical hazard mitigation. Thus, the waste management facilities use different leak detection techniques to control leachate contamination.

Many different methods for leak detection are available, however, the electrical resistivity method is most feasible owing to its low operational cost and easy operability. Most soils have very high electrical resistivity values compared to that of contaminating fluids such as landfill

leachates. Consequently, the leakage of even a small amount of leachate may cause significant rise in the electrical resistivity of the underlying soil, which can be easily detected. Therefore, resistivity measurements can be used as an effective tool to detect contamination. Hence, there is a significant scope for an innovative method of leak detection which can detect leakages at the onset.

In this research, an attempt has been made to assess the current state of landfilling in Australia with a focus on the lining practices and leak detection methods. An extensive study was conducted involving different private and public waste handling and management facilities in all the States and territories of Australia.

In addition, this research also presents the results of an investigation into the effect of the state of compaction on the resistivity of sand-bentonite mixtures, with the bentonite content varying from 0 to 100%. The resistivity of mixtures at their different states of compaction are investigated.

Further, this study introduces an innovative diagnostic technique for the detection of leaks through liners using the changes in the electrical resistivity of base soil. It has been developed and investigated by the Geotechnical and Geoenvironmental Research Group at Edith Cowan University with a view to applying them in landfilling facilities for leakage monitoring. The system design is based on the well-known principles of the electrical resistivity method. A new leak detection system is developed by pairing a resistivity sensing technique with a four-probe ground resistance testing equipment. The guidelines given by the Australian Standard AS 1289.4.4.1-1997 are used for the system design. The details for the fabrication of the system are presented extensively in this paper.

Tests were conducted to substantiate the efficacy of the system in determining leakage issues through liners. Liner leakage was simulated in the laboratory using the controlled leakage of different leachates into the soil layer beneath the liner. Tap water, two leachates procured from Western Australian municipal solid waste (MSW) landfill sites, and Bayer liquor procured from an aluminium manufacturing company in Perth, Australia, were used as the leachates. Resistivity testing was then conducted to evaluate the performance of this technique. Various resistivity profiles were obtained at regular time-intervals to investigate the effect of leakage duration, leachate composition, and electrode location on the resistivity of soil.

Finally, based on the leak detection test results, newly developed empirical correlations and analytical modelling were presented for the relationship between the electrical resistivity of liner base material, the leakage duration and the distance/depth of point of measurement.

In addition, a numerical model was developed using GeoStudio SEEP/W, for the seepage analysis of the leak detection test. The flow velocity obtained from this model was used in conjunction with the new correlations to generate resistivity profiles for any specific soil type and leachate.

10.2 Conclusions

Based on the current study, the following general conclusions are made from each of the individual research aspects and the analysis of the literature.

1. Landfilling is the predominant method of waste disposal in Australia with nearly 51% of the generated waste ending up in landfills.
2. In Australia, majority of the landfill facilities are owned and operated by public sector entities such as cities, counties/parishes, regional authorities, state governments, and the federal government.
3. Australians landfills generally consist of varying combinations of compacted clay and geomembrane liners. However, they do not follow any one unifying guideline for ground preparation, siting, design, operation, and rehabilitation.
4. Groundwater monitoring wells were the principal method of leakage detection practiced by the Australian landfills.
5. The use of the electrical resistivity technique for leak detection is proven to be very effective in determining leakages.
6. The compaction behavior of the sand-bentonite mixture resembles that of bentonite at higher bentonite contents.
7. The electrical resistivity of each sand-bentonite mixture decreases rapidly with an increase in water content. However, after a certain water content, this rate of decrease reduces significantly. This specific water content is different for each of the sand-bentonite mixtures.
8. The change in the decreasing trend of resistivity occurs on the wet-side of the optimum for sand-bentonite mixtures and on the dry-side of the optimum for sand and bentonite.
9. The effect of bentonite addition is negligible on the electrical resistivity of sand-bentonite mixture at bentonite contents over 20%.
10. The use of pre-laid sensor beds based on electrical resistivity method was observed to be marginal. Further, the need for the online monitoring of lining systems for the proper management of waste containment facilities in Australia, has been discussed.

11. An innovative leak detection technique to determine the electrical resistivity behavior of soils as a result of leachate contamination, as developed and used by the Geotechnical and Geoenvironmental research group at Edith Cowan University (ECU), is presented.
12. Results for the experimental demonstration of the leak detection test using the tap water, two municipal solid waste (MSW) landfill leachate, and Bayer liquor, are presented.
13. For leak detection tests using any type of leachate, the resistivity of the soil increases with an increase in the depth or the distance, of the mid-point of the pair of electrodes, from the liner leak.
14. The effect of distance and depth is found to be negligible at greater depths, for the leakage duration of 30 min, for tests done with tap water as leachate.
15. For tap water as leaching fluid, the resistivity values are in the range of 90-100 Ωm.
16. The effect of distance/depth on the soil resistivity is negligible at leakage duration greater than 60 min for landfill leachate #1 and 160 min for landfill leachate #2.
17. The resistivity of soil ranges from 7-15 Ωm for Leachate #1 to 20-50 Ωm for Leachate #2.
18. The resistivity values obtained with water are nearly 10 times the values observed with landfill leachates as the leaching liquid.
19. The resistivity values were found to range from 1 to 3 Ωm when using Bayer liquor as leachate.
20. Resistivity of the soil decreases rapidly with an increase in the leakage duration.
21. The leak detection system is effective in determining leakage in the liner, irrespective of the leakage duration.
22. Electrode sensing system which is closest to the liner has the better ability to detect leakage. The resistivities recorded using sensors at the depth of 120 mm and above, showed insignificant variation with distance and leakage duration.
23. The newly developed system is effective in determining and locating liner leaks at the onset. It has further applications in sensor development for real-time monitoring of lining systems in waste containment facilities.
24. This innovative methodology for the testing of the electrical resistivity of soils can be adopted as a standard method for soil testing by the Australian government and Standards Australia, in accordance to their policies.
25. The innovative diagnostic technique can find several applications in designing the monitoring systems for waste storage and handling facilities, subbase contamination

detection, liner leak detection, soil and corrosion studies, anomaly detection, and subsurface water profiling and prospecting.

26. New empirical correlations have been developed and presented for the relationship between resistivity, leakage duration and distance/depth. The equations have also been given to predict the flow velocity of leachate at any point within a soil specimen, for known resistivity at a given time. These correlations can be used with any software that deals with seepage analysis and provides the velocity vector at different locations, to predict expected resistivity values.
27. The application of newly developed correlationa has been demonstrated by designing a numerical model for seepage analysis using the SEEP/W software. Then, the velocity vector generated from this numerical model has been replaced in the developed correlations to obtain electrical resistivity.
28. The newly developed correlations were demonstrated to be useful for practicing engineers in the design of lining systems as well as for various numerical modelling applications in waste containment facilities.
29. The findings reported here should not be extrapolated to soil and leachate types which differ significantly from the soil used in this study.
30. It may be noted that the leak detection system will not be able to detect leakages in the liner if the soil is completely saturated.

10.3 Contributions to Knowledge

This research can be particularly useful in generating awareness about the state of landfilling and will help various environmental protection agencies in making informed decisions for the development of rules and regulations to govern landfills. The newly developed leak detection technique was found to be effective in the timely detection and location of liner leakages, irrespective of the leakage duration and leachate composition.

The new technique can be useful in designing the monitoring systems for waste storage and handling facilities, contamination detection, liner leak detection, development of sensors, development of numerical models, and so on. The use of graphical presentations, empirical correlations, analytical expressions and numerical models presented in this research can assist in actively monitoring the lining systems and taking timely action for contamination control.

10.4 Future Research Trajectories

The following research trajectories have been identified:

- Further research to identify the feasibility and possible methods of commercialisation for these research findings.
- Investigation of the effect of changing the subbase material on the resistivity profiles obtained in leak detection test.
- Development of numerical model based on the experimental results for the design of sensor systems in waste containment facilities.